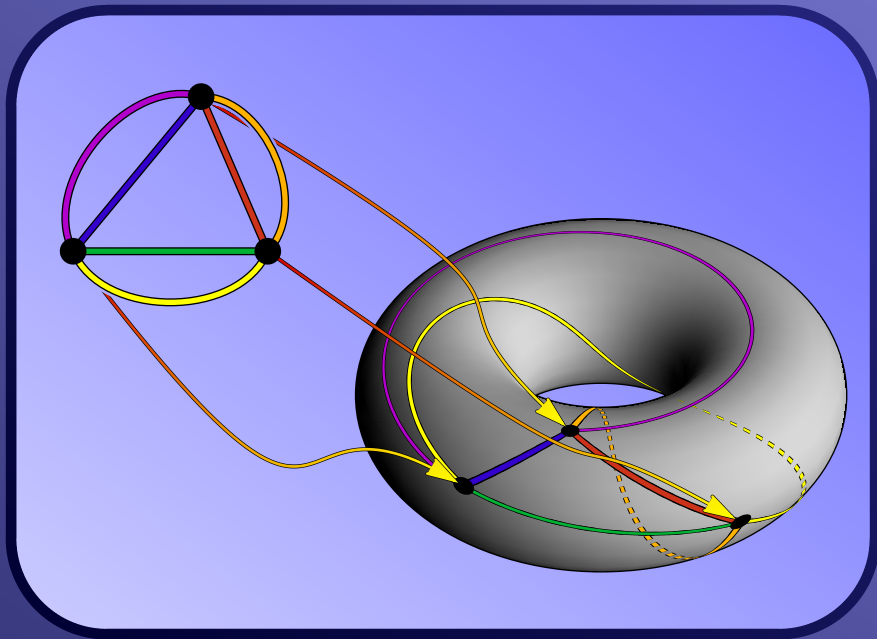# The combinatorics of
the Jack parameter
and
the genus series
for topological maps

Michael Andrew La Croix

The combinatorics of the Jack parameter and the genus series for topological maps

by

Michael Andrew La Croix

A thesis
presented to the University of Waterloo
in fulfillment of the
thesis requirement for the degree of

Doctor of Philosophy

in

Combinatorics and Optimization

Waterloo, Ontario, Canada, 2009

Author's declaration

I hereby declare that I am the sole author of this thesis. This is a true copy of the thesis, including any required final revisions, as accepted by my examiners.

I understand that my thesis may be made electronically available to the public.

Abstract

Informally, a rooted map is a topologically pointed embedding of a graph in a surface. This thesis examines two problems in the enumerative theory of rooted maps.

The b-Conjecture, due to Goulden and Jackson, predicts that structural similarities between the generating series for rooted orientable maps with respect to vertex-degree sequence, face-degree sequence, and number of edges, and the corresponding generating series for rooted locally orientable maps, can be explained by a unified enumerative theory. Both series specialize $M(\mathbf{x}, \mathbf{y}, z; b)$, a series defined algebraically in terms of Jack symmetric functions, and the unified theory should be based on the existence of an appropriate integer valued invariant of rooted maps with respect to which $M(\mathbf{x}, \mathbf{y}, z; b)$ is the generating series for locally orientable maps. The conjectured invariant should take the value zero when evaluated on orientable maps, and should take positive values when evaluated on non-orientable maps, but since it must also depend on rooting, it cannot be directly related to genus.

A new family of candidate invariants, η, is described recursively in terms of root-edge deletion. Both the generating series for rooted maps with respect to η and an appropriate specialization of M satisfy the same differential equation with a unique solution. This shows that η gives the appropriate enumerative theory when vertex degrees are ignored, which is precisely the setting required by Goulden, Harer, and Jackson for an application to algebraic geometry. A functional equation satisfied by M and the existence of a bijection between rooted maps on the torus and a restricted set of rooted maps on the Klein bottle show that η has additional structural properties that are required of the conjectured invariant.

The q-Conjecture, due to Jackson and Visentin, posits a natural combinatorial explanation, for a functional relationship between a generating series for rooted orientable maps and the corresponding generating series for 4-regular rooted orientable maps. The explanation should take the form of a bijection, φ, between appropriately decorated rooted orientable maps and 4-regular rooted orientable maps, and its restriction to undecorated maps is expected to be related to the medial construction.

Previous attempts to identify φ have suffered from the fact that the existing derivations of the functional relationship involve inherently non-combinatorial steps, but the techniques used to analyze η suggest the possibility of a new derivation of the relationship that may be more suitable to combinatorial analysis. An examination of automorphisms that must be induced by φ gives evidence for a refinement of the functional relationship, and this leads to a more combinatorially refined conjecture. The refined conjecture is then reformulated algebraically so that its predictions can be tested numerically.

Acknowledgements

This Thesis could not have been produced without input and support from many people. I am extremely grateful to the Department of Combinatorics and Optimization for providing a fertile working environment. I would particularly like to thank my supervisors, David Jackson, for introducing me to the subject of map enumeration, and Ian Goulden, for helping me to understand bureaucracy. Courses taught by David Wagner, Bruce Richter, and Jim Geelen gave me the tools I needed to study combinatorics. Thanks are also owed to my colleagues, who had the patience to listen as I tried to refine my presentation of the subject.

If my department gave me the tools I needed to succeed, then it was my friends and family who provided me with raw materials. A special thanks is reserved for my parents: to my father, who taught me to love mathematics, and to my mother, who was always available to offer late-night editorial assistance, thank you for raising me to be the person I am today. It would be unjust to proceed without additionally singling out the rôle played by Aaron Williams, who convinced me to apply to graduate school in the first place. The lessons he taught me, on the importance of recreation and the power of perseverance, gave me the grounding I needed to undertake a project of this magnitude.

Lastly, none of this would have been possible without the support of my loving wife, Kathleen, who always offered me a second opinion when I found myself unable to opine a first. Her tolerance was immeasurable, and I only hope that I will eventually be able to repay it in kind. With tools and raw materials in hand, I obtained my vision from Kathleen.

Michael LaCroix

Michael Andrew La Croix
Friday, August 14, 2009

Table of Contents

List of Tables

List of Figures

Chapter 1

Introduction

This Thesis is an examination of two conjectures related to the enumeration of rooted maps: the b-Conjecture, and the q-Conjecture. Informally, a rooted map is a pointed 2-cell embedding of a topological graph in a compact 2-manifold without boundary, and each map is classified as either orientable or non-orientable according to the orientability of its underlying manifold. Equivalence of maps is defined up to homeomorphism, and the resulting equivalence classes also admit a combinatorial characterization that is closely related to the symmetric group in the case of orientable maps, and to the hyperoctahedral group in the case of locally orientable maps. As a consequence, the study of maps can be used as a tool to study these groups, and has applications in such diverse fields as algebraic geometry, physics, and symmetric functions.

Emphasis is placed on the b-Conjecture of Goulden and Jackson, first introduced in [GJ96a]. It predicts the existence of a topological invariant of hypermaps that measures departure from orientability with respect to which an appropriately refined generating series has a particular expression in terms of Jack symmetric functions. The main result of the Thesis, Theorem 4.16, establishes a concrete relationship between the combinatorics of rooted maps and a parameter of Jack symmetric functions. In the process, the theorem resolves a special case of the b-Conjecture that Goulden, Harer, and Jackson predicted in [GHJ01] could be used to establish properties of a conjectured space that interpolates between two moduli spaces of pointed algebraic curves. Structural properties of the algebraic presentation of the relevant generating series suggest that the invariants used to prove this specialization are also the invariants predicted by Goulden and Jackson in the most general form of the b-Conjecture, though no proof of this stronger claim is known at present.

Of secondary emphasis, the q-Conjecture of Jackson and Visentin, first introduced in [JV90a], calls for a natural bijection to explain a functional relationship between two generating series appearing in the study of two models of 2-dimensional quantum gravity. Though both involve generating series for rooted maps, the two conjectures appear to be structurally unrelated, but the analy-

sis of the former introduces tools that are used in Chapter 7 first to suggest a refinement of the latter, and then to provide an analytic formulation that has survived numerical testing.

1.1 Structure of the Thesis

After a brief review of relevant properties of surfaces, Chapter 2 gives a precise definition of rooted maps. It then proceeds to familiarize the Reader with the correspondence between various topological and combinatorial representations. A combinatorialization of topological maps is outlined in Section 2.3, and underpins the development of the subject: maps are defined topologically, and both the invariant predicted by the b-Conjecture, and the bijection predicted by the q-Conjecture are expected to have natural topological descriptions, but the enumerative results on which the conjectures are based have combinatorial derivations. The Chapter concludes with a description of an operation, in Section 2.4, of root-edge deletion that is subtly different from operations used previously to study the b-Conjecture. This new operation gives a framework for a recursive definition of the invariants used to analyze the b-Conjecture in Chapter 4, and later, in Chapter 7, the operation acts as the basis for an attack on the q-Conjecture.

The b-Conjecture was formulated by Goulden and Jackson in an attempt to explain algebraic similarities between two generating series: the generating series for orientable hypermaps, obtained by Jackson and Visentin in [JV90a] in terms of Schur functions, and the analogous generating series for all hypermaps, both orientable and non-orientable, obtained by Goulden and Jackson in [GJ96b] in terms of zonal polynomials. Both series have a common algebraic generalization, the hypermap series, $H(\mathbf{x}, \mathbf{y}, \mathbf{z}; b)$, expressed in terms of Jack symmetric functions. The b-Conjecture predicts that this generalized series is a generating series for hypermaps with respect to an unidentified invariant called a b-invariant. Chapter 3 begins with a review of symmetric functions, and proceeds by precisely describing the algebraic form of the b-Conjecture. After surveying several relaxations of the Conjecture, some with independent combinatorial derivations, the Chapter concludes by summarizing elementary properties of b-invariants. This culminates with Theorem 3.35, a proof of the non-existence of any b-invariant that is both additive, in a sense made precise in Conjecture 3.32, and invariant under duality.

Chapter 4 introduces a family of candidate b-invariants, similar in form to an invariant previously described by Brown and Jackson in [BJ07]. Analysis of the new invariants uses root-edge deletion as described in Section 2.4. By introducing a refined generating series that tracks the degree of the root face of a map separately from the degrees of other faces, the Chapter establishes the main result of the Thesis, Theorem 4.16, that the generating series for rooted maps with respect to any invariant that satisfies Definition 4.1 is a specialization of $H(\mathbf{x}, \mathbf{y}, \mathbf{z}; b)$. The series are identified by verifying that both the combinatorially

and algebraically defined series satisfy the same partial differential equation, (4.2), with a unique solution. The analysis used to prove Theorem 4.16 is tight, and cannot directly be applied to the most general version of the b-Conjecture, but structural and numerical evidence presented in Chapter 5 and Chapter 6 further suggest that these invariants are the ones required by the full b-Conjecture.

Chapter 5 uses combinatorial properties of the invariants defined in Chapter 4 to predict algebraic properties of the hypermap series. Algebraically, the b-Conjecture states that a family of triply indexed coefficients of the hypermap series, $\{c_{\nu,\varphi,\epsilon}(b)\}$, known *a priori* to be rational functions in $\mathbb{Q}(b)$, are in fact polynomials in $\mathbb{Z}_+[b]$. Extrapolation from Theorem 4.22 predicts that these rational functions satisfy functional equations that depend on their indices. A subsequent verification of this prediction by algebraic methods, Theorem 5.18, provides evidence that the invariants can be used to resolve a more general form of the conjecture. A secondary implication is that Corollary 5.22 imposes a degree bound and permits efficient computation of the low order terms of H.

Chapter 6 outlines a programme for verifying that a particular function is a b-invariant. The main tool is that the generating series for maps with respect to any b-invariant must possess properties imposed on H by its algebraic presentation. A consequence of Corollary 5.22 is that the existence of a b-invariant implies a bijective correspondence between certain restricted classes of rooted maps that are defined in terms of the invariant. The major portion of the Chapter details the search for natural descriptions of these induced bijections relative to some of the invariants satisfying Definition 4.1. Partial success, in the form of Theorems 6.11 and 6.22, supports the claim that the invariants satisfy the general form of the b-Conjecture.

Chapter 7 offers evidence that the approach to the b-Conjecture can be applied more generally. The Chapter shifts focus to the q-Conjecture, which posits the existence of a natural bijection between suitably decorated rooted orientable maps and rooted orientable 4-regular maps as an explanation for a functional equation relating two generating series. Tools developed for the proof of Theorem 4.16 are used first to refine the conjecture by predicting structural properties of the bijection in Conjecture 7.15, and then to formulate an analytic condition that is both necessary and sufficient to guarantee the existence of a bijection with this additional structure. Numerical testing using the analytic characterization provides additional evidence for the refinement. The Chapter concludes by describing possible restricted actions of the conjectured bijection that are suggested by the refinement.

Chapter 8 concludes the Thesis with a summary of topics for future research.

Chapter 2

Background and Definitions

This Chapter defines objects used in this enumerative study of rooted maps; that is, topologically pointed embeddings of graphs in surfaces. Its aim is to present enough topology to provide a foundation for the combinatorics used in later chapters, though it is intended as a survey. Beginning with a review of surfaces, the Chapter develops the concepts required to describe an equivalence relation on rooted maps. A brief survey of maps, from a topological perspective, emphasizes the need for a combinatorial description of the equivalence classes of this relation; one such combinatorialization, generalizing to hypermaps, is given. Several representations of maps are discussed, and their equivalence is used to give a precise definition to a new root-edge deletion operation.

2.1 Surfaces

This section collects classical facts about surfaces, with an emphasis on those needed to represent maps. A more robust treatment, emphasizing graph embeddings, is presented by Gross and Tucker in [GT01].

Definition 2.1 (surface, orientable surface, non-orientable surface, locally orientable surface)**.** *A Surface is a compact connected 2-manifold without boundary. It is* non-orientable *if any subset is homeomorphic to a Möbius strip, otherwise it is* orientable*. A neighbourhood of every point is homeomorphic to an open disc, and collectively, all surfaces are* locally orientable*.*

Since all surfaces are locally orientable, the adjective is not strictly necessary, but non-orientability is a somewhat exotic concept. In particular, orientable surfaces can be embedded in three-dimensional Euclidean space, but non-orientable surfaces can be embedded in Euclidean spaces only of dimension at least 4. For this reason, it is convenient to have a term for emphasizing the departure from the familiar, especially when orientable examples are used to illustrate general concepts.

4
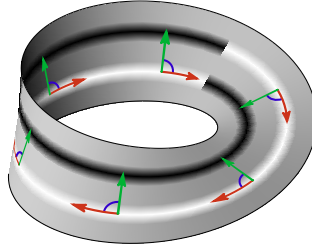
Figure 2.1: A Möbius strip embedded in Euclidean 3-space.

Example 2.2. *Every orientable surface is homeomorphic to a sphere or an n-handled torus. A complete set, O, of orientable surfaces up to homeomorphism is given by*

Remark 2.3. A Möbius strip can be embedded in Euclidean 3-space. Figure 2.1 shows one such embedding. Without opposite sides of the strip identified, the model would be an orientable double-cover of a Möbius strip. Similar embeddings are not possible for non-orientable manifolds without boundary.

Beginning with a surface, Σ, a *cross-cap* or *handle* is added to Σ by removing the interior of a closed disc and stitching the boundary of a Möbius strip or punctured torus, respectively, along the boundary of the resulting hole. Since a Möbius strip can be contracted across its width, adding a cross-cap is homeomorphically equivalent to identifying antipodal points on the boundary of the excised disc: see Figure 2.2. Adding a handle is homeomorphically equivalent to identifying opposite sides of an excised square: see Figure 2.3. More generally, removing an open disc from each of two surfaces, and then identifying the boundaries of the resulting holes produces the *connected sum* of the two surfaces.

By a classical result (attributed by Gross and Tucker, [GT01, p. 95] to Rado), every abstract surface can be triangulated. The Euler characteristic of a surface is then defined in terms of such a triangulation.

Definition 2.4 (Euler characteristic). *For a surface, Σ, homeomorphic to the combinatorial surface defined by the simplicial complex K, the* Euler characteristic *of Σ is*

$$\chi(\Sigma) = f_0 - f_1 + f_2,$$

where f_i denotes the number of simplices of dimension i in K.

Theorem 2.5 (Classification Theorem, Möbius and others). *Surfaces, up to homeomorphism, are characterized by Euler characteristic and orientability. Every orientable surface is homeomorphic to a sphere with $n \geq 0$ handles, and every non-orientable surface is homeomorphic to a sphere with $n \geq 1$ cross-caps.*
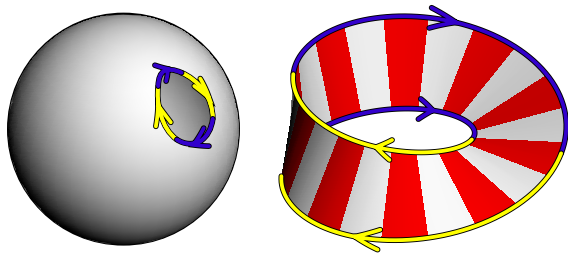
Figure 2.2: Adding a cross-cap to a sphere produces a projective plane.
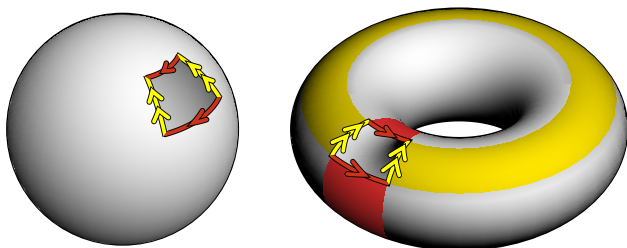
Figure 2.3: Adding a handle to a sphere produces a torus.

Remark 2.6. Thomassen gives a an accessible proof of the Classification Theorem in [Tho92].

Remark 2.7. The Euler characteristic of the sphere with n handles and i cross-caps is $2 - 2n - i$. In particular, if i is at least 1, then a sphere with $2n + i$ cross-caps is homeomorphic to a sphere with n handles and i cross-caps.

Definition 2.8 (genus)**.** *For an orientable or non-orientable surface, Σ, the* genus *of Σ is the maximum number of non-intersecting simple closed curves along which Σ can be cut without becoming disconnected.*

A non-orientable surface with Euler characteristic χ has genus $g = 2 - \chi$, while an orientable surface with Euler characteristic χ has genus $\frac{1}{2}(2 - \chi)$. The parameter $g = 2 - \chi$ plays a prominent rôle in the enumerative theory of locally orientable maps as developed in Chapters 3, 4, 5, and 6; when considering locally orientable surfaces, this parameter will be referred to as *genus*, even when the surface is orientable. Where the distinction is significant, it may be emphasized by referring to the parameter as *Euler genus*. Using this terminology, genus is additive with respect to connected sums.

Example 2.9. *As locally orientable surfaces, both the torus and the Klein bottle have genus 2.*

Remark 2.10. For a Riemannian manifold, Σ, the Euler characteristic $\chi(\Sigma)$ has an additional interpretation given by the Gauß-Bonnet theorem, which states
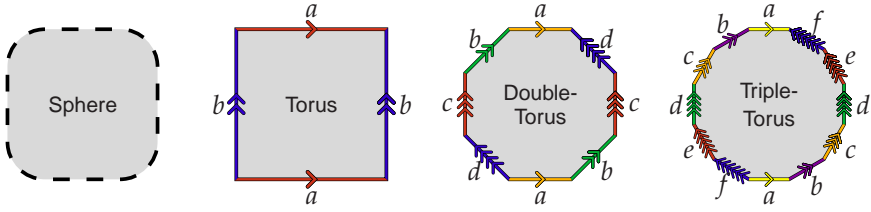
Figure 2.4: Polygonal representations of orientable surfaces
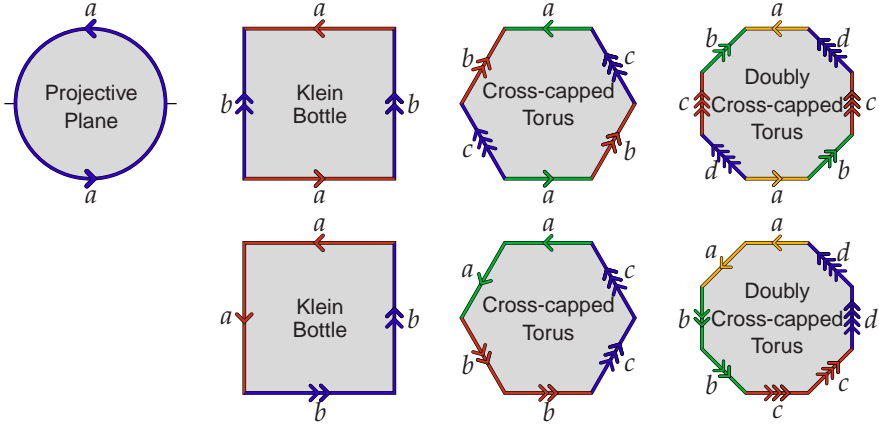
Figure 2.5: Polygonal representations of non-orientable surfaces

that

$$\chi(\Sigma) = \frac{1}{2\pi} \int_{\Sigma} \kappa \, \mathrm{d}A,$$

where κ is Gaußian curvature, and $\mathrm{d}A$ is the area measure. As a notable consequence, average Gaußian curvature is positive for the sphere and projective plane, zero for the torus and Klein bottle, and negative for all other surfaces. This property is used in Section 2.2.5 in a discussion of tiling.

A polygon with an even number of sides, together with a labelling specifying how to identify pairs of sides, describes a surface *via* the identification topology. Identifying opposite sides of a polygon with $4n$ or $4n + 2$ sides, in an orientation preserving way, produces an n-handled torus. Figures 2.6 and 2.7, on page 8, show how a torus is obtained from a square and hexagon by identification. Polygonal representations of orientable surfaces as polygons with $4n$ sides are shown in Figure 2.4. Figure 2.5 shows identifications that produce the sphere with n cross-caps from a polygon with $2n$ sides. Though homeomorphically equivalent, the two representations of the Klein bottle appear to be distinguished by an invariant of rooted maps introduced in Chapter 4.
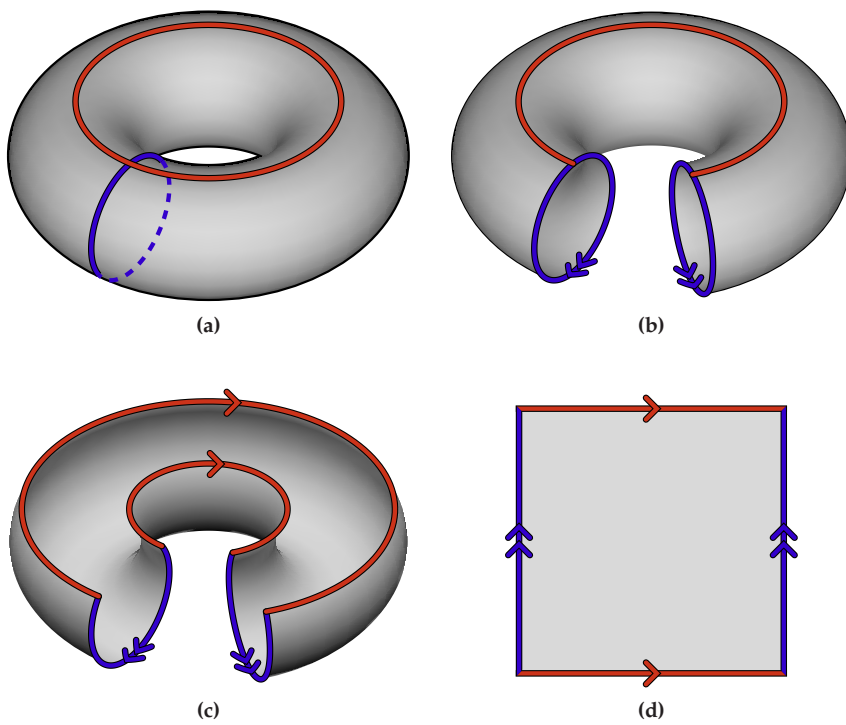
Figure 2.6: Cutting a torus along the two curves shown in (a) leaves a square. The torus can be recovered by identifying opposite sides of the square as indicated in (d).
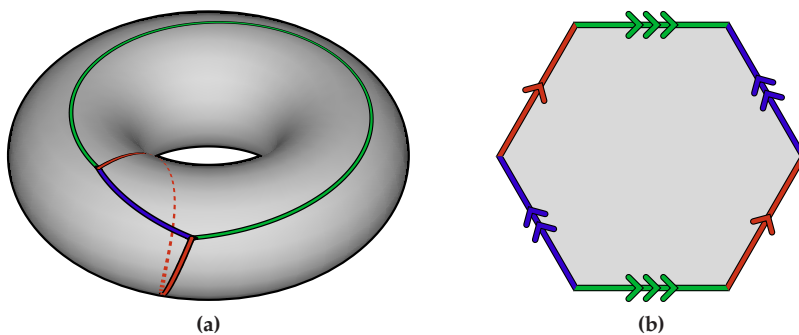
Figure 2.7: Cutting along the curves indicated in (a) leaves a hexagon, (b). Any two of these curves define a simple closed curve, with each pair determining a distinct homotopy class of non-contractible curves on the torus.

2.2   Graphs and Maps

This section provides a topological definition of maps. For enumerative purposes, it is sensible to define maps using the combinatorialization of Section 2.3, but the formalism has topological origins, and combinatorial conjectures introduced in Chapters 3 and 7 are expected to have topological explanations. The goal of this section is not to construct a rigorous foundation, but rather to provide a topological setting into which combinatorial conjectures can be lifted, for analysis and visualization.

2.2.1   Graphs

Graphs are introduced as an intermediate step in defining maps. As with surfaces, many notational choices are possible for graphs. Most objects are defined similarly in this section and in [GT01], but where Gross and Tucker emphasized nomenclature that avoids ambiguity between topological and graph theoretic terms, the present discussion reverts to usage more common in combinatorial graph theory. Several significant deviations from [GT01] are noted, and used with an aim of streamlining the subsequent enumerative theory.

Definition 2.11 (graph, vertex, edge, loop, link). *A* graph, G, *consists of a finite set,* $V = V_G$, *of* vertices *together with a finite set,* $E = E_G$, *of* edges*. Each edge,* $e \in E_G$, *is associated with a set of endpoints,* $V_G(e) \subseteq V_G$, *such that* $1 \le |V_G(e)| \le 2$. *An edge with one endpoint is a* loop, *while an edge with two endpoints is a* link. *Two distinct edges are* parallel *if they have the same endpoints. A graph is* simplicial *if it has no loops or parallel edges.*

A simplicial graph defines a simplicial 1-complex, and this topological interpretation has a natural extension to all graphs. In [HR84], Hoffman and Richter describe the following representation.

1. A graph, G, is a Hausdorff space with a non-empty finite subset of singletons, V, called vertices.
2. The connected components of $G \setminus V$ are a finite set of edges, E, such that, with cl(e) denoting the topological closure of e:
   (a) every edge is homeomorphic to $\mathbb{R}$, and
   (b) for any edge e, cl(e) $- e \subseteq V$ with $1 \le |\text{cl}(e) - e| \le 2$.

Note that the closure of an edge is either the one-point or two-point compactification of the line, and may be homeomorphic either to a circle or to a closed interval, depending on whether the edge is a loop or a link.

Remark 2.12. If the graph H is obtained from G by subdivision, then the two graphs define homeomorphic topological spaces.

Two graphs, G and H are *isomorphic* if there are bijections

$$f: V_G \to V_H \qquad \text{and} \qquad g: E_G \to E_H$$

such that $v \in V_G(e)$ if and only if $f(v) \in g(V_G(e))$. Such bijections can be found precisely when the topological representations of G and H are homeomorphic *via* a homeomorphism that bijectively maps the vertex set of one graph onto the vertex set of the other graph. It is typically unnecessary to distinguish between combinatorial graphs and their topological representations. A graph is *connected* if its topological representation is connected.

For a vertex $v \in V_G$, the *degree* (Gross and Tucker [GT01] use *valence*), of v is

$$\deg(v) = \deg_G(v) := \left| \{ e \in E_G : v \in V_G(e) \} \right| + \left| \{ e \in E_G : v = V_G(e) \} \right|.$$

A classic result of Euler shows that

$$\sum_{v \in V_G} \deg(v) = 2|E_G|,$$

so in a graph with n edges, the degrees of the vertices of G form an integer partition, v, of $2n$. This is the *vertex degree partition* of G.

2.2.2 Maps

Definition 2.13 (embedding, face, cellular embedding). *An* embedding, $i: G \to \Sigma$ *of a graph, G, in a surface, Σ, is a continuous one-to-one function from the topological representation of the graph into the surface. The components of the complement of $i(G)$ are the* faces *of the embedding. If every face is homeomorphic to an open disc, then the embedding is a* cellular *embedding.*

Remark 2.14. It is possible to find a surface in which G has a cellular embedding precisely when G is connected. Note that the graph with a single vertex and no edges has a cellular embedding in the sphere.

Definition 2.15 (map, orientable map, non-orientable map). *A* map *is a cellular embedding of a graph in a surface. The map is* orientable *if the surface is orientable, otherwise it is* non-orientable. *All maps are* locally orientable.

Remark 2.16. An embedding, or by extension a map, is properly a function, but one that implicitly references a graph as its domain. By a slight abuse of notation, a vertex of the graph that is the domain of an embedding is referred to as a vertex of the embedding. Other properties of the underlying graph may also be considered to be inherited by the embedding when convenient.

Two maps, $i: G \to \Sigma_1$ and $j: H \to \Sigma_2$ are *equivalent* if there is a homeomorphism $h: \Sigma_1 \to \Sigma_2$ such that $h(i(G)) = j(H)$ and $h(i(V_G)) = j(V_H)$. If such a homeomorphism exists, then it follows that G and H are isomorphic graphs. This definition of equivalence coincides neither with the definition given by
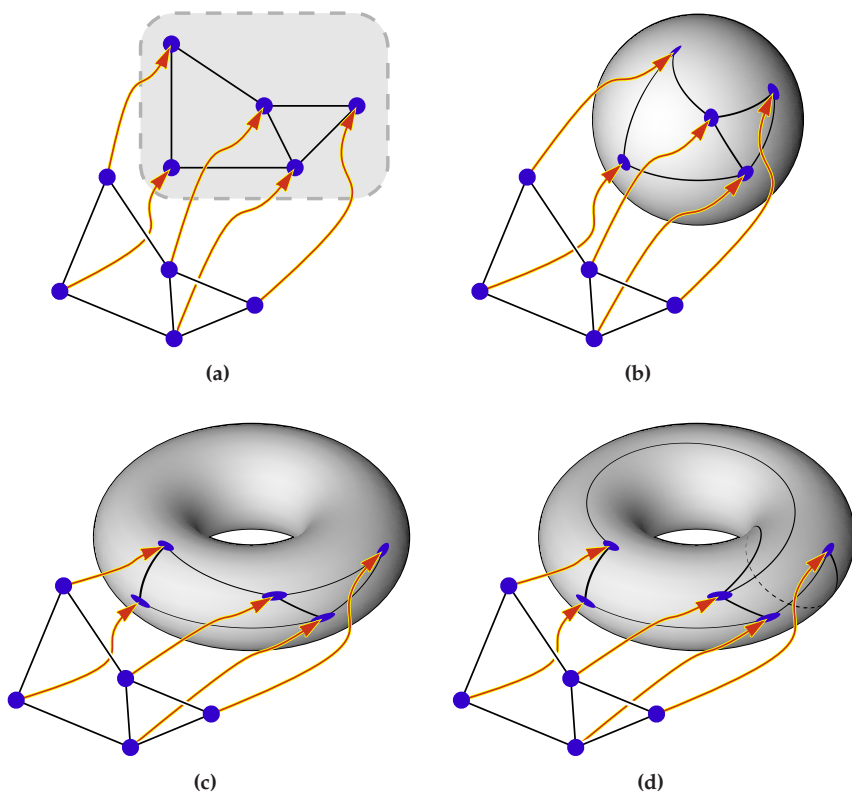
Figure 2.8: Four embeddings of a graph in orientable surfaces
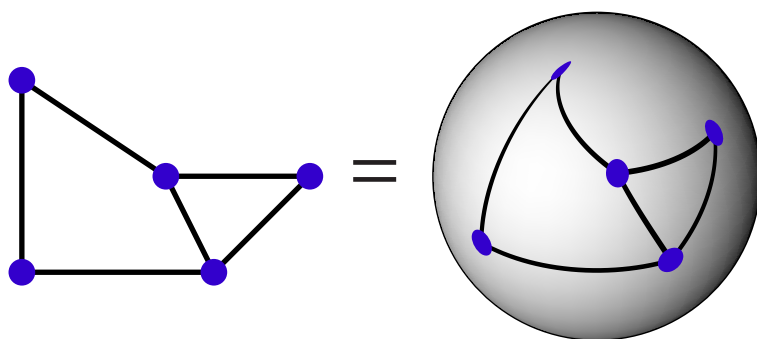
Figure 2.9: The maps in figures 2.8a and 2.8b are equivalent, since by convention, the plane represents its one-point compactification.
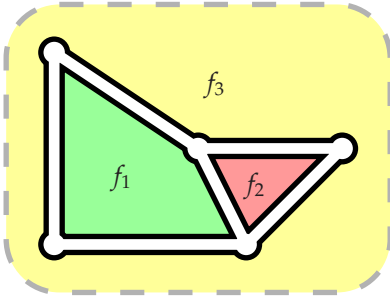
Figure 2.10: The faces of a map
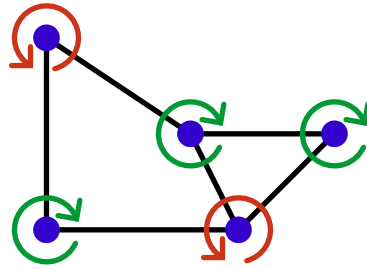
Figure 2.11: Vertex permutations

Gross and Tucker in [GT01] for equivalence, which requires in addition that $hi = j$, nor with their definition of weak equivalence, which requires only that $h(i(G)) = j(G)$. The subtle variations are not required in the present context, because the enumerative theory described in later chapters is primarily concerned with rooted maps, that is maps that are topologically pointed.

Example 2.17. *Figure 2.8 shows four embeddings of a graph. Figures 2.8a, 2.8b, and 2.8d all depict maps. The embedding in Figure 2.8c is not a map, since one of its faces is homeomorphic to a punctured torus. Using the convention that the plane represents its one point compactification, the embeddings in Figures 2.8a and 2.8b are equivalent maps. With the understanding that a graph is to be identified with its image under the embedding, the equivalence can be illustrated concisely, as in Figure 2.9.*

The *degree of a face* is the length of a closed walk passing once around its boundary. In a map with n edges, the degrees of the faces form an integer partition of $2n$. This partition, denoted by φ, is the *face degree partition* of the map. While the vertex degree partition of a map is inherited from the underlying graph, the face degree partition is determined by the embedding. The embedding also determines cyclic permutations on the half-edges incident with each vertex. Figure 2.11 illustrates one collection of vertex permutations. These permutations are unique up to order reversal. Homeomorphism preserves vertex permutations and face boundaries: see Figure 2.12.

Example 2.18. *Figure 2.10 shows the faces, f_1, f_2, and f_3, of the map in Figure 2.9. They have degrees 4, 3, and 5, so the map has face degree partition $\varphi = [3, 4, 5]$. Every embedding in Figure 2.8 has vertex degree partition $\nu = [2^3, 3^2]$.*

2.2.3 Ribbon Graphs, Flags, and Duality

When specifying a map, it is necessary to describe which cycles in the graph are orientation preserving in the embedding. This information is encoded in a neighbourhood of the image of the graph.
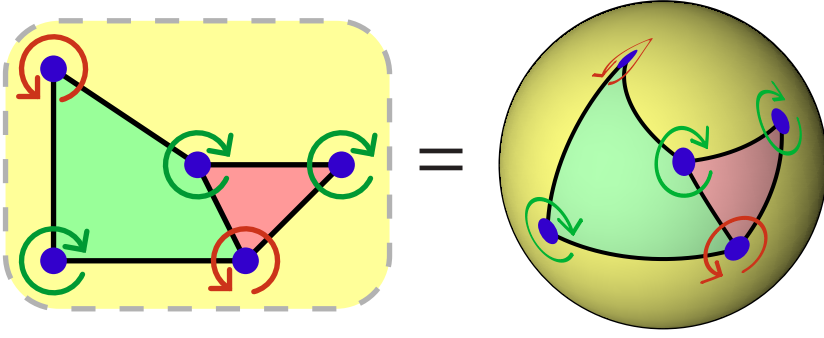
Figure 2.12: Faces and vertex permutations are invariant under homeomorphism.

Definition 2.19 (ribbon graph, ribbon). *Given a map $i\colon G \to \Sigma$, a ribbon graph representing i is a family $\mathcal{F}$ of closed discs satisfying the following properties.*

1. *The union of the discs is a closed neighbourhood of $i(G)$, and this neighbourhood has $i(G)$ as a retract in Σ.*
2. *There is a bijection $\Gamma\colon E_G \cup V_G \to \mathcal{F}$.*
3. *For every vertex $v \in V_G$, $i(v) \in \Gamma(v)$.*
4. *For every edge e in E_G, $\Gamma(e) \cap i(G)$ is connected and contained in $i(e)$.*
5. *If u and v are distinct vertices, then $\Gamma(u) \cap \Gamma(v) = \varnothing$.*
6. *If e and f are distinct edges, then $\Gamma(e) \cap \Gamma(f) = \varnothing$.*
7. *If e is an edge, and v is a vertex, then $\Gamma(e) \cap \Gamma(v)$ is:*
   (a) *empty if $v \notin V_G(e)$,*
   (b) *two disjoint Jordan arcs if $V_G(e) = \{v\}$, and*
   (c) *a Jordan arc if $V_G(e) = \{u, v\}$ for some $u \neq v$.*

For every edge e, the disc $\Gamma(e)$ is the ribbon *representing e.*

Remark 2.20. The existence of a ribbon graph representing a particular map is a nontrivial consequence of the topological definition, but is guaranteed by the existence of an open neighbourhood of each vertex with its boundary intersecting each incident edge precisely once, a fact proved by Hoffman and Richter in [HR84, Thm. 3.1].

Ribbon graphs correspond to the *reduced band decompositions* used by Gross and Tucker in [GT01, Sec. 3.2.1]. They are studied directly, without reference to the underlying graph embedding, by Bollobás and Riordan in [BR02], and get their name from the fact that they can be physically modelled in three-dimensional space by gluing flexible ribbons, representing edges, to rigid discs, representing vertices. Corresponding to this physical realization, it is sometimes convenient to draw open neighbourhoods of the discs, so that the intersections between discs can be emphasized.
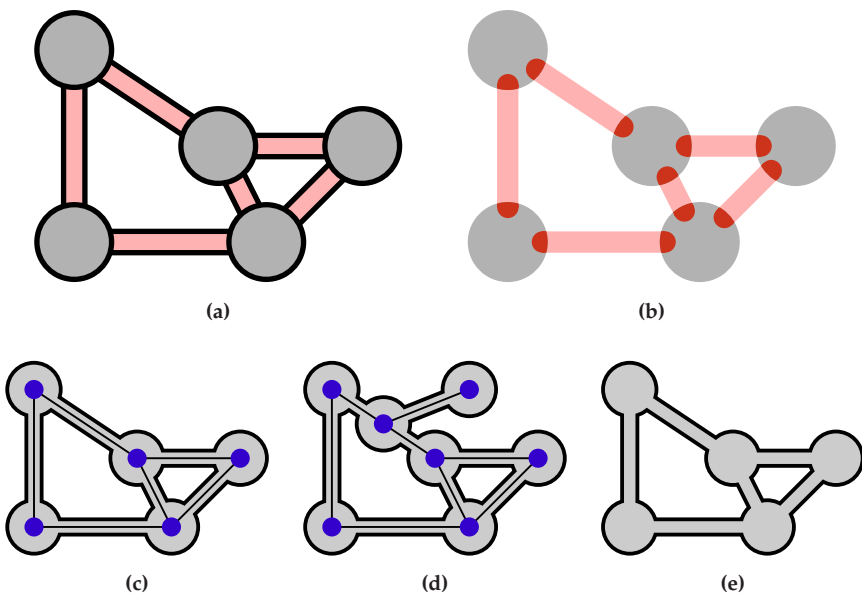
Figure 2.13: Ribbon graph representations of maps

Example 2.21. *The ribbon graph in Figure 2.13a represents the map from Figure 2.9. It is redrawn in Figure 2.13b using open discs to emphasize the intersections between discs representing vertices and discs representing edges.*

The equivalence class of a map is uniquely determined by any ribbon graph representing it. Specifying which elements of $\mathcal{F}$ correspond to vertices and which correspond to edges is unnecessary. Intersections between elements of $\mathcal{F}$ can be used to define an auxiliary bipartite graph with vertex set $\mathcal{F}$. The edges of the ribbon graph can be identified unambiguously with the class of degree two vertices in this auxiliary graph, unless both classes consist entirely of degree two vertices, in which case the map is a cycle and the two choices are equivalent.

Two maps that differ only by the addition of degree one vertices or by the subdivision of edges have homeomorphic neighbourhoods, so it is necessary to specify the decomposition $\mathcal{F}$ to describe a ribbon graph. In practice, visual cues can be used to distinguish vertices from edges, and it is often sufficient to draw only the neighbourhood.

Example 2.22. *Figures 2.13c and 2.13d give two maps with homeomorphic neighbourhoods. Figure 2.13e unambiguously represents the same map as Figure 2.13c, even though only the neighbourhood is shown; shape is used to distinguish the vertices from the edges, without specifying explicit boundaries.*

Definition 2.23 (flag). *With respect to an embedding, each edge has two sides and*

(a) Flags as quarter edges

(b) Flags as boundary points

(c) Flags as quarter edges

(d) Flags as boundary points
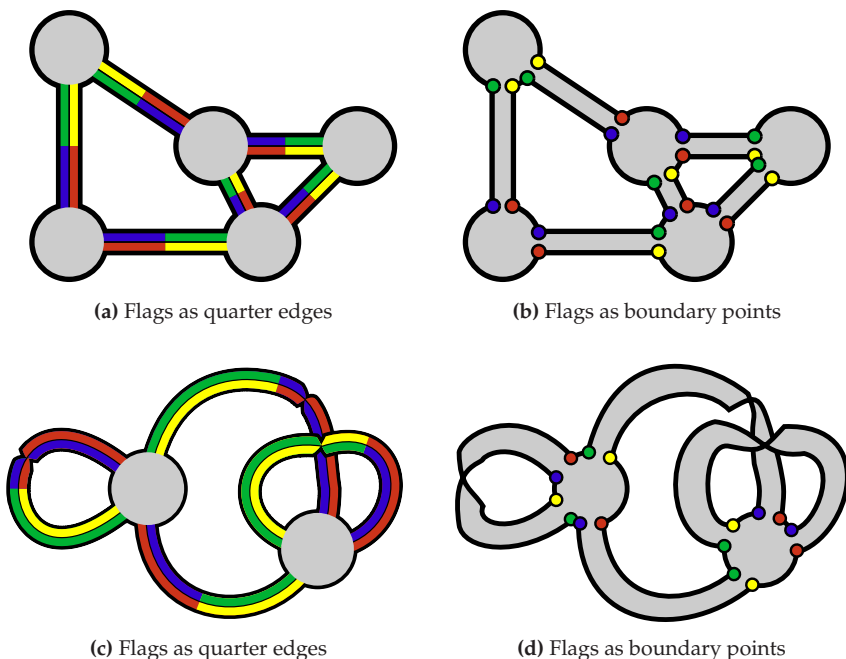
Figure 2.14: Drawing flags

two ends, giving a total of four side-end positions, referred to as flags.

The best way to interpret flags as topological objects depends on context. For combinatorial purposes, flags should be thought of as points on the boundary of the intersections between discs representing edges and discs representing vertices. This interpretation is used in Section 2.3 to describe a combinatorialization of the equivalence classes of topological maps. For visualization, however, it is sometimes convenient to depict flags as quarter edges. Most flags can be described uniquely by a triple (f, e, v), consisting of a face f, an edge on its boundary e, and a vertex v incident with e. This description is used in an informal introduction to the subject in [GR01, Sec. 17.10], but is ambiguous when e is a loop or incident with the same face on both sides: the map in Figure 2.13d, for example, has 32 flags but has only 30 distinct face-edge-vertex triples.

Example 2.24. *Figure 2.14 illustrates the flags of a map. In Figures 2.14a and 2.14c flags are shown as quarter ribbons, while in Figures 2.14b and 2.14d flags are shown as boundary points. The twisted ribbons used in Figures 2.14c and 2.14d are necessary because the map they show is non-orientable.*

Given a ribbon graph, $\mathcal{F}$, representing the map $i\colon G \to \Sigma$, every component of the boundary of the neighbourhood of $i(G)$ is a simple closed curve corresponding to a face of the map. The surface, Σ, can be recovered by stitching a closed

(a) A band decomposition

(b) The dual decomposition

(c) A map

(d) Its dual

(e) Poincaré duality
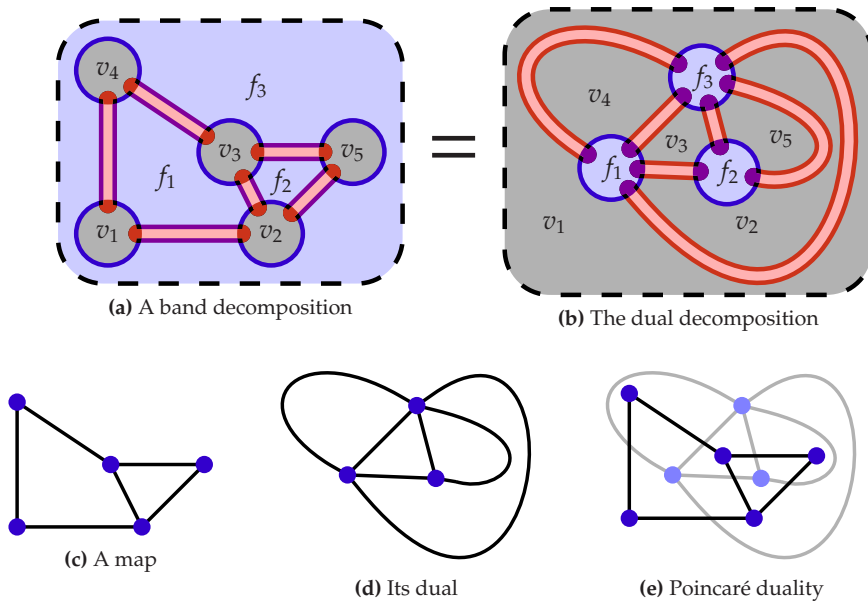
Figure 2.15: Band decompositions and their relationship to duality

disc along each boundary component. Augmenting $\mathcal{F}$ by adding these face discs, and specifying which elements of $\mathcal{F}$ correspond to vertices, edges, and faces, gives a *band decomposition* of the surface, as described in [GT01, Sec. 3.2.1], where Gross and Tucker use 0-band, 1-band, and 2-band to describe the three classes of discs. Interchanging the rôles of vertices and faces in a band decomposition gives the *dual* band decomposition, and implicitly defines a *dual* map. In the context of duality, the original map is referred to as the *primal* map.

This form of duality is an involution, and is sometimes referred to as Poincaré duality. It preserves orientability, and interchanges vertex and face degree partitions, but primal and dual maps share an edge degree partition. See [GT01, Sec. 1.4.8] for a direct construction of dual maps that does not involve band decompositions. If $i\colon G \to \Sigma$ is a map, and $i^*\colon G^* \to \Sigma$ is its dual, then the only intersections between $i(G)$ and $i^*(G^*)$ are transverse intersections between edges and their duals. There is a natural bijection between the flags of a map and the flags of its dual.

Example 2.25. *Figures 2.15a and 2.15b show the open disc drawings of two band decompositions that correspond to the same family of discs; shape is used to distinguish between vertices and faces. The decompositions are dual to each other and represent the maps in Figures 2.15c and 2.15d. The drawing in Figure 2.15e shows that the two maps are Poincaré duals of each other. Additional examples of duality are given in Figures 3.5, 3.8, and 3.7.*

2.2.4 Rooted Maps

Rooted maps are introduced as an enumeratively tractable variant of maps. A general technique for enumerating topological objects, is to:

1. label constituent parts of the objects (in the case of maps, edges or flags are convenient constituent parts),

2. give a combinatorial description to labelled objects,

3. enumerate the labelled objects, and

4. account for multiplicative factors introduced by equivalent labellings.

For maps, the final step presents an obstacle, since a map may have a non-trivial automorphism group. The following definition is prompted by noting that the automorphism group of a map acts by permuting flags.

Definition 2.26 (rooted map, root, root edge, root vertex, root face)**.** *A root of a map is a distinguished orbit of flags under the action of the automorphism group of the map. A* rooted map *is a map, together with a root. For a rooted map with at least one edge, the root may be distinguished by marking one flag in the orbit. The edge containing this flag is the* root edge *of the map. The point representing the flag is contained in the boundary of a single vertex and a single face, referred to as the* root vertex *and* root face*.*

Remark 2.27. This differs from the standard definition of a rooted map. In common usage (see [JV90a], [GJ96b], [GJ96a], [Bro00], [GHJ01], or [RW95], for example), a rooted map is a map together with a distinguished flag, with equivalence up to homeomorphisms that send the root flag of one map onto the root flag of the other. The two definitions are equivalent except when considering the map with no edges, which cannot be rooted under the standard definition. The subtle difference simplifies the analysis in Chapter 4.

Remark 2.28. The unique map with no edges and one vertex has a root but does not have a root edge. Its face and vertex are the root face and root vertex of the map.

Without drawing a ribbon graph, a root can be indicated schematically. This requires an implicit local sense of clockwise that can be inherited from the drawing. Except where otherwise noted, an arrow pointing at the side of an edge indicates the orbit containing the flag immediately *counterclockwise* from the arrow; an arrow contained in a face and pointing at a vertex, indicates the orbit containing the flag immediately *clockwise* of the arrow. Using these conventions, it may be necessary to reflect a drawing of a map in order to indicate a particular root. The two forms of root indication will be used interchangeably, with suitability often depending on whether it is most convenient to emphasize root vertices, root edges, or root faces. The first form is more conventional, but the second can be used to draw the rooted map with no edges.

(a) An orbit

(b) A single flag

(c) The side of an edge

(d) A vertex-face incidence
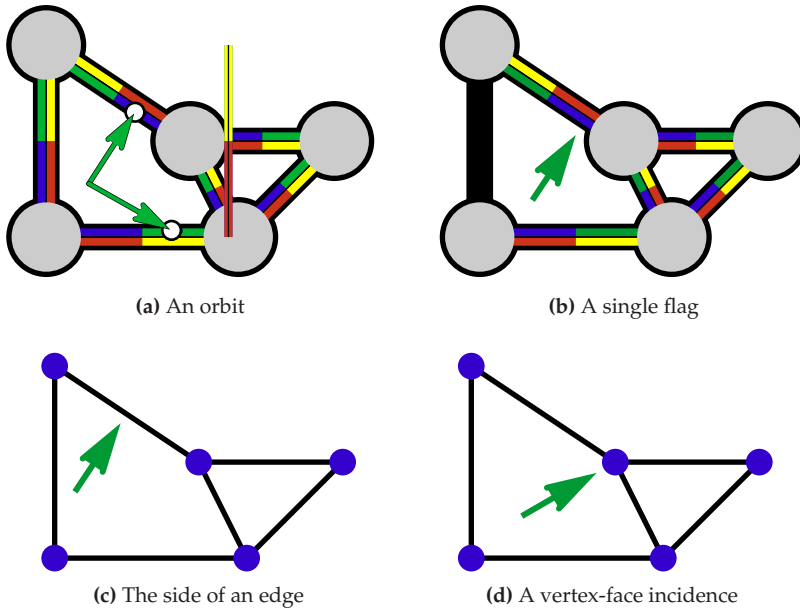
Figure 2.16: Four ways to mark the root of a map

Example 2.29. *Figure 2.16 illustrates four ways of marking the root of a map. In (a), all of the flags in an orbit are decorated. The same orbit is marked in (b) by an arrow pointing at a single flag. Figures (a) and (b) represent the same rooted map when reflected, while Figures (c) and (d) do not.*

In practice, the generality lost by working with rooted maps instead of maps is often negligible in enumerative applications. Many exact enumerative results about rooted maps can be applied asymptotically to unrooted maps. A result of Richmond and Wormald, [RW95], shows that asymptotically almost all maps have only trivial symmetries, so a typical map with n edges can be rooted in $4n$ inequivalent ways.

2.2.5 Diagrammatic Conventions

An essential tool for investigating maps is a visual shorthand for drawing them. It is convenient to have a variety of ways to represent a particular map. This Section describes several conventions and emphasizes the advantages and disadvantages of each. Table 2.1 summarizes the analysis. Figures 2.17 and 2.18 illustrate the representations for two particular maps.
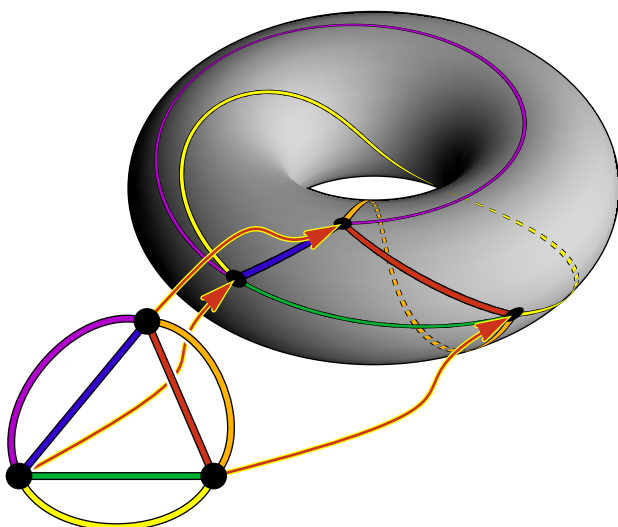
(a) An embedding in three-dimensional Euclidean space
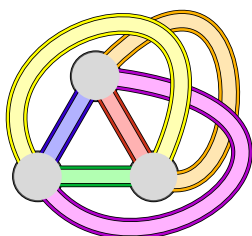
(b) A ribbon graph
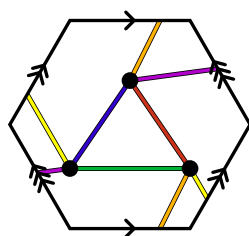
(c) A polygon
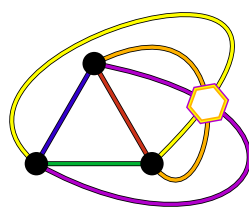
(d) A handle

Figure 2.17: Four representations of a map on the torus
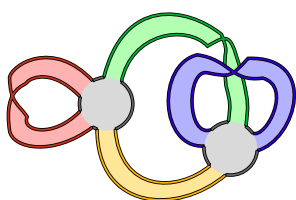
(a) A ribbon graph
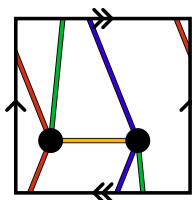
(b) A polygon
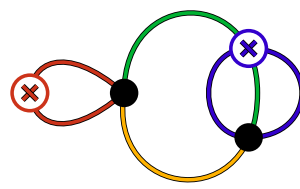
(c) Two cross-caps

Figure 2.18: Three representations of a map on the Klein Bottle

Table 2.1: A comparison of map representation techniques

Representation	Concrete	Faces	Surface	Cellular	Incidence
Physical Embedding	✔	✗	✔	✗	✔
Ribbon Graph	✔	✗	✗	✔	✔
Polygonal Surface	✗	✔/✗	✔	✗	✗
Tiled	✗	✔	✔	✔	✔/✗
Handles & Cross-caps	✗	✔/✗	✔	✗	✔

Physical Embeddings

Drawing a map by embedding its surface in three-dimensional Euclidean space provides a sense of concreteness, but physical intuitions are not always consistent with the topological formalism: see, in particular, Section 2.2.6 for a discussion of non-isotopic homeomorphisms. Figure 2.17a shows a map on the torus, using dashed lines to indicate occluded portions of edges. In this representation, the surface and vertex-edge incidence are recognizable, but part of the surface is occluded and it is difficult to verify that the embedding is cellular or to trace face boundaries. The extra dimension required for non-orientable surfaces makes physical embeddings practical only for orientable surfaces. Section C.3 of Appendix C includes a PostScript program for drawing straight-line embeddings of maps on the torus.

Ribbon Graphs

A ribbon graph can be used to provide a concrete realization of any map. Since every ribbon graph represents a cellular embedding, the representation is particularly suited to recursive decompositions of maps, and is used in Section 2.4 in the description of root-edge deletion. Ribbon graphs are also used in Section 2.3 to show the flags used in describing a combinatorialization of maps. Figures 2.17b and 2.18a show ribbon graph representations of two maps. It is difficult to recognize the surface or to trace face boundaries of ribbon graphs, and ribbon graphs are not well suited to hand drawing.

Polygonal Representations of Surfaces

Every surface can be represented as a polygon with opposite sides identified, as in Figures 2.4 and 2.5. Figures 2.17c and 2.18b illustrate maps using this representation. The surface is easily recognized, but the vertex-edge incidence of the underlying graph is obscured, and it is difficult to verify that the embedding is cellular. In the polygonal representation, faces can be coloured, as in Figures 2.20a and 2.21a, but it is not easy to trace face boundaries. Jackson and Visentin used polygon representations in [JV01] to catalogue maps.
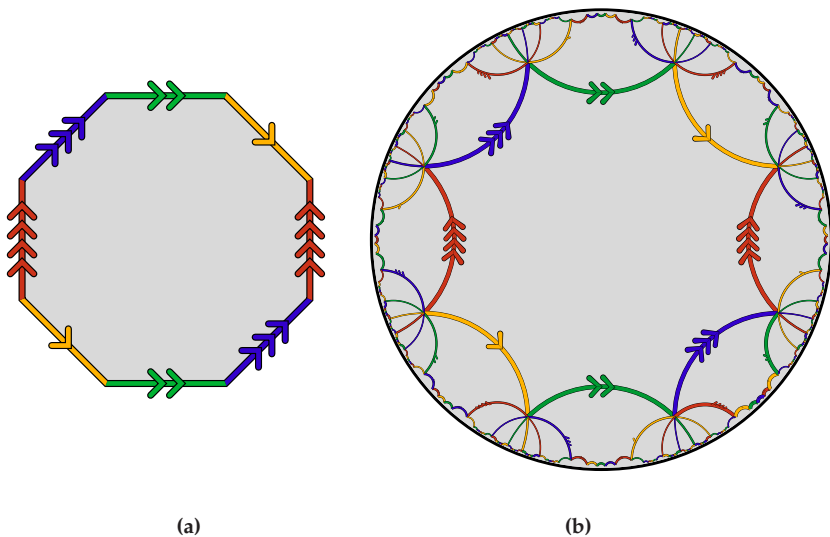
Figure 2.19: An octagon, (a), is used to tile the hyperbolic plane, (b).

Tiled Polygonal Representations

At the cost of additional space, the polygonal representation of a surface can be tiled to represent a map in the universal covering space of its surface. Face boundaries can be recognized easily in a tiled map, and this property of tilings was used in investigating the q-Conjecture (discussed in Chapter 7). The universal covering space of both the torus and Klein bottle is the plane, and partial tilings of the plane in Figures 2.20c and 2.21c reveal the faces of the maps from Figures 2.17 and 2.18. Surfaces with Euler genus greater than two have negative average Gaußian curvature (recall Remark 2.10), so polygonal representations of these surfaces can be used to tile only hyperbolic space.

Remark 2.30. Euler genus occurs in Theorem 4.22 and (5.8) as a bound on the degree of b-polynomials (from Definition 3.7). Given this rôle of genus in the enumerative theory of maps, and the relationship between genus and curvature, it is an intriguing possibility that the combinatorial property of maps underlying the b-Conjecture might be describable in terms of a metric property of their tiled representations.

Example 2.31. *The Poincaré disc model represents hyperbolic space as the interior of a disc with boundary circle C. Line segments in this model are arcs of circles that intersect C orthogonally, and the axioms of incidence are as in Euclidean geometry. Figure 2.19 gives a tiling of hyperbolic space by an octagon. Using the same tiling, a polygonal representation of the map in Figure 2.22a is tiled to give Figure 2.22c. Figure 2.22a shows that the map has vertex degree partition $v = [6^2, 8]$, and Figure 2.22c shows that the map has face degree partition $\varphi = [3, 4^3, 5]$.*
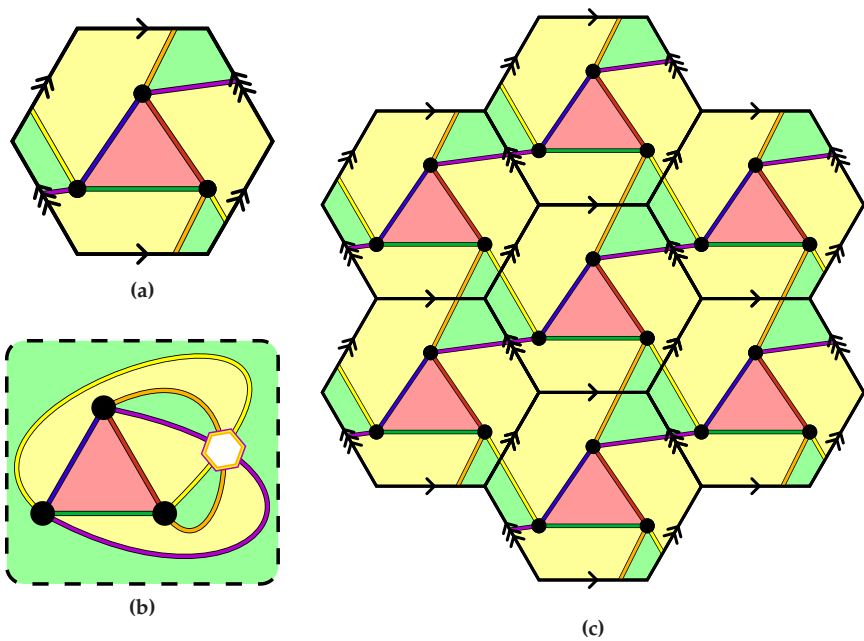
Figure 2.20: Colouring faces of a map on the torus
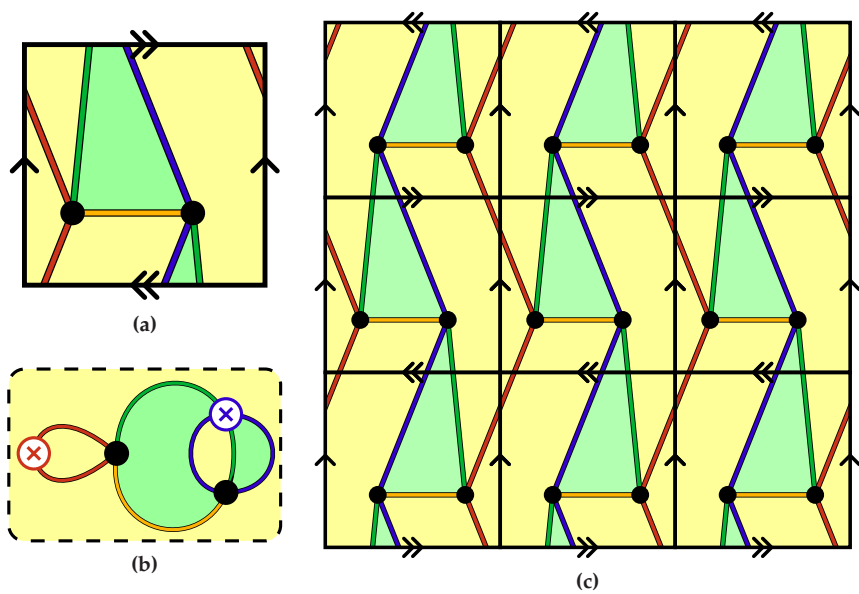
Figure 2.21: Colouring faces of a map on the Klein bottle
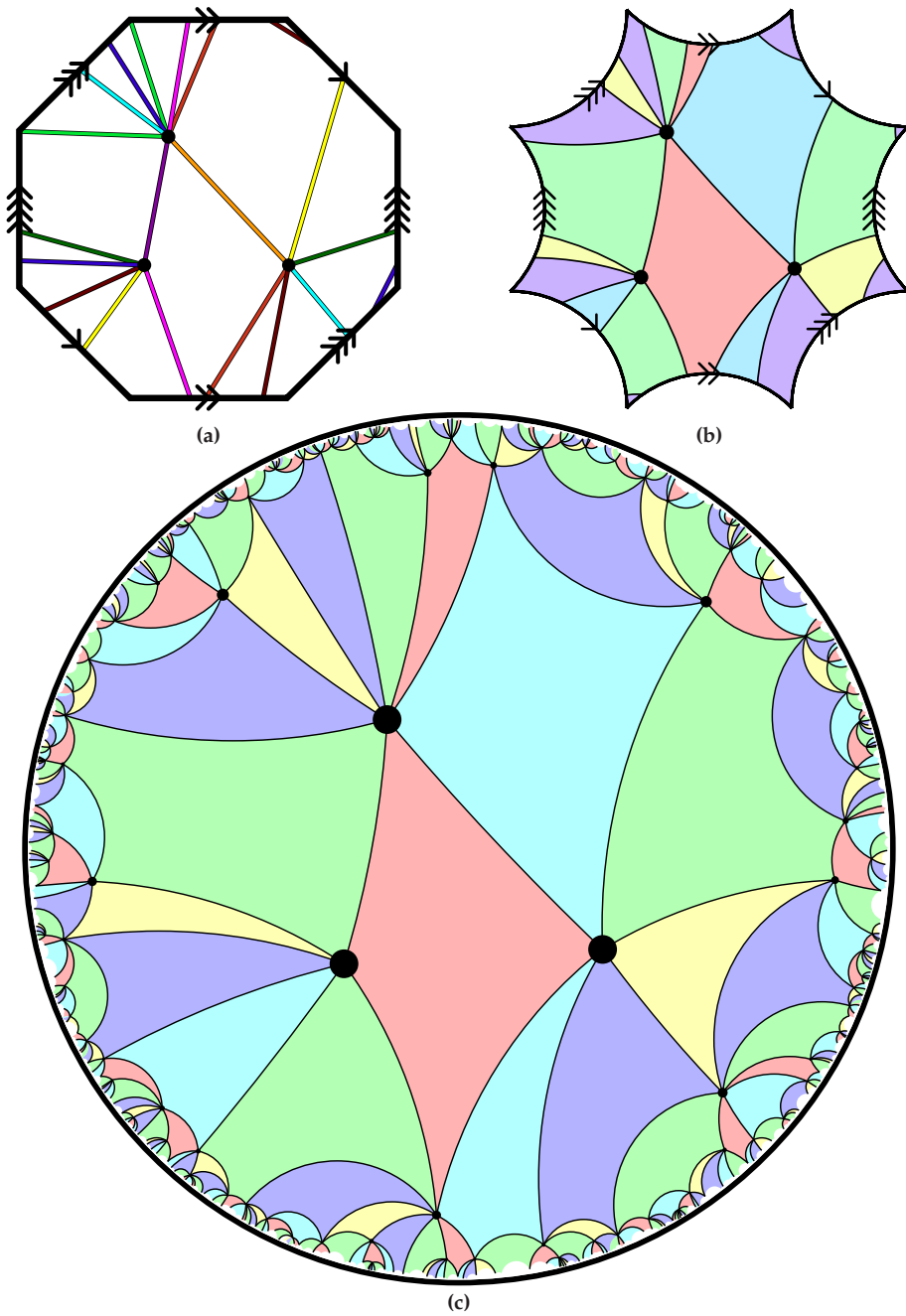
Figure 2.22: A polygonal representation of a map on the double-torus, (a), is used to tile the Poincaré hyperbolic disc, (c), where faces are coloured. A single tile is given in (b).

Remark 2.32. Sections C.2 and C.4 of Appendix C include PostScript programs for drawing tiled maps on the torus and double-torus.

Localized Handles and Cross-caps

Most of the figures in later chapters are drawn schematically, with icons representing localized handles and cross-caps. The icons, given in Figure 2.23, represent discs excised from the plane. Identifying opposite points on the boundaries of cross-caps, or opposite sides of the boundaries of handles, corresponds to the surgeries used to add cross-caps and handles to a surface (recall Figures 2.3 and 2.2). This representation is used in Figures 2.17d and 2.18c, and like the ribbon graph representation, it emphasizes the incidence structure of the underlying graphs. As with the polygonal representation, faces can be coloured, but tracing face boundaries and verifying that a drawing represents a cellular embedding is non-trivial: see Figures 2.20b and 2.21b. Of all the representations discussed, this is the most suitable for hand drawing, and is particularly convenient for representing monopoles. It is also the natural representation for discussing connected sums of maps, as in Section 3.6.2.

Representations are not unique. For non-orientable surfaces of genus at least three, two cross-caps can be substituted for a handle: see Figures 2.24a and 2.24b. This flexibility is useful for finding visually simple drawings of maps, but makes verifying the equivalence of two maps somewhat difficult. The use of two different, though topologically equivalent, icons representing handles provides some flexibility when drawing orientable maps, and the preferred choice is often related to homotopy: compare Figures 2.24c and 2.24d.

(a) A cross-cap   **(b)** A handle   **(c)** Another handle
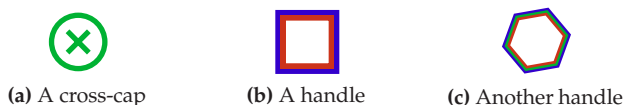
Figure 2.23: Icons for representing surfaces

(a)   **(b)**   **(c)**   **(d)**
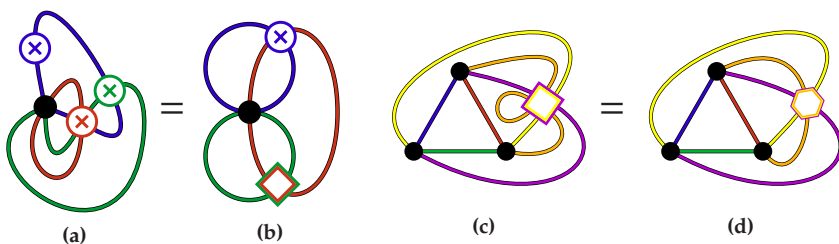
Figure 2.24: Equivalent maps drawn using localized handles and cross-caps

2.2.6 Equivalent Maps

Determining whether two maps are equivalent requires finding a particular homeomorphism, or verifying its nonexistence. Since the space of possible homeomorphisms is neither discrete nor finite, a naïve search of all candidate functions is not feasible. A combinatorial characterization of equivalence classes, described in Section 2.3, reduces the problem to an exhaustive search through a finite set of permutations. This Section uses the example of Dehn twists of the torus to illustrate the gap between intuition and topological formalism (in [LZ04, p. 30], Lando and Zvonkin refer to this gap by writing, "the seemingly harmless definition contains a trap"), and to show why such a combinatorialization is necessary.

The most visually recognizable homeomorphisms are reflections and isotopies. Recall that two embeddings, $i_0, i_1 \colon G \to \Sigma$ are *isotopic* if there is a continuous function $F \colon G \times [0,1] \to \Sigma$ such that $F(x,0) = f_0(x)$, $F(x,1) = f_1(x)$, and $F(\cdot, t) \colon G \to \Sigma$ is an embedding for every t. Experience with planar maps (on the sphere) suggests that every map equivalence can be verified using an isotopy of surfaces embedded in Euclidean space. But homeomorphism is defined in terms of intrinsic properties of a surface, and except for maps on the sphere and real projective plane, an isotopy view of homeomorphisms is not complete. For the torus, it is necessary, in addition to isotopies and reflection, to consider homeomorphisms involving Dehn twists. These homeomorphisms are obtained in 3-dimensional Euclidean space by first cutting the surface along a closed curve that does not bound a disc, and then re-identifying the boundaries after twisting the surface within the ambient space: see Figure 2.25.
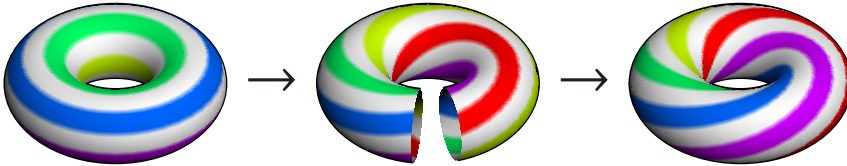
Figure 2.25: A Dehn twist of a torus embedded in three-dimensional space

Example 2.33. *Since the homotopy class of a curve is invariant under isotopy, the embeddings in Figures 2.26a and 2.26e are not isotopic. Tiled polygonal representations of these maps are given in Figures 2.26b and 2.26d. A Dehn twist, represented by a continuous deformation of the covering space of the torus, in Figure 2.26c, shows the equivalence of the two tiled representations.*

Remark 2.34. The isotopy classes of homeomorphisms of a surface have a group structure, defining the *mapping class group*, a discussion of which is beyond the scope of this Thesis, but it is worth noting that the mapping class group of an orientable surface is generated by a reflection together with Dehn twists, while the mapping class group of a non-orientable surface is generated by Dehn twists and *y*-homeomorphisms.
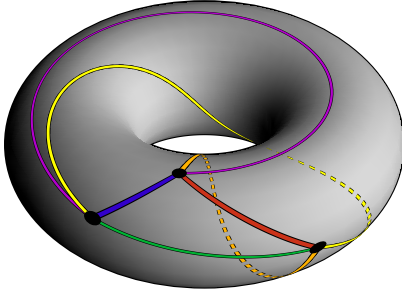
(a) A map on the torus
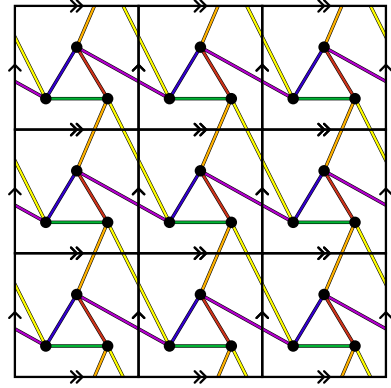
(b) The same map as a tiling
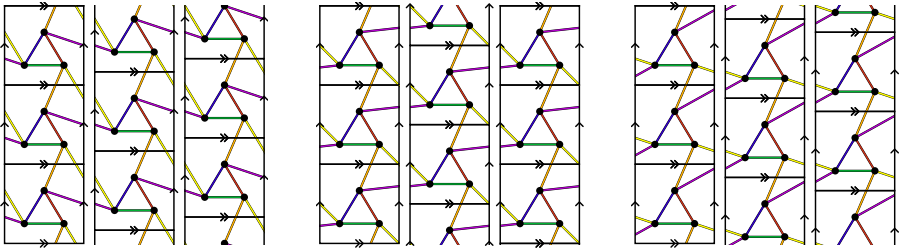
(c) A Dehn twist transforms (b) into (d) by deforming the covering space of the map.
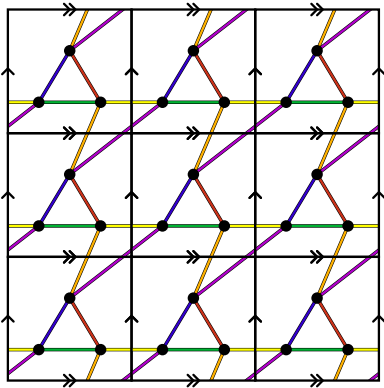
(d) A homeomorphic tiling
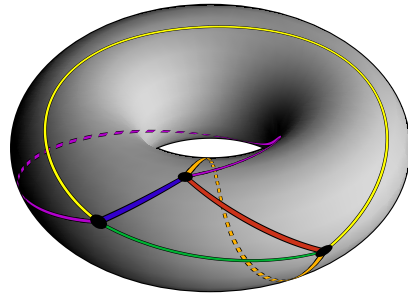
(e) Its physical embedding

Figure 2.26: The map in (a) is homeomorphic to the map in (e) *via* a Dehn twist. The homeomorphism is not an isotopy, but can be represented as a continuous deformation of the covering space of the map: see (b), (c), and (d).

2.3 A Combinatorialization

This section describes a combinatorialization that characterizes equivalence classes of a map in terms of the relationships between its flags in its ribbon graph representation. The combinatorial description resolves the problem of recognizing equivalent maps. It forms a foundation for the enumerative theory of rooted maps, and could have been used as a definition. Indeed, the problem motivating this Thesis, the Hypermap b-Conjecture (Conjecture 3.10), originated in [GJ96a] from purely combinatorial considerations. But the conjecture calls for a topological interpretation, and the partial resolution presented in Chapter 4 is best understood with respect to a topological underpinning.

Definition 2.35 (matching graph). *If $\mathcal{F}$ is a family of closed discs in the ribbon graph representation of a map with flag set F, then the union of the boundaries of the discs forms a topological graph with vertex set F. This is the* matching graph *of the map.*

If B_e is the union of the boundaries of edge ribbons, and B_v is the union of the boundaries of vertex ribbons, then the edges of the matching graph can be partitioned into three disjoint class given by

$$M_v = B_e \setminus B_v, \qquad M_e = B_v \setminus B_e, \qquad \text{and} \qquad M_f = (B_v \cap B_e) \setminus F.$$

By a slight abuse of notation, each of M_v, M_e, and M_f is identified with an edge set consisting of its connected components, so that each is a perfect matching on the set of flags. Each cycle of $M_v \cup M_f$ corresponds to the boundary of an edge ribbon, and has length four. The cycles of $M_e \cup M_f$ and $M_v \cup M_e$ correspond to the boundaries of vertices and faces, each cycle having length equal to twice the degree of the vertex or face it corresponds to. Figure 2.27 illustrates a matching graph. Each matching can be used to construct a fixed-point-free involution with cycles acting on the vertex set of the matching graph by transposing flags joined by an edge of the matching. Using this correspondence, the combinatorial properties of a matching graph are encapsulated by the following definition of a combinatorial map used by Tutte in [Tut84], but given in its present form in [GR01, Sec. 17.10].

Definition 2.36 (combinatorial map). *For a finite set of flags, F, the triple $\mathfrak{m} = (\tau_v, \tau_e, \tau_f)$ is a* combinatorial map *if:*

1. *τ_v, τ_e, and τ_f are fixed-point-free involutions acting on F,*
2. *$\tau_v \tau_f = \tau_f \tau_v$, and $\tau_v \tau_f$ is fixed-point free, and*
3. *the group generated by τ_v, τ_e, and τ_f acts transitively on F.*

Every combinatorial map can be used to construct a ribbon graph by translating the cycles of $\tau_e \tau_f$ and $\tau_v \tau_f$ into the boundaries of discs representing vertices and edges (the cycles of $\tau_v \tau_e$ correspond to face boundaries). With this interpretation, the definition of combinatorial maps can be deconstructed as

(a) A matching graph

(b) M_v

(c) M_e

(d) M_f

(e) $M_v \cup M_e$

(f) $M_v \cup M_f$

(g) $M_e \cup M_f$
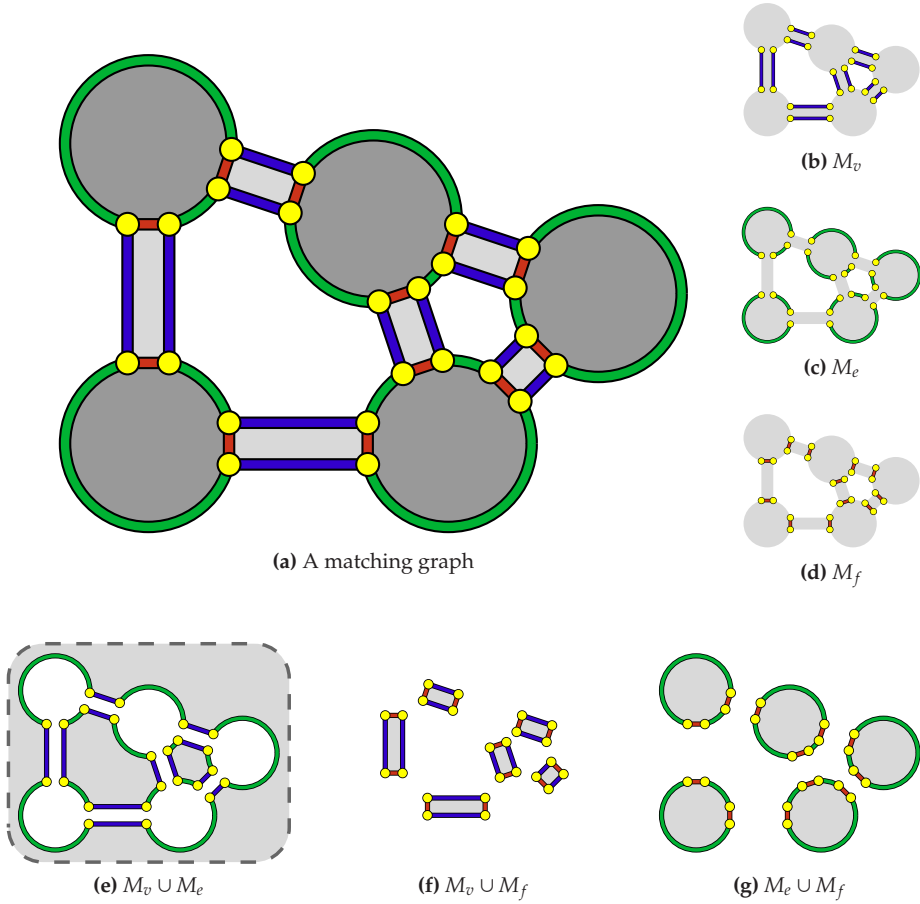
Figure 2.27: The boundaries of ribbons define a three-regular graph with the flags of the map as its vertex set, (a). The edges can be partitioned into three perfect matchings, (b), (c), and (d). The union of any two matchings determines a two-regular subgraph, the cycles of which are the boundaries of a class of bands, (e), (f), and (g).

follows: the first condition states that each of τ_v, τ_e, and τ_f corresponds to a perfect matching, the second condition forces edge boundaries to have length four, and the final condition forces the map to be connected. The symmetry between the conditions on τ_0 and τ_2 is a consequence of map duality, since if $\mathfrak{m} = (\tau_0, \tau_1, \tau_2)$ represents a map, then $\mathfrak{m}^* = (\tau_2, \tau_1, \tau_0)$ represents its dual.

Two combinatorial maps, $\mathfrak{m} = (\tau_v, \tau_e, \tau_f)$ with flag set F, and $\mathfrak{m}' = (\tau'_v, \tau'_e, \tau'_f)$ with flag set F', are equivalent if there is a bijection $\Gamma \colon F \to F'$ such that

$$\Gamma(\tau_v) = \tau'_v, \qquad \Gamma(\tau_e) = \tau'_e, \qquad \text{and} \qquad \Gamma(\tau_f) = \tau'_f.$$

Using this definition, there is a bijective correspondence between equivalence classes of combinatorial maps and equivalence classes of topological maps. The correspondence has been known in various forms since the nineteenth century: a brief history is provided by Gross and Tucker in [GT01, Sec. 3.2]. Hoffman and Richter verify a similar correspondence between topological and combinatorial maps in [HR84], albeit with respect to different definitions of maps. A proof of the correspondence involves more topological subtlety than the present discussion warrants, but the argument hinges on the correspondence between maps and ribbon graphs. It uses compactness of graphs and several applications of Schönflies Theorem, that any homeomorphism between Jordan curves on a sphere can be extended to a homeomorphism of the sphere, to show that:

1. every topological map can be represented as a ribbon graph,
2. every ribbon graph represents a map,
3. a homeomorphism between maps can be extended to a homeomorphism between ribbon graph representations,
4. a homeomorphism between two ribbon graphs can be used to construct a homeomorphism between the maps they represent, and
5. the correspondence between matching graphs and ribbon graphs is invariant under homeomorphism.

Using the correspondence, determining if two maps are equivalent amounts to determining whether they have isomorphic matching graphs with the same ordered partition of edge sets into three matchings.

Example 2.37. *Figure 2.28 illustrates the matching graph of the map from Figure 2.18 with explicitly labelled flags. With τ_v, τ_e, and τ_f determined by the matchings M_v, M_e, and M_f, the pairwise products are given by:*

$$\tau_v\tau_f = (1\ 3')(1'\ 3)(2\ 5')(2'\ 5)(4\ 8)(4'\ 8')(6\ 7')(6'\ 7)$$
$$\tau_f\tau_e = (1\ 4\ 3\ 2)(1'\ 2'\ 3'\ 4')(5\ 8\ 7\ 6)(5'\ 6'\ 7'\ 8')$$
$$\tau_v\tau_e = (1\ 4'\ 5')(1'\ 2\ 6'\ 6\ 8')(2'\ 8\ 3)(3'\ 4\ 7\ 7'\ 5).$$

The cycle type of $\tau_f\tau_e$ is $[4^4]$, and the cycle type of $\tau_v\tau_e$ is $[3^2, 5^2]$. These correspond to vertex degree partition $[4^2]$ and face degree partition $[3, 5]$.
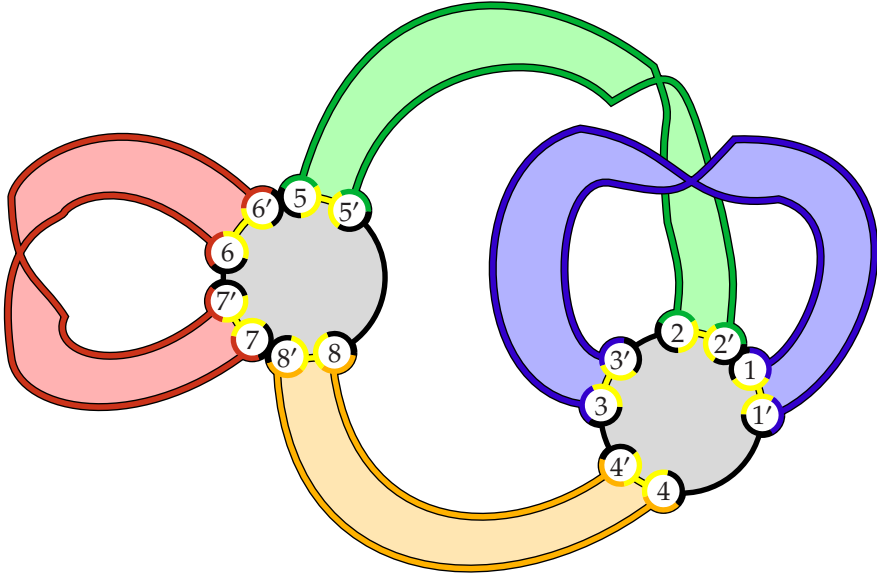
(a) With labelled flags, the matching graph can be written explicitly using three matchings.

$$M_v = \Big\{ \{1,3\}, \{1',3'\}, \{2,5\}, \{2',5'\}, \{4,8'\}, \{4',8\}, \{6,7\}, \{6',7'\} \Big\}$$

$$M_e = \Big\{ \{1,2'\}, \{1',4\}, \{2,3'\}, \{3,4'\}, \{5,6'\}, \{5',8\}, \{6,7'\}, \{7,8'\} \Big\}$$

$$M_f = \Big\{ \{1,1'\}, \{2,2'\}, \{3,3'\}, \{4,4'\}, \{5,5'\}, \{6,6'\}, \{7,7'\}, \{8,8'\} \Big\}$$
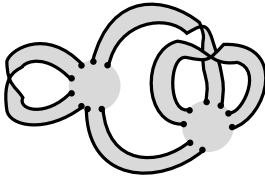
(b) M_v
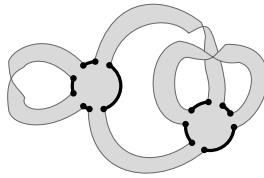
(c) M_e
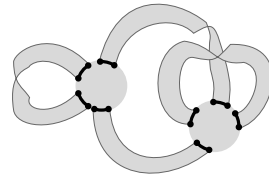
(d) M_f
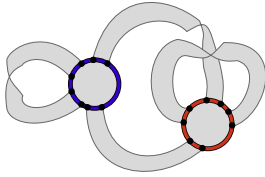
(e) $M_e \cup M_f$
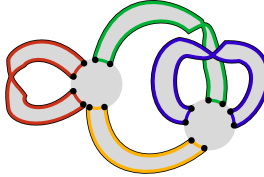
(f) $M_v \cup M_f$
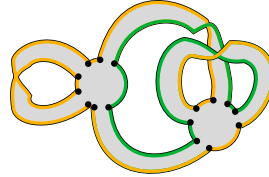
(g) $M_v \cup M_e$

Figure 2.28: The matching graph of the map in Figure 2.18

2.3.1 Specialization to Orientable Maps

The combinatorial encoding is simplified for orientable maps, which are characterized as maps with bipartite matching graphs. This bipartition defines two classes of flags, and the equivalence class of a rooted map can be recovered from the actions of $\tau_v \tau_e$, $\tau_v \tau_f$, and $\tau_e \tau_f$ on the class of flags containing the root flag. As in [Tut84], the equivalence class of an oriented combinatorial map, $\mathfrak{m} = (\tau_v, \tau_e, \tau_f)$, can be encoded by the pair (ϵ, ν) with ϵ and ν the restrictions of $\tau_v \tau_f$ and $\tau_f \tau_e$ to a single class of flags. This encoding is equivalent to the definition used by Lando and Zvonkin in [LZ04]. The permutation ϵ is a fixed-point-free involution, and if the map has n edges, then for the purpose of map equivalence, without loss of generality, after relabelling,

$$\epsilon = (1\ 1')(2\ 2')(3\ 3') \cdots (n\ n').$$

This choice implicitly labels and orients each edge of the map, so that the edge containing flags i and i' is labelled i and directed from i to i'. A pair (ϵ, ν) encodes a map if ϵ is a fixed-point-free involution, ν is a permutation acting on the same set, and ϵ and ν act transitively on this set.

To encode a rooted oriented map with n edges, label the edges bijectively with the elements of $\{1, 2, 3, \ldots, n\}$, and orient each edge arbitrarily, with the convention that the edge containing the root flag is labelled with 1 and directed away from the root flag. The flags of the root class can then be identified with the elements of $S = \{1, 2, \ldots, n\} \cup \{1', 2, \ldots, n'\}$, such that edge with label i is directed from flag i to flag i'. The permutation ν is given by clockwise circulations of flags around each vertex. Counterclockwise tours around the boundaries of faces can be recovered from the cycles of $\varphi = \epsilon \nu$, which is the restriction of $\tau_v \tau_e$ to the class of flags containing the root. Permuting the non-root edge labels, and reorienting the non-root edges, produces $2^{n-1}(n-1)!$ distinct permutations representations for a rooted oriented map with n edges. When encoding an unrooted map, there is no restriction on which edge is labelled 1, or the orientation assigned to this edge, but the labelling induces an implicit rooting, and the number of distinct representations depends on the size of the automorphism group of the map.

Example 2.38. *Figure 2.29 illustrates an encoding of the rooted map in Figure 2.16. First the edges are directed and labelled in Figure 2.29a using the convention that the root edge is labelled* 1 *and directed away from the root flag. The edge labels are associated with flags in Figure 2.29b. Reading clockwise cycles of flags at each vertex in Figure 2.29c gives the permutation ν. The permutation $\varphi = \epsilon \nu$ can be recovered by reading counterclockwise cycles of flags around each face boundary: note that the orientation of the infinite face appears reversed as an artifact of the planar representation of the sphere.*

Example 2.39. *Figure 2.30 illustrates an encoding of the map from Figure 2.17. The root was chosen arbitrarily. Since the map has two rootings, it is represented by $2 \cdot 2^5 5!$ distinct permutations.*
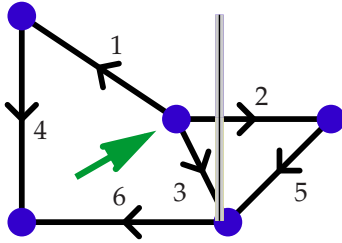
(a) A map is labelled.

(b) Labels are associated with flags.

$$\epsilon = (1\ 1')(2\ 2')(3\ 3')(4\ 4')(5\ 5')(6\ 6')$$
$$\nu = (1\ 2\ 3)(1'\ 4)(2'\ 5)(3'\ 5'\ 6)(4'\ 6')$$
$$\varphi = (1\ 4\ 6'\ 3')(1'\ 2\ 5\ 6\ 4')(2'\ 3\ 5')$$
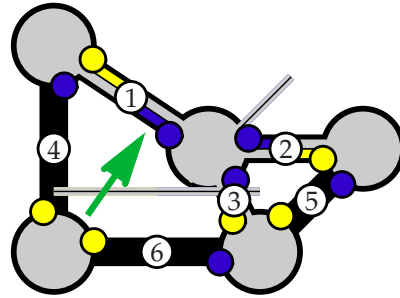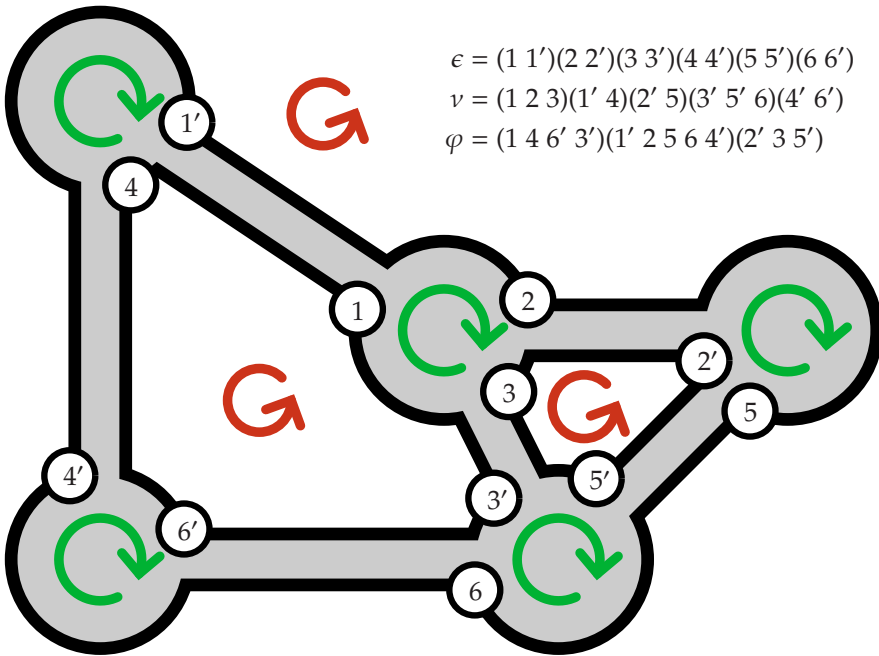
(c) Permutations ν and φ can be read from the map.

Figure 2.29: The map from Figure 2.16 is encoded as the pair of permutations (ϵ, ν).

$$\epsilon = (1\ 1')(2\ 2')(3\ 3')(4\ 4')(5\ 5')(6\ 6')$$
$$\nu = (1\ 2\ 5\ 4)(1'\ 6'\ 5'\ 3')(2'\ 3\ 4'\ 6)$$
$$\varphi = (1\ 6'\ 2'\ 5\ 3'\ 4')(1'\ 2\ 3)(4\ 6\ 5')$$
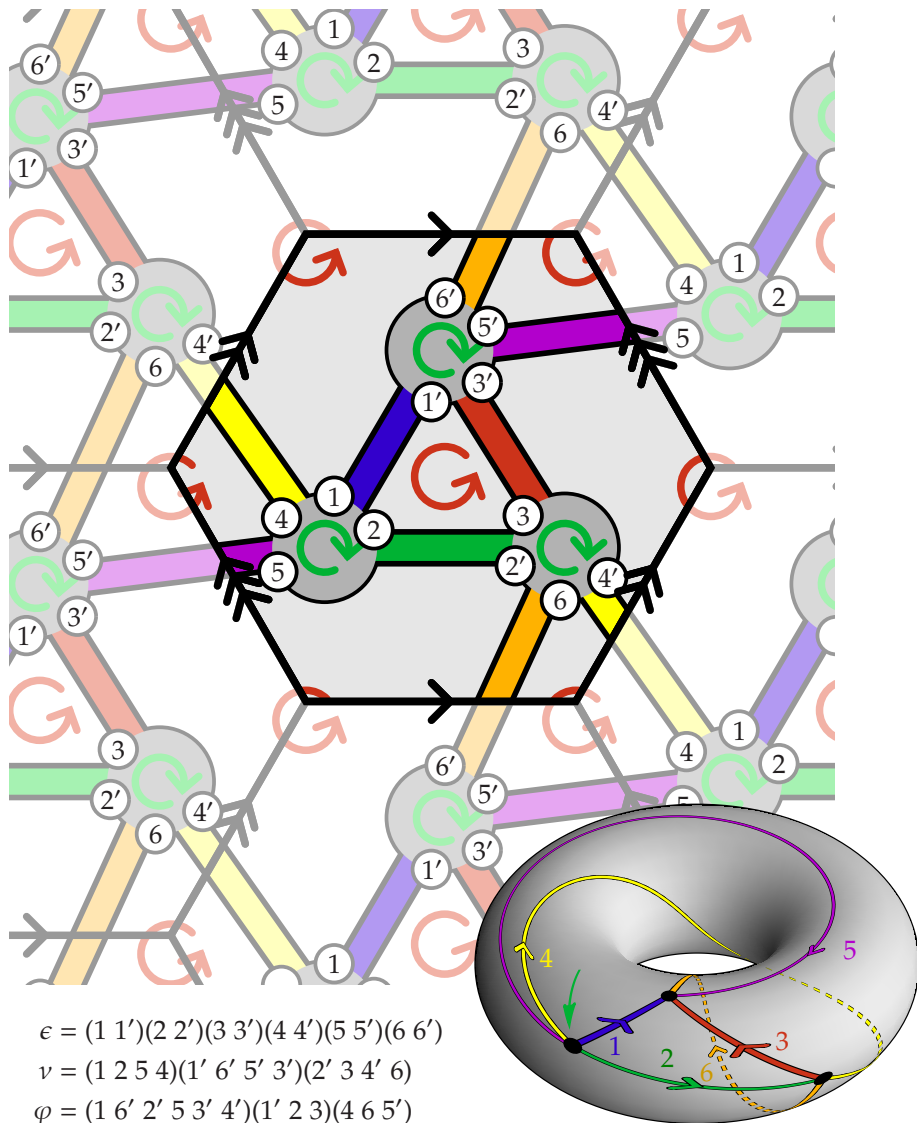
Figure 2.30: An edge-labelling of a map on the torus, and its permutation representation. The permutations are related through $\varphi = \epsilon\nu$.

2.3.2   Hypermaps

A more symmetric version of the enumerative theory of maps is obtained by considering the generalized objects obtained by dropping the second condition, the restrictions on $\tau_v \tau_f$, from Definition 2.36. The conditions on τ_v, τ_e, and τ_f become completely symmetric, and this symmetry generalizes duality. The resulting objects can be thought of as embeddings of hypergraphs in surfaces, and are called *hypermaps*. The following combinatorial definition is convenient for enumerative purposes.

Definition 2.40 (hypermap, hyperedge, hyperface). *A hypermap is a three-regular connected graph with an ordered partition, (M_v, M_e, M_f), of its edges into three perfect matchings. The cycles of $M_e \cup M_f$ are called* vertices, *the cycles of $M_v \cup M_f$ are called* hyperedges, *and the cycles of $M_v \cup M_e$ are called* hyperfaces. *Every cycle has even length, and the degree of a vertex, hyperedge, or hyperface is half the length of its corresponding cycle.*

Orientable hypermaps were introduced in terms of pairs of permutations (ϵ, ν) acting transitively on their ground sets. Using this presentation, Walsh, in [Wal75], exhibited a genus preserving bijection between orientable hypermaps and orientable two-coloured maps. Walsh's bijection extends to locally orientable maps, but in the present discussion it is more convenient to describe the dual correspondence relating hypermaps and face two-coloured maps.

Up to homeomorphism, a matching graph has a unique embedding, such that the face boundaries are the cycles of $M_e \cup M_f$, $M_v \cup M_f$, and $M_v \cup M_e$. Beginning with this embedding, contracting the faces bounded by cycles of $M_e \cup M_f$ leaves a map in the same surface, with M_v as its edge set and two classes of faces, one class corresponding to hyperfaces and the other class corresponding to hyperedges. The degree of each vertex of the hypermap is half its degree as a vertex of the map representation. To construct a matching graph from a face-two-coloured map, truncate each vertex, and partition the resulting edges appropriately. Note that the correspondence requires that the maps are face-coloured with distinguishable colours, otherwise it is not possible to distinguish between M_e and M_f in the reconstructed matching graph.

Example 2.41. *Figure 2.31 illustrates the relationship between the representations of a hypermap. A matching graph representation is given in (a). The vertices, hyperedges, and hypervertices are given in (b), (c), and (d). Contracting the vertices produces a representation of the hypermap as a face-two-coloured map (e). The face-two-coloured maps in (f) and (g) represent the same matching graph, but with different ordered partitions of the edges into perfect matchings.*

A hypermap in which every hyperedge has degree two shares a matching graph with a map. Using the face-two-coloured representation of such a hypermap, and deleting one edge from the boundary of each hyperedge, a process called *digon conflation*, produces the map with the same matching graph. Figure 2.32 illustrates this process.

(b) Vertices

(c) Hyperedges

(d) Hyperfaces

(a) A matching graph of a hypermap

(e)

(f)

(g)
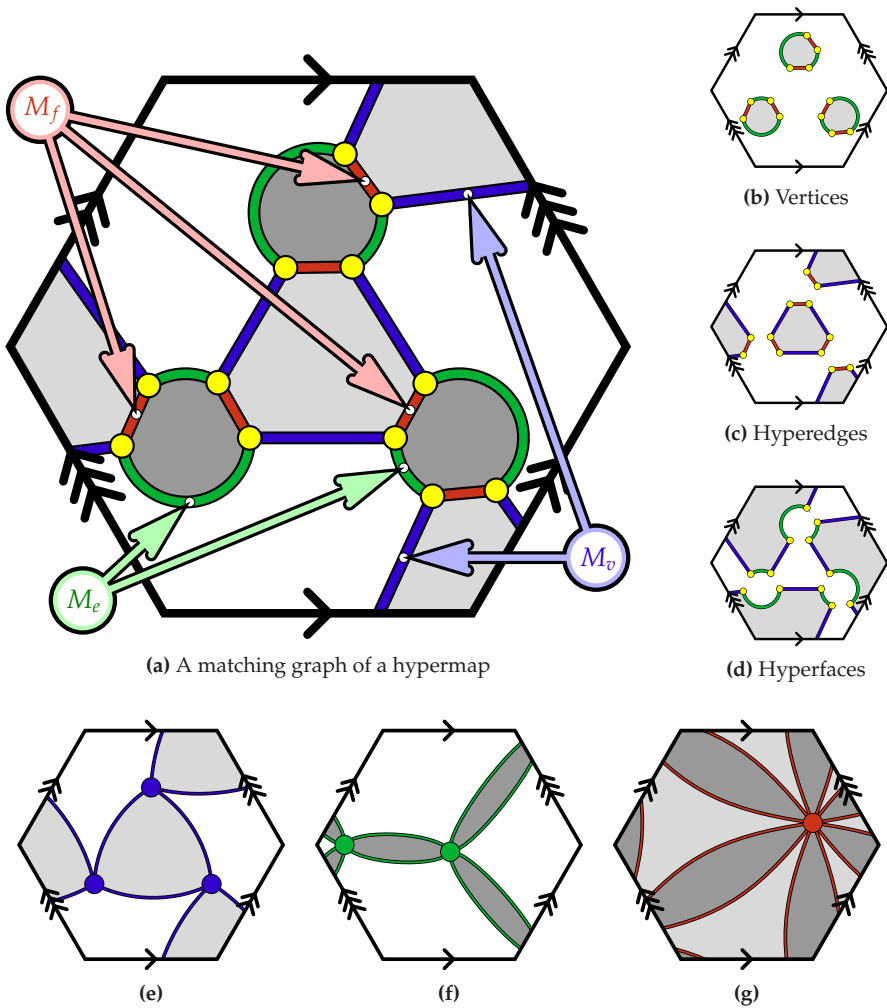
Figure 2.31: A hypermap with vertex degree partition $[2^3]$, hyperface degree partition $[6]$, and hyperedge degree partition $[3^2]$
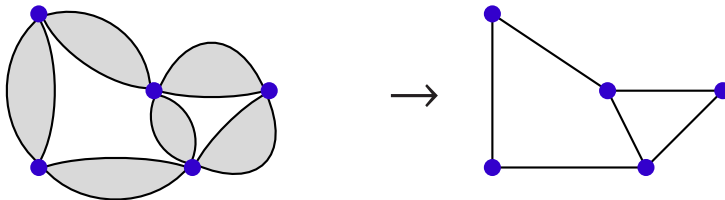
Figure 2.32: If every hyperedge has degree two, then *digon conflation* produces a map with the same matching graph.

2.4　Root-Edge Deletion

This Section describes a new operation of root-edge deletion. Its precise formulation, appealing to the equivalence of the representations of maps discussed in this Chapter, resolves some issues that make alternative definitions unsuitable for the analysis in Chapter 4, where the operation is used as the basis of a recursive decomposition of rooted maps.

Deleting an edge from a map produces a graph embedding with fewer edges than the original map. This embedding is cellular only if the deleted edge separated faces in the original map. Working in the ribbon graph model, deleting the disc associated with an edge leaves either one or two new ribbon graphs, depending on whether or not the deleted edge was a cut edge; in this model, each component can be interpreted as a map. Deletion preserves the incidence of non-deleted edges around each vertex and preserves the orientability of every cycle not containing the deleted edge.

For root-edge deletion to form the basis of a recursive analysis of maps, it is necessary to specify a canonical choice of which edge to delete, and how to root the resulting map or maps. The first choice is natural, since, in a map with at least one edge, the root flag is part of a distinguished root edge. Using the traditional convention of identifying a root with a side of an end of an edge, it is unclear how the resulting map or maps should be rooted. To resolve this dilemma, we use the convention of marking a root using an arrow contained in a face and pointing at a vertex (recall Figure 2.16d). If the root edge is not a cut edge, then after the root edge is deleted, this arrow continues to point from a face to a vertex and indicates a root of the new map: see Figure 2.33a. Deleting the root edge decreases the Euler genus by at most two.

If the root edge is a cut-edge, then it is necessary to additionally indicate the root of the second component, which can be accomplished by drawing a root arrow along the deleted edge, pointing at the second component: see Figure 2.33b. In this case, the Euler genus of the original map is the sum of the Euler genera of the resulting components, and the original map is non-orientable if and only if at least one of the resulting components is non-orientable.

(a) A typical edge　　　　(b) A cut edge
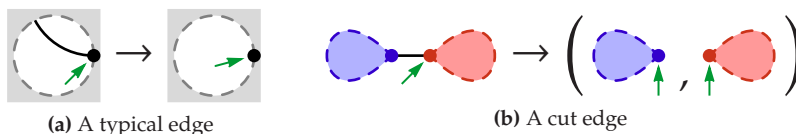
Figure 2.33: A schematic description of root-edge deletion

Example 2.42. *Figure 2.34 gives an example of root-edge deletion. The root edge of (a) is not a cut-edge. Deleting it produces the map in (b). The root edge of (b) is a cut-edge, and deleting it produces the ordered pair of rooted maps, given in (c).*
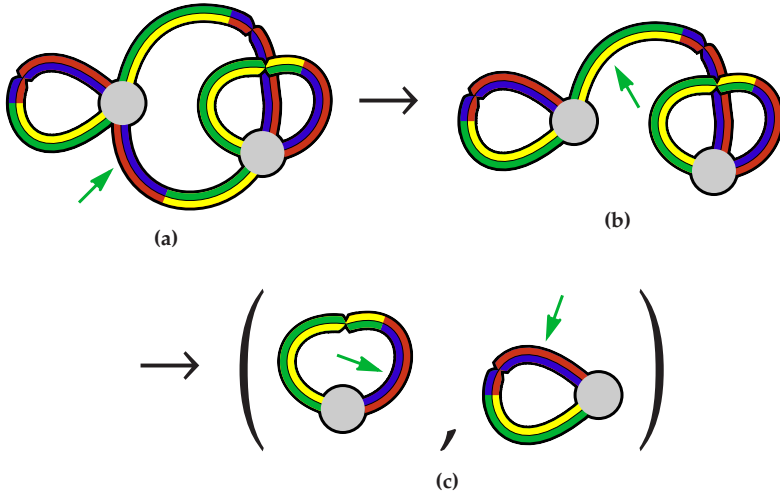
Figure 2.34: An example of root-edge deletion

2.5 Summary

This Chapter surveyed several equivalent topological and combinatorial representations of rooted maps. An emphasis on the topological characterization of maps provided a setting for defining a root-edge deletion operation in Section 2.4. This operation gives a topological interpretation to an essentially combinatorial invariant of rooted maps that is introduced in Chapter 4 to address the b-Conjecture described in Chapter 3. The combinatorial description of maps given in Section 2.3 forms the foundation of the enumerative theory of maps discussed in later chapters. It was used to define hypermaps, the combinatorial objects most naturally enumerated by the symmetric function techniques discussed in Section 3.5.1.

Chapter 3

The b-Conjecture

This Chapter introduces a conjecture of Goulden and Jackson, [GJ96a, Conj. 6.3], referred to throughout as the *Hypermap b-Conjecture*. The conjecture relates b, a shifted version of the Jack parameter from symmetric function theory, to an unidentified topological invariant of rooted hypermaps. Structural similarities between a generating series for rooted orientable hypermaps and an analogous generating series for rooted locally orientable hypermaps suggest a common generalization from which both series can be recovered by specialization. Despite a precise algebraic formulation, this generalized series lacks a combinatorial foundation: verifying that it specializes correctly requires a foreknowledge of the specialized series. The Hypermap b-Conjecture predicts that the generalizations can be explained in terms of a b-invariant, an invariant of rooted hypermaps that is non-negative integer valued and quantifies departure from orientability. A description of such an invariant might be used to derive a unified enumerative theory from which generating series for orientable and locally orientable rooted maps can be recovered by specialization.

The chapter reverses the historical development of the subject. After reviewing the required terminology from symmetric function theory, it proceeds by introducing the generalized series itself, before describing its origins. Several relaxations of the conjecture are also described. Then a brief survey of parallel enumerative techniques motivates the Hypermap b-Conjecture by exploring its origins and its applications. Emphasis is placed on reasons that the techniques do not extend to a general setting; this stresses the need for a new approach.

The conjecture originated with a comparison of series presented in terms of symmetric functions and derived from character theoretic analyses in [JV90a], [JV90b], and [GJ96b]. Jack symmetric functions assume a rôle in the generalized series that is played by Schur functions in the generating series for orientable maps, and by zonal polynomials in the generating series for locally orientable maps. A second enumerative technique presents generating series for maps in terms of integrals evaluated against Gaußian measures on appropriate spaces of matrices. This integral presentation is combinatorially less refined, but cor-

respondingly more computationally tractable, than the presentation involving symmetric functions. Jackson adapted the technique to enumerate orientable maps in [Jac94], and together with Goulden in [GJ97], extended it to locally orientable maps. With Harer, in [GHJ01], they used the corresponding generalized series as a starting point for computing a parametrized interpolation between the virtual Euler characteristics of two moduli spaces, and they explicitly conjectured a combinatorial foundation for this geometric setting. Chapter 4 resolves the resulting weaker conjecture. An integration formula for Jack symmetric functions links the two generalizations, and was proved by Okounkov in [Oko97] after being conjectured by Goulden and Jackson in [GJ96b]. Originating with the enumeration of rooted maps, the b-Conjecture is related to symmetric functions, characters, integration formulae, and algebraic geometry.

Superficially, a framework for generalizing the enumeration of locally orientable and orientable rooted hypermaps appears unnecessary; combinatorially one class clearly generalizes the other, but the generating series of the latter class cannot be recovered by specializing the generating series of the former class. Algebraic generalizations are not consistent with the simple dichotomy of orientable *versus* non-orientable, and demand a refinement of the second concept. From this perspective, a resolution of the b-Conjecture might illuminate why there is no independent theory for the enumeration of non-orientable maps, or why there do not appear to be significant applications for such a theory.

The chapter concludes by presenting preliminary observations about the nature of b-invariants, in preparation for Chapters 4, 5, and 6. A new result, Theorem 3.35, proves that a b-invariant cannot simultaneously satisfy two apparently natural conditions, and clears the way for the description of a family of invariants in Chapter 4 that do not obviously satisfy either.

3.1   Symmetric Functions

Symmetric functions form the algebraic foundation for the enumerative theory of rooted maps. Macdonald's development in [Mac95] is considered the definitive reference on the subject, though Stanley's systematic development of Jack symmetric functions in [Sta89] is more suited to the present discussion, since he presents several essential results in a more immediately applicable form. This Section is intended only as a review of notation, following primarily Macdonald's usage, though adjusted through Stanley's where it applies to Jack symmetric functions. One notable exception is that, in standard usage, z_λ denotes the size of the centralizer in $\mathfrak{S}_{|\lambda|}$ of a permutation with cycle type λ. This conflicts with the desire to preserve z as an indeterminate marking edges in generating series for maps, having reserved x for vertices and y for faces. In place of z_λ, the present discussion uses ω_λ: potential conflict with the use of ω as the fundamental involution on the ring of symmetric functions is minimal, since the involution is not used in this Thesis, and the non-standard use of ω is noted when the quantity is needed explicitly.

The *ring of symmetric functions* over the field $\mathbb{Q}(\alpha)$ consists of polynomial functions that are invariant under the action of the infinite symmetric group permuting indeterminates, and it is denoted by $\Lambda_{\mathbb{Q}(\alpha)} := \Lambda \otimes_{\mathbb{Z}} \mathbb{Q}(\alpha)$. As it applies to hypermap enumeration, it is convenient to begin by considering $\Lambda_{\mathbb{Q}(\alpha)}$ as the $\mathbb{Q}(\alpha)$-algebra generated by algebraically independent indeterminates $\{p_i : i \geq 1\}$. For a partition $\lambda = [\lambda_1, \lambda_2, \ldots, \lambda_k]$, with no parts equal to zero, p_λ is defined multiplicatively by $p_\lambda := p_{\lambda_1} p_{\lambda_2} \cdots p_{\lambda_k}$, and the set $\{p_\lambda : \lambda \in \mathscr{P}\}$ is a basis for $\Lambda_{\mathbb{Q}(\alpha)}$ as a $\mathbb{Q}(\alpha)$-vector space. The ring has a natural grading, given by

$$\Lambda_{\mathbb{Q}(\alpha)} = \bigoplus_{k \geq 0} \Lambda_{\mathbb{Q}(\alpha)}^k \qquad \text{where} \qquad \Lambda_{\mathbb{Q}(\alpha)}^k = \operatorname{span}_{\mathbb{Q}(\alpha)} \{p_\lambda : \lambda \in \mathscr{P}, |\lambda| = k\}.$$

The p_λ's are collectively referred to as *power-sum* symmetric functions. A second basis for $\Lambda_{\mathbb{Q}(\alpha)}^k$ is the *monomial* symmetric functions, $\{m_\lambda : \lambda \in \mathscr{P}, |\lambda| = k\}$. For $n \geq k$, the relationship between the two bases of $\Lambda_{\mathbb{Q}(\alpha)}^k$ can be determined by identifying the basis elements with polynomial functions given by

$$p_r(\mathbf{x}) = \sum_{i=1}^{n} x_i^r \quad \text{(for } r \geq 1) \qquad \text{and} \qquad m_\lambda(\mathbf{x}) = \sum_{\pi \in S_\lambda} \prod_{j=1}^{\ell(\lambda)} x_{\pi(j)}^{\lambda_j},$$

where $S_\lambda \subseteq \mathfrak{S}_n$ is a maximal set such that the monomials in the sum are unique. Thus $p_\lambda(\mathbf{x})$ and $m_\lambda(\mathbf{x})$ are polynomials in $\mathbb{Q}(\alpha)[x_1, x_2, \ldots, x_n]$ that are invariant under the action of $\mathfrak{S}_n$ permuting indeterminates (hence symmetric functions). Since the relationships are unchanged by increasing n, the identifications can be made as formal sums in the $n \to \infty$ limit.

Remark 3.1. Distinction must be made between $p_\varnothing(\mathbf{x}) = 1$, the power-sum symmetric function indexed by the empty partition, and $p_0(\mathbf{x})$ which is not a generator of the algebra, and is reserved in this Thesis for use when $\mathbf{x}$ is a finite set of indeterminates.

The ring of symmetric functions may be equipped with a scalar product $\langle \cdot, \cdot \rangle_\alpha$ defined with respect to the power-sum basis by

$$\left\langle p_\lambda, p_\mu \right\rangle_\alpha := \delta_{\lambda,\mu} \omega_\lambda \alpha^{\ell(\lambda)}, \tag{3.1}$$

where ω_λ is the size of the centralizer in $\mathfrak{S}_{|\lambda|}$ of a permutation with cycle type λ, and δ is Kronecker's delta function. By considering a more general scalar product, Macdonald showed, in [Mac95, Chap. VI (4.7)], that there is a unique family $\{J_\lambda : \lambda \in \mathscr{P}\}$ of elements of $\Lambda_{\mathbb{Q}(\alpha)}$ satisfying the following criteria.

(P1) (Orthogonality) If $\lambda \neq \mu$, then $\left\langle J_\lambda, J_\mu \right\rangle_\alpha = 0$.

(P2) (Triangularity) Expressing J_λ in the monomial basis,

$$J_\lambda = \sum_{\mu \leqslant \lambda} v_{\lambda\mu}(\alpha) m_\mu,$$

where $v_{\lambda\mu}(\alpha)$ is a rational function in α, and '$\preccurlyeq$' denotes the natural order on partitions (called the *dominance order* by Stanley).

(P3) (Normalization) If $|\lambda| = n$, then $v_{\lambda,[1^n]}(\alpha) = n!$.

If the partial order, $\preccurlyeq$, in the triangularity criterion is replaced by any compatible total order, then the existence follows by Gram-Schmidt orthogonalization, from the fact that the scalar product is positive definite whenever α is a positive real number. The content of Macdonald's result is that the coefficients are independent of which refinement of $\preccurlyeq$ is chosen.

Remark 3.2. For combinatorial applications, the choice of normalization used in (P3) has the advantage that the coefficient of $p_{[1^n]}$ in J_λ is $\delta_{n,|\lambda|}$. A second normalization, with respect to which the functions are monic, is often preferred when deriving analytic properties of Jack symmetric functions as in [Oko97].

The functions, $\{J_\lambda : \lambda \in \mathscr{P}\}$, are called *Jack* symmetric functions. They were introduced by Jack, in [Jac71], using an analytic characterization, as a parametrized generalization of Schur functions and zonal polynomials. Lapointe and Vinet, [LV95], showed that the rational functions $v_{\lambda\mu}(\alpha)$ are polynomials in α with coefficients in $\mathbb{Z}$, and Knop and Sahi, [KS97], extended this result to show that $v_{\lambda\mu}$ is in $\mathbb{Z}_+[\alpha]$. It is thus possible to interpret J_λ as a function of α; when this is the intended interpretation, it is written $J_\lambda(\alpha)$. It can be evaluated at arbitrary complex numbers, even those for which the inner product is degenerate. Most of this Thesis is concerned with the coefficient of $J_\lambda(b+1)$ with respect to the power-sum basis.

Remark 3.3. The `Maple` procedure *FastJack*, in Section B.4 of Appendix B can be used to compute Jack symmetric functions in terms of the power-sum basis when α is a positive integer. In fact, the procedure works when α is an indeterminate, but the corresponding computations are prohibitively slow. A more robust system for working with Jack symmetric functions is provided by the *MOPS* package, as described by Dumitriu, Edelman, and Shuman in [DES07].

Jack symmetric functions appear in the study of rooted hypermaps. Their relationship to Schur functions and zonal polynomials can be stated explicitly using some additional notation. If a partition is identified with its Ferrers diagram, so that
$$\lambda = \{(i,j) : 1 \le i \le \ell(\lambda), 1 \le j \le \lambda_i\},$$
then for $x = (s,t)$ in λ, the *arm length* and *leg length* of x, denoted by $a_\lambda(x)$ and $l_\lambda(x)$, are given by

$$a_\lambda(x) := \left|\{(s,j) \in \lambda : j > t\}\right| \qquad \text{and} \qquad l_\lambda(x) := \left|\{(i,t) \in \lambda : i > s\}\right|. \qquad (3.2)$$

The quantity $a_\lambda(x) + l_\lambda(x) + 1$ is the *hook length* of x, and the product of all the hook lengths of boxes of λ,

$$H_\lambda := \prod_{x \in \lambda} \left(a_\lambda(x) + l_\lambda(x) + 1\right),$$

appears in the representation theory of the symmetric group. In terms of these quantities, Stanley found an explicit formula for the norms of Jack symmetric functions.

Proposition 3.4 (Stanley [Sta89, Thm. 5.8]). *The value of $\langle J_\lambda, J_\lambda \rangle_\alpha$ is given by*

$$\langle J_\lambda, J_\lambda \rangle_\alpha = \prod_{x \in \lambda} \Big(\alpha\, a_\lambda(x) + l_\lambda(x) + \alpha \Big) \Big(\alpha\, a_\lambda(x) + l_\lambda(x) + 1 \Big).$$

Since *Schur* functions, $\{s_\lambda \colon \lambda \in \mathscr{P}\}$, are known to satisfy (P1) and (P2) for $\alpha = 1$, and similarly *zonal* polynomials, $\{Z_\lambda \colon \lambda \in \mathscr{P}\}$, for $\alpha = 2$, their relationship to Jack symmetric functions is determined by choice of normalization, (P3). The following proposition summarizes these relationships.

Proposition 3.5 (Stanley [Sta89, Prop. 1.2]). *Jack symmetric functions generalize Schur functions and zonal polynomials in the sense that*

$$\langle J_\lambda, J_\lambda \rangle_1 = H_\lambda^2, \quad J_\lambda(1) = H_\lambda s_\lambda, \quad \langle J_\lambda, J_\lambda \rangle_2 = H_{2\lambda}, \quad and \quad J_\lambda(2) = Z_\lambda,$$

where 2λ denotes the partition obtained from λ by multiplying each part by two.

Jack symmetric functions are used in the next section to construct the hypermap series.

3.2 The Hypermap Series

As a common generalization of series appearing in [JV90a], [JV90b], and [GJ96b], Goulden and Jackson, in [GJ96a], introduced the series

$$\Phi(\mathbf{x}, \mathbf{y}, \mathbf{z}; t, b) := \sum_{\theta \in \mathscr{P}} \frac{t^{|\theta|}}{\langle J_\theta, J_\theta \rangle_{1+b}} J_\theta(\mathbf{x}; 1 + b) J_\theta(\mathbf{y}; 1 + b) J_\theta(\mathbf{z}; 1 + b), \qquad (3.3)$$

and a related series

$$\Psi(\mathbf{x}, \mathbf{y}, \mathbf{z}; b) := (1 + b) t \frac{\partial}{\partial t} \ln \Phi(\mathbf{x}, \mathbf{y}, \mathbf{z}; t, b) \Big|_{t=1}. \qquad (3.4)$$

The sum is over the class $\mathscr{P}$, of all integer partitions, including the empty partition. A complete development of Jack symmetric functions shows that Φ has no poles at $b = 0$, and so the series can be thought of as a formal power series in t with coefficients that are symmetric functions in $\mathbf{x}$, $\mathbf{y}$, and $\mathbf{z}$ with coefficients in the field $\mathbb{Q}(b)$. Since the unique Jack symmetric function indexed by the empty partition is the constant function 1, and the term of the summation corresponding to this partition contributes 1 to the sum, the logarithm of Φ, and hence Ψ, are well-defined as formal power series in the algebraically independent indeterminates $\{p_i(\mathbf{x}), p_i(\mathbf{y}), p_i(\mathbf{z}) \colon i \geq 1\}$ with coefficients in $\mathbb{Q}(b)$. Evaluating Φ at $b \in \{0, 1\}$, and expressing the result in the power-sum basis,

produces coefficients that enumerate matchings. A corresponding resolution of Ψ produces coefficients that enumerate hypermaps. The primary goal of this and the next three chapters is to extend the combinatorial interpretation of this second collection of coefficients to general values of b.

Remark 3.6. An analogous sum with similar algebraic grounding is the Cauchy sum

$$\sum_{\theta \in \mathscr{P}} \frac{J_\theta(\mathbf{x}, \alpha) J_\theta(\mathbf{y}, \alpha)}{\langle J_\theta, J_\theta \rangle_\alpha} = \prod_{i,j} (1 - x_i y_j)^{-\frac{1}{\alpha}}, \tag{3.5}$$

given by Stanley as [Sta89, Prop. 2.1].

Definition 3.7 (b-polynomial, hypermap series). *The coefficients, $c_{\nu,\varphi,\epsilon}(b)$, referred to collectively as* b-polynomials, *are implicitly constructed by expressing Ψ in the power-sum basis as*

$$\Psi(\mathbf{x}, \mathbf{y}, \mathbf{z}; b) = \sum_{\nu, \varphi, \epsilon \in \mathscr{P}} c_{\nu,\varphi,\epsilon}(b) p_\nu(\mathbf{x}) p_\varphi(\mathbf{y}) p_\epsilon(\mathbf{z}).$$

Using the algebraic independence of $\{ p_i(\mathbf{x}) \colon i \geq 1 \}$, *$\Psi$ can be evaluated at* $p_i(\mathbf{x}) = x_i$, $p_i(\mathbf{y}) = y_i$, *and* $p_i(\mathbf{z}) = z_i$ *for all i, to produce the* hypermap series, *H, given by*

$$H(\mathbf{x}, \mathbf{y}, \mathbf{z}; b) := \Psi(\mathbf{x}, \mathbf{y}, \mathbf{z}; b) \Big|_{\substack{p_i(\mathbf{x}) = x_i \\ p_i(\mathbf{y}) = y_i \\ p_i(\mathbf{z}) = z_i}} = \sum_{\nu, \varphi, \epsilon \in \mathscr{P}} c_{\nu,\varphi,\epsilon}(b) \mathbf{x}^\nu \mathbf{y}^\varphi \mathbf{z}^\epsilon. \tag{3.6}$$

Remark 3.8. Using the notation $\mathbf{p}(\mathbf{x}) = (p_1(\mathbf{x}), p_2(\mathbf{x}), \dots)$, the relationship between H and Ψ can be expressed functionally as

$$H\big(\mathbf{p}(\mathbf{x}), \mathbf{p}(\mathbf{y}), \mathbf{p}(\mathbf{z}); b\big) = \Psi(\mathbf{x}, \mathbf{y}, \mathbf{z}; b).$$

Remark 3.9. By homogeneity of Φ, the coefficient $c_{\nu,\varphi,\epsilon}(b)$ is identically zero unless $|\nu| = |\varphi| = |\epsilon|$. Numerical evidence suggests that all $c_{\nu,\varphi,\epsilon}(b)$ are polynomials in b with non-negative integer coefficients, but they are only known to be rational functions except in specific cases. Polynomiality of the coefficients of Ψ with respect to the power-sum basis does not follow from the polynomiality of Jack symmetric functions, because zeroes of $\langle J_\lambda, J_\lambda \rangle_{1+b}$ are not cancelled by zeroes of the corresponding numerators. In particular, as a consequence of Proposition 3.4 and the non-vanishing of $J_\lambda(0) = e'_\lambda \prod_i \lambda'_i!$ (see [Sta89, Prop. 7.6]), every summand of (3.3), except the term indexed by the empty partition, has a pole at $b = -1$.

There is no known combinatorial interpretation for H, but Proposition 3.5 gives its specializations at $b = 0$ and $b = 1$:

$$H(\mathbf{p}(\mathbf{x}), \mathbf{p}(\mathbf{y}), \mathbf{p}(\mathbf{z}); 0) = t \frac{\partial}{\partial t} \ln \left(\sum_{\theta \in \mathscr{P}} t^{|\theta|} H_\theta s_\theta(\mathbf{x}) s_\theta(\mathbf{y}) s_\theta(\mathbf{z}) \right) \Bigg|_{t=1} \tag{3.7}$$

and

$$H(\mathbf{p}(\mathbf{x}), \mathbf{p}(\mathbf{y}), \mathbf{p}(\mathbf{z}); 1) = 2t\frac{\partial}{\partial t}\ln\left(\sum_{\theta\in\mathscr{P}}t^{|\theta|}\frac{1}{H_{2\theta}}Z_\theta(\mathbf{x})Z_\theta(\mathbf{y})Z_\theta(\mathbf{z})\right)\Bigg|_{t=1.} \tag{3.8}$$

From [JV90a], [JV90b], and [GJ96b], (3.7) and (3.8) are recognized as generating series, in the power-sum basis, for rooted orientable and rooted locally orientable hypermaps with at least one hyperedge. In particular, $c_{\nu,\varphi,\epsilon}(0)$ and $c_{\nu,\varphi,\epsilon}(1)$ have combinatorial interpretations as the number of rooted orientable and rooted locally orientable hypermaps with vertex-degree partition ν, hyperface-degree partition φ, and hyperedge-degree partition ϵ. These specializations motivated the definition of Ψ and led Goulden and Jackson to the following conjecture, which they called "The Hypermap-Jack conjecture", but which shall be referred to throughout as the *Hypermap b-Conjecture*:

Conjecture 3.10 (Hypermap *b*-Conjecture, Goulden and Jackson [GJ96a, Conj. 6.3]). *There exists a non-negative integer valued function β on the class of locally orientable rooted hypermaps such that, $\beta(\mathfrak{m})$ equals 0 precisely when $\mathfrak{m}$ is orientable, and for partitions ν, φ, and ϵ of size at least one, the b-polynomial $c_{\nu,\varphi,\epsilon}(b)$ has the combinatorial interpretation:*

$$c_{\nu,\varphi,\epsilon}(b) = \sum_{\mathfrak{m}\in\mathcal{H}_{\nu,\varphi,\epsilon}} b^{\beta(\mathfrak{m})}, \tag{3.9}$$

where the sum is taken over all rooted hypermaps with vertex degree partition ν, face degree partition φ, and hyperedge degree partition ϵ.

Remark 3.11. For algebraic reasons, the hypermap with no edges is not enumerated by *b*-polynomials.

Definition 3.12 (*b*-invariant for hypermaps). *An invariant, β, such that (3.9) is satisfied for all ν, φ, and ϵ, is called a b-invariant for hypermaps.*

Remark 3.13. The term anticipates that β may be topological in nature, in which case it should be invariant under equivalence of rooted maps.

As defined, the hypermap series and *b*-polynomials depend on the normalization used in defining Jack symmetric functions. Noting $[p_{[1^{|\theta|}]}]J_\theta(1 + b) = 1$, Φ may be rewritten as

$$\Phi(\mathbf{x}, \mathbf{y}, \mathbf{z}; b, t) = \sum_{\theta\in\mathscr{P}}t^{|\theta|}\frac{J_\theta(\mathbf{x}; 1 + b)J_\theta(\mathbf{y}; 1 + b)J_\theta(\mathbf{z}; 1 + b)}{\langle J_\theta, J_\theta\rangle_{1+b}[p_{[1^{|\theta|}]}]J_\theta(1 + b)}, \tag{3.10}$$

to remove this dependence. The existence of a homogeneous form of the series suggests that its significant properties are a consequence of orthogonality and triangularity of Jack symmetric functions, and hints that their analytic description might be useful, since using their characterization as eigenfunctions, (see for example [Mac87]), Jack symmetric functions are unique only up to scalar

multiples. Replacing H_θ and $\dfrac{1}{H_{2\theta}}$ with

$$H_\theta = \frac{1}{\langle s_\theta, s_\theta \rangle_1 \, [p_{[1^{|\theta|}]}] s_\theta} \qquad \text{and} \qquad \frac{1}{H_{2\theta}} = \frac{1}{\langle Z_\theta, Z_\theta \rangle_2 \, [p_{[1^{|\theta|}]}] Z_\theta} \tag{3.11}$$

puts (3.7) and (3.8) in homogeneous form, and emphasizes the extent of the symmetry between (3.10), (3.7), and (3.8).

3.3 The Map Series

The hypermap series, (3.7) and (3.8), were introduced as byproducts of the study of maps. Character theoretic methods used in [JV90a] and [GJ96b] to enumerate rooted maps applied equally well to the study of hypermaps. Given the relationship between maps and hypermaps, that there is a genus preserving embedding of each class in the other, it is not clear which class is more fundamental. The enumerative theory of maps can, however, be recovered from the enumerative theory of hypermaps. Assuming that H has an interpretation as a generating series for hypermaps, a corresponding generating series for maps, M, is obtained as an evaluation of H by algebraically suppressing terms involving hyperfaces of degrees other than two.

Definition 3.14 (map series). *The* map series, M, *is defined by*

$$M(\mathbf{x}, \mathbf{y}, z; b) := H(\mathbf{x}, \mathbf{y}, z\mathbf{e}_2; b) = \sum_{n \geq 0} \sum_{\nu, \varphi \vdash 2n} c_{\nu, \varphi, [2^n]}(b) \mathbf{x}^\nu \mathbf{y}^\varphi z^n. \tag{3.12}$$

Remark 3.15. The symbol M will take on a polymorphic rôle, and will be used to refer to both specializations and refinements of the series defined by (3.12). All versions are properly considered map series and any ambiguity is resolved by context.

When H is evaluated at $\mathbf{z} = z\mathbf{e}_2$, the degree of every monomial as a function of t is equal to twice its degree as a function of z. It follows that, in the definition of M, the operator $t\frac{\partial}{\partial t}$ can be replaced by $2z\frac{\partial}{\partial z}$ to give

$$M(\mathbf{p}(\mathbf{x}), \mathbf{p}(\mathbf{y}), z; b)$$
$$= (1 + b) 2z \frac{\partial}{\partial z} \ln \sum_{\substack{n \geq 0 \\ \theta \vdash 2n}} z^n \frac{J_\theta(\mathbf{x}; 1 + b) J_\theta(\mathbf{y}; 1 + b)}{\langle J_\theta, J_\theta \rangle_{1+b}} \, [p_{[2^n]}] \, J_\theta(1 + b). \tag{3.13}$$

The map series exhibits less algebraic symmetry than the hypermap series, but the approach used in Chapter 4 relies on this broken symmetry.

3.3.1 An Integration Formula

In practice, M is not computationally tractable, but applications of map enumeration do not always require the fully refined series. Jackson, in [Jac94], used an approach originating in physics literature [BIZ80] to express evaluations of the generating series for orientable maps in terms of integrals over the space of complex Hermitian matrices. A related formula was used by Goulden and Jackson in [GJ97] to express evaluations of the generating series for locally orientable maps in terms of integrals over the space of real symmetric matrices. They simplified the expressions and found that when N is a positive integer evaluations of the series can be computed as

$$M(N, \mathbf{y}, z; 0) = 2z \frac{\partial}{\partial z} \ln \int_{\mathbb{R}^N} V(\lambda)^2 \exp\left(\frac{-p_2(\lambda)}{2} + \sum_{k \geq 1} \frac{p_k(\lambda)}{k} y_k \sqrt{z}^k \right) d\lambda \qquad (3.14)$$

and

$$M(N, \mathbf{y}, z; 1) = 4z \frac{\partial}{\partial z} \ln \int_{\mathbb{R}^N} |V(\lambda)| \exp\left(\frac{-p_2(\lambda)}{4} + \sum_{k \geq 1} \frac{p_k(\lambda)}{2k} y_k \sqrt{z}^k \right) d\lambda, \qquad (3.15)$$

where $V(\lambda)$ is the Vandermonde determinant, and as before, $p_k(\lambda)$ is the k-th power-sum symmetric function. They are given by

$$V(\lambda) := \prod_{1 \leq i < j \leq N} (\lambda_i - \lambda_j) \qquad \text{and} \qquad p_k(\lambda) = \sum_{1 \leq i \leq N} \lambda_i^k,$$

Note that N occurs on the right side of both (3.14) and (3.15) as the dimension of the space of integration, but in both cases, coefficients of M, considered as a power series in z, are known, from the generating function interpretation, to depend polynomially on N. Evaluating the series for indeterminate x is thus a matter of presenting M as an element of $\mathbb{Z}_+[N, \mathbf{y}][\![z]\!]$ and replacing every occurrence of N with an x: the validity of this substitution is a consequence of the Fundamental Theorem of Algebra.

Remark 3.16. Pedantically, the evaluations should be written $M(N\mathbf{1}, \mathbf{y}, z; \cdot)$, but the notation is simplified in the interest of aesthetics.

A common generalization of (3.14) and (3.15) that specializes (3.12) is best described using some additional notation.

Definition 3.17 ($\langle \cdot \rangle$, $\langle \cdot \rangle_e$)**.** *For a function $f : \mathbb{R}^N \to \mathbb{R}$, two expectation operators $\langle \cdot \rangle$ and $\langle \cdot \rangle_e$, are defined by*

$$\langle f \rangle := \int_{\mathbb{R}^N} |V(\lambda)|^{\frac{2}{1+b}} f(\lambda) e^{-\frac{1}{2(1+b)} p_2(\lambda)} \, d\lambda, \qquad (3.16)$$

and

$$\langle f \rangle_e := \left\langle f(\lambda) \exp^{\frac{1}{1+b} \sum_{k \geq 1} \frac{1}{k} y_k p_k(\lambda) \sqrt{z}^k} \right\rangle. \tag{3.17}$$

By comparing (3.14) and (3.15) to (3.7) and (3.8), Goulden and Jackson conjectured an integration formula for Jack symmetric functions in [GJ97]. Okounkov proved the formula in [Oko97] to give the following theorem.

Theorem 3.18 (Okounkov [Oko97])**.** *If N is a positive integer, $1 + b$ is a positive real number, and θ is an integer partition of $2n$, then*

$$\langle J_\theta(\lambda, 1 + b) \rangle = J_\theta(\mathbf{1}_N, 1 + b)[p_{[2^n]}]J_\theta \langle 1 \rangle, \tag{3.18}$$

where $\mathbf{1}_N = (1, \ldots, 1, 0, 0, \ldots)$ is the vector consisting of N leading ones followed by zeroes.

Corollary 3.19 (Goulden, Jackson, and Harer [GHJ01, Prop. 7.1])**.** *For any positive integer N and any real number $b > -1$, the map series can be evaluated as*

$$M(N, \mathbf{y}, z; b) = (1 + b)2z \frac{\partial}{\partial z} \ln \frac{\langle 1 \rangle_e}{\langle 1 \rangle}. \tag{3.19}$$

Proof. The proof is based on [GHJ01, Prop. 7.1]. Notice that $J_\theta(\mathbf{1}_N; 1 + b)$ is obtained from $J_\theta(\mathbf{x}; 1 + b)$ by replacing $p_i(\mathbf{x})$ with N for every i. Starting with (3.13) and applying Theorem 3.18, shows that

$$M(N, \mathbf{p}(\mathbf{y}), z; b) = (1 + b)2z \frac{\partial}{\partial z} \ln \left\langle \sum_{\theta \in \mathscr{P}} z^{\frac{|\theta|}{2}} \frac{J_\theta(\lambda; 1 + b)J_\theta(\mathbf{y}; 1 + b)}{\langle J_\theta, J_\theta \rangle_{1+b}} \right\rangle$$

$$= (1 + b)2z \frac{\partial}{\partial z} \ln \left\langle \prod_i \prod_{j=1}^N \left(1 - \sqrt{z} y_i \lambda_j \right)^{-\frac{1}{1+b}} \right\rangle$$

$$= (1 + b)2z \frac{\partial}{\partial z} \ln \left\langle \exp \left(\frac{1}{1 + b} \sum_{k \geq 1} \frac{1}{k} p_k(\mathbf{y}) p_k(\lambda) \sqrt{z}^k \right) \right\rangle,$$

where the second equality is by restricting (3.5) to a finite set of indeterminates. Appealing to the algebraic independence of $\{ p_i(\mathbf{y}) : i \geq 1 \}$, and replacing every occurrence of $p_i(\mathbf{y})$ with y_i completes the proof. $\square$

Remark 3.20. It is necessary to include the restriction $b > -1$ to guarantee that the expectation operator is well-defined, but the expression can be used to derive properties of M for arbitrary values of b, since in Chapter 4, the series is shown to have an expression in $\mathbb{Z}_+[N, \mathbf{y}, b][\![z]\!]$.

Remark 3.21. The factor $\langle 1 \rangle$ does not depend on z, and can be omitted from (3.19), but its inclusion is consistent with the derivations of (3.14) and (3.15) described in 3.5.2, that involve giving combinatorial interpretations to $\frac{\langle 1 \rangle_e}{\langle 1 \rangle}\big|_{b=0}$ and $\frac{\langle 1 \rangle_e}{\langle 1 \rangle}\big|_{b=1}$.

3.4   A Hierarchy of Conjectures

This Section outlines a sequence of relaxations of the Hypermap b-Conjecture, Conjecture 3.10. Each calls for a combinatorial interpretation of only particular sums of b-polynomials corresponding to maps. The relaxed conjectures are introduced not only because they appear to be more tractable than the original, but also because they are interesting in their own right. In particular, Conjecture 3.23, which is resolved in Chapter 4 has applications to algebraic geometry.

The first relaxation involves sums of b-polynomials corresponding to maps with identical face-degree partitions. Brown proved it in [Bro00, Lemm. 7.1] using a character theoretic result of Jackson and Goulden from [GJ96a], and gave a combinatorial interpretation to the sum as [Bro00, Lemm. 7.2]. A new and shorter proof of the algebraic content is given here using (3.19) to evaluate the map series at $\mathbf{x} = \mathbf{1}$, with a combinatorial interpretation implicit in the proof of Theorem 4.16.

Lemma 3.22 (Brown [Bro00, Lemm. 7.1]). *The coefficient of $\mathbf{y}^{\varphi}z^n$ in $M(\mathbf{1}, \mathbf{y}, z; b)$ is given by the marginal sum*

$$\sum_{\nu \vdash 2n} c_{\nu, \varphi, [2^n]}(b) = (1 + b)^{n - \ell(\varphi) + 1} \sum_{\nu \vdash 2n} c_{\nu, \varphi, [2^n]}(0).$$

Proof. Expanding $M(\mathbf{1}, \mathbf{y}, z; b)$ in terms of an integral over $\mathbb{R}^1$, using (3.19), and changing the variable of integration, *via* the substitution $\lambda = \rho \sqrt{1 + b}$, gives

$$M(\mathbf{1}, \mathbf{y}, z; b) = (1 + b)2z \frac{\partial}{\partial z} \ln \int_{\mathbb{R}} \exp \left(\frac{1}{1 + b} \sum_{k \geq 1} \frac{1}{k} y_k \lambda^k \sqrt{z}^k - \frac{\lambda^2}{2(1 + b)} \right) d\lambda$$

$$= (1 + b)2z \frac{\partial}{\partial z} \ln \int_{\mathbb{R}} \exp \left(\sum_{k \geq 1} \frac{1}{k} \left(\frac{y_k}{1 + b} \right) \rho^k \sqrt{z(1 + b)}^k - \frac{\rho^2}{2} \right) d\rho$$

$$= (1 + b) M\left(\mathbf{1}, \frac{\mathbf{y}}{1 + b}, (1 + b)z; 0 \right).$$

The result follows by comparing coefficients of $\mathbf{y}^{\varphi}z^n$. $\square$

A second relaxation, the topic of Chapter 4, was stated explicitly by Goulden, Harer, and Jackson in [GHJ01, p. 4422], and provides precisely the setting needed to combinatorialize a parametrized function interpolating between the virtual Euler characteristics of two moduli spaces of curves. The relaxation is resolved in Chapter 4, where a strengthened version appears as Corollary 4.17.

Conjecture 3.23 (The Marginal b-Conjecture, [GHJ01]). *For $\varphi \vdash 2n$, the coefficient of $x^\nu \mathbf{y}^\varphi z^n$ in $M(x\mathbf{1}, \mathbf{y}, z; b)$ has a combinatorial interpretation as*

$$d_{\nu, \varphi}(b) := \sum_{\ell(\nu) = \nu} c_{\nu, \varphi, [2^n]}(b) = \sum_{\mathfrak{m} \in \mathcal{M}_{\nu, \varphi}} b^{\beta(\mathfrak{m})},$$

where β is a non-negative integer valued function on the class of locally orientable rooted maps such that β(m) is zero precisely when m is orientable, and the second sum is over all rooted maps with v vertices and face-degree partition φ.

Definition 3.24 (marginal *b*-polynomial, marginal *b*-invariant). *The coefficients $d_{v,\varphi}$ are* marginal *b*-polynomials, *and an invariant β such that Conjecture 3.23 is satisfied for all v and φ is called a* marginal *b*-invariant.

The final conjecture in this sequence is the strongest relaxation of Conjecture 3.10 to involve only maps, though a further refinement, that is not a specialization of Conjecture 3.10, appears as Conjecture 4.9. Chapter 6 describes a programme for verifying a combinatorial interpretation of the coefficients of M for all maps of sufficiently low genus, but a general approach to this conjecture remains elusive.

Conjecture 3.25 (The *b*-Conjecture). *There exists a non-negative integer valued function β on the class of locally orientable rooted maps such that, β(m) equals 0 precisely when m is orientable, and for $v, \varphi \vdash 2n$, the b-polynomial $c_{v,\varphi,[2^n]}(b)$ has the combinatorial interpretation:*

$$c_{v,\varphi,[2^n]}(b) = \sum_{m \in \mathcal{M}_{v,\varphi}} b^{\beta(m)}, \qquad (3.20)$$

where the sum is taken over all rooted maps with vertex degree partition v and face degree partition φ.

Definition 3.26 (*b*-invariant for maps). *An invariant, β, such that* (3.20) *is satisfied for all v and φ, is called a* b-invariant for maps. *When clear from context, such an invariant will be referred to as a* b-invariant.

Each relaxed conjecture described in this section anticipates a combinatorial interpretation for a particular marginal sum of coefficients from H. Corresponding algebraic forms of the conjectures predict that the marginal sums are polynomials in $\mathbb{Z}_+[b]$ but do not require combinatorial interpretations in terms of maps. Table 3.1 summarizes the evaluations of H and the coefficients involved in each relaxation. Two of the relaxations have been resolved as true, and the final column refers to these resolutions.

Despite the lack of a general approach to its solution, Conjecture 3.25 appears more tractable than Conjecture 3.10, and is the subject of the majority of this Thesis. The emphasis on maps is justified both by the fact that the Hypermap *b*-Conjecture originated from work on the enumeration of maps, with attention given to hypermaps only when the algebraic techniques proved to be extensible, and by the belief encapsulated in the following conjecture. It suggests that *b*-invariants and *b*-invariants for hypermaps are compatible in the sense that when each of $\mathcal{H}$ and $\mathcal{M}$ is embedded in the other, the invariant does not change.

Conjecture 3.27. *If there is a b-invariant for hypermaps, then it is induced by the restriction to face-two-coloured maps of a b-invariant for maps.*

Table 3.1: Relaxations of Conjecture 3.10

Relaxation	Series	Coefficients	Resolved in
Conjecture 3.10	$H(\mathbf{x}, \mathbf{y}, \mathbf{z}; b)$	$c_{v,\varphi,\epsilon}(b)$	Unresolved
Conjecture 3.25	$M(\mathbf{x}, \mathbf{y}, z; b)$	$c_{v,\varphi,[2^n]}(b)$	Unresolved
Conjecture 3.23	$H(x\mathbf{1}, \mathbf{y}, z\mathbf{e}_2; b)$	$\displaystyle\sum_{\ell(v)=v} c_{v,\varphi,[2^n]}(b)$	Corollary 4.17
Lemma 3.22	$H(\mathbf{1}, \mathbf{y}, z\mathbf{e}_2; b)$	$\displaystyle\sum_{v\vdash 2n} c_{v,\varphi,[2^n]}(b)$	Lemma 7.1 of [Bro00]

Remark 3.28. The converse is necessarily true; if maps are identified with hypermaps having hyperedges only of degree two, then every b-invariant for hypermaps induces a b-invariant for maps. Similarly, every b-invariant is also a marginal b-invariant.

3.5 Historical Developments

A survey of the techniques originally used to derive (3.7), (3.8), (3.14), and (3.15) is presented to emphasize the difficulty associated with extending the derivations to general values of b. Parallels between the formulae suggest a common generalization, but the generalization does not exist at the level of the combinatorics used to derive the specialized expressions. The combinatorial derivations of all four expressions follow the same format, a two-stage process involving first deriving evaluations of Φ directly as an exponential generating series for collections of labelled hypermaps (maps in the cases of (3.14) and (3.15)), and then extending this interpretation to Ψ by giving combinatorial interpretations to the actions of the logarithm and partial derivative: a standard enumerative technique, due to Hurwitz, shows that the logarithm restricts the generating series to connected components, and the partial derivative removes multiplicative factors introduced by labelling the hypermaps. For technical reasons involving the action of the logarithm, the map with no edges is not considered connected when interpreted as a labelled object.

An analogous approach is not possible for general values of b. Because of the leading factor of $(b + 1)$ in the expression for Ψ, either every b-polynomial is divisible by $b+1$, or Φ has an essential singularity at $b = -1$. Direct computation shows the first possibility is not the case, in particular $c_{[2],[2],[2]}(b) = b$. Any combinatorial interpretation of Φ for general b must thus involve a rescaling of coefficients, or involve considering the series Φ^{1+b}. The proof of Conjecture 3.23

in Chapter 4 avoids this complication by working directly with connected maps, and not using labelled or disconnected objects as intermediaries.

3.5.1   A Symmetric Function Approach

The Hypermap b-Conjecture originated from a symmetric-function-based approach to the enumeration of rooted hypermaps. Jackson and Visentin used a character theoretic derivation, in [JV90a], to obtain the generating series for rooted orientable maps with respect to vertex- and face-degree partitions, and extended their analysis to hypermaps in [JV90b]. Goulden and Jackson recast the result in terms of Schur functions in [GJ96b], where they used a parallel derivation to express the generating series for locally orientable hypermaps in terms of zonal polynomials.

   The derivations use the combinatorializations described in Section 2.3 to rephrase the problem of enumerating hypermaps as one of computing a multiplication table for an appropriate algebra: the class algebra of the symmetric group for orientable hypermaps, and the double coset algebra of the hyperoctahedral group for locally orientable hypermaps. In both cases the multiplication is carried out by working over a basis of orthogonal idempotents described using irreducible characters. The link to symmetric functions is made by noting that the character evaluations involved are the coefficients of Schur functions and zonal polynomials with respect to the power-sum basis. There is no corresponding algebra known with respect to which the coefficients of Jack symmetric functions in the power-sum basis are character evaluations.

Orientable Hypermaps

This Section sketches the derivation of (3.7) as the generating series for rooted orientable hypermaps with respect to vertex-, hyperface-, and hyperedge-degree partitions. The series was originally derived by Jackson and Visentin for maps in [JV90a], and extended to hypermaps in [JV90b]. Emphasis is placed on parallels with the development of (3.8) from [GJ96b]. The necessary algebraic tools are discussed in [Mac95] and [HSS92]. Starting with the combinatorialization for orientable maps from Section 2.3.1 and its generalization to orientable hypermaps from Section 2.3.2, arbitrary pairs of permutations are interpreted as representing unordered collections of edge-labelled hypermaps. Counting these representations is phrased as a problem in the class algebra of the symmetric group, and the solution is expressed using character sums before being recast using Schur functions.

   As in [JV90b], if two permutations, ϵ and ν in $\mathfrak{S}_n$, do not act transitively on $\{1, 2, \ldots, n\}$, then $\{1, 2, \ldots, n\}$ can be partitioned into its orbits under the action of the group generated by ϵ and ν,

$$\{1, 2, \ldots, n\} = \mathcal{S}_1 \cup \mathcal{S}_2 \cup \cdots \cup \mathcal{S}_k,$$

and ϵ and ν can be written as products

$$\epsilon = \epsilon_1 \epsilon_2 \cdots \epsilon_k \qquad \text{and} \qquad \nu = \nu_1 \nu_2 \cdots \nu_k,$$

such that ϵ_i and ν_i act transitively on $\mathcal{S}_i$ and fix all other elements of $\{1, 2, \ldots, n\}$. In this way, an arbitrary pair of permutations (ϵ, ν) acting on the same set represents an unordered collection,

$$\{(\epsilon_i, \nu_i) \colon 1 \leq i \leq k\},$$

of labelled orientable hypermaps, and in this context, following the terminology of [JV90b], such a collection is called a *permutation system*. The concepts of vertex-, hyperedge-, and hyperface-degree partitions are extended to permutations systems as the cycle types of ϵ, ν, and $\epsilon\nu$. Notably, some $\mathcal{S}_i$ may consist of a singleton, in which case ϵ_i and ν_i fix every element of $\{1, 2, \ldots, n\}$, but hypermaps without edges, that is hypermaps represented by permutations acting on the empty set, do not appear in these collections. The machinery needed to count permutations systems using the class algebra of the symmetric group is summarized from [HSS92, Sec. 2].

If G is any finite group, with conjugacy classes $C_1, C_2, \ldots, C_t$, then its complex group algebra, $\mathbb{C}G$, is semisimple by Maschke's Theorem (see, for example, [Her94, Thm. 1.4.1]), and so $Z(\mathbb{C}G)$ has a basis of orthogonal idempotents given by

$$\mathsf{E}_i = \frac{d_i}{|G|} \sum_{j=1}^{t} \overline{\chi}_j^{(i)} \mathsf{C}_j \qquad (1 \leq i \leq t), \tag{3.21}$$

where $\chi_j^{(i)}$ is obtained by evaluating the irreducible complex character $\chi^{(i)}$ at any $w \in C_j$, the degree of $\chi^{(i)}$ is d_i, and C_i is the formal sum of elements of C_i. The relationship is inverted, using orthogonality of characters to give

$$\mathsf{C}_j = |C_j| \sum_{i=1}^{t} \frac{\chi_j^{(i)}}{d_i} \mathsf{E}_i. \tag{3.22}$$

When G is $\mathfrak{S}_n$, the symmetric group on n elements, the conjugacy classes are naturally indexed by integer partitions of n. In this case C_λ is the set of permutations with cycle type λ, and if $\lambda \vdash n$, then χ^λ has degree $\frac{n!}{H_\lambda}$. Coefficients $a_{\mu,\nu}^\varphi$ are defined implicitly by the multiplication

$$\mathsf{C}_\mu \mathsf{C}_\nu = \sum_\lambda a_{\mu,\nu}^\lambda \mathsf{C}_\lambda,$$

so $a_{\mu,\nu}^\lambda$ is the number of pairs of permutations $(u, v) \in C_\mu \times C_\nu$ such that $uv = w$ for a fixed $w \in C_\lambda$. It follows that the number of permutation systems with vertex-degree partition ν, hyperface-degree partition φ, and hyperedge-degree partition ϵ is $|C_\epsilon| a_{\nu,\varphi}^\epsilon$, or the corresponding expressions with ν, φ, and ϵ

permuted. Explicit computation of $a_{\nu,\varphi}^{\epsilon}$ is possible by using (3.21) and (3.22) to give

$$a_{\nu,\varphi}^{\epsilon} = \omega_\nu^{-1}\omega_\varphi^{-1} \sum_{\lambda \in \mathscr{P}} H_\lambda \chi^\lambda(\nu)\chi^\lambda(\varphi)\chi^\lambda(\epsilon), \qquad (3.23)$$

since the irreducible characters are real-valued, and $\omega_\lambda = \frac{n!}{|C_\lambda|}$, when $\lambda \vdash n$. Schur functions were developed to record these character evaluations, and the link to symmetric functions is made *via* the relationship,

$$s_\lambda = \sum_{\mu \vdash k} \omega_\mu^{-1} \chi^\lambda(\mu) p_\mu,$$

due to Frobenius [Mac95, Sec. I.7.10]. It follows that an exponential generating series for permutations systems in the power-sum basis is given by

$$\sum_{\nu,\varphi,\epsilon \in \mathscr{P}} \frac{t^{|\nu|}}{|\nu|!} |C_\epsilon| a_{\nu,\varphi}^{\epsilon} p_\nu(\mathbf{x}) p_\varphi(\mathbf{y}) p_\epsilon(\mathbf{z}) = \sum_{\theta \in \mathscr{P}} t^{|\theta|} H_\theta s_\theta(\mathbf{x}) s_\theta(\mathbf{y}) s_\theta(\mathbf{z}).$$

A logarithm restricts the series to labelled connected hypermaps with at least one edge, and (3.7) is recovered as the generating series for rooted orientable hypermaps by taking a partial derivative with respect to t to remove the labelling, since each rooted hypermap has $(n-1)!$ distinct labellings.

Locally Orientable Hypermaps

This Section describes the derivation of (3.8) as the generating series for rooted locally orientable hypermaps with respect to vertex-, hyperface-, and hyperedge-degree partitions. It follows the derivation used by Goulden and Jackson in [GJ96b], but without an explicit derivation of the specialization to maps. Necessary algebraic tools are discussed in [BG92], [HSS92, Sec. 2], and [Mac95, VII.2]. Beginning with the combinatorialization of hypermaps in Section 2.3.2, the problem of counting finite collections of hypermaps, called *corner systems*, is phrased as a problem in the double-coset algebra of the hyperoctahedral group, and then the solution is expressed using zonal polynomials.

As in [GJ96b], a *corner system* is an ordered triple (M_v, M_e, M_f) of perfect matchings on the same vertex set. If the matching graph G with edge set $M_v \cup M_e \cup M_f$ is connected, then the corner system (M_v, M_e, M_f) represents a hypermap, but in general a corner system represents an unordered collection of hypermaps with at least one hyperedge: there are no isolated vertices in G since M_v is a perfect matching. For two perfect matchings M_1 and M_2, let $\Lambda(M_1, M_2)$ be the partition with parts equal to half the lengths of the cycles in the graph with edge set $M_1 \cup M_2$. Vertex-, hyperface-, and hyperedge-degree partitions are generalized to corner systems as $\Lambda(M_e, M_f)$, $\Lambda(M_v, M_e)$, and $\Lambda(M_v, M_f)$.

The hyperoctahedral group of order n, is the wreath product $\mathfrak{B}_n = \mathfrak{S}_n[\mathfrak{S}_2]$. It can be embedded in $\mathfrak{S}_{2n}$ as the centralizer of a fixed-point-free involution π. As described in [BG92] and [HSS92], the double cosets of $\mathfrak{B}_n$ in $\mathfrak{S}_{2n}$ are naturally

indexed by partitions, with $\mathcal{K}_\theta$ given by

$$\mathcal{K}_\theta := \{\, \sigma \in \mathfrak{S}_{2n} \colon \Lambda(M, \sigma M) = \theta \,\},$$

where M is the matching that pairs elements transposed by π. If K_θ is the formal sum of elements of $\mathcal{K}_\theta$, then $\{\,\mathsf{K}_\theta \colon \theta \vdash n\,\}$ is a basis for a commutative sub-algebra of $\mathbb{C}\mathfrak{S}_{2n}$, identified as $\mathscr{H}(\mathfrak{S}_{2n}, \mathfrak{B}_n)$, the Hecke algebra of the Gel'fand pair $(\mathfrak{S}_{2n}, \mathfrak{B}_n)$. Self-contained descriptions of $\mathscr{H}(\mathfrak{S}_{2n}, \mathfrak{B}_n)$ are given by Bergeron and Garsia in [BG92] and by Macdonald in [Mac95, Chap. VII]. Coefficients $b^\lambda_{\mu, \nu}$ are implicitly defined by multiplication in $\mathscr{H}(\mathfrak{S}_{2n}, \mathfrak{B}_n)$ using the expansion

$$\mathsf{K}_\mu \mathsf{K}_\nu = \sum_\lambda b^\lambda_{\mu, \nu} \mathsf{K}_\lambda,$$

and they are given a combinatorial description by Hanlon, Stanley, and Stembridge in [HSS92, Sec. 3]. From the correspondence,

$$
\begin{aligned}
\sigma \in \mathcal{K}_\nu &\Longleftrightarrow \Lambda(\sigma M, M) = \Lambda(M, \sigma^{-1} M) = \nu \\
\tau \in \mathcal{K}_\varphi &\Longleftrightarrow \Lambda(\tau M, M) = \varphi \\
\sigma \tau \in \mathcal{K}_\epsilon &\Longleftrightarrow \Lambda(\sigma \tau M, M) = \Lambda(\tau M, \sigma^{-1} M) = \epsilon,
\end{aligned}
$$

it follows that if $(\sigma, \tau) \in \mathcal{K}_\nu \times \mathcal{K}_\varphi$ contributes to $b^\epsilon_{\nu, \varphi}$, then $(M, \sigma^{-1}M, \tau M)$ is a corner system with vertex-, hyperface-, and hyperedge-degree partitions ν, φ, and ϵ. Counting multiplicities, it follows, as in [GJ96b], that the number of corner systems with these degree partitions is given by

$$\frac{|\mathfrak{S}_{2n}| \cdot |\mathcal{K}_\epsilon|}{|\mathfrak{B}_n|^3} \, b^\epsilon_{\nu, \varphi}. \tag{3.24}$$

As in the orientable case, the coefficients $b^\epsilon_{\nu, \varphi}$ can be computed directly by using the fact that $\mathscr{H}(\mathfrak{S}_{2n}, \mathfrak{B}_n)$ is a semisimple commutative algebra, and thus has a basis of orthogonal idempotents $\{\, E_\mu \colon \mu \vdash n \,\}$. In [HSS92, Sec. 3], these idempotents are related to the coset sums by

$$\mathsf{E}_\mu = \frac{1}{H_{2\mu}} \sum_{\nu \vdash n} \frac{1}{|\mathcal{K}_\nu|} \phi^\mu(\nu) \mathsf{K}_\nu \qquad \text{and} \qquad \mathsf{K}_\mu = \sum_{\nu \vdash n} \phi^\nu(\mu) \mathsf{E}_\nu, \tag{3.25}$$

where

$$\phi^\lambda(\theta) = \sum_{\mu \in \mathcal{K}_\theta} \chi^{2\lambda}(\mu) \qquad (\lambda \vdash n)$$

are irreducible characters of $\mathscr{H}(\mathfrak{S}_{2n}, \mathfrak{B}_n)$, as described in [BG92]. It follows that

$$b^\lambda_{\mu, \nu} = \frac{1}{|\mathcal{K}_\lambda|} \sum_{\beta \vdash n} \frac{1}{H_{2\beta}} \phi^\beta(\lambda) \phi^\beta(\mu) \phi^\beta(\nu).$$

From [BG92], zonal polynomials, evaluations of Jack symmetric functions at

54

$\alpha = 2$, are given by

$$Z_\lambda(\mathbf{x}) = \frac{1}{|\mathfrak{B}_n|} \sum_{\theta \vdash n} \phi^\lambda(\theta) p_\theta(\mathbf{x}),$$

so a generating series for corner systems, exponential with respect to the number of vertices in the matching graph, is given in the power-sum basis by

$$\sum_{\nu,\varphi,\epsilon \in \mathscr{P}} t^{|\nu|} \frac{|\mathcal{K}_\epsilon|}{|\mathfrak{B}_n|^3} b^\epsilon_{\nu,\varphi} p_\nu(\mathbf{x}) p_\varphi(\mathbf{y}) p_\epsilon(\mathbf{z}) = \sum_{\theta \in \mathscr{P}} t^{|\theta|} \frac{1}{H_{2\theta}} Z_\theta(\mathbf{x}) Z_\theta(\mathbf{y}) Z_\theta(\mathbf{z}),$$

and (3.8) is obtained as in the orientable case. The leading factor of 2 accounts for the fact that a hypermap with n edges has a matching graph with $2n$ vertices.

3.5.2   An Integration Approach to Map Enumeration

The integral expressions for evaluations of the map generating series, (3.14) and (3.15), can be obtained by considering maps with painted vertices. If N is a positive integer, then the coefficients of $\mathbf{y}^\varphi z^n$ in $M(N, \mathbf{y}, z; 0)$ and $M(N, \mathbf{y}, z; 1)$ are the numbers of orientable and locally orientable rooted maps with n edges, face-degree partition φ, and each vertex painted independently with a colour from a set of cardinality N. A map with k vertices is thus counted with multiplicity N^k. Both series were originally obtained combinatorially, in dual form, by considering rooted maps with painted faces. Each face-painted map can be decomposed as a collection of painted vertex neighbourhoods, together with instructions for attaching ribbons to connect the vertices in a manner respecting the face painting.

   Given a collection of face-painted vertex neighbourhoods, each embedded in an oriented plane, a clockwise tour around each vertex induces a cyclic sequence of face colours. Encode the sequence $(c_1, c_2, \ldots, c_k)$ as the monomial $m_{c_1 c_2} m_{c_2 c_3} \ldots m_{c_k c_1}$ in indeterminates $\{m_{ij} : 1 \le i, j \le N\}$, so that m_{ij} encodes a half-edge such that its sides are painted i and j, and the side painted i is encountered before the side painted j in a clockwise tour around the associated vertex. With this encoding, the number of ways to draw colour-respecting ribbons is determined by the product of the monomials encoding the vertices. In general, when the monomial m encodes a collection of vertices, let $\langle m \rangle_{\mathcal{L}}$ be the number of ways to match the half-edges by joining them with colour-respecting ribbons, and let $\langle m \rangle_O$ be the number of ways to do this in an orientation-preserving fashion. Then

$$\left\langle m_{ii}^{2n} \right\rangle_O = \frac{(2n)!}{2^n n!}, \qquad \left\langle m_{ij}^n m_{ji}^k \right\rangle_O = n! \, \delta_{n,k}, \qquad \langle pq \rangle_O = \langle p \rangle_O \langle q \rangle_O,$$

$$\left\langle m_{ii}^{2n} \right\rangle_{\mathcal{L}} = \frac{(2n)!}{n!}, \qquad \left\langle m_{ij}^n m_{ji}^k \right\rangle_{\mathcal{L}} = \frac{(n+k)!}{2^{\frac{n+k}{2}} \left(\frac{n+k}{2} \right)!}, \qquad \text{and } \langle pq \rangle_{\mathcal{L}} = \langle p \rangle_{\mathcal{L}} \langle q \rangle_{\mathcal{L}},$$

provided that all m_{ij} and m_{ji} appear in the same factor of pq for every i and j.
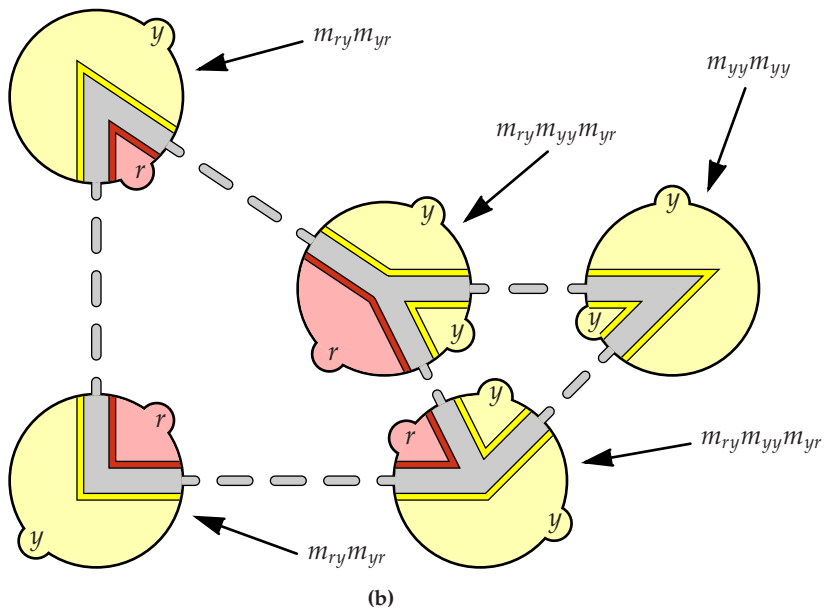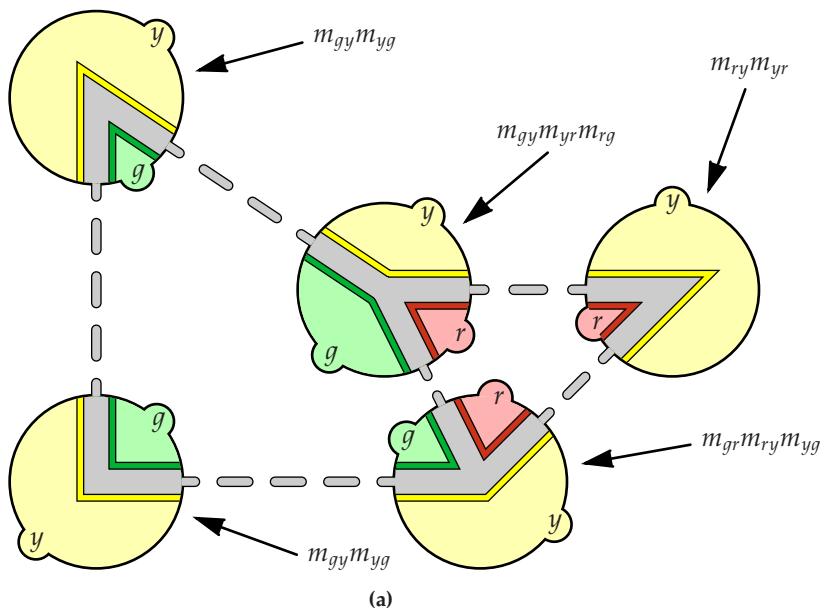
Figure 3.1: Painted neighbourhoods of vertices are encoded by monomials representing half-edges.

Example 3.29. *Figure 3.1 shows two decompositions of the map from Figure 2.10 into collections of vertex neighbourhoods, each face-painted using the colours $\{g, r, y\}$. The collection shown in Figure 3.1a is represented by the monomial*

$$(m_{gy}m_{yg})^2(m_{gr}m_{ry}m_{yr})(m_{gy}m_{yr}m_{rg})(m_{ry}m_{yr}) = (m_{gr}m_{rg})(m_{gy}^3 m_{yg}^3)(m_{ry}^2 m_{yr}^2).$$

There are $1!3!2! = 12$ *orientation-preserving and* $\frac{2!}{2^1 1!} \frac{6!}{2^3 3!} \frac{4!}{2^2 2!} = 45$ *ways to join its half-edges with ribbons. The collection shown in Figure 3.1b is represented by the monomial*

$$(m_{ry}m_{yr})^2(m_{ry}m_{yy}m_{yr})^2(m_{yy}m_{yr}) = (m_{ry}^4 m_{yr}^4)(m_{yy}^4).$$

Its half-edges can be connected with ribbons in $4!\frac{4!}{2^2 2!} = 72$ *orientation-preserving ways, and* $\frac{8!}{2^4 4!} \frac{4!}{2!} = 1260$ *ways.*

Integral representations of $\langle \cdot \rangle_O$ and $\langle \cdot \rangle_{\mathcal{L}}$ are obtained by noting that, for non-negative integers m and n,

$$\int_{\mathbb{R}^2} (x_1 + \mathrm{i}x_2)^n (x_1 - \mathrm{i}x_2)^m e^{-x_1^2 - x_2^2} \, d\mathbf{x} = \begin{cases} n!\,\pi & \text{if } n = m \\ 0 & \text{if } n \neq m, \end{cases}$$

and

$$\int_{\mathbb{R}} x^n e^{-\frac{x^2}{2}} \, dx = \begin{cases} 0 & \text{if } n \text{ is odd} \\ \frac{(2i)!}{2^i i!} \sqrt{2\pi} & \text{if } n = 2i \text{ is even.} \end{cases}$$

Let $\mathcal{V}_N$ be the space of $N \times N$ complex Hermitian matrices. A typical element of $\mathcal{V}_N$ is a matrix M with entries $m_{ij} = r_{ij} + \mathrm{i}c_{ij}$. In particular, $r_{ij} = r_{ji}$ and $c_{ij} = -c_{ji}$, so

$$\operatorname{tr} M^2 = 2 \sum_{1 \leq i < j \leq N} (r_{ij}^2 + c_{ij}^2) + \sum_{1 \leq i \leq N} r_{ii}^2,$$

and it follows that

$$\langle f \rangle_O = \frac{\int_{\mathcal{V}_N} f \exp\left(-\frac{1}{2} \operatorname{tr} M^2\right) dM}{\int_{\mathcal{V}_N} 1 \exp\left(-\frac{1}{2} \operatorname{tr} M^2\right) dM},$$

where $dM = \left(\prod_{i<j} c_{i,j}\right)\left(\prod_{i \leq j} r_{i,j}\right)$ is a Haar measure. Similarly, let $\mathcal{W}_N$ denote the space of $N \times N$ real symmetric matrices with entries $m_{ij} = r_{ij}$. Then

$$\langle f \rangle_{\mathcal{L}} = \frac{\int_{\mathcal{V}_N} f \exp\left(-\frac{1}{4} \operatorname{tr} M^2\right) dM}{\int_{\mathcal{V}_N} 1 \exp\left(-\frac{1}{4} \operatorname{tr} M^2\right) dM},$$

where $dM = \prod_{i \leq j} r_{i,j}$ is again a Haar measure. These matrix models are particularly useful, since the monomials representing paintings of the neighbourhood of a degree k vertex with colours $\{1, 2, \ldots, N\}$ are generated by $\operatorname{tr} M^k$. It follows, using factors of $\frac{1}{k}$ and $\frac{1}{2k}$ to account for cyclic and dihedral symmetries in the

orientable and locally orientable cases, that

$$M(N, \mathbf{y}, z; 0) = 2z \frac{\partial}{\partial z} \ln \frac{\int_{\mathcal{V}_N} \exp\left(\sum_{k \geq 1} \frac{1}{k} y_k \sqrt{z}^k \operatorname{tr} M^k\right) \exp\left(-\frac{1}{2} \operatorname{tr} M^2\right) dM}{\int_{\mathcal{V}_N} \exp\left(-\frac{1}{2} \operatorname{tr} M^2\right) dM} \quad (3.26)$$

and

$$M(N, \mathbf{y}, z; 1) = 4z \frac{\partial}{\partial z} \ln \frac{\int_{\mathcal{W}_N} \exp\left(\sum_{k \geq 1} \frac{1}{2k} y_k \sqrt{z}^k \operatorname{tr} M^k\right) \exp\left(-\frac{1}{4} \operatorname{tr} M^2\right) dM}{\int_{\mathcal{V}_N} \exp\left(-\frac{1}{4} \operatorname{tr} M^2\right) dM}. \quad (3.27)$$

As in Section 3.5.1, the logarithm restricts the series to edge-connected compo-
nents, and the differential operator removes the order on the half-edges that is
implicit from the encoding. A `Maple` program in Section B.3 of Appendix B can
be used to work with these expressions directly for small values of N. There are
no natural candidates to interpolate between $\mathcal{V}_N$ and $\mathcal{W}_N$ as topological groups,
but the integral over $\mathcal{W}_N$ can be represented as an integral over $\mathcal{V}_N$ by changing
the measure to include Dirac-delta functions of the complex components. This
approach has not been used to generalize the two series.

Algebraic manipulation is used to generalize (3.26) and (3.27) by first express-
ing them in terms of integrals over $\mathbb{R}^N$. Every element of $\mathcal{V}_N$ (respectively $\mathcal{W}_N$)
can be represented as a product of the form $M = UDU$, with D diagonal and U
unitary (respectively orthogonal). Since the measures factor according to this
representation, and since the integrands are invariant under conjugation, the
series can be transformed into integrals over $\mathbb{R}^N$ using integration theorems
of Weyl to obtain (3.14) and (3.15), as in [Jac94], [GJ97], and [LZ04]: integra-
tion over a space of $N \times N$ matrices is replaced by integration over N-element
sets of eigenvalues of such matrices. The generalization to (3.19) is implicit in
[GJ97] and appears explicitly in [GHJ01], where Goulden, Harer, and Jackson
conjecture that it has a geometric interpretation. An indirect method is used in
Chapter 4 to verify a combinatorial interpretation of $M(N, \mathbf{y}, z; b)$, but there is no
apparent way to lift the approach to a representation involving matrix integrals,
and a combinatorial derivation of the generalized series remains elusive.

3.5.3   Motivation (The Ubiquity of b)

As a consequence of the varied approaches to map and hypermap enumeration,
the parameter b interpolates between several different classes of structures. With
a positive resolution of the Hypermap b-Conjecture, it might be possible to lift
the constructions used to derive the map and hypermap series to more gen-
eral settings. In addition to giving a new combinatorial interpretation to Jack
symmetric functions, a description of a b-invariant could potentially be used to
describe algebraic objects interpolating between $Z(\mathbb{C}[\mathfrak{S}_n])$ and $\mathscr{H}(\mathfrak{S}_{2n}, \mathfrak{B}_n)$, or
between $\mathcal{V}_N$ and $\mathcal{W}_N$. Strebel differentials link map enumeration to moduli
spaces of complex and real algebraic curves, and Goulden, Harer, and Jackson

conjecture, in [GHJ01], that b might appear as a parameter of an as yet unidentified interpolating space. Promisingly, only the symmetric-function-based derivation leads to the full Hypermap b-Conjecture, so the marginal b-invariant described in Chapter 4 might be sufficient for the remaining applications.

3.6 Approaching the Conjecture

Approaches to identifying a b-invariant fit into two broad categories. One approach relies on the principle that a b-invariant should be natural: from this perspective, it should be possible to search for combinatorial properties of maps, and then check which properties are manifested algebraically by M. A second approach involves finding algebraic properties of the series, and then interpreting the combinatorial implications of those properties. The first approach is used in Chapter 4 to construct a marginal b-invariant, and the second approach is used in Chapter 5 to verify that a degree bound predicted by Goulden and Jackson in [GJ96a] holds for all b-invariants.

The derivations in Section 3.5 do not provide an independent enumerative theory for non-orientable maps, though they can be enumerated as the complement of orientable maps within the class of locally orientable maps. It is more natural to consider maps on the Klein bottle and the torus, than to consider maps on the Klein bottle alone. If the b-Conjecture is true, then a b-invariant can be interpreted as a measure of non-orientability, and from the perspective of the enumerative theory of rooted maps, the classification theorem for surfaces presents a false dichotomy: though orientability is a binary concept, there are degrees of non-orientability. That it is more natural to study rooted maps for which the invariant is at most zero, than it is to study maps for which the invariant is at least one, suggests that the analysis implicitly uses a partial order with respect to which down-sets are more natural than up-sets. This is the basis for the assumption that root-edge deletion recursively decomposes a map into pieces that are each 'less non-orientable' than the original map, and motivates the description of the marginal b-invariants discussed in Chapter 4.

This Chapter concludes by examining some known b-polynomials. Elementary observations reveal some properties that cannot be satisfied by b-invariants, and provide a grounding for some of the assumptions made in later chapters. In particular, the non-existence result of Theorem 3.35 is new, and shows that an apparent deficiency of the invariant described in Chapter 4 is an essential property of b-invariants. The emphasis is on maps, but most of the statements also apply to hypermaps.

3.6.1 Dependence on Rooting

Since b-invariants are conjectured to measure non-orientability, and orientability is independent of rooting, it might be expected that some b-invariant is
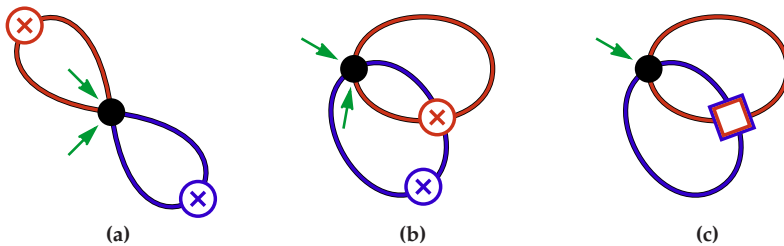
Figure 3.2: Rooted monopoles with two edges and one face

independent of rooting. Examining the coefficients of $c_{[4],[4],[2^2]}(b) = 1 + b + 3b^2$, obtained by direct computation, shows that this is not the case.

Theorem 3.30 (Goulden and Jackson [GJ96a])**.** *If there is a b-invariant of rooted maps, then it depends on rooting, and it is not an invariant of unrooted maps.*

Proof. The 5 rooted maps shown in Figure 3.2 are the only rooted maps with vertex-degree partition [4] and face-degree partition [4]. Since the rooted map in Figure 3.2c is orientable, it accounts for the constant term in $c_{[4],[4],[2^2]}(b)$, so the combined contribution of the rooted maps in Figures 3.2a and 3.2b to $c_{[4],[4],[2^2]}(b)$ is $b + 3b^2$. However, for *any* invariant of unrooted maps, the total contribution of these two maps to each term must be even. □

Remark 3.31. The presence of a linear term in $c_{[4],[4],[2^2]}(b)$ also shows that the parity of a b-invariant is not determined by the number of cross-caps used to construct the surface in which a map is embedded.

3.6.2 Known Values of b-Invariants

If $c_{v,\varphi,[2^n]} = ab^k$ is a monomial, then every b-invariant has value k for every rooted map with vertex-degree partition v and face-degree partition φ. Goulden and Jackson noted, in [GJ96a], that every known b-polynomial is either identically zero, or has degree equal to the Euler genus of the surfaces on which it is conjectured to enumerate maps. This bound is explored in more detail in Chapter 5. In the present context, it is sufficient to note that numerical evidence suggests that, when a b-invariant is evaluated at a rooted map in the projective plane, it takes the value 1. As a consequence, b-invariants do not depend on rooting for projective-planar maps. Besides planar and projective-planar maps, the only known maps for which all possible b-invariants can be uniquely determined are some embeddings in the Klein bottle; their corresponding b-polynomials are the monomials of degree 2 that are tabulated in Figure 3.2.

Of particular interest, the polynomial $c_{[4^2],[3,5],[2^4]}(b) = 8b^2$ corresponds to a unique map with face-degree partition $[4^2]$ and vertex-degree partition $[3, 5]$ (see [JV01, p. 125]), so all eight of its rootings, illustrated in Figure 3.3a, must
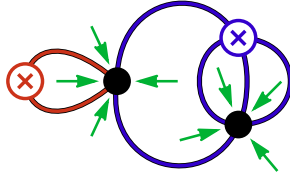
(a) $c_{[4^2],[3,5],[2^4]}(b) = 8b^2$
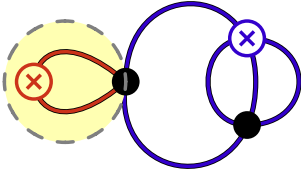
(b) A decomposition
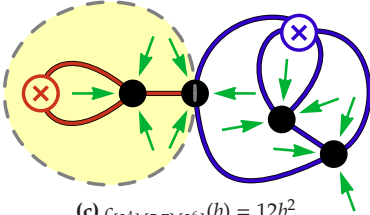
(c) $c_{[3^4],[5,7],[2^6]}(b) = 12b^2$

Figure 3.3: Rooted maps for which all b-invariants take the value two

Table 3.2: Degree 2 monomials

ν	φ	n	$c_{\nu,\varphi,[2^n]}(b)$
$[4^2]$	$[3,5]$	4	$8b^2$
$[3,5]$	$[4^2]$	4	$8b^2$
$[2,3,5]$	$[5^2]$	5	$30b^2$
$[5^2]$	$[2,3,5]$	5	$30b^2$
$[3^4]$	$[5,7]$	6	$12b^2$
$[4^3]$	$[3,4,5]$	6	$36b^2$
$[2^2,3,5]$	$[6^2]$	6	$60b^2$
$[3,4,5]$	$[4^3]$	6	$36b^2$
$[6^2]$	$[2^2,3,5]$	6	$60b^2$
$[5,7]$	$[3^4]$	6	$12b^2$
$[2^3,3,5]$	$[7^2]$	7	$126b^2$
$[7^2]$	$[2^3,3,5]$	7	$126b^2$
$[1,3^5]$	$[8^2]$	8	$48b^2$
$[4^4]$	$[3,4^2,5]$	8	$96b^2$
$[4^4]$	$[1,5^3]$	8	$48b^2$
$[4^4]$	$[1,3,6^2]$	8	$144b^2$
$[4^4]$	$[3^3,7]$	8	$16b^2$
$[4^4]$	$[2^2,5,7]$	8	$112b^2$
$[2^4,3,5]$	$[8^2]$	8	$192b^2$
$[3,4^2,5]$	$[4^4]$	8	$96b^2$
$[1,5^3]$	$[4^4]$	8	$48b^2$
$[1,3,6^2]$	$[4^4]$	8	$144b^2$
$[3^3,7]$	$[4^4]$	8	$16b^2$
$[2^2,5,7]$	$[4^4]$	8	$112b^2$
$[8^2]$	$[1,3^5]$	8	$48b^2$
$[8^2]$	$[2^4,3,5]$	8	$192b^2$

have weight two with respect to every b-invariant. The map is notable for the fact that it can be decomposed as the connected sum of two maps on the projective plane: see Figure 3.3b. The other monomials in the list appear to enumerate other maps with the same property, and this provides numerical evidence that it may be possible to construct a b-invariant that is additive with respect to connected sums: for example, the twelve rootings of the map in Figure 3.3c are enumerated by $c_{[3^4],[5,7],[2^6]}(b) = 12b^2$, and the underlying map can be decomposed as the connected sum of two maps on the projective plane in two different ways, one of which is indicated.

Brown and Jackson approached the problem of describing a b-invariant by working with edge-labelled maps. In [BJ07], they introduced a candidate invariant and showed that, for edge-labelled maps, it is additive with respect to

connected sums. Because b-invariants are necessarily dependent on rooting (recall Theorem 3.30), it is not clear how to define additivity with respect to connected sums for unlabelled rooted maps, so a weaker property, satisfied by all 'reasonable' forms of additivity, is used in the following conjecture.

Conjecture 3.32. *There is a b-invariant β such that if $\mathfrak{m}$ is a rooted map that can be decomposed as the connected sum of smaller maps so that there are k non-orientable pieces, and so that the total genus of the non-orientable pieces is g_n, then $k \le \beta(\mathfrak{m}) \le g_n$.*

3.6.3 Symmetry Breaking

The combinatorial definition of maps exhibits several symmetries, but it is impossible for a b-invariant to respect all of these symmetries. This is reminiscent of modern particle physics, where explaining broken symmetries in apparently symmetric systems has been a notable theme of the past century, and interesting because several problems in map enumeration arose from physical models. The theme of symmetry breaking is revisited in the context of the q-Conjecture in Section 7.5.

From Definition 2.36, a combinatorial map can be represented as a triple, $\mathfrak{m} = (\tau_v, \tau_e, \tau_f)$, of fixed-point-free involutions, and the definition of hypermaps is symmetric with respect to these three involutions. Using the convention that a root is indicated by an arrow pointing from a face to a vertex, reflection acts by replacing the root flag with its image under the action of τ_e. Since τ_v, τ_e, and τ_f act transitively on the flags of a hypermap, any function that is constant under the action of all three involutions cannot depend on rooting, and thus, by Theorem 3.30, cannot be a b-invariant.

For maps, only the conditions on τ_v and τ_f are symmetric, but if additivity is required, in the sense of Conjecture 3.32, then a b-invariant cannot even be constant under the action of τ_e. If β is an additive b-invariant, then the two rooted maps in Figure 3.4 have different weights with respect to β. Since the two diagrams are related by reflection, it follows that additive b-invariants exhibit a form of chirality with respect to this representation of rooting. The symmetry between τ_v and τ_f corresponds to duality, and is discussed in the next section.
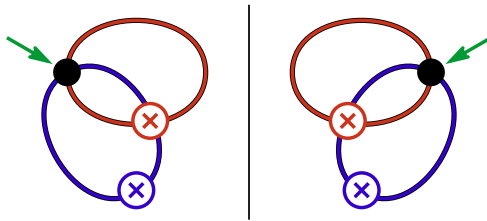
Figure 3.4: These rooted maps, with diagrams related by reflection across a vertical line, have different weights with respect to every additive b-invariant.

3.6.4 Duality

The map series is symmetric with respect to **x** and **y**. A combinatorial interpretation is that, if β is a b-invariant, then there is a bijection acting on the class of rooted maps that interchanges vertex- and face-degree partitions while preserving β. This is not necessarily true of marginal b-invariants. In both the $b = 0$ and $b = 1$ cases, duality is one such bijection, and it might be expected that duality explains the symmetry in the case of arbitrary b. This leads to the following conjecture.

Conjecture 3.33. *There is a b-invariant, β, such that for every map $\mathfrak{m}$, the rootings of $\mathfrak{m}$ and the rootings of the dual of $\mathfrak{m}$ have the same multi-set of values with respect to β.*

The conjecture intentionally avoids specifying a particular form of rooted duality. In fact, it is not obvious how the concept of duality, inherently a relationship between unrooted maps, should be extended to rooted maps. The natural choice, using the bijection between the flags of a map and the flags of its dual that is induced by exchanging M_v with M_f in the matching representation, is not the unique choice, and it is immediately shown to be inconsistent with additivity.

Example 3.34. *Figure 3.5 gives the maps from Figure 3.2 superimposed with their duals, and shows that every map with vertex-degree partition [4] and face-degree partition [4] is self-dual. Suppose β satisfies the conclusion of Conjecture 3.32, then it would follow, by additivity, that Figure 3.5b has one rooting with weight 1 and one rooting with weight 2, with respect to β. But in this map, the two equivalence classes of flags are distinguished by whether they lie on an orientation-preserving edge, or on an orientation-reversing edge, and duality exchanges these two classes.*

It would appear that an alternate form of rooted duality is required, but even this is not sufficient to provide compatibility with additivity. Somewhat surprisingly, the conclusions of Conjectures 3.32 and 3.33 cannot be satisfied by the same invariant.

Theorem 3.35. *A b-invariant cannot be both additive with respect to connected sums, and invariant under any form of rooted duality that is a refinement of unrooted duality.*
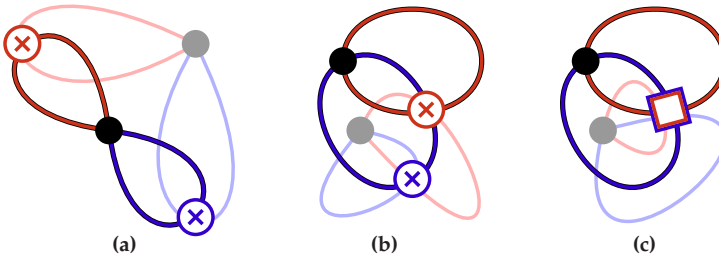
Figure 3.5: Monopoles with $\nu = [4]$ and $\varphi = [4]$ superimposed with their duals.
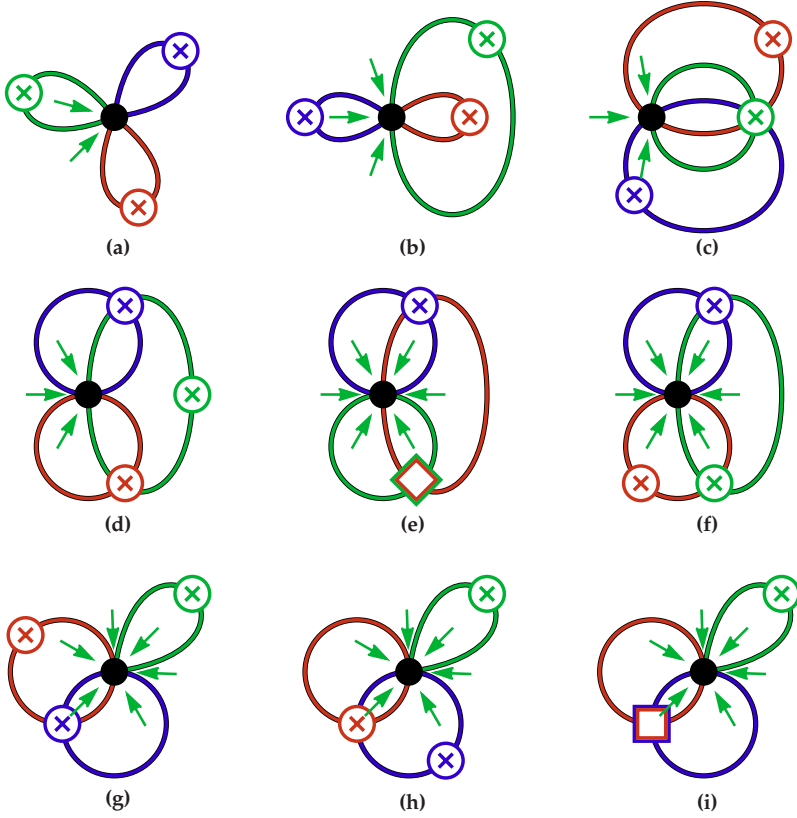
Figure 3.6: Rooted monopoles with three edges and one face

Proof. Let β be a b-invariant that is additive in the sense of Conjecture 3.32. There are 41 rooted maps with three edges, one vertex, and one face, and the corresponding b-polynomial is $c_{[6],[6],[2^3]}(b) = 13b + 13b^2 + 15b^3$. The maps are given in Figure 3.6. With an illustration inheriting a local orientation from its drawing, Figures 3.6g and 3.6h give the same unrooted map.

Of the eight maps, those given in Figures 3.6a, 3.6b, 3.6g=3.6h, and 3.6i are self-dual. By additivity, the invariant is independent of rooting for Figures 3.6a, 3.6b, and 3.6i, which contribute a total of $6b + 5b^3$ to the sum. Since Figure 3.6g=3.6h is a connected sum of two non-orientable maps, it cannot contribute to the linear term. This means that precisely $13 - 6 = 7$ rootings of the remaining 4 maps have weight 1 with respect to β.

Figure 3.7 shows that Figures 3.6c and 3.6d give dual maps, while Figure 3.8 shows that Figures 3.6e and 3.6f give dual maps. So if β is invariant under duality, then the rootings given in Figures 3.6c, 3.6d, 3.6e, and 3.6f must make an even contribution to each term of $c_{[4],[4],[2^4]}(b)$. Since 7 is not even, it follows that β is not invariant under duality, in the sense of Conjecture 3.33. □
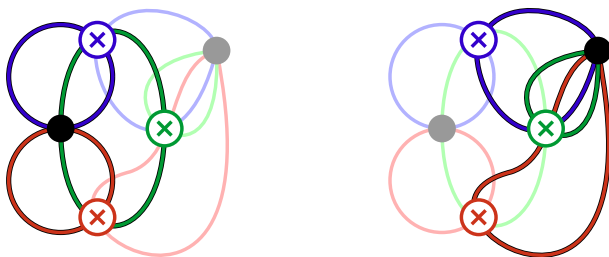
Figure 3.7: The maps in Figures 3.6c and 3.6d are duals with three rootings each.
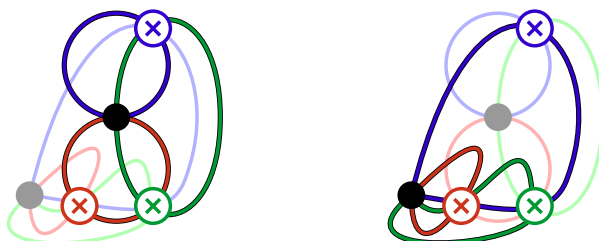
Figure 3.8: The maps in Figures 3.6e and 3.6f are duals with six rootings each.

Remark 3.36. The contradiction used in the proof of Theorem 3.35 involves two pairs of dual maps. Tiled representations of these maps are superimposed with their duals in Figure 3.9, but this representation does not suggest any structural reasons that at least one of the maps is not invariant under duality with respect to every b-invariant that is additive in the sense of Conjecture 3.32.

Remark 3.37. Since $c_{[6],[6],[2^3]}(b) = d_{1,[6]}(b)$, Theorem 3.35 also applies to marginal b-invariants, although in this setting it is less clear that invariance under duality should be expected. The marginal b-invariants described in Chapter 4 were constructed without any consideration given to duality invariance.

3.7 Summary

This Chapter introduced the b-Conjecture, a conjecture that posits the existence of a combinatorial interpretation for the algebraic generalization of two generating series. The enumerative techniques leading to the conjecture were discussed, and several elementary observations were used to examine the nature of the b-invariants that are needed to resolve it.
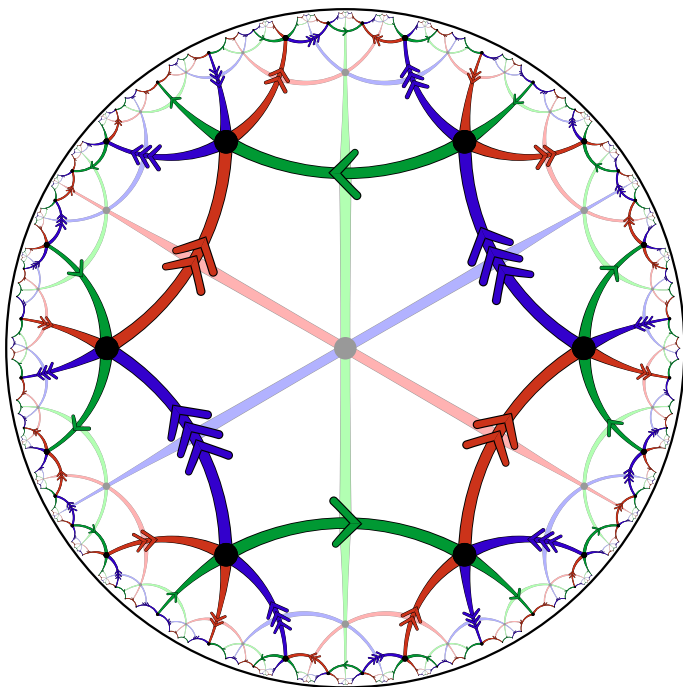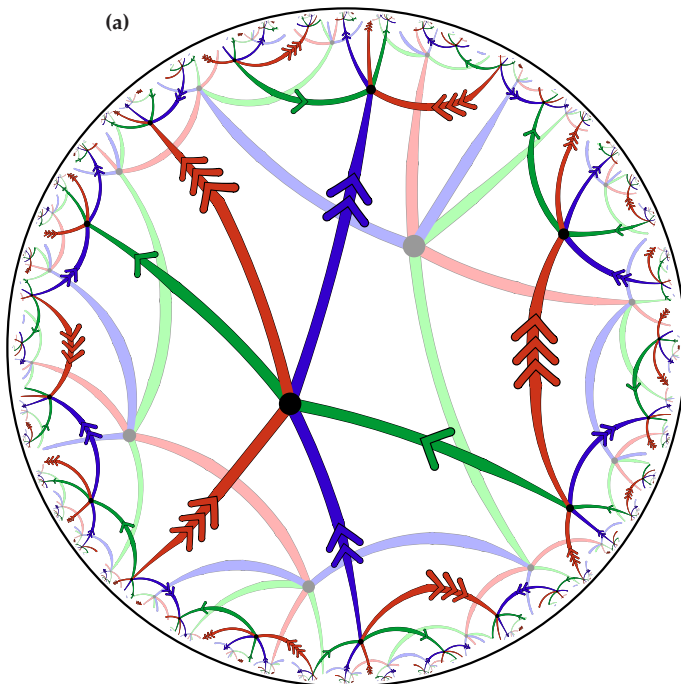
Figure 3.9: Tiled representations of Figures 3.6c and 3.6d are superimposed in (a), and tiled representations of Figures 3.6e and 3.6f are superimposed in (b).

Chapter 4

A Marginal b-Invariant

Theorem 4.16, the main result of this Chapter, resolves Conjecture 3.23, the Marginal b-Conjecture, by introducing a family of new invariants, and showing that each of the new invariants is a marginal b-invariant. These new invariants are defined inductively in terms of root-edge deletion, and are more easily analyzed than a similar invariant introduced by Brown and Jackson in [BJ07]. Their invariant is defined in terms of directed maps with edge labels, and its description for rooted maps uses the rooting to construct a canonical edge-labelling. They analyzed the invariant in terms of the associated exponential generating series for edge-labelled multi-component maps, but were unable to determine whether or not they had defined a marginal b-invariant.

Since the new invariants are defined in terms of root-edge deletion, it is possible to work directly with rooted maps, and this reveals a partial differential equation, (4.2), that is satisfied by a generating series for rooted maps, with respect to each of the new invariants. To obtain the partial differential equation, the generating series must be refined to distinguish between the degree of the root face and the degrees of non-root faces. Conjecture 4.9 is used to predict the analogous refinement for the algebraic form of the map generating series. The two series are identified by showing that the algebraically defined series also satisfies (4.2), and that the partial differential equation has a unique solution.

By resolving the Marginal b-Conjecture, this Chapter provides a concrete link between the Jack parameter and the topology of rooted maps. In particular, each of the new invariants gives a combinatorial interpretation to all terms of M that correspond to monopoles. An analysis of the new invariants reveals structural properties of marginal b-polynomials: Theorem 4.22 gives a strengthened form of non-negativity for the coefficients of marginal b-polynomials, and this reveals a combinatorial interpretation for the series $M(-x, -\mathbf{y}, -z; -1)$. These properties are extended to all b-polynomials in Chapter 5. The new invariants are conjectured to be b-invariants, and this possibility is examined in Chapter 6. The framework developed in this Chapter is used in Chapter 7 to explore another enumerative conjecture involving rooted maps.

4.1 The Invariants

Definition 4.1. *For a rooted map $\mathfrak{m}$, an invariant $\eta(\mathfrak{m})$ is defined inductively as follows.*

1. *If $\mathfrak{m}$ has no edges, then $\eta(\mathfrak{m}) = 0$.*

2. *Otherwise $\mathfrak{m}$ has a root edge e, and this edge can be deleted to produce one or two rooted maps with fewer edges, as described in Section 2.4.*

   (a) *If e is a* bridge *of $\mathfrak{m}$, then deleting e decomposes $\mathfrak{m}$ into two rooted components $\mathfrak{m}_1$ and $\mathfrak{m}_2$, and $\eta(\mathfrak{m}) = \eta(\mathfrak{m}_1) + \eta(\mathfrak{m}_2)$.*

   (b) *Otherwise, deleting e from $\mathfrak{m}$ leaves a single rooted map $\mathfrak{m}'$. The number of faces of $\mathfrak{m}'$ differs from the number of faces of $\mathfrak{m}$ by at most one.*

      i. *If $\mathfrak{m}'$ has one fewer face than $\mathfrak{m}$, then e is a* border, *and $\eta(\mathfrak{m}) = \eta(\mathfrak{m}')$.*

      ii. *If $\mathfrak{m}'$ has the same number of faces as $\mathfrak{m}$, then e is a* cross-border, *and $\eta(\mathfrak{m}) = \eta(\mathfrak{m}') + 1$.*

      iii. *If $\mathfrak{m}'$ has one more face than $\mathfrak{m}$, then e is a* handle. *There is a second map $\tau(\mathfrak{m})$ obtained from $\mathfrak{m}$ by twisting the ribbon associated with e. The edge e is also a handle of $\tau(\mathfrak{m})$, and deleting e from $\tau(\mathfrak{m})$ also produces $\mathfrak{m}'$. In this case,*

      $$\{\eta(\mathfrak{m}), \eta(\tau(\mathfrak{m}))\} = \{\eta(\mathfrak{m}'), \eta(\mathfrak{m}') + 1\}.$$

      At most one of $\mathfrak{m}$ and $\tau(\mathfrak{m})$ is orientable, and for the present purpose, it is sufficient to allow any canonical choice such that if $\mathfrak{m}$ is orientable, then $\eta(\mathfrak{m}) = 0$ and $\eta(\tau(\mathfrak{m})) = 1$.

Definition 4.2 (twisted). *For a map $\mathfrak{m}$ with root edge e, the edge e is said to be* twisted *if it is not a bridge and $\eta(\mathfrak{m}) = \eta(\mathfrak{m}\backslash e) + 1$.*

Using this terminology, $\eta(\mathfrak{m})$ is the number of twisted edges encountered when $\mathfrak{m}$ is decomposed using iterated root-edge deletion. The definition of η is ambiguous; when the root edge is a handle, 2(b)iii does not specify which of $\mathfrak{m}$ and $\tau(\mathfrak{m})$ has the twisted rooting, unless $\mathfrak{m}\backslash e$ is orientable. Each choice produces a distinct invariant, but in the present context, every choice produces the same enumerative result, so for now, η represents a family of related invariants. The definition can be made concrete by defining twisting relative to any canonically constructed spanning tree, but this is not necessary, and a discussion of particular invariants is deferred to Section 6.4.

Remark 4.3. Though the description of η is combinatorial, its definition is motivated by topological considerations. Handles, borders, and cross-borders can be distinguished by topological properties related to map duality. To see this, work in the ribbon graph model for maps, as described in Section 2.2.3, and consider the ribbon graph representing the dual of a rooted map. The space T, formed by the union of the root edge and its vertices is homeomorphic to a
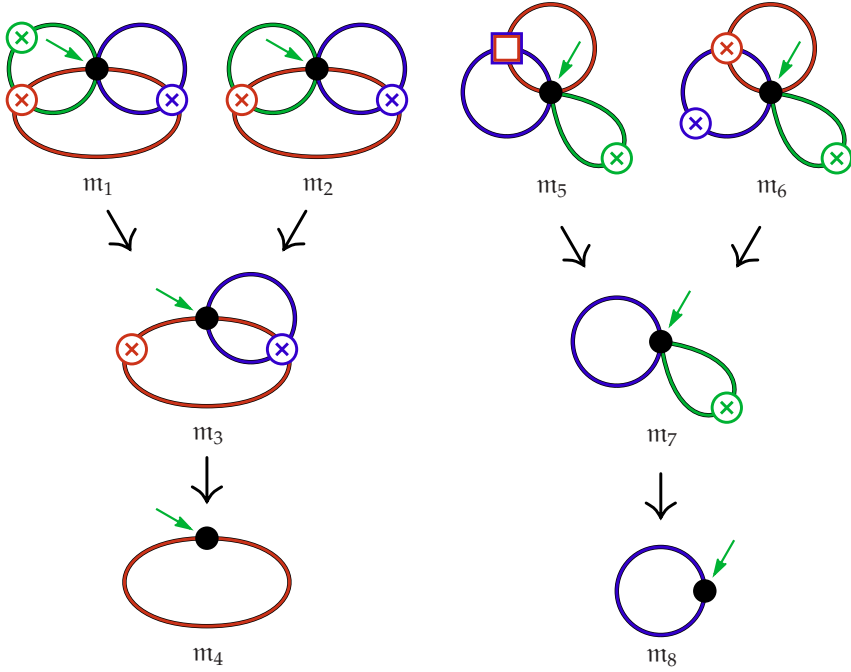
Figure 4.1: Root-edge deletion is used to compute η.

Möbius strip, an open disc, or a cylinder. If T is a Möbius strip, then the root edge is a cross-border. If T is a disc, then the root edge is a border. Otherwise, T is a cylinder, and the root edge is either a handle or bridge. These final two cases are distinguished by considering the connectivity of the complement of T in the surface in which the map is embedded. A further topological link is the following degree bound.

Theorem 4.4. *If $\mathfrak{m}$ is a map on the surface Σ, then $\eta(\mathfrak{m}) = 0$ if Σ is orientable, and $1 \le \eta(\mathfrak{m}) \le k$ if Σ is the sphere with k cross-caps.*

Proof. If iterated root-edge deletion of $\mathfrak{m}$ encounters b borders, c cross-borders, r bridges, and h handles, then $\mathfrak{m}$ has $r+1$ vertices, $b-h+1$ faces, and $b+c+r+h$ edges. It follows that the Euler characteristic of Σ is $(r+1)-(b+c+r+h)+(b-h+1) = 2-c-2h$ and $c \le \eta(\mathfrak{m}) \le c+h \le c+2h$. $\qquad\square$

The same bound was shown by Brown and Jackson in [BJ07] to hold for their invariant, and the analogous degree bound was conjectured for b-polynomials by Goulden and Jackson in [GJ96a]. In Chapter 5, Corollary 5.24 shows that the bound is satisfied by all b-invariants.

Example 4.5. *Consider the rooted maps $\mathfrak{m}_1$ and $\mathfrak{m}_2$ given in Figure 4.1, with 1 and 2 faces respectively. Deleting the root edge of either, leaves $\mathfrak{m}_3$, which has 1 face. It*

follows that the root edge of $\mathfrak{m}_1$ is a cross-border, and that the root edge of $\mathfrak{m}_2$ is a border. Deleting the root edge of $\mathfrak{m}_3$ leaves $\mathfrak{m}_4$, and increases the number of faces from 1 to 2, so the root edge of $\mathfrak{m}_3$ is a handle. Since $\tau(\mathfrak{m}_3)$ is orientable, $\eta(\mathfrak{m}_3) = \eta(\mathfrak{m}_4) + 1$. The root edge of $\mathfrak{m}_4$ is a border, so since its deletion leaves a map with no edges, $\eta(\mathfrak{m}_4) = 0$. It follows, by back substitution, that $\eta(\mathfrak{m}_3) = \eta(\mathfrak{m}_4) + 1 = 1$, $\eta(\mathfrak{m}_2) = \eta(\mathfrak{m}_3) = 1$, and $\eta(\mathfrak{m}_1) = \eta(\mathfrak{m}_3) + 1 = 2$.

Example 4.6. *Each of $\mathfrak{m}_5$ and $\mathfrak{m}_6$, also given in Figure 4.1, has 1 face. Deleting the root edge of either leaves $\mathfrak{m}_7$, which has 2 faces. It follows that the root edges of both $\mathfrak{m}_5$ and $\mathfrak{m}_6$ are handles, and that $\{\eta(\mathfrak{m}_5), \eta(\mathfrak{m}_6)\} = \{\eta(\mathfrak{m}_7), \eta(\mathfrak{m}_7) + 1\}$. Deleting the root edge of $\mathfrak{m}_7$ leaves $\mathfrak{m}_8$, which also has 2 faces, so the root edge of $\mathfrak{m}_7$ is a cross-border. Since $\mathfrak{m}_8$ is orientable, $\eta(\mathfrak{m}_8) = 0$. It follows, by back substitution, that $\eta(\mathfrak{m}_7) = \eta(\mathfrak{m}_8) + 1 = 1$, and that $\{\eta(\mathfrak{m}_5), \eta(\mathfrak{m}_6)\} = \{1, 2\}$. Since neither $\mathfrak{m}_5$ nor $\mathfrak{m}_6$ is orientable, the values of $\eta(\mathfrak{m}_5)$ and $\eta(\mathfrak{m}_6)$ depend on the particular invariant, but if η is chosen to be additive, in the sense of Conjecture 3.32, then $\eta(\mathfrak{m}_5) = 1$.*

As with the invariant of Brown and Jackson from [BJ07], each invariant η is dependent on rooting, with the rooting of a map being used to define a deletion order on its edges. For a given deletion order, η uses effectively the same deletion types and interpretations as its precursor, but the number of cases is reduced from 9 to 4 by not excluding the rooted map with no edges and by treating all handles uniformly. The key difference between the invariants is the order in which edges are deleted. In contrast to the work of Brown and Jackson, no attempt is made to specify the relative deletion order for edges in different components after the deletion of a bridge, so η is defined in terms of a partial order induced by the rooting. An advantage of this approach is that inductive analysis is localized to the root face. In particular, by deleting the root edge first, instead of last, it becomes possible to analyze a refined combinatorial sum that records the degree of the root face.

4.2 A Partial Differential Equation

Brown and Jackson suggested, in [BJ07], that finding a partial differential equation satisfied by the map generating series would be a key tool for linking a combinatorial sum to the algebraically defined map series. In the case of η, the generating series for maps is refined to mark the root face separately from non-root faces. This leads to a differential equation arising from a recurrence with non-negative integer coefficients. Using cues from the $b = 0$ and $b = 1$ cases, the corresponding algebraic refinement is identified and shown to satisfy the same partial differential equation.

Consider the combinatorial sum M defined by

$$M = M(x, \mathbf{y}, z, \mathbf{r}; b) := \sum_{\mathfrak{m} \in \mathcal{M}} x^{|V(\mathfrak{m})|} \mathbf{y}^{\varphi(\mathfrak{m}) \smallsetminus r(\mathfrak{m})} z^{|E(\mathfrak{m})|} r_{\rho(\mathfrak{m})} b^{\eta(\mathfrak{m})}, \qquad (4.1)$$

where the sum is taken over all rooted maps, including the map with no edges, $V(\mathfrak{m})$ is the vertex set of $\mathfrak{m}$, $\varphi(\mathfrak{m})$ is the face-degree partition of $\mathfrak{m}$, $\rho(\mathfrak{m})$ is the degree of the root face of $\mathfrak{m}$, and $E(\mathfrak{m})$ is the edge set of $\mathfrak{m}$. This sum refines the generating series appearing in Conjecture 3.23, by treating the root face as qualitatively different from other faces with the same degree. Corollary 4.17 justifies the notational abuse by showing that

$$M(x, \mathbf{y}, z, \mathbf{y}; b) = xy_0 + M(x\mathbf{1}, \mathbf{y}, z; b),$$

where the first series is the combinatorial sum from (4.1), and the second series is the algebraically defined map series of (3.12). The present proof relies on Theorem 3.18 for evaluating the maps series, and cannot be extended to include the vertex degrees.

Lemma 4.7. *The combinatorial sum M, given in* (4.1), *satisfies the partial differential equation for f:*

$$
\begin{aligned}
f = r_0 x &+ z \sum_{i \geq 0} (i+1) b r_{i+2} \frac{\partial}{\partial r_i} f + z \sum_{i \geq 0} \sum_{j=1}^{i+1} r_j y_{i-j+2} \frac{\partial}{\partial r_i} f \\
&+ z \sum_{i,j \geq 0} (1+b) j r_{i+j+2} \frac{\partial^2}{\partial r_i \partial y_j} f + z \sum_{i,j \geq 0} r_{i+j+2} \left(\frac{\partial}{\partial r_i} f \right) \left(\frac{\partial}{\partial r_j} f \right).
\end{aligned}
\tag{4.2}
$$

Proof. The map with no edges is enumerated by $r_0 x$, and each sum corresponds to one deletion type for the root edge. The proof proceeds by induction on the number of edges in a rooted map, examining in turn the contributions from each type of root edge.

Given a map $\mathfrak{m}$ with root-face degree i, a *cross-border* can be added as the root edge in any of $i + 1$ ways. The second end can be attached to any of the i, counting multiplicities, vertices on the boundary of the root face, and a loop has two distinct rootings. The following figure illustrates this schematically.
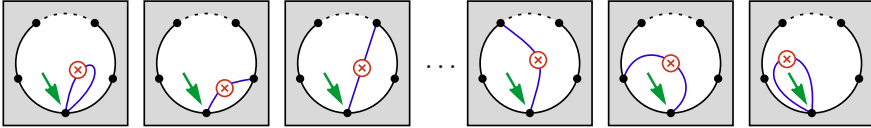
Each resulting map has root-face degree $i + 2$ and weight $\eta(\mathfrak{m}) + 1$ with respect to η. Every cross-border-rooted map is obtained in this way precisely once, so such maps are enumerated by

$$z \sum_{i \geq 0} (i+1) b r_{i+2} \frac{\partial}{\partial r_i} M.$$

Similarly, using the same end points with untwisted root edges, a *border* can be added in $i + 1$ ways. The following figure illustrates this schematically.
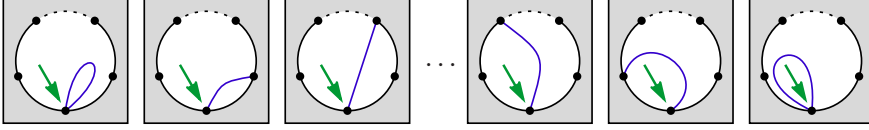
Each resulting map has one more face than $\mathfrak{m}$. The degrees of the two new faces sum to $i + 2$, with the root faces taking each degree in the range 1 to $i + 1$ inclusive precisely once. It follows that border-rooted maps are enumerated by

$$z \sum_{i \geq 0} \sum_{j=1}^{i+1} r_j y_{i-j+2} \frac{\partial}{\partial r_i} M.$$

A *handle* can be added as the root edge by picking an end for the edge on any non-root face and either twisting the ribbon or not. If the chosen non-root face has degree j, then the end point can be selected in j ways. Each end point can be used to attach a twisted handle and an untwisted handle. The resulting root face has degree $i + j + 2$. This is illustrated schematically in the following figure.
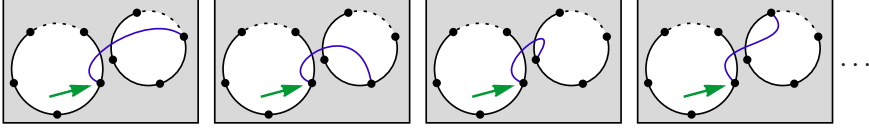
The sum is independent of the canonical choice made in the definition of η, since precisely one of $\mathfrak{m}$ and $\tau(\mathfrak{m})$ contributes to each of

$$z \sum_{i,j \geq 0} j r_{i+j+2} \frac{\partial^2}{\partial r_i \partial y_j} M \qquad \text{and} \qquad z b \sum_{i,j \geq 0} j r_{i+j+2} \frac{\partial^2}{\partial r_i \partial y_j} M.$$

When the roots of two maps $\mathfrak{m}_1$ and $\mathfrak{m}_2$ with respective root-face degrees i and j are joined by a bridge, the boundary of the root face of the resulting map contains the boundaries of both $\mathfrak{m}_1$ and $\mathfrak{m}_2$ together with the new root edge, which occurs twice. The new map has root-face degree $i + j + 2$, as in the following figure.
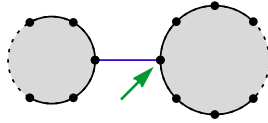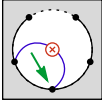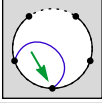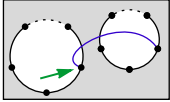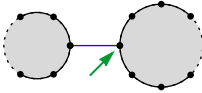
Since every bridge-rooted map is produced in this way precisely once, such maps are enumerated by

$$z \sum_{i,j \geq 0} r_{i+j+2} \left(\frac{\partial}{\partial r_i} M \right) \left(\frac{\partial}{\partial r_j} M \right).$$

The cases partition all root-edge types, and this completes the proof. $\qquad\square$

Remark 4.8. The root-edge types and their contributions to M are summarized

Table 4.1: The contribution to M from maps with each root-edge type

Root-edge type	Schematic	Contribution to M
Cross-border		$z \sum_{i \geq 0} (i+1) b r_{i+2} \dfrac{\partial}{\partial r_i} M$
Border		$z \sum_{i \geq 0} \sum_{j=1}^{i+1} r_j y_{i-j+2} \dfrac{\partial}{\partial r_i} M$
Handle		$z \sum_{i,j \geq 0} (1+b) j r_{i+j+2} \dfrac{\partial^2}{\partial r_i \partial y_j} M$
Bridge		$z \sum_{i,j \geq 0} r_{i+j+2} \left(\dfrac{\partial}{\partial r_i} M \right) \left(\dfrac{\partial}{\partial r_j} M \right)$

in Table 4.1. Since the proof of Lemma 4.7 does not involve edge-labelled maps, the classification might be useful in the analysis of the q-Conjecture, as discussed in Chapter 7.

4.3   A Refined b-Conjecture

Finding an analytic solution to (4.2) requires refining the map series, M, to record the degree of the root face. For $b = 0$ and $b = 1$, since a map can be re-rooted at any flag without changing its orientability, this is accomplished by replacing $2z \frac{\partial}{\partial z}$ with $\sum_{j \geq 1} j r_j \frac{\partial}{\partial y_j}$ in (3.13), the definition of the series. The justification is not valid for general values of b, since Theorem 3.30 shows that b-invariants depend on rooting, but numerical evidence suggests that the substitution remains combinatorially meaningful in this more general setting. As a special case, Corollary 4.20 shows that the substitution maintains its combinatorial interpretation for general values of b when the series is specialized at $x_i = x$ for all i. The validity of a similar substitution in (3.4), the definition of H, has not been investigated.

With the assumption that the coefficients of the map series are polynomials in b, the Maple worksheet in Section B.4 of Appendix B was used to compute the map series up to coefficients of z^8. That the validity of this computation depends only on the assumption of polynomiality, is a consequence of Corollary 5.22. Applying the substitution to the definition of the resulting series produces a polynomial with $130,044$ terms, each monomial of which has a coefficient that is a non-negative integer. This provides numerical evidence for the following
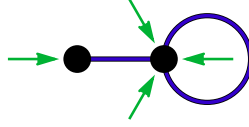
Figure 4.2: The unique map with $\varphi = \nu = [1,3]$

refinement of the *b*-Conjecture.

Conjecture 4.9 (Refined *b*-Conjecture). *When* $2z\frac{\partial}{\partial z}$ *is replaced with* $\sum_{j\geq 1} jr_j\frac{\partial}{\partial y_j}$ *in the definition of the map series, the coefficients of the resulting series,*

$$(1+b)\sum_{j\geq 1} jr_j\frac{\partial}{\partial y_j}\ln\sum_{\substack{n\geq 0 \\ \theta \vdash 2n}} z^n\frac{J_\theta(\mathbf{x};1+b)J_\theta(\mathbf{y};1+b)}{\langle J_\theta, J_\theta\rangle_{1+b}}\left[p_{[2^n]}\right]J_\theta(1+b)\Bigg|_{\substack{p_i(\mathbf{x})=x_i \\ p_i(\mathbf{y})=y_i}}\forall i,$$

are non-negative integers. Furthermore, there is an interpretation for this refined series as a generating series for maps with r_i *marking a root face of degree i.*

A proof of this conjecture would explain why many *b*-polynomials for *n*-edge maps are multiples of 2*n*. In particular, by considering the action of the differential operators, the refinement predicts that

$$\frac{i\,m_i(\varphi)}{2n}c_{\nu,\varphi,[2^n]}(b)\in\mathbb{Z}_+[b]$$

for every part *i* of φ. It would follow from the symmetry between **x** and **y** that

$$c_{\nu,\varphi,[2^n]}(b)\in\frac{2n}{\gcd\{i\gcd(m_i(\nu),m_i(\varphi))\}_{i\in\mathbb{Z}_+}}\mathbb{Z}_+[b].$$

Combinatorially, the conjecture is a statement that, among all maps with specified vertex- and face-degree partitions, there is no correlation between the degree of the root face and the value of η. The obvious combinatorial explanation for this property, that η is independent of rooting, is *false*.

By duality, the series can be refined instead to record the degree of the root vertex, but there is no apparent algebraic operation that refines the series to simultaneously record the degrees of both the root face and the root vertex. Without a simultaneous refinement, an analysis of Conjecture 4.9 must be asymmetrical with respect to vertices and faces, and this asymmetry partially explains the difficulties inherent in analyzing the behaviour of η with respect to duality.

One obstacle to simultaneous refinement is that, among maps with given vertex- and face-degree partitions, the degrees of the root vertex and root face are correlated, even in the case of orientable maps. In particular, Figure 4.2 gives the rooted maps with $\nu = \varphi = [1,3]$, and every rooting on a vertex of degree 1 is on a face of degree 3. As a result, any algebraic operation
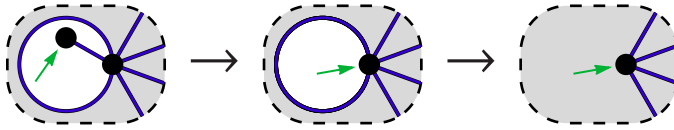
Figure 4.3: A rooted map with root-vertex degree 1 and root-face degree 3

$$2b^2 \qquad\qquad b + b^2 \qquad\qquad 1$$
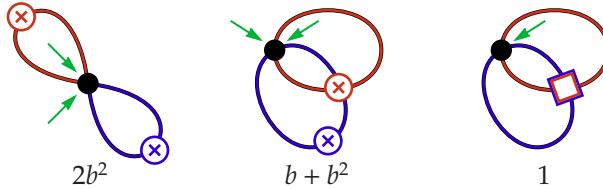
Figure 4.4: The weights with respect to η of the five rooted maps with $\nu = \varphi = [4]$

that simultaneously refines the map series to record root-face and root-vertex degrees cannot act independently on **x** and **y**. In fact, no linear operator can carry out the simultaneous refinement.

Theorem 4.10. *There is no operator that acts linearly on b-polynomials to produce refined polynomials that record the degrees of both the root vertex and the root face.*

Proof. Consider the polynomial $c = c_{[1,7],[3,5],[2^4]}(b) = 16 + 16b + 64b^2$. Any linear operator acting on c produces coefficients in the ratio $1 : 1 : 4$, but there are precisely five rooted maps with $\nu = [1,7]$ and $\varphi = [3,5]$ that are rooted on a vertex of degree 1 and a face of degree 3. To see this, note that deleting the root edge of such a map leaves a rooted map with $\nu = [6]$, $\varphi = [1,5]$, and root-face degree 1. Deleting the root edge of the resulting map leaves a rooted map with $\nu = [4]$ and $\varphi = [4]$. The root-deletion process is illustrated in Figure 4.3, and the resulting maps are given in Figure 4.4. Since five maps cannot have weights occurring in the ratio $1 : 1 : 4$, the result follows. $\qquad\square$

Remark 4.11. The choice of $\nu = [1,7]$ and $\varphi = [3,5]$ was arrived at by algebraic considerations. Assuming that Conjecture 4.9 holds, it follows from Corollary 5.22 that a refinement is possible for all polynomials corresponding to maps with a single vertex, a single face, or Euler genus less than two.

Example 4.12. *After two root-edge deletions, the five maps used in the proof correspond to the maps enumerated by $c_{[4],[4],[2^2]}(b) = 1 + b + 3b^2$. With respect to η, their weights are given in Figure 4.4.*

As a consistency check, among rooted maps with $\nu = [1,7]$ and $\varphi = [3,5]$, there are seven *rooted maps with root-vertex degree 1 and root-face degree 5. After a single root-edge deletion, they correspond to the rooted maps enumerated by $c_{[6],[3^2],[2^3]}(b) = 1 + b + 5b^2$. These maps are given, together with their weights with respect to η, in Figure 4.5.*

$$b + 2b^2 \qquad\qquad 3b^2 \qquad\qquad 1$$
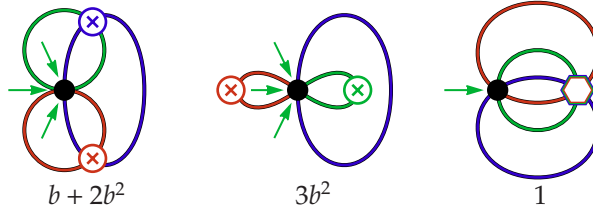
Figure 4.5: Seven rooted maps with $\nu = [1, 7]$ and $\varphi = [3, 5]$

Together, these twelve *rooted maps are the only rooted maps with vertex-degree partition $\nu = [1, 7]$, face-degree partition $\varphi = [3, 5]$, and root-vertex degree 1. Since $(1 + b + 5b^2) + (1 + b + 3b^2) = \frac{1}{8}(16 + 16b + 64b^2)$, this is consistent with the prediction of Conjecture 4.9.*

4.4 Solving the Equation

Assuming Conjecture 4.9, the Refined b-Conjecture, the solution to the partial differential equation (4.2) is given in terms of the expectation operators of Section 3.3.1 by replacing $2z\frac{\partial}{\partial z}$ with $\sum_{j\geq 1} jr_j\frac{\partial}{\partial y_j}$ in the expression

$$M = (1 + b)2z\frac{\partial}{\partial z}\ln\frac{\langle 1\rangle_e}{\langle 1\rangle},$$

as given in Corollary 3.19. Recall from Definition 3.17 that

$$\langle f\rangle := \int_{\mathbb{R}^N} |V(\lambda)|^{\frac{2}{1+b}} f(\lambda)\mathrm{e}^{-\frac{1}{2(1+b)}p_2(\lambda)}\mathrm{d}\lambda \quad \text{and} \quad \langle f\rangle_e := \left\langle f(\lambda)\mathrm{e}^{\frac{1}{1+b}\sum_{k\geq 1}\frac{1}{k}y_k p_k(\lambda)\sqrt{z}^k}\right\rangle,$$

so $\frac{\partial}{\partial y_j}\langle 1\rangle_e = \frac{1}{j(1+b)}\left\langle p_j\sqrt{z}^j\right\rangle_e$. Since the set of indeterminates is finite, it is convenient, for this Section, to use the convention that $p_0(\lambda) = \sum_{i=1}^N \lambda_i^0 = N$, so that, in particular,

$$\sum_{i=1}^N \frac{\partial}{\partial\lambda_i}p_k(\lambda) = kp_{k-1}(\lambda) \qquad (k\geq 1).$$

Using this convention, $\langle p_0\rangle = N\langle 1\rangle$, and the Refined b-Conjecture predicts that, if $\Re(b) > -1$, then

$$M(N, \mathbf{y}, z, \mathbf{r}; b) = r_0 N + (1 + b)\left(\sum_{j\geq 1} jr_j\frac{\partial}{\partial y_j}\right)\ln\frac{\langle 1\rangle_e}{\langle 1\rangle} = \sum_{j\geq 0} r_j\frac{\left\langle p_j\sqrt{z}^j\right\rangle_e}{\langle 1\rangle_e}.$$

This is verified by using the following recurrence property for expectation.

Lemma 4.13. *For a fixed positive integer N, expectations of power-sum symmetric functions in the variables $\lambda_1, \lambda_2, \ldots, \lambda_N$ satisfy the recurrence:*

$$\left\langle p_{j+2} p_\theta \right\rangle = (j+1)b \left\langle p_j p_\theta \right\rangle + (1+b) \sum_{i \in \theta} i\, m_i(\theta) \left\langle p_{j+i} p_{\theta \setminus i} \right\rangle + \sum_{i=0}^{j} \left\langle p_i p_{j-i} p_\theta \right\rangle. \quad (4.3)$$

Proof. As in Mehta's commentary on Aomoto's proof of Selberg's integration theorem [Meh04, Chap. 17], let

$$\gamma := \frac{1}{1+b} \qquad \text{and} \qquad \Omega := e^{-\frac{\gamma}{2} p_2(\mathbf{x})} |V(\mathbf{x})|^{2\gamma}$$

so that, in particular, $\langle f \rangle = \int_{\mathbb{R}^N} f \Omega \, d\mathbf{x}$. Consider the partial derivative:

$$\frac{\partial}{\partial x_1} x_1{}^{j+1} p_\theta \Omega = (j+1) x_1{}^j p_\theta \Omega - \gamma x_1{}^{j+2} \Omega$$

$$+ \sum_{i \in \theta} i\, m_i(\theta) x_1{}^{i+j} p_{\theta \setminus i} \Omega + 2\gamma \sum_{i=2}^{N} \frac{x_1{}^{j+1} p_\theta}{x_1 - x_i} \Omega. \quad (4.4)$$

Thus, provided that $\mathfrak{R}(\gamma) > 0$,

$$\int_{-\infty}^{\infty} \left(\frac{\partial}{\partial x_1} x_1{}^{j+1} p_\theta \Omega \right) dx_1 = \lim_{x_1 \to \infty} x_1{}^{j+1} p_\theta \Omega - \lim_{x_1 \to -\infty} x_1{}^{j+1} p_\theta \Omega = 0,$$

since the exponential factor of Ω, namely $e^{-\frac{\gamma}{2} x_1^2}$, dominates in the limit. Integrating (4.4) and rearranging terms gives

$$\gamma \left\langle x_1{}^{j+2} p_\theta \right\rangle = (j+1) \left\langle x_1{}^j p_\theta \right\rangle + \sum_{i \in \theta} i\, m_i(\theta) \left\langle x_1{}^{i+j} p_{\theta \setminus i} \right\rangle + 2\gamma \sum_{i=2}^{N} \left\langle \frac{x_1{}^{j+1} p_\theta}{x_1 - x_i} \right\rangle. \quad (4.5)$$

By symmetry, $\left\langle \frac{x_1{}^{j+1} p_\theta}{x_1 - x_i} \right\rangle = \left\langle \frac{x_i{}^{j+1} p_\theta}{x_i - x_1} \right\rangle$. So

$$2 \left\langle \frac{x_1{}^{j+1} p_\theta}{x_1 - x_i} \right\rangle = \left\langle \frac{x_1{}^{j+1} p_\theta}{x_1 - x_i} \right\rangle - \left\langle \frac{x_j{}^{j+1} p_\theta}{x_1 - x_i} \right\rangle = \left\langle \frac{x_1{}^{j+1} - x_j{}^{j+1}}{x_1 - x_i} p_\theta \right\rangle = \sum_{l=0}^{j} \left\langle x_1{}^l x_i{}^{j-l} p_\theta \right\rangle.$$

Using this in (4.5) and multiplying by $N(1+b)$ gives

$$N \left\langle x_1{}^{j+2} p_\theta \right\rangle = N(1+b)(1+j) \left\langle x_1{}^j p_\theta \right\rangle + (1+b)N \sum_{i \in \theta} i\, m_i(\theta) \left\langle x_1{}^{i+j} p_{\theta \setminus i} \right\rangle$$

$$+ N \sum_{i=2}^{N} \sum_{l=0}^{j} \left\langle x_1{}^l x_i{}^{j-l} p_\theta \right\rangle.$$

But $N\left\langle x_1{}^j p_\theta \right\rangle = \left\langle p_j p_\theta \right\rangle$ and $N\left(\left\langle x_1{}^j p_\theta \right\rangle + \sum_{i=2}^{N}\left\langle x_1{}^l x_i{}^{j-l} p_\theta \right\rangle\right) = \left\langle p_l p_{j-l} p_\theta \right\rangle$, giving the desired recurrence. $\qquad\square$

Lemma 4.14. *If N is a fixed positive integer and $\mathfrak{R}(b) > -1$, then equation (4.2) with $x = N$ is satisfied by*

$$f = \sum_{j\geq 0} r_j \frac{\left\langle p_j \sqrt{z}^j \right\rangle_e}{\langle 1 \rangle_e}.$$

Proof. The condition on b is required so that the integrals are well defined. Mehta gives an explicit evaluation of $\langle 1 \rangle$ in [Meh04, Eq. (17.6.7)], but for the present purposes the existence of the integral is sufficient. The existence of $\langle 1 \rangle_e$ and $\left\langle p_j \sqrt{z}^j \right\rangle_e$ then follow from the recurrence in Lemma 4.13.

When g is independent of y, as in the case of $g = 1$ or $g = p_j \sqrt{z}^j$,

$$\frac{\partial}{\partial y_i} \langle g \rangle_e = \frac{\partial}{\partial y_i}\left\langle g \cdot \exp\left(\frac{1}{1+b}\sum_{k\geq 1}\frac{1}{k}y_k p_k(\lambda)\sqrt{z}^k\right)\right\rangle = \frac{\sqrt{z}^i}{i(1+b)}\langle g \cdot p_i \rangle_e,$$

so the partial differential equation is satisfied if

$$\sum_{j\geq 1} r_j \frac{\left\langle p_j \sqrt{z}^j \right\rangle_e}{\langle 1 \rangle_e} = z\sum_{j\geq 0} r_{j+2}(j+1)b\frac{\left\langle p_j \sqrt{z}^j \right\rangle_e}{\langle 1 \rangle_e} + z\sum_{j\geq 0}\sum_{i=1}^{j+1} r_i y_{j-i+2}\frac{\left\langle p_j \sqrt{z}^j \right\rangle_e}{\langle 1 \rangle_e}$$

$$+ z\sum_{j\geq 0}\sum_{i\geq 1} r_{i+j+2}\frac{\left\langle p_j p_i \sqrt{z}^{i+j} \right\rangle_e}{\langle 1 \rangle_e} - z\sum_{j\geq 0}\sum_{i\geq 1} r_{i+j+2}\frac{\left\langle p_j \sqrt{z}^j \right\rangle_e \left\langle p_i \sqrt{z}^i \right\rangle_e}{\langle 1 \rangle_e^2}$$

$$+ z\sum_{j\geq 0}\sum_{i\geq 0} r_{i+j+2}\frac{\left\langle p_i \sqrt{z}^i \right\rangle_e \left\langle p_j \sqrt{z}^j \right\rangle_e}{\langle 1 \rangle_e^2}.$$

A cancellation between the last two sums leaves only the $i = 0$ terms, and is a reflection of the intrinsic similarity between handles and bridges discussed in Remark 4.3. Coefficients of r_{j+2} for $j \geq -1$ are homogeneous in $\sqrt{z}$, so by cancelling the denominators and using the fact that $\langle p_0 \rangle_e = N \langle 1 \rangle_e$ it is sufficient to show that, for every $j \geq -1$,

$$\left\langle p_{j+2} \right\rangle_e = (j+1)b\left\langle p_j \right\rangle_e + \sum_{i\geq j+1} y_{i-j}\left\langle p_i \right\rangle_e + \sum_{i=1}^{j}\left\langle p_i p_{j-i} \right\rangle_e + N\left\langle p_j \right\rangle_e$$

$$= (j+1)b\left\langle p_j \right\rangle_e + \sum_{i\geq 1} y_i\left\langle p_{j+i} \right\rangle_e + \sum_{i=0}^{j}\left\langle p_i p_{j-i} \right\rangle_e. \tag{4.6}$$

When g is independent of $\mathbf{y}$, the coefficient of $\mathbf{y}_\theta$ in $\langle g \rangle_e$ is given by

$$[\mathbf{y}_\theta] \langle g \rangle_e = [\mathbf{y}_\theta] \left\langle g \exp \left(\frac{1}{1+b} \sum_{k \geq 1} \frac{1}{k} y_k p_k(\lambda) \sqrt{z}^k \right) \right\rangle = \frac{\omega_\theta^{-1} \sqrt{z}^{|\theta|}}{(1+b)^{\ell(\theta)}} \langle g p_\theta \rangle .$$

Here ω_θ is the order of the centralizer of a permutation of cycle-type θ: in particular, if $\theta = [1^{m_1} 2^{m_2} \cdots i^{m_i}]$, then

$$\omega_\theta = m_1! m_2! \cdots m_i! 1^{m_1} 2^{m_2} \cdots i^{m_i}. \tag{4.7}$$

By using this to compare coefficients of $\mathbf{y}_\theta$ in (4.6), the equation is equivalent to

$$\frac{\omega_\theta^{-1}}{(1+b)^{\ell(\theta)}} \langle p_{j+2} p_\theta \rangle = \frac{\omega_\theta^{-1}}{(1+b)^{\ell(\theta)}} (j+1) b \langle p_j p_\theta \rangle + \sum_{i \in \theta} \frac{\omega_{\theta \smallsetminus i}^{-1}}{(1+b)^{\ell(\theta \smallsetminus i)}} \langle p_{j+i} p_{\theta \smallsetminus i} \rangle$$

$$+ \sum_{i=0}^{j} \frac{\omega_\theta^{-1}}{(1+b)^{\ell(\theta)}} \langle p_i p_{j-i} p_\theta \rangle ,$$

for every partition θ. Removing common factors in this recurrence, using the fact that $\omega_{\theta \smallsetminus i}^{-1} = i \, m_i(\theta) \, \omega_\theta^{-1}$, leaves precisely the recurrence in the statement of Lemma 4.13. □

Corollary 4.15. *If N is a fixed positive integer and $\mathfrak{R}(b) > -1$, then*

$$M(N, \mathbf{y}, z, \mathbf{r}; b) = \sum_{j \geq 0} r_j \frac{\left\langle p_j \sqrt{z}^j \right\rangle_e}{\langle 1 \rangle_e} .$$

Proof. The partial differential equation (4.2) leads to a recurrence for the coefficients of its solution as a power series in z, so its solution is uniquely determined in the ring $\mathbb{R}[N, \mathbf{y}, \mathbf{r}, b][\![z]\!]$ by its evaluation at $z = 0$. At $z = 0$, both expressions evaluate to

$$r_0 N = r_0 \frac{\langle p_0 \rangle_e}{\langle 1 \rangle_e},$$

so the series are identical. □

This is sufficient to produce the main result of this Chapter by giving a combinatorial interpretation to the map series M. The Marginal b-Conjecture is then resolved as a corollary by specializing to $\mathbf{r} = \mathbf{y}$.

Theorem 4.16. *The generating series M can be expressed in terms of Jack symmetric functions as*

$$M(x, \mathbf{y}, z, \mathbf{r}; b) = r_0 x + (1+b) \left(\sum_{k \geq 1} k r_k \frac{\partial}{\partial y_k} \right) \ln \left(\Phi(x, \mathbf{y}, z; b) \right),$$

where

$$\Phi(x, \mathbf{y}, z; b) = \sum_{\theta \in \mathscr{P}} \frac{J_\theta(\mathbf{x}; 1 + b) J_\theta(\mathbf{y}; 1 + b) J_\theta(\mathbf{z}; 1 + b)}{\langle J_\theta, J_\theta \rangle_{1+b}} \left. \right|_{\substack{p_i(\mathbf{x})=x, \\ p_i(\mathbf{y})=y_i, \\ p_i(\mathbf{z})=\delta_{i,2}z}} \left. \right\} \forall i \geq 0.$$

Proof. The combinatorial sum is in the ring $\mathbb{Z}[x, \mathbf{y}, \mathbf{r}, b][\![z]\!]$, since there are only finitely many rooted maps with any given number of edges, while the analytic expression is in $\mathbb{Q}(b)[x, \mathbf{y}, \mathbf{r}][\![z]\!]$ by construction.

Evaluating either expression at $x = N$ for any positive integer N and any real $b \geq 1$, the second condition so that $\langle ., . \rangle_{1+b}$ is an inner product, gives

$$\sum_{j \geq 0} r_j \frac{\left\langle p_j \sqrt{z}^j \right\rangle_e}{\langle 1 \rangle_e} \in \mathbb{Q}[\mathbf{y}, \mathbf{r}][\![z]\!],$$

the combinatorial sum by Corollary 4.15, and the algebraic expression by substituting $\sum_{k \geq 1} k r_k \frac{\partial}{\partial y_k}$ for $2z \frac{\partial}{\partial z}$ in (3.19). It follows that the coefficients of $r_k \mathbf{y}_\theta z^n$ in both expressions are elements of $\mathbb{Q}(b)[x]$ that agree at every non-negative real b and every positive integer N. This is sufficient to show that the coefficients agree as rational functions and that the series are equal. □

Corollary 4.17. *The Marginal b-Conjecture, Conjecture 3.23, is true with η as a marginal b-invariant. In particular,*

$$M(x, \mathbf{y}, z, \mathbf{y}; b) = xy_0 + M(x\mathbf{1}, \mathbf{y}, \mathbf{z}; b),$$

and for $\varphi \vdash 2n$, the marginal sums

$$d_{v,\varphi}(b) = \sum_{\ell(\nu)=v} c_{\nu,\varphi,[2^n]}(b)$$

are polynomials with non-negative integer coefficients. Moreover, the coefficient of b^l in $d_{v,\varphi}(b)$ has a combinatorial interpretation as the number of rooted maps with v vertices, face-degree partition φ, and a total of l twisted edges when decomposed by iterative root deletion. This number is divisible by

$$\frac{2n}{\gcd\{i\, m_i(\varphi) : i \in \varphi\}}.$$

Proof. Specializing the combinatorial sum, through $\mathbf{r} = \mathbf{y}$, has the effect of treating the root face and non-root faces identically. In the algebraic series, the action of $\sum_{j \geq 0} j y_j \frac{\partial}{\partial y_j}$ is to scale $\mathbf{y}_\theta$ by a factor of $|\theta|$, which, by homogeneity, is the same as the action of $2z \frac{\partial}{\partial z}$. Divisibility is guaranteed by the fact that replacing $2z \frac{\partial}{\partial z}$ with $\sum_{j \geq 1} j r_j \frac{\partial}{\partial y_j}$ produces a refinement of the series with integer coefficients. □

Remark 4.18. Corollary 4.17 resolves precisely the case required by Goulden, Harer, and Jackson in [GHJ01] to give a combinatorial interpretation to the virtual Euler characteristic of the moduli space of curves.

Remark 4.19. As a particular case of Corollary 4.17, the coefficients of the map series corresponding to monopoles are polynomials with a combinatorial interpretation, since, if $\varphi \vdash 2n$, then $c_{[2n],\varphi,[2^n]}(b) = d_{1,\varphi}(b)$. By symmetry, the coefficient $c_{v,[2n],[2^n]}(b)$ corresponding to one-faced maps is also a polynomial, but a combinatorial interpretation consistent with η has not been verified.

The substitution of differential operators shows implicitly that Conjecture 4.9 is true when vertex degrees are ignored. A direct combinatorial proof remains elusive, but interpreting the substitution combinatorially shows the following property of η.

Corollary 4.20 (The Root-Face Degree Distribution Property)**.** *If a rooted maps is selected uniformly at random after specifying a given face-degree partition and a fixed number of vertices, then root-face degree and η are independent statistics.*

Remark 4.21. By using this property, it is possible to analyze some enumerative problems as though η is independent of rooting. In particular, if φ has a part equal to i, then to compute $d_{v,\varphi}(b)$, it is sufficient to determine the generating series for rooted maps with root-face degree i, since this restriction introduces a known multiplicative factor. This observation is used in Section 4.7 and Chapter 7.

4.5 Commentary on the Proof of Theorem 4.16

After specializing Theorem 4.16 to $b = 0$ and $b = 1$, this Chapter provides a simultaneous proof of the integration formulae for the orientable and locally orientable map series. The new proof differs from the approaches described in Section 3.5 by working directly with rooted maps; it avoids introducing a multiplicative factor associated with edge decoration and does not require the use of multi-component analogues. Chapter 7 exploits this to provide insight into a conjecture on the enumerative properties of orientable maps.

The proof requires foreknowledge of the analytic form of the map series, and does not provide any new insight into the rôle played by Jack symmetric functions: their defining properties have not been given a combinatorial explanation. It might be informative to show directly that the Jack function presentation of the map series satisfies the differential equation, although such a proof would be equivalent to verifying Theorem 3.18.

4.6 Implications

Lemma 4.7 gives a recurrence for the coefficients of $M(x, \mathbf{y}, z, \mathbf{r}; b)$ as a power series in z. Namely, with $m_n = m_n(x, \mathbf{y}, \mathbf{r}; b)$ denoting the coefficient of z^n in M,

the constant term is given by $m_0 = r_0 x$, and for $n \geq 0$,

$$
\begin{aligned}
m_{n+1} = \sum_{i=0}^{2n} \sum_{j=0}^{2n-i} r_{i+j+2} & \left((1+b)j \frac{\partial^2}{\partial r_i \partial y_j} m_n + \sum_{k=0}^{n} \left(\frac{\partial}{\partial r_i} m_k \right) \left(\frac{\partial}{\partial r_j} m_{n-k} \right) \right) \\
+ \sum_{i=0}^{2n} & \left((i+1) b r_{i+2} + \sum_{j=1}^{i+1} r_j y_{i-j+2} \right) \frac{\partial}{\partial r_i} m_n.
\end{aligned}
\tag{4.8}
$$

For computational purposes, it is more convenient to specialize to $\mathbf{r} = \mathbf{y}$ using Corollary 4.20. Under this specialization,

$$
\frac{\partial}{\partial r_j} m_n(x, \mathbf{y}, \mathbf{r}; b) = \frac{j}{2n} \frac{\partial}{\partial y_j} m_n(x, \mathbf{y}, \mathbf{y}; b),
$$

when $n \neq 0$. In this case, the recurrence is given by two initial conditions,

$$
m_0 = x y_0 \qquad \text{and} \qquad m_1 = x^2 y_2 + x y_1^2 + b x y_2,
$$

and for $n \geq 1$

$$
\begin{aligned}
m_{n+1} = \sum_{i=1}^{2n} \sum_{j=1}^{2n-i} y_{i+j+2} & \left((1+b) \frac{ij}{2n} \frac{\partial^2}{\partial y_i \partial y_j} m_n \right) \\
+ \sum_{i=1}^{2n} \sum_{j=1}^{2n-i} y_{i+j+2} & \left(\sum_{k=1}^{n-1} \frac{ij}{4k(n-k)} \left(\frac{\partial}{\partial y_i} m_k \right) \left(\frac{\partial}{\partial y_j} m_{n-k} \right) \right) \\
+ \sum_{i=1}^{2n} & \left((ib + b + 2x) y_{i+2} + \sum_{j=1}^{i+1} y_j y_{i-j+2} \right) \frac{i}{2n} \frac{\partial}{\partial y_i} m_n.
\end{aligned}
\tag{4.9}
$$

Terms of (4.8) involving $\frac{\partial}{\partial r_0}$ vanish except when $k = 0$ or $n-k = 0$, and these terms have been redistributed into the second sum, accounting for the presence of $2x$. Section B.1 of Appendix B contains a computer algebra implementation of this recurrence that was used to compute all marginal b-polynomials corresponding to maps with at most 16 edges. The recurrence also reveals the following structure for marginal b-polynomials.

Theorem 4.22. *For a particular $\varphi \vdash 2n$ and v, if $g = 2 - v - \ell(\varphi) + n$ is the genus of maps enumerated by $d_{v,\varphi}(b)$, then integers $h_{v,\varphi,i}$ are implicitly defined by*

$$
d_{v,\varphi}(b) = \sum_{i=0}^{g/2} h_{v,\varphi,i} b^{g-2i} (1+b)^i,
\tag{4.10}
$$

and there are $2^i h_{v,\varphi,i}$ rooted maps with v vertices, face degree partition φ, and i handles encountered in the computation of η through Definition 4.1.

Proof. Recall that it was not necessary to specify a rule to distinguish between twisted and untwisted handles in order to establish the differential equation in Lemma 4.7. As an algebraic reflection of this fact, consider a new variable a defined by the relation $2a = 1 + b$. Making the formal substitution $1 + b = 2a$ in recurrence (4.8) has the effect of refining the computed polynomials so that handles are marked by a, and b marks only cross-borders. Since $d_{v,\varphi}$ is a coefficient of $m_n(x, \mathbf{y}, \mathbf{r}; b)$, it follows that

$$d_{v,\varphi}(b) = \sum_{i=0}^{g/2} h_{v,\varphi,i} b^{g-2i} (2a)^i.$$

Replacing $2a$ by $1+b$ recovers the original polynomials and proves the result. $\square$

The form of (4.10) highlights the topological nature of η. Polynomial degree is bounded by genus, and the interplay between handles and cross-borders alludes to the relationship between handles and cross-caps in the Classification Theorem for surfaces, Theorem 2.5. The theorem also strengthens the non-negativity results for the coefficients of $d_{v,\varphi}(b)$ by showing that the polynomials are non-negative with respect to the basis

$$B_g = \left\{ b^{g-2i}(1 + b)^i : 0 \leq i \leq g/2 \right\}.$$

Theorem 4.22 arises here from combinatorial considerations, but Chapter 5 explores how its algebraic form is a consequence of properties of Jack symmetric functions. It implies that any b-invariant should share combinatorial properties with η. Theorem 4.22 also shows how the top coefficients of the marginal b-polynomials may be determined.

Corollary 4.23. *For $\varphi \vdash 2n$ with $\ell(\varphi) = f$, the polynomial $d_{v,\varphi}(b)$ is non-zero precisely when $v - n + f \leq 2$. In this case, it has degree $g = g(v, \varphi) = 2 - v - f + n$, and its top coefficient is given by*

$$h_{v,\varphi,0} = (-1)^{v+f+n} d_{v,\varphi}(-1). \tag{4.11}$$

Proof. From the combinatorial interpretation of $d_{v,\varphi}(b)$ in Corollary 4.17, if the polynomial is not identically zero, then there is a map with Euler characteristic $v - n + f$. This is not possible if $v - n + f > 2$.

Alternatively, if $v - n + f \leq 2$, then consider the map $\mathfrak{m}$ given in Figure 4.6a. Borrowing terminology from flowers, the stem consists of v vertices and the map has g petals, each a cross-border. The map has a single face with degree $2g+2v-2$, and $\eta(\mathfrak{m}) = g$ for every rooting of $\mathfrak{m}$. Represent m as a $(2g+2v-2)$-gon with edges identified, then construct a new map $\mathfrak{m}'$ by adding $f - 1$ chords to the interior of the face, each incident with the root, to induce the face-degree partition φ: see Figure 4.6b. From this construction $\mathfrak{m}'$ has v vertices, face partition φ, and $\eta(m') = \eta(\mathfrak{m}) = g$. It follows that the degree of $d_{v,\varphi}(b)$ is at least g. But g is also an upper bound for the degree, as a consequence of Theorem 4.4, so the polynomial has degree exactly g.

(a) A map with one face **(b)** Its polygonal representation
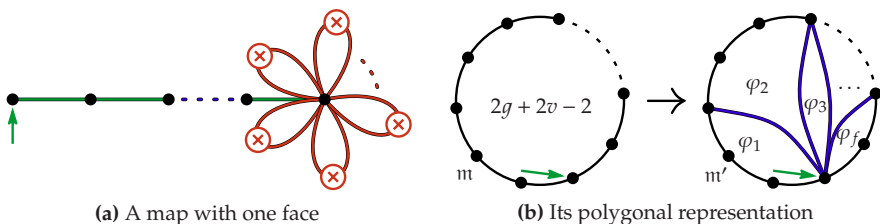
Figure 4.6: The genus of $\mathfrak{m}'$ is equal to $\eta(\mathfrak{m}')$.

The evaluation follows from (4.10), since every term of lower degree contains a factor of $1 + b$ in that presentation. □

Remark 4.24. By selectively replacing adjacent pairs of cross-caps with handles, the same proof can be used to show that $d_{v,\varphi}(b)$ has a non-zero term of degree i for every i in the range $0 \leq i \leq g$ when g is even, or in the range $1 \leq i \leq g$ when g is odd.

The proof of Corollary 4.23 motivates the following definition for a class of maps that is analyzed in more detail in Section 5.7.

Definition 4.25 (unhandled map)**.** *A rooted map $\mathfrak{m}$ is said to be* unhandled *if $\eta(\mathfrak{m})$ can be computed, using the recursive description from Definition 4.1, without encountering any handles. The class of all such maps is denoted by $\mathcal{U}$.*

Remark 4.26. Brown used the term *fully non-orientable* to refer to a related family of ordered digraphs in [Bro00, Cor. 6.4], but did not give them a combinatorial characterization.

With this terminology, the rooted maps enumerated by the top coefficients of marginal b-polynomials are precisely the unhandled maps. As a consequence of Corollary 4.23, the generating series for such maps, with respect to number of vertices, face-degree partition, and number of edges, is given by

$$U(x, \mathbf{y}, z; b) := M(-x, -\mathbf{y}, -z; -1). \tag{4.12}$$

All planar and projective-planar maps are unhandled, but in general, being unhandled is a property of a rooting and not of the underlying surface or the unrooted map. In particular Figure 4.7 gives two rooted maps; only Figure 4.7a is unhandled. This is to be contrasted with the classes of orientable maps and non-orientable maps corresponding to the $b = 0$ and $b = 1$ evaluations of M, both of which are closed under re-rooting. In fact, all previously known specializations of the map series correspond to classes of maps that are closed under re-rooting.

Despite its simple form, this evaluation is algebraically unwieldy, since both the integral- and Jack-based presentations of M are degenerate at $b = -1$. In

(a) Unhandled   **(b)** Handled
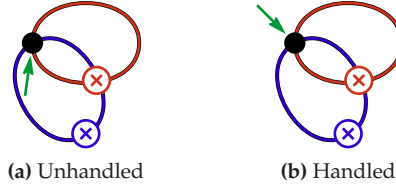
Figure 4.7: One map may have both handled and unhandled rootings.

particular, unhandled maps correspond to the pole of $\frac{1}{1+b}M$. The maps are thus unhandled both in the literal sense, of lacking combinatorial handles, and in the sense that there is an algebraic difficulty with computing their generating series. In practice, it appears necessary to compute U indirectly, using a limiting process or polynomial interpolation, for example. As an alternative approach, U, up to alternating signs, is determined by the constant coefficient of M as a polynomial in $1 + b$. Work in this direction appears in [GHJ01], where Goulden, Harer, and Jackson expand M as an asymptotic series in $\gamma = (1 + b)^{-1}$, but only after a specialization that discards face degree information. In specific cases, coefficients of U can be recovered by other methods.

Corollary 4.27. *Unhandled monopoles with face-degree partition $\varphi \vdash 2n$ are enumerated by*

$$h_{1,\varphi,0} = \sum_{\nu \vdash 2n} c_{\nu,\varphi,[2^n]}(0).$$

Proof. Appealing to Lemma 3.22,

$$\sum_{\nu \geq 1} d_{\nu,\varphi}(b) = \sum_{\nu \vdash 2n} c_{\nu,\varphi,[2^n]}(b) = (1 + b)^{n-\ell(\varphi)+1} \sum_{\nu \vdash 2n} c_{\nu,\varphi,[2^n]}(0).$$

The result follows by comparing coefficients of $b^{n-\ell(\varphi)+1}$, since one consequence of Corollary 4.23 is that $b^{n-\ell(\varphi)+1}$ only occurs in the left hand sum when $\nu = 1$. □

Remark 4.28. As in the proof of Lemma 3.22, the right hand sum is a coefficient of $M(1, \mathbf{y}, z; 0)$, a series that can be evaluated in terms of an integral over $\mathbb{R}$. Using the fact that

$$\int_{\mathbb{R}} x^{2n} e^{-\frac{x^2}{2}} \, dx = \frac{(2n)!}{2^n n!} \int_{\mathbb{R}} e^{-\frac{x^2}{2}} \, dx,$$

the generating series for unhandled monopoles with respect to face degree partition and number of edges is

$$\sum_{n \geq 1} \sum_{\varphi \vdash 2n} h_{1,\varphi,0} \mathbf{y}^\varphi z^n = 2z \frac{\partial}{\partial z} \ln \left(\sum_{n \geq 0} \frac{(2n)!}{2^n n!} z^n \sum_{\theta \vdash 2n} \frac{\mathbf{y}^\theta}{\omega_\theta} \right),$$

where ω_θ is defined in (4.7).

85

Example 4.29. *The number of unhandled one-faced monopoles with n edges is*

$$h_{1,[2n],0} = \sum_{\nu \vdash 2n} c_{\nu,[2n],[2^n]}(0) = \frac{(2n)!}{2^n n!},$$

since rooted orientable one-faced maps can be identified with matchings on the the edges of a 2n-gon. Alternatively, this result can be obtained inductively, since every edge of an unhandled one-faced monopole is a cross-border.

4.7 Degree-One and Degree-Two Faces

This Section uses properties of low-degree faces, together with the Root-Face Degree Distribution Property, Corollary 4.20, to verify and strengthen patterns conjectured from numerical evidence by Brown in [Bro00]. The analysis is motivated by dual considerations, and reinforces the claim that η has a natural topological interpretation.

Definition 4.30 (Smooth map)**.** *The class of* smooth maps *consists of all rooted maps without any vertices of degree less than three.*

This is the class of maps required in the application of map enumeration to the moduli space of curves, in [GHJ01]. The generating series for smooth maps cannot be recovered directly from the series presented in this Chapter, since $M(x, \mathbf{y}, z; b)$ does not record the degrees of vertices. Effectively, smooth maps are representative rooted maps with respect to a weakened equivalence relation, the relation defined such that two rooted maps are equivalent if the first can be transformed into the second using a combination of leaf deletions, edge subdivisions, and their inverses. With respect to this equivalence, each class of rooted maps contains either precisely one smooth map, or a representative from the set

$$\mathcal{I} = \left\{ \vcenter{\hbox{}} , \vcenter{\hbox{}} , \vcenter{\hbox{}} \right\}.$$

Every invariant described by Definition 4.1 is unchanged by leaf deletion, and Item 2(b)iii of the definition can be strengthened to impose invariance with respect to subdivision of edges.

Since η is also constant under the duals of these operations, equivalent results can be obtained by considering rooted maps without any faces of degree one or degree two. In any map, every face of degree one is bounded by a loop, and if the map has at least two edges, then every face of degree two is bounded by a pair of parallel edges. Since the boundaries of such faces are borders, these edges do not contribute to η, and thus, except when dealing with the non-orientable rooted map with one edge, deleting the root edge from a map with root-face degree one or two does not change the value of η. In the case that the root face had degree two, this operation also does not change the

number of vertices or the degree of any other face. Appealing to Corollary 4.20, the restriction from maps *with* a degree-two face to maps *rooted* on a degree-two face introduces a known multiplicative factor, and leads to the functional equation in Proposition 4.31

Refining the map series to record root-face degree provides precisely the setting required to prove an identity 'anticipated' by Brown. In [Bro00, Sec. 7.4], he noted that his invariant remains constant under the operations of adding and conflating parallel edges, and incorrectly implied in [Bro00, Lemm. 7.9] that every rooted map uniquely decomposes as a digon-free map with each edge independently replaced by the dual of a path. The stated decomposition fails to maintain bijectivity for maps rooted on faces of degree two: in particular, two of the rooted maps with one edge, the duals of maps in $\mathcal{I}$, have degree-two faces not bounded by parallel edges. Correcting the implication to account for this, requires the refined series, with r_i marking a root face with degree i.

Proposition 4.31. *The map series M satisfies the functional equation*

$$M\left(x, \mathbf{y}|_{y_2=0}, \frac{z}{1-y_2 z}, \mathbf{r}; b\right) = M\left(x, \mathbf{y}, z, \mathbf{r}; b\right).$$

Proof. Rewriting the expression for M from Corollary 4.15, if A is defined by

$$
\begin{aligned}
A := & \left(\sum_{k \geq 1} \frac{y_k p_k(\lambda)}{(1+b)k}\bigg|_{y_2=0} \sqrt{\frac{z}{1-y_2 z}}^{\,-k}\right) - \frac{p_2(\lambda)}{2(1+b)} \\
= & \left(\sum_{k \geq 1} \frac{y_k p_k(\lambda)}{(1+b)k} \sqrt{\frac{z}{1-y_2 z}}^{\,-k}\right) - \left(1 + \frac{y_2 z}{1-y_2 z}\right)\frac{p_2(\lambda)}{2(1+b)} \\
= & \left(\sum_{k \geq 1} \frac{y_k p_k(\lambda)}{(1+b)k} \sqrt{\frac{z}{1-y_2 z}}^{\,-k}\right) - \frac{1}{1-y_2 z}\frac{p_2(\lambda)}{2(1+b)},
\end{aligned}
$$

then for any fixed positive integer N,

$$
\begin{aligned}
& M\left(N, \mathbf{y}|_{y_2=0}, \frac{z}{1-y_2 z}, \mathbf{r}; b\right) \\
& = \sum_{j \geq 0} r_j \frac{\int_{\mathbb{R}^N} |V(\lambda)|^{\frac{1}{1+b}} p_j(\lambda) \sqrt{\frac{z}{1-y_2 z}}^{\,j} \exp\left(A\right) d\lambda}{\int_{\mathbb{R}^N} |V(\lambda)|^{\frac{1}{1+b}} \exp\left(A\right) d\lambda} \\
& = \sum_{j \geq 0} r_j \frac{\int_{\mathbb{R}^N} |V(\rho)|^{\frac{1}{1+b}} p_j(\rho) \sqrt{z}^{\,j} \exp\left(\sum_{k \geq 1} \frac{y_k p_k(\rho)}{(1+b)k} \sqrt{z}^{\,-k} - \frac{p_2(\rho)}{2(1+b)}\right) d\rho}{\int_{\mathbb{R}^N} |V(\rho)|^{\frac{1}{1+b}} \exp\left(\sum_{k \geq 1} \frac{y_k p_k(\rho)}{(1+b)k} \sqrt{z}^{\,-k} - \frac{p_2(\rho)}{2(1+b)}\right) d\rho} \\
& = M\left(N, \mathbf{y}, z, \mathbf{r}; b\right).
\end{aligned}
$$

Additional factors introduced by changing the variables of integration, using
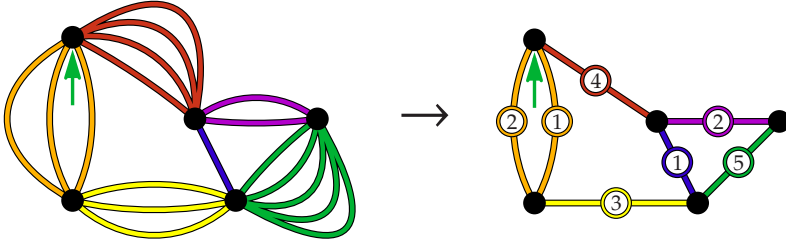
Figure 4.8: By conflating non-root digons, a rooted map can be represented by a rooted map in which every face except the root face has degree different from two. The number on each edge records the number of edges in a parallel class.

the substitution $\lambda = \rho \sqrt{1 - y_2 z}$, do not affect the final sum because they occur in both the numerator and denominator of each summand. Since the coefficients of the series are polynomials in N, the identity continues to hold when N is replaced by the indeterminate x. □

Remark 4.32. As in [Bro00], the combinatorial explanation of the functional equation is that η is constant under the addition of parallel edges bounding digons. Such edges are deleted consecutively during the computation of η, and all but at most one edge from each parallel class are borders when deleted. The result follows by noting that every rooted map can be expressed uniquely as a rooted map with the same root-face degree, no non-root faces of degree two, and each edge replaced independently by the dual of a path: see Figure 4.8.

The restriction of maps to those with root-face degree at most two can be used to compute specific marginal b-polynomials more efficiently. Typical computations, using the recurrence (4.9) directly, involve a large number of terms, but the Root-Face Degree Distribution Property, Corollary 4.20, can be used to simplify these computations. The following two propositions illustrate this technique.

Proposition 4.33. If $\varphi \vdash 2n$, $\ell(\varphi) \geq 2$, and $m_2(\varphi) \geq 1$, then

$$\frac{m_2(\varphi)}{n} d_{i,\varphi}(b) = d_{i,\varphi \setminus 2}(b).$$

Proof. By Corollary 4.20, rooted maps with i vertices, face-degree partition φ, and root-face degree two are enumerated by $\frac{m_2(\varphi)}{n} d_{i,\varphi}(b)$. The root edge of such a map is a border, and deleting this edge leaves a map with i vertices and face-degree partition $\varphi \setminus 2$. This deletion is uniquely reversible, and the result follows. □

Proposition 4.34. For $k > 2$ and $n \geq 1$,

$$\frac{m}{kn + m} d_{i,[1^m,k^n]}(b) = \frac{k-1}{kn + m - 2} d_{i,[1^{m-1},k-1,k^{n-1}]}.$$

Proof. For a rooted map with root-face degree one and face-degree partition $[1^m, k^n]$, the root edge is a border. By connectivity, the faces it separates do not both have degree one, so deleting it leaves a map rooted on a face of degree $k - 1$, with $n - 1$ faces of degree k and $m - 1$ faces of degree one. Applying Corollary 4.20 twice produces the result. $\qquad\square$

Remark 4.35. Combining these results and specializing, gives

$$\frac{1}{2k} d_{i,[1,2k-1]}(b) = d_{i,[2k-2]}(b) = \frac{1}{k} d_{i,[2,2k-2]}(b) \qquad \text{for } k \geq 3,$$

which supersedes a result obtained by Brown, [Bro00, Lemm. 7.10].

Example 4.36. *By Propositions 4.33 and 4.34:*

$$
\begin{aligned}
d_{i,[1,2^3,3^3]}(b) &= \left(\tfrac{8}{3}\right) d_{i,[1,2^2,3^3]}(b) \\
&= \left(\tfrac{8}{3}\right)\left(\tfrac{7}{2}\right) d_{i,[1,2,3^3]}(b) \\
&= \left(\tfrac{8}{3}\right)\left(\tfrac{7}{2}\right)\left(\tfrac{6}{1}\right) d_{i,[1,3^3]}(b) \\
&= \left(\tfrac{8}{3}\right)\left(\tfrac{7}{2}\right)(6)(10)\left(\tfrac{2}{8}\right) d_{i,[2,3^2]}(b) \\
&= \left(\tfrac{8}{3}\right)\left(\tfrac{7}{2}\right)(6)(10)\, d_{i,[3^2]}(b) \\
&= 560 d_{i,[3^2]}(b),
\end{aligned}
$$

which agrees with the direct computation

φ	$d_{1,\varphi}(b)$	$d_{2,\varphi}(b)$	$d_{3,\varphi}(b)$
$[3^2]$	$1 + b + 5b^2$	$9b$	4
$[1, 2^3, 3^3]$	$560 + 560b + 2800b^2$	$5040b$	$2240.$

Example 4.37. *When $j \geq 1$,*

$$\frac{1}{4} d_{i,[1^j,3^j]}(b) = \frac{2}{4j-2} d_{i,[1^{j-1},2,3^{j-1}]}(b) = d_{i,[1^{j-1},3^{j-1}]}(b).$$

Since $d_{1,[2]}(b) = b$ and $d_{2,[2]}(b) = 1$, it follows inductively that $d_{1,[1^j,3^j]}(b) = 4^j b$ and $d_{2,[1^j,3^j]}(b) = 4^j$.

4.8 Summary

This chapter introduced a family of invariants of rooted maps. All these invariants, generically written η, were shown to be marginal b-invariants by verifying that the generating series for rooted maps with respect to η satisfies a partial differential equation with a unique solution that is also satisfied by the map series M. This resolved the Marginal b-Conjecture of Goulden, Harer, and Jackson from [GHJ01]. In the process, an algebraic operation for refining the map
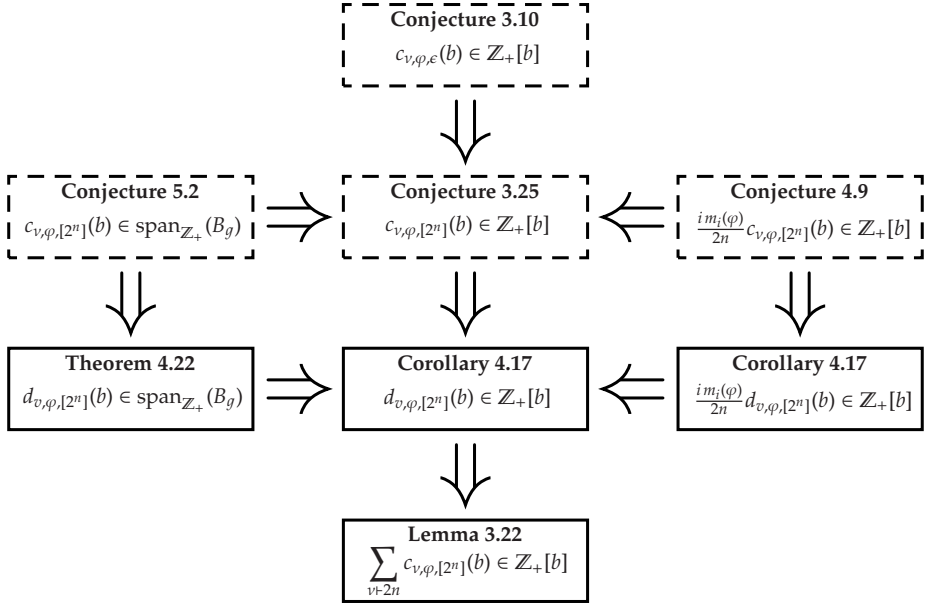
Figure 4.9: The relationships between the conjectures from Section 3.4 and the refinements introduced in this Chapter are summarized, with dashed boxes indicating open conjectures.

series to record the degree of the root face was shown to apply in the context of b-weighted maps, leading to a strengthened form of the b-Conjecture, and explaining divisibility properties observed from numerical evidence.

The proof revealed a strengthened form of non-negativity, by expressing marginal b-polynomials in the basis B_g, a basis tied to the topological rôles of handles and cross-caps, and in the process gave a combinatorial interpretation to a 'strange evaluation' of the map series at $b = -1$. Chapter 5 explores this further, by showing that B_g is related to algebraic properties of Jack symmetric functions, and is the natural basis in which to study all b-polynomials.

Figure 4.9 gives a summary of the relationships between the conjectures of Chapter 3 and their refinements introduced in this Chapter. Unproven statements are indicated by dashed boxes.

Proving the Marginal b-Conjecture relied on the full strength of Theorem 3.18. The existing proof cannot be refined to show that η is a b-invariant, but Chapter 6 explores how the algebraic properties of the map series and the combinatorial properties of η might be used to verify that it is a b-invariant for all maps of low genus. In the process, it investigates the issue of which choices of η should be considered the most natural invariants.

Chapter 5

Algebraic Properties of b-Polynomials

Chapter 4 introduced η and showed that every invariant in the family is a marginal b-invariant, thus giving, in Corollary 4.17, a combinatorial interpretation of the sums

$$d_{v,\varphi}(b) := \sum_{\ell(v)=v} c_{v,\varphi,[2^n]}(b).$$

This Chapter uses combinatorial properties of η as a guide for finding structural results about the individual b-polynomials. Since the techniques used in Chapter 4 to verify the combinatorial interpretation relied, in an essential way, on ignoring the degrees of vertices, the proof cannot be extended to show that η is a b-invariant. Instead, this Chapter uses combinatorial properties of η to predict algebraic properties of the maps series, and to refine Conjecture 3.25. Most significantly, a direct proof of one of the implications of this refinement reveals combinatorial properties of *all b-invariants*.

  Analyzing η gave structure to the sums $d_{v,\varphi}(b)$. Theorem 4.22 shows that each can be written in the basis B_g with non-negative integer coefficients, and computational evidence suggests that this structure is preserved in individual $c_{v,\varphi,\epsilon}(b)$. Standard facts about Jack symmetric functions are used to verify a relaxation of this result. By re-interpreting the result combinatorially, it is possible to draw conclusions about all possible b-invariants, though the approach does not address existence. In particular, the degree bound for marginal b-polynomials is extended to b-polynomials, first under the assumption of non-negativity of the coefficients, and then, using structural properties, as a consequence of polynomiality. This second approach extends to arbitrary coefficients of the hypermap series, and not just those associated with maps. Structural properties of b-polynomials also suggest that the $b = -1$ evaluation of the map series continues to have combinatorial significance as the generating series for unhandled maps when the series is refined to record vertex degrees.

5.1 A Degree Bound

Since $c_{v,\varphi,[2^n]}(0)$ can be interpreted combinatorially as the number of orientable maps with n edges, vertex-degree partition v, and face-degree partition φ, it follows that $c_{v,\varphi,[2^n]}(b)$ does not have a pole at $b = 0$. Being a rational function, it is thus analytic in a neighbourhood of 0, and determines a formal power series in the ring $\mathbb{Q}[\![b]\!]$. The b-Conjecture predicts further that every b-polynomial has a representation in $\mathbb{Z}_+[b]$, and a weakened form of this prediction is sufficient to provide a degree bound on all b-polynomials.

Theorem 5.1. *For a given $\varphi \vdash 2n$, if $c_{v,\varphi,[2^n]}(b)$ is analytic in a neighbourhood of 0 with a representation in $\mathbb{Q}_+[\![b]\!]$ for every $v \vdash 2n$ such that $\ell(v) = v$, then $c_{v,\varphi,[2^n]}(b)$ is a polynomial with degree at most $g = n + 2 - \ell(v) - \ell(\varphi)$ for every v with $\ell(v) = v$.*

Proof. If the coefficients of $c_{v,\varphi,[2^n]}(b)$ are non-negative for every partition v with length v, then the degree of $d_{v,\varphi,[2^n]}(b) := \sum_{\ell(v)=v} c_{v,\varphi,[2^n]}(b)$ is at least the degree of every summand, and the result follows from Corollary 4.23. $\qquad\square$

In particular, the existence of any b-invariant is sufficient to show that the hypotheses of Theorem 5.1 are satisfied. As in the marginal case, g is the Euler genus of the maps enumerated by $c_{v,\varphi,[2^n]}(1)$, and the degree bound offers algebraic evidence of the topological nature of all b-invariants. A weaker degree bound, $n+1-\ell(\varphi)$, can be obtained by considering the marginal sums appearing in Lemma 3.22.

5.2 The Basis B_g

Theorem 4.22 emphasizes the topological nature of marginal b-polynomials by expressing them in the form

$$d_{v,\varphi}(b) := \sum_{\ell(v)=v} c_{v,\varphi,[2^n]}(b) = \sum_{i=0}^{\lfloor g/2 \rfloor} h_{v,\varphi,i} b^{g-2i}(1+b)^i,$$

for $\varphi \vdash 2n$ and $g = 2 - v - \ell(\varphi) + n$. The coefficients, $h_{v,\varphi,i}$ are non-negative integers with a combinatorial significance, and the rôle of the basis

$$B_g := \left\{ b^{g-2i}(1+b)^i : 0 \le i \le \tfrac{g}{2} \right\},$$

is explained by the fact that η distinguishes between handles, marked by $1 + b$, and cross-caps, marked by b. By Corollary 4.23, $h_{v,\varphi,0} = 0$ precisely when $d_{v,\varphi}(b)$ is identically zero, consequently the degree of a marginal b-polynomial determines the ratio between its coefficients of lowest degree; in a marginal b-polynomial of degree $2i$, the linear term and constant term are in the ratio $i : 1$, which is also the ratio between the quadratic and linear terms of marginal

b-polynomials of degree $2i + 1$. That these ratios hold for all known b-polynomials, provides phenomenological evidence of the following conjecture, which predicts that all b-polynomials can be expressed in terms of B_g for appropriate choices of g. If the conjecture is true, then it can be used to implicitly define coefficients, analogous to $h_{v,\varphi,i}$, that may have combinatorial interpretations in terms of handles and cross-caps.

Conjecture 5.2. *With $v, \varphi, \epsilon \vdash n$ and $g = 2 + n - \ell(v) - \ell(\varphi) - \ell(\epsilon)$, the rational function $c_{v,\varphi,\epsilon}(b)$ is an element of* $\mathrm{span}_{\mathbb{Z}_+}(B_g)$.

Remark 5.3. Elements of $\mathrm{span}(B_g)$ are naturally bounded in degree by g. When $\epsilon = [2^n]$, the expression simplifies, since $2n - \ell(\epsilon) = n$, so g is equal to the degree bound predicted by Theorem 5.1. For general values of ϵ, g is the degree bound conjectured by Goulden and Jackson in [GJ96a].

The conjecture should be viewed as a strengthening of the algebraic form of the hypermap b-Conjecture, Conjecture 3.10, which predicts that $c_{v,\varphi,\epsilon}(b)$ is an element of $\mathbb{Z}_+[b]$. Its utility arises from the relaxations obtained by considering $\mathrm{span}_R(B_g)$, with R a semi-ring containing $\mathbb{Z}_+$. Figure 5.1 summarizes the relationships between several algebraic relaxations of Conjecture 5.2.
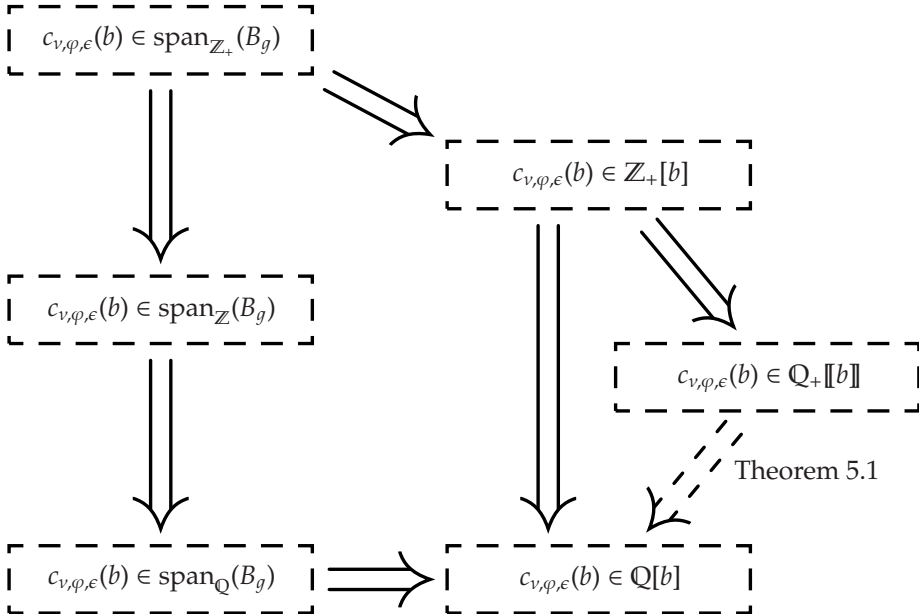
Figure 5.1: A summary of relationships between algebraic relaxations of Conjecture 5.2. That $c_{v,\varphi,\epsilon}(b) \in \mathbb{Q}_+[\![b]\!]$ implies $c_{v,\varphi,\epsilon}(b) \in \mathbb{Q}[b]$, is a consequence of Theorem 5.1, but only applies when $\epsilon = [2^n]$ and in the presence of the quantifier, "for all v such that $\ell(v) = v$." All other implications hold for individual polynomials as a consequence of set inclusion.

5.3 A Functional Equation

Focusing on the implication that $c_{v,\varphi,\epsilon}(b)$ is an element of $\text{span}_{\mathbb{Q}}(B_g)$ has proved to be particularly fruitful. By characterizing the elements of $\text{span}_{\mathbb{Q}}(B_g)$ as the polynomial solutions to a functional equation, and then using algebraic properties of the hypermap series to show that this functional equation is satisfied by all b-polynomials, it becomes feasible to draw conclusions about all possible combinatorial interpretations of the hypermap series, without deriving an explicit presentation for general b-polynomials. This approach is used to show that the degree bound of Theorem 5.1 must hold independently for each $c_{v,\varphi,\epsilon}(b)$ that is a polynomial (recall that $c_{v,\varphi,\epsilon}(b)$ is conjectured to be a polynomial but only known, in general, to be a rational function). The functional equation also suggests a potential method for proving that $c = c_{v,\varphi,\epsilon}(b)$ is indeed a polynomial in b.

Notice that for integers g and i, and with $p(b) := b^{g-2i}(1+b)^i$, then

$$p(b-1) = (b-1)^{g-2i} b^i$$
$$= (-b)^g \left(\tfrac{1}{b} - 1\right)^{g-2i} (-b)^{-2i} b^i$$
$$= (-b)^g \left(\tfrac{1}{b} - 1\right)^{g-2i} \left(\tfrac{1}{b}\right)^i$$
$$= (-b)^g p\left(\tfrac{1}{b} - 1\right).$$

Rational functions of this form generalize the elements of B_g, and are polynomials precisely when g and i are non-negative integers with $0 \le i \le \left\lfloor \tfrac{g}{2} \right\rfloor$. This observation leads to the definition of a class of rational functions.

Definition 5.4 (Ξ_g-function)**.** *A rational function $p(b)$ satisfying*

$$p(b-1) = (-b)^g p\left(\tfrac{1}{b} - 1\right) \tag{5.1}$$

is said to be a Ξ_g*-function. The set of all such functions is denoted by* Ξ_g.

Lemma 5.5. *The set of* Ξ_g*-functions is closed under finite linear combinations.*

Proof. If $p(b), q(b) \in \Xi_g$, then by trivial calculation

$$(p + \alpha q)(b-1) = p(b-1) + \alpha q(b-1) = (-b)^g (p + \alpha q)\left(\tfrac{1}{b} - 1\right). \qquad \square$$

It follows from Lemma 5.5 that every element of $\text{span}(B_g)$ is a Ξ_g-function. In particular, 0 is a Ξ_g-function for every choice of g, and $d_{v,\varphi}(b)$ is a Ξ_g-function for g equal to the Euler genus of maps enumerated by $d_{v,\varphi}(b)$. With this second example in mind, the index g can be thought of as encapsulating genus. For marginal b-polynomials, additivity of genus with respect to connected sums is reflected in the fact that

$$\text{span}(B_g) \cdot \text{span}(B_h) \subseteq \text{span}(B_{g+h}),$$

where '·' denotes multiplication in the algebra of polynomials. Equality holds unless g and h are both odd. An analogous result for Ξ_g is given in the following lemma.

Lemma 5.6. *If $p \in \Xi_g$ and $q \in \Xi_h$, then $pq \in \Xi_{g+h}$.*

Proof. This is an immediate consequence of the definition, since

$$(pq)(b-1) = p(b-1)q(b-1) = (-b)^{g+h}(pq)(\tfrac{1}{b}-1). \qquad \square$$

In general, elements of Ξ_g are not polynomials. Varying i outside of the range $0 \leq i \leq \left\lfloor \frac{g}{2} \right\rfloor$ produces Ξ_g-functions of the form $b^{g-2i}(1+b)^i$ with poles of any order at $b = -1$ or any order with parity equal to g at $b = 0$. Additionally, for any rational function $f(b)$, the function

$$k(b) = f(b+1) + (-1-b)^g f\left(\tfrac{1}{1+b}\right) \tag{5.2}$$

is a Ξ_g-function, since

$$k(b-1) = f(b) + (-b)^g f\left(\tfrac{1}{b}\right) = (-b)^g \left(f\left(\tfrac{1}{b}\right) + \left(-\tfrac{1}{b}\right)^g f(b) \right) = (-b)^g k\left(\tfrac{1}{b}-1\right).$$

If $f(b) = \frac{1}{1+x-b}$, then for general values of x, the construction produces a Ξ_g-function with poles at x and $\frac{-x}{x+1}$. Thus all but finitely many rational numbers occur as the pole of a Ξ_g-function with at most two poles. From the location and multiplicity of these poles, it follows that Ξ_g does not have a finite basis.

After algebraic manipulation, sums of the form in (5.2) appear in the defining expression for the hypermap series. This leads to the conclusion that each coefficient, $c_{\nu,\varphi,\epsilon}(b)$, is in Ξ_g for an appropriate choice of g. The following lemma provides a characterization of the polynomials in Ξ_g, which then further circumscribes the search for a combinatorial interpretation of b-polynomials.

Lemma 5.7. *For any ring R, a polynomial $p(b)$ in $R[b]$ is a Ξ_g-function if and only if it is an element of $\mathrm{span}_R(B_g)$.*

Proof. Consider a non-zero polynomial, p, satisfying (5.1). Since $(-b)^g p\left(\tfrac{1}{b}-1\right)$ is a polynomial, the degree of p is at most g. Additionally, if p has degree d, then $(-b)^g p\left(\tfrac{1}{b}-1\right)$ has degree at least $g-d$. It follows that $d \geq g-d$, and so any non-zero polynomial solution to (5.1) is bounded in degree between $\left\lceil \frac{g}{2} \right\rceil$ and g.

If p has degree $d = g - i$ and top coefficient α, then $p - \alpha \cdot b^{g-2i}(1+b)^i$ is a solution to (5.1) with degree less than d. Thus, for every non-zero polynomial solution to (5.1), there is another solution of lower degree, differing from the original solution by an element of $\mathrm{span}_R(B_g)$. Since the number of possible positive degrees is finite, it follows, by induction, that $p(b)$ differs from 0 by an element of $\mathrm{span}_R(B_g)$. $\qquad \square$

Since the proof of Lemma 5.7 makes use of additive inverses in R, this characterization cannot be used to address the question of non-negativity, but it can be used to split the task of proving that $c_{\nu,\varphi,\epsilon}(b)$ is an element of $\text{span}_{\mathbb{Q}}(B_g)$ into proving the following two intermediate conjectures.

Conjecture 5.8. *If $g = 2 + |\nu| - \ell(\nu) - \ell(\varphi) - \ell(\epsilon)$, then $c_{\nu,\varphi,\epsilon}(b)$ is a Ξ_g-function.*

Conjecture 5.9. *The rational function $c_{\nu,\varphi,\epsilon}(b)$ is a polynomial.*

Conjecture 5.8 is resolved in the next section, but Conjecture 5.9 remains open.

5.4 b-Polynomials Are Ξ_g-Functions

Addressing Conjecture 5.8 involves unpacking the definition of the hypermap series, Definition 3.7, and appealing to two technical results relating the Jack symmetric functions J_λ and $J_{\lambda'}$. The results are due to Macdonald, and a discussion of their derivation can be found in [Mac95], but the present form is described by Stanley in [Sta89]. As usual, λ' denotes the conjugate partition of λ.

Definition 5.10 ($c_{\lambda,\mu}$, $v_{\lambda,mu}$). *The coefficients $c_{\lambda\mu}(\alpha)$ and $v_{\lambda\mu}(\alpha)$ are defined implicitly by expressing $J_\lambda(\alpha)$ in terms of the power-sum and monomial bases:*

$$J_\lambda(\alpha) = \sum_\mu c_{\lambda\mu}(\alpha)p_\mu = \sum_\mu v_{\lambda\mu}(\alpha)m_\mu. \tag{5.3}$$

Distinguishing between the doubly indexed c's defined here, and the triply indexed c's used to denote b-polynomials is unambiguous, and the present choice was made to agree with the cited source material.

Lemma 5.11 (Stanley [Sta89, Cor. 3.5]).

$$J_{\lambda'}(\alpha) = \sum_\mu (-\alpha)^{|\lambda|-\ell(\mu)} c_{\lambda\mu}\left(\tfrac{1}{\alpha}\right)p_\mu.$$

In the present context, it is useful to restate the lemma in the form,

$$c_{\lambda'\mu}(\alpha) = (-\alpha)^{|\lambda|-\ell(\mu)} c_{\lambda\mu}\left(\tfrac{1}{\alpha}\right). \tag{5.4}$$

Lemma 5.12 (Stanley [Sta89, Prop. 3.6]).

$$\langle J_\lambda, J_\lambda \rangle_\alpha = \alpha^{|\lambda|} v_{\lambda\lambda}(\alpha) v_{\lambda'\lambda'}\left(\tfrac{1}{\alpha}\right). \tag{5.5}$$

Remark 5.13. Proposition 3.4 gives $\langle J_\lambda, J_\lambda \rangle_\alpha$ explicitly as a function of λ, but this level of detail is not required in the present context.

Recalling the defining expression for b-polynomials from Definition 3.7,

$$\sum_n \sum_{\nu,\varphi,\epsilon \vdash n} c_{\nu,\varphi,\epsilon}(b) p_\nu(\mathbf{x}) p_\varphi(\mathbf{y}) p_\epsilon(\mathbf{z}) := (1+b)t \frac{\partial}{\partial t} \ln \Phi(\mathbf{x},\mathbf{y},\mathbf{z};t,b) \bigg|_{t=1},$$

it is useful to examine the expansion of Φ in terms of the power-sum basis. Define $q_{\nu,\varphi,\tau}(b)$ by

$$\sum_{\nu,\varphi,\epsilon} q_{\nu,\varphi,\epsilon}(b) p_\nu(\mathbf{x}) p_\varphi(\mathbf{y}) p_\epsilon(\mathbf{z}) := \Phi(\mathbf{x},\mathbf{y},\mathbf{z};1,b)$$

$$:= \sum_{\theta \in \mathcal{P}} \frac{1}{\langle J_\theta, J_\theta \rangle_{b+1}} J_\theta(\mathbf{x};b+1) J_\theta(\mathbf{y};b+1) J_\theta(\mathbf{z};b+1),$$

where the latter equality is from (3.3).

Lemma 5.14. *The rational function $q_{\nu,\varphi,\epsilon}(b)$ is a Ξ_g-function, provided that $g = |\nu| - \ell(\nu) - \ell(\varphi) - \ell(\epsilon)$.*

Proof. By homogeneity of Jack symmetric functions, $q_{\nu,\varphi,\epsilon}(0)$ is identically 0 unless $|\nu| = |\varphi| = |\epsilon|$. Since 0 is a Ξ_g-function for every value of g, it remains only to consider the case of $\nu, \varphi, \epsilon \vdash n$ for some n. In this case, by noting that

$$\{\theta : \theta \vdash n\} = \{\theta' : \theta \vdash n\},$$

expanding $q_{\nu,\varphi,\epsilon}(b)$ using (5.3) and (5.5) gives

$$q_{\nu,\varphi,\epsilon}(b-1) = \sum_{\theta \vdash n} \frac{1}{b^n v_{\theta'\theta'}(b) v_{\theta''\theta''}\left(\frac{1}{b}\right)} c_{\theta'\nu}(b) c_{\theta'\varphi}(b) c_{\theta'\epsilon}(b)$$

$$= \sum_{\theta \vdash n} \frac{(-b)^{n-\ell(\nu)-\ell(\varphi)-\ell(\epsilon)}}{\left(\frac{1}{b}\right)^n v_{\theta\theta}\left(\frac{1}{b}\right) v_{\theta'\theta'}(b)} c_{\theta\nu}\left(\frac{1}{b}\right) c_{\theta\varphi}\left(\frac{1}{b}\right) c_{\theta\epsilon}\left(\frac{1}{b}\right)$$

$$= (-b)^{n-\ell(\nu)-\ell(\varphi)-\ell(\epsilon)} q_{\nu,\varphi,\epsilon}\left(\frac{1}{b}-1\right),$$

with the second equality using (5.4) and the fact $(-b)^{3n} = (-b)^n \left(\frac{1}{b}\right)^{-2n}$. $\qquad\square$

Example 5.15. *Directly computing J_ν for $\nu \vdash 2$ gives*

$$J_{[1^2]}(1+b) = p_{[1^2]} - p_{[2]}, \quad \text{and} \quad J_{[2]}(1+b) = p_{[1^2]} + (1+b)p_{[2]},$$

so the norms of $J_{[1^2]}$ and $J_{[2]}$ are given by

$$\langle J_{[1^2]}, J_{[1^2]} \rangle_{1+b} = 4 + 6b + 2b^2, \quad \text{and} \quad \langle J_{[2]}, J_{[2]} \rangle_{1+b} = 4 + 10b + 8b^2 + 2b^3.$$

The corresponding $q_{\nu,\varphi,\epsilon}(b)$ for $\nu, \varphi, \epsilon \vdash 2n$ are thus

$$q_{[1^2],[1^2],[1^2]}(b) = \frac{1}{4 + 6b + 2b^2} + \frac{1}{4 + 10b + 8b^2 + 2b^3} = \frac{1}{2(1+b)^2},$$

$$q_{[1^2],[1^2],[2]}(b) = \frac{-1}{4 + 6b + 2b^2} + \frac{1+b}{4 + 10b + 8b^2 + 2b^3} = 0,$$

$$q_{[1^2],[2],[2]}(b) = \frac{1}{4 + 6b + 2b^2} + \frac{(1+b)^2}{4 + 10b + 8b^2 + 2b^3} = \frac{1}{2(1+b)}, \text{ and}$$

$$q_{[2],[2],[2]}(b) = \frac{-1}{4 + 6b + 2b^2} + \frac{(1+b)^3}{4 + 10b + 8b^2 + 2b^3} = \frac{b}{2(1+b)},$$

with the unlisted functions recoverable through symmetry.

Remark 5.16. Structurally, the appearance of Ξ_g-functions is a consequence of a pairing between terms indexed by conjugate partitions. Using the notation

$$r_\theta(b) := \frac{c_{\theta\nu}(b) c_{\theta\varphi}(b) c_{\theta\epsilon}(b)}{b^{|\theta|} v_{\theta\theta}(b) v_{\theta'\theta'}\left(\frac{1}{b}\right)},$$

$q_{\nu,\varphi,\epsilon}(b)$ can be written in the form

$$q_{\nu,\varphi,\epsilon}(b) = \sum_{\theta \vdash n} r_\theta(b+1) = \frac{1}{2} \sum_{\theta \vdash n} \left(r_\theta(b+1) + r_{\theta'}(b+1) \right).$$

The proof of Lemma 5.14 implicitly shows that $r_{\theta'}(b+1) = (-1-b)^g r_\theta(\frac{1}{b+1})$, so it follows that each term in the second sum is in the form prescribed by (5.2), and is thus a Ξ_g-function. Despite the proof revealing this additional algebraic structure, a further investigation of these revised terms is not expected to expose any additional combinatorial structure of the map series. In general, the intermediate terms are not polynomials, nor do they have non-negative coefficients, and many have several distinct poles.

Example 5.17. *Computing $J_\nu(1+b)$ for $\nu \vdash 3$ gives*

$$J_{[1^3]}(1+b) = p_{[1^3]} - 3p_{[1,2]} + 2p_{[3]},$$

$$J_{[1,2]}(1+b) = p_{[1^3]} + bp_{[1,2]} - (1+b)p_{[3]},$$

$$J_{[3]}(1+b) = p_{[1^3]} + 3(1+b)p_{[1,2]} + 2(1+b)^3 p_{[3]},$$

$$\left\langle J_{[1^3]}, J_{[1^3]} \right\rangle_{1+b} = 6(1+b)(2+b)(3+b),$$

$$\left\langle J_{[1,2]}, J_{[1,2]} \right\rangle_{1+b} = (3+b)(3+2b)(1+b)^2, \text{ and}$$

$$\left\langle J_{[3]}, J_{[3]} \right\rangle_{1+b} = 6(2+b)(2b+3)(1+b)^3.$$

Applying Remark 5.16, $q_{[1^3],[1^3],[1^3]}(b)$ can be written as a sum of Ξ_{-6}-functions, giving

$$q_{[1^3],[1^3],[1^3]}(b) = \frac{1}{(3+b)(3+2b)(1+b)^2} + \frac{3+3b+2b^2}{6(3+2b)(3+b)(1+b)^3} = \frac{1}{6(1+b)^3}.$$

By examining the actions of the logarithm and differential operator in the construction of the hypermap series, the results of Lemma 5.14 can be lifted to arbitrary b-polynomials. The leads to the following, which is the main result of this Section.

Theorem 5.18. *For $v, \varphi, \epsilon \vdash n$, the rational function $c_{v,\varphi,\epsilon}(b)$ is a Ξ_g-function with $g = 2 + n - \ell(v) - \ell(\varphi) - \ell(\epsilon)$.*

Proof. Since Φ has unit constant term, $\ln \Phi$ is given by

$$\ln \Phi = \sum_{i \geq 1} (-1)^i \frac{(\Phi - 1)^i}{i}.$$

Thus, if $q_{v,\varphi,\epsilon}^{(i)}(b)$ is defined by

$$\sum_{v,\varphi,\epsilon \in \mathscr{P}} q_{v,\varphi,\epsilon}^{(i)}(b) t^{|v|} p_v(\mathbf{x}) p_\varphi(\mathbf{y}) p_\epsilon(\mathbf{z}) := \left(\Phi(\mathbf{x}, \mathbf{y}, \mathbf{z}; t, b) - 1 \right)^i,$$

then the b-polynomial, $c_{v,\varphi,\epsilon}(b)$, can be written explicitly as

$$c_{v,\varphi,\epsilon}(b) = (1 + b) \sum_{i=1}^{|v|} (-1)^i \frac{|v|}{i} q_{v,\varphi,\epsilon}^{(i)}(b).$$

The upper bound on the summation is finite, since by homogeneity, $q_{v,\varphi,\epsilon}^{(i)}(b)$ is identically zero unless $v, \varphi, \epsilon \vdash n$ for some $n \geq i$. Since $1 + b$ is a Ξ_2-function, and Ξ_g is closed under finite linear combinations, it is sufficient to show, for every $i, v, \varphi,$ and ϵ, that $q_{v,\varphi,\epsilon}^{(i)}(b)$ is a Ξ_t-function with t defined by

$$t := t(v, \varphi, \epsilon) := |v| - \ell(v) - \ell(\varphi) - \ell(\epsilon).$$

The proof proceeds by induction on i. The base case is $q_{v,\varphi,\epsilon}^{(1)}(b) = q_{v,\varphi,\epsilon}(b)$ when $|v| > 0$, and this is a Ξ_t-function by Lemma 5.14. Viewing partitions as multi-sets, when $\hat{\kappa}$ is a submulti-set of κ, let $\overline{\kappa} := \kappa \setminus \hat{\kappa}$ denote the complement of $\hat{\kappa}$ with respect to κ. Then for $i \geq 1$,

$$q_{v,\varphi,\epsilon}^{(i+1)}(b) = \sum_{(\hat{v},\hat{\varphi},\hat{\epsilon}) \in R_{v,\varphi,\epsilon}} q_{\hat{v},\hat{\varphi},\hat{\epsilon}}^{(1)}(b) \, q_{\overline{v},\overline{\varphi},\overline{\epsilon}}^{(i)}(b), \tag{5.6}$$

where the sum is taken over

$$R_{v,\varphi,\epsilon} = \left\{ (\hat{v}, \hat{\varphi}, \hat{\epsilon}) : \hat{v} \subseteq v, \hat{\varphi} \subseteq \varphi, \hat{\epsilon} \subseteq \epsilon, \text{ and } |\hat{v}| = |\hat{\varphi}| = |\hat{\epsilon}| \right\}.$$

Inductively, $q^{(1)}_{\hat{v},\hat{\varphi},\hat{\epsilon}}(b)$ is a $\Xi_{\hat{t}}$-function and $q^{(i)}_{\overline{v},\overline{\varphi},\overline{\epsilon}}(b)$ is a $\Xi_{\overline{t}}$-function, where

$$\hat{t} := t(\hat{v},\hat{\varphi},\hat{\epsilon}) \qquad \text{and} \qquad \overline{t} := t(\overline{v},\overline{\varphi},\overline{\epsilon}).$$

Since, for $\hat{\kappa} \subseteq \kappa$, $|\hat{\kappa}| + |\overline{\kappa}| = |\kappa|$ and $\ell(\hat{\kappa}) + \ell(\overline{\kappa}) = \ell(\kappa)$, it follows by Lemma 5.6 that each term of (5.6) is in Ξ_t, and, by Lemma 5.5, that so is $q^{(i+1)}_{v,\varphi,\epsilon}(b)$. □

Remark 5.19. A comment of Brown, [Bro00, Cor. 6.6], suggests that he knew of this proof in the setting of marginal b-polynomials, but, lacking the equivalent of Lemma 5.7, did not realize its potential applications.

Example 5.20. *If $g = |v| + \ell(v) + \ell(\varphi) + \ell(\epsilon)$ is odd, then*

$$c_{v,\varphi,\epsilon}(0) = c_{v,\varphi,\epsilon}(1-1) = (-1)^g c_{v,\varphi,\epsilon}\left(\tfrac{1}{1} - 1\right) = -c_{v,\varphi,\epsilon}(0),$$

so $c_{v,\varphi,\epsilon}(0) = 0$. Combining this with the combinatorial interpretation of $H(\mathbf{x}, \mathbf{y}, \mathbf{z}; 0)$ gives an indirect proof that every orientable hypermap has even Euler characteristic.

5.5 Implications

Theorem 5.18 resolves Conjecture 5.8, and reduces the problem of proving that $c_{v,\varphi,\epsilon}(b)$ is in $\mathrm{span}_{\mathbb{Q}}(B_g)$ to proving that $c_{v,\varphi,\epsilon}(b)$ is a polynomial, that is verifying Conjecture 5.9. This conjecture remains open, but Theorem 5.18 offers some additional insights. From the construction of the map series, any pole of a b-polynomial must occur as a zero of a $\langle J_\lambda, J_\lambda \rangle_{1+b}$ for some partition λ, since, by the polynomiality results of Lapointe and Vinet, [LV95], or Knop and Sahi, [KS97], the numerators of Φ are polynomials in b. Recall from Proposition 3.4 that

$$\langle J_\lambda, J_\lambda \rangle_\alpha = \prod_{x \in \lambda} \left(\alpha a_\lambda(x) + l_\lambda(x) + \alpha \right)\left(\alpha a_\lambda(x) + l_\lambda(x) + 1 \right), \tag{5.7}$$

where $a_\lambda(x)$ and $l_\lambda(x)$ are defined in (3.2), and denote the arm and leg lengths of x as a box of the Ferrers diagram of λ. This can only vanish when α is a rational number with $\alpha \leq 0$, since for every box $x \in \lambda$, both $a_\lambda(x)$ and $l_\lambda(x)$ are non-negative integers. Taking into account the change of variables, $\alpha = b + 1$, every complex pole of every b-polynomial must occur at a rational number on the interval $(-\infty, -1]$. But, from Theorem 5.18, if $c_{v,\varphi,\epsilon}(b)$ has a pole at x, then it also has a pole at $\frac{1}{x+1} - 1$. It follows that for every pole in the interval $(-\infty, -2)$, the function has a second pole in the interval $(-2, -1)$. Thus, to show that $c_{v,\varphi,\epsilon}(b)$ is a polynomial, it is sufficient to show that it has no poles in the interval $[-2, -1]$, which gives the following alternative characterization of polynomiality.

Proposition 5.21. *If $c_{v,\varphi,\epsilon}(b)$ has the Maclaurin series expansion $\sum_{i\geq 0} a_i b^i$, then it is a polynomial if and only if $\sum_{i\geq 0} a_i(-2)^i$ converges.*

Even without resolving the question of polynomiality, it is still possible to infer combinatorial properties of all b-invariants. Together, Theorem 5.18 and
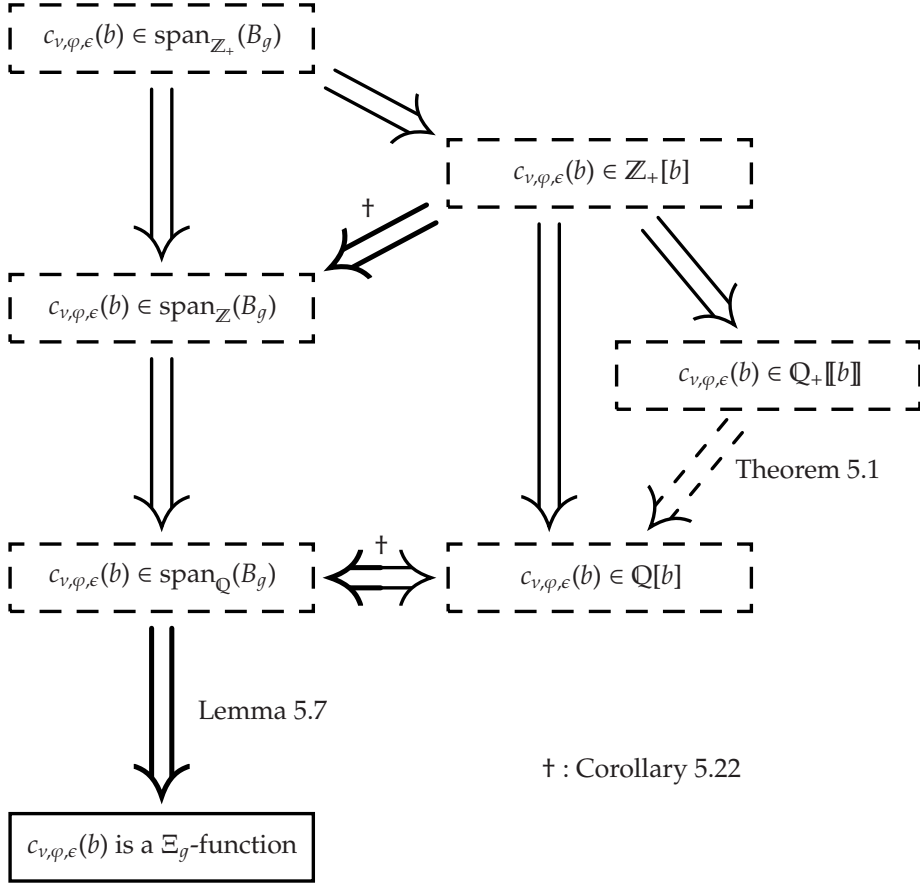
Figure 5.2: A revised summary of relationships between relaxations of Conjecture 5.2. New implications are indicated by bold arrows.

Lemma 5.7 have the following immediate corollary, the implications of which are incorporated into Figure 5.2, an updated version of Figure 5.1, giving a revised summary of relaxations of Conjecture 5.2 that have been obtained in this Chapter.

Corollary 5.22. *If $c_{v,\varphi,\epsilon}(b)$ is a polynomial in b over the ring R, then it has degree at most $g = 2 + |v| - \ell(v) - \ell(\varphi) - \ell(\epsilon)$, and*

$$c_{v,\varphi,\epsilon}(b) \in \mathrm{span}_R(B_g).$$

Remark 5.23. It is most notable that the existence of a b-invariant is sufficient to show that the hypothesis of Corollary 5.22 is satisfied with $R = \mathbb{Z}$. It is thus possible, without addressing existence, to draw conclusions about all possible b-invariants.

Assuming polynomiality, and writing $c_{v,\varphi,\epsilon}(b)$ as an element of span(B_g), emphasizes the relationship between b-invariants and edges. In the specialization to maps, $h_{v,\varphi,i}$ can be refined by writing $c_{v,\varphi,[2^n]}(b) = \sum_i h_{v,\varphi,i} b^{g-2i}(1+b)^i$, so that $h_{v,\varphi,i} = \sum_{\ell(v)=v} h_{v,\varphi,i}$. Then using z as a scalar gives

$$M(\mathbf{x},\mathbf{y},z;b) = \frac{1}{z^2} \sum_{v,\varphi \vdash 2n} \sum_i h_{v,\varphi,i}(\mathbf{x}z)^v(\mathbf{y}z)^\varphi(bz)^{g-2i}\left((1+b)z^2\right)^i, \qquad (5.8)$$

with $g = g(n,v,\varphi) = 2 + n - \ell(v) - \ell(\varphi)$, and i ranging between 0 and $\left\lfloor \frac{g}{2} \right\rfloor$. Expressing M in this form, with b occurring together with z, emphasizes why a combinatorial interpretation of the series may be expected to be derived from an invariant that is naturally described in terms of edge deletion, and why such an invariant is expected, like η, to involve contributions from two qualitatively different classes of edges. The form of M in (5.8) also reinforces the relationship between b-invariants and Euler genus.

Corollary 5.24. *If β is any b-invariant, and $\mathfrak{m}$ is a rooted map on the sphere with $k \geq 1$ cross-caps, then $1 \leq \beta(\mathfrak{m}) \leq k$.*

Corollary 5.25. *If there is a b-invariant, then it agrees with η for all rooted maps on the sphere and projective plane. For such maps, the invariant remains unchanged under duality and re-rooting.*

Corollary 5.26. *For $v, \varphi, \epsilon \vdash n$, if $g = 2 + n - \ell(v) - \ell(\varphi) - \ell(\epsilon)$ is negative and $c_{v,\varphi,\epsilon}(b)$ is a polynomial, then $c_{v,\varphi,\epsilon}(b)$ is identically zero.*

Proof. The set B_g is empty when g is negative. □

Interpreting $H(\mathbf{x},\mathbf{y},\mathbf{z};0)$ and $H(\mathbf{x},\mathbf{y},\mathbf{z};1)$ as generating series for hypermaps, shows that $c_{v,\varphi,\epsilon}(b)$ vanishes at $b = 0$ and $b = 1$ whenever $g = 2 + |v| - \ell(v) - \ell(\varphi) - \ell(\epsilon)$ is negative. Corollary 5.26 shows that, assuming polynomiality, these b-polynomials vanish for general b, which is an algebraic prerequisite of the conjectured combinatorial interpretation for H as a generating series for rooted hypermaps.

Remark 5.27. With the structural restrictions imposed on b-polynomials by Corollary 5.22, it becomes possible, at least in theory, to verify that a function is a b-invariant, without relating its computation to the algebraic definition of the map series. If $c_{v,\varphi,\epsilon}(b)$ can be shown to be a polynomial, then it can be identified with a combinatorial sum by equating evaluations at specific values of b. In practice, evaluations of the map series at $b = 0$ and $b = 1$ are well understood, and the evaluation at $b = -1$ has a conjectured combinatorial significance (see Conjecture 5.28), so this approach could potentially be used to verify that a function is a b-invariant for all maps with Euler genus at most four. This approach is explored in Chapter 6.

Table 5.1: Families of $h_{v,\varphi,i}$ that can be shown to be non-negative with appropriate assumptions on the coefficients of $c_{v,\varphi,[2^n]}(b)$ with respect to the standard basis.

Family	Assumption	Reason
$\ell(v) = 1$	None	Remark 4.19
$\ell(\varphi) = 1$	None	Remark 4.19 and symmetry
$i = \frac{g}{2}$, g even	None	Coefficients of $M(\mathbf{x}, \mathbf{y}, z; 0)$
$g = 0$	Polynomiality	Coefficients of $M(\mathbf{x}, \mathbf{y}, z; 0)$
$g = 1$	Polynomiality	Coefficients of $M(\mathbf{x}, \mathbf{y}, z; 1)$
$i = 0$	Polynomiality, Non-negativity	$h_{v,\varphi,i}$ is the only contribution to the b^g term of $c_{v,\varphi,[2^n]}(b)$
$i = 1$	Polynomiality, Non-negativity	$h_{v,\varphi,i}$ is the only contribution to the b^{g-1} term of $c_{v,\varphi,[2^n]}(b)$
$i = \frac{g-1}{2}$, g odd	Polynomiality, Non-negativity	$h_{v,\varphi,i}$ is the only contribution to the linear term of $c_{v,\varphi,[2^n]}(b)$

5.6 Non-Negativity and Numerical Evidence

Knowing that b-polynomials are elements of span(B_g), provided that they are polynomials at all, narrows the gap between non-negativity with respect to the standard basis and non-negativity with respect to B_g. Table 5.1 lists families of coefficients for which Conjecture 5.2 and Conjecture 3.10 have identical implications. These families include all $h_{v,\varphi,i}$ corresponding to maps with at most seven edges, or corresponding to maps in surfaces with Euler genus at most five.

In the absence of a proof that η is a b-invariant, the best evidence for non-negativity of the coefficients of b-polynomials, both as elements of span(B_g) and with respect to the standard basis, is currently numerical. Using the degree bound of Corollary 5.22 and assuming polynomiality, it is possible to compute b-polynomials *via* polynomial interpolation. This replaces arithmetic over the field of rational functions, $\mathbb{Q}(b)$, with arithmetic over $\mathbb{Q}$, and offers a significant improvement in run-time and memory usage, when compared to direct computation. Section B.4 of Appendix B includes a procedure for computing low-degree terms of the map series using `Maple`, a symbolic algebra system. The procedure was used to compute the map series up to (and including) coefficients of z^8.

Assuming polynomiality, every map polynomial, $c_{v,\varphi,[2^n]}(b)$, with $n \leq 8$ has

non-negative integer coefficients in both the standard basis and as an element of span(B_g). This accounts for 24,187 polynomials, with 48,249 non-zero coefficients in the standard basis, enumerating 2,319,581,295 (this is over two billion!) rooted maps. Expressing these polynomials as elements of span$_\mathbb{Z}(B_g)$ produces 36,218 positive coefficients, of which 64 do not occur in any family listed in Table 5.1. These exceptional coefficients correspond to maps with eight edges, two vertices, and two faces, and, up to symmetry, appear as the 36 coefficients of $b^2(1 + b)^2$ in Table A.1 of Appendix A.

In contrast to Corollary 4.23, not every pair $\nu, \varphi \vdash 2n$ with $g = 2 + n - \ell(\nu) - \ell(\varphi) \geq 0$ can be realized as the vertex- and face-degree partitions of rooted maps. For example, $c_{[3^2],[3^2],[2^3]}(b) = 0$, but $2 + 3 - \ell([3^2]) - \ell([3^2]) = 1$. Non-realizable pairs of partitions are listed by Jackson and Visentin in [JV01, Chap. 11]. Of the $37,011$ triples (ν, φ, i) with $\nu, \varphi \vdash 2n$, $g = 2 + n - \ell(\nu) - \ell(\varphi) \geq 0$, $0 \leq i \leq \lfloor \frac{g}{2} \rfloor$, and $n \leq 8$, the only triples for which $h_{\nu,\varphi,i}$ is zero occur with $i = \lfloor \frac{g}{2} \rfloor$ and $g \leq 2$. In particular, every computed polynomial is either identically zero or has degree equal to the bound predicted by Theorem 5.1.

Brown speculated, [Bro00, App. A.1], that coefficients might be shown to be non-negative by relating them to ranks of appropriate homology groups, noting that the dual of the matching graph is a simplicial complex. In this setting, the relationship between the coefficients of $c_{\nu,\varphi,\epsilon}(b)$ in the standard basis and in the basis B_g is reminiscent of the correspondence between f-vectors and h-vectors in the study of simplicial complexes, with (5.1) taking the rôle of the Dehn-Sommerville equations.

5.7   Top Coefficients and Unhandled Maps

As in the marginal case, assuming polynomiality, the coefficient of b^g in $c_{\nu,\varphi,\epsilon}(b)$ can be recovered, up to a factor of -1, by an evaluation at $b = -1$. Specializing (5.8) shows that, for maps,

$$M(-\mathbf{x}, -\mathbf{y}, -z; -1) = \frac{1}{z^2} \sum_{\nu,\varphi \vdash 2n} h_{\nu,\varphi,0}(\mathbf{x}z)^\nu (\mathbf{y}z)^\varphi z^g.$$

For hypermaps, recovering the top coefficients requires additionally evaluating Φ at $t = -1$. Motivated by the combinatorial interpretation of the top coefficients in the marginal case, the procedure from Section B.5 of Appendix B was used to compute the generating series for unhandled maps (recall Definition 4.25) with at most six edges. This series agrees with $M(-\mathbf{x}, -\mathbf{y}, -z; -1)$, providing numerical evidence for the following two conjectures, both generalizing Corollary 4.23.

Conjecture 5.28. *The series, $U(\mathbf{x}, \mathbf{y}, z) := M(-\mathbf{x}, -\mathbf{y}, -z; -1)$, is the generating series for unhandled maps with respect to vertex-degree partition, face-degree partition, and number of edges.*

Conjecture 5.29. *If there is a rooted map with vertex-degree partition ν and face-degree partition φ, then there is an unhandled rooted map with the same vertex- and face-degree partitions.*

Remark 5.30. Conjecture 5.29 is related to the essential nature of the factor $1 + b$ in the definition of the map series, and suggests that every non-zero $q_{\nu,\varphi,[2^n]}(b)$ has a pole at $b = -1$. Verifying Conjecture 5.28 would confirm that these poles do not survive in M. It might then be possible to conclude that the coefficients of the map series are polynomials in b by checking that each $q_{\nu,\varphi,[2^n]}(b)$ has no poles except at $b = -1$.

Conjecture 5.28 predicts that a third distinguished specialization of the map series, at $b = -1$, complements its specializations at $b = 0$ and $b = 1$. This suggests that unhandled maps may play a rôle comparable to that played by orientable and locally orientable rooted maps. Besides extending the applicability of the technique described in Remark 5.27 to maps with Euler genus at most four, the existence of a third combinatorially significant specialization offers a test for the validity of a b-invariant, and this test is likely more tractable than the general problem. In particular, in a direct enumeration of unhandled maps, as used to generate the numerical evidence for the conjecture, it is possible to ignore the structure of non-root faces.

It remains to find a presentation of the map series for which evaluation at $b = -1$ is possible, since the symmetric function presentation is degenerate there. The Jack symmetric functions themselves can only be constructed directly for positive values of the parameter α, but the limit, $\lim_{\alpha \to 0} J_\theta(\alpha)$, is well understood and can be taken as a definition, since the functions are known to be polynomials in α by [LV95] and [KS97]. Using this definition, $J_\theta(0)$ is a renormalized elementary symmetric function, with the normalizing factor given by Stanley in [Sta89, Prop. 7.6] as

$$J_\lambda(\mathbf{x}; 0) = e_{\lambda'}(\mathbf{x}) \prod_i \lambda'_i!.$$

This suggests that there is a relationship between elementary symmetric functions and unhandled maps, but from (5.7), every column of the Ferrers diagram of λ contributes a factor of $1 + b$ to $\langle J_\lambda, J_\lambda \rangle_{b+1}$, so the denominators of Φ all vanish at $b = -1$. Since the pole is removable in the conjectured combinatorial interpretation, further asymptotics of the limits of the numerators are required.

It might also be possible to recover the top coefficients by analytic methods. Since the top coefficients correspond to the pole of $\frac{1}{1+b}M$, integrating the Jack parameter around the contour $|\alpha| = 1$ gives potentially the most compact expression for U, and provides a bridge to the rich integration theory of Jack symmetric functions as developed by Kadell (see [Kad93], for example).

5.8 Summary

This Chapter used combinatorial properties of η, the marginal b-invariant introduced in Chapter 4, to predict, in Conjecture 5.2, that $c_{\nu,\varphi,\epsilon}(b)$ is an element of $\text{span}_{\mathbb{Z}_+}(B_g)$ with $g = 2 + |\nu| - \ell(\nu) - \ell(\varphi) - \ell(\epsilon)$. A weaker result, that if $c_{\nu,\varphi,\epsilon}(b)$ is a polynomial then it is in $\text{span}_{\mathbb{Q}}(B_g)$, was verified, as Corollary 5.22, using properties of Jack symmetric functions. The degree bound inherent to elements of $\text{span}(B_g)$, makes it possible to compute b-polynomials using rational arithmetic, and was used to provide additional numerical evidence that η is a b-invariant.

Writing b-polynomials in terms of B_g provides a structural explanation for the degree bound conjectured by Goulden and Jackson in [GJ96a], and for the numerical relationship observed between low degree terms. It also emphasizes the topological nature of all b-invariants, and restricts possible combinatorial interpretations of the hypermap series. Additional evidence suggests that the 'strange evaluation' at $b = -1$ of the map series extracts its top coefficients and enumerates unhandled maps, generalizing an observation from Chapter 4. Chapter 6 examines how these properties might be used to show that η is a b-invariant for all maps of low genus.

Chapter 6

Recognizing a *b*-Invariant

This Chapter explores the problem of how to show that a particular function is a *b*-invariant, with an emphasis on the functions satisfying Definition 4.1. While the existence of a *b*-invariant has not been verified, conditional on this existence, the Chapter outlines an approach for verifying that functions are *b*-invariants for all maps on surfaces of Euler genus at most 4. Together with Theorem 4.16, this would be sufficient to give a combinatorial interpretation to coefficients of z^5 in the map series $M(\mathbf{x}, \mathbf{y}, z; b)$. If in addition a combinatorial explanation for the symmetry between $\mathbf{x}$ and $\mathbf{y}$ in the map series is supplied, then the interpretation could be extended to coefficients of z^6.

Algebraic properties of *b*-polynomials, as given by Corollary 5.22, are used to make concrete predictions about the combinatorics of *b*-invariants, and these are sufficient to describe the behaviour of *b*-invariants for all rooted maps with a small number of edges or sufficiently low genus. This description is sufficient to achieve, in Corollary 6.13, the more modest goal of verifying that the functions described in Definition 4.1 are *b*-invariants for the infinite class of rooted maps on the Klein bottle with at most three vertices.

The general approach is to classify rooted maps according to genus, number of edges, and number of vertices, and then to verify that a function is a *b*-invariant for each class. To extend this analysis beyond the simplest cases, clues are taken from the marginal case discussed in Chapter 4. These suggest that the appearance of B_g in Corollary 5.22 is an expression of the relationship between twisted and untwisted handles (recall Definition 4.2), so Section 6.4 examines the question of which handles should be considered twisted, and whether this is indeed the correct question.

Section 6.4 isolates two refinements of Definition 4.1 for further study. One specialization has enough structure for verifying that it defines *b*-invariants for rooted maps with two vertices and at most six edges on the cross-capped torus and doubly cross-capped torus, with the tangible consequence, given in Corollary 6.29, that all such functions are *b*-invariants for all maps with at most four edges. This is notable for the fact that it exhausts the list of 4428 non-

orientable maps presented by Jackson and Visentin in [JV01], an atlas compiled with an eye towards examining problems like the b-Conjecture. Computer assistance in the proof of Corollary 6.29 is minimal, being limited to verifying the polynomiality of coefficients of $M(\mathbf{x}, \mathbf{y}, z; b)$ and generating the 260 unhandled rooted maps with 4 edges, 2 vertices, and 1 face.

6.1 A Classification of Rooted Maps

At present, there is no uniform approach for verifying that a particular function is a b-invariant for all maps, but Chapters 4 and 5 provide tools for dealing with collections of rooted maps on a case-by-case basis. An armamentarium of these tools can be used to analyze all sufficiently small maps: small in the sense of having few edges, or few vertices and low genus. A precise description of these tools reveals structural subtleties that are useful for analyzing the general problem. In particular, a specialization of Definition 4.1 is described in Section 6.4, and is motivated by a bijection used Section 6.2 for analyzing rooted maps on the Klein bottle: the specialized family of invariants is used in Section 6.5 to analyze rooted maps on the cross-capped torus.

A brute force approach is infeasible, even for rooted maps with relatively few edges, since the number of rooted maps grows quickly as the number of edges is allowed to increase. This is summarized in the following table.

Edges	1	2	3	4	5	6	7
Rooted Maps	3	24	297	4 896	100 278	2 450 304	69 533 397

Table 6.1 offers a further refinement by giving the distribution of rooted maps with respect to genus, number of edges, and number of vertices. Recall the convention that η denotes any invariant that satisfies Definition 4.1. Two infinite classes of rooted maps for which existing results are sufficient to show that η is a b-invariant are highlighted in Table 6.1: Remark 4.19 shows that η is a b-invariant for all monopoles, and Corollary 5.25 shows that η agrees with every b-invariant for planar and projective planar rooted maps.

Two additional approaches are available for verifying that a function is a b-invariant for maps on the Klein bottle. Direct computation applies when considering rooted maps with a small number of edges, while a bijective analysis applies when considering rooted maps on the Klein bottle with at most three vertices. A combination of the two approaches is needed in Section 6.5 for analyzing invariants for rooted dipoles on the cross-capped torus, so both approaches are examined in more detail.

Remark 6.1. All invariants satisfying Definition 4.1 take the same values when evaluated on rooted maps with Euler genus at most 2, so in this limited domain, it is not necessary to distinguish between them.

Proposition 6.2. *If there is a b-invariant for rooted maps on the Klein bottle with at most 6 edges, then η is such an invariant.*

Table 6.1: This table shows the distributions of rooted maps with respect to genus, number of edges, and number of vertices. Shaded regions indicate infinite classes of rooted maps for which η is known to be a b-invariant, if any such invariant exists.

Edges	Vertices	$g = 0$	$g = 1$	$g = 2$	$g = 3$	$g = 4$	$g = 5$
1	1	1	1				
	2	1					
2	1	2	5	5			
	2	5	5				
	3	2					
3	1	5	22	52	41		
	2	22	54	52			
	3	22	22				
	4	5					
4	1	14	93	374	690	509	
	2	93	398	899	690		
	3	164	398	374			
	4	93	93				
	5	14					
5	1	42	386	2 290	7 150	12 143	8 229
	2	386	2 480	9 490	16 925	12 143	
	3	1 030	4 330	9 490	7 150		
	4	1 030	2 480	2 290			
	5	386	386				
	6	42					

Proof. If v and φ are the vertex- and face-degree partitions of a rooted map with n edges on the Klein bottle, then $c_{v,\varphi,[2^n]}(b) = h_{v,\varphi,1}(1 + b) + h_{v,\varphi,0}b^2$, by Corollary 5.22. By Theorem 4.4, the generating series for rooted maps with vertex-degree partition v and face-degree partition φ with respect to η is of the form

$$\sum_{m \in \mathcal{M}_{v,\varphi}} b^{\eta(m)} = a_{v,\varphi,0} + a_{v,\varphi,1}b + a_{v,\varphi,2}b^2,$$

where $\mathcal{M}_{v,\varphi}$ denotes the set of rooted maps with vertex-degree partition v and face-degree partition φ. Since $c_{v,\varphi,[2^n]}(0)$ and $c_{v,\varphi,[2^n]}(1)$ enumerate orientable and locally orientable rooted maps, it follows that

$$h_{v,\varphi,1} = a_{v,\varphi,0} \qquad \text{and} \qquad 2h_{v,\varphi,1} + h_{v,\varphi,0} = a_{v,\varphi,0} + a_{v,\varphi,1} + a_{v,\varphi,2}.$$

For maps with at most 6 edges, the result follows by direct computation, since the procedure from Section B.5 of Appendix B shows that $h_{v,\varphi,0}$ enumerates unhandled maps whenever $|v| \leq 12$, and so $h_{v,\varphi,0} = a_{v,\varphi,2}$. $\qquad\square$

The proof of Proposition 6.2 relies on combinatorial interpretations for evaluations of the map polynomials at $b = 0$, $b = 1$, and $b = -1$. Since the significance of the third evaluation has been verified only numerically, this approach does not apply for maps with arbitrarily many edges. Extending the analysis to infinite classes of rooted maps involves giving a bijective explanation for the appearance of B_2 in Corollary 5.22, and using the fact that elements of span(B_2) can be reconstructed from their evaluations at $b = 0$ and $b = 1$. The bijective content of the approach is predicted by the following theorem.

Theorem 6.3. *If β is a b-invariant for rooted maps on the Klein bottle, then there is a vertex- and face-degree partition preserving bijection between all rooted maps on the torus and those rooted maps on the Klein bottle for which β takes the value 1.*

Proof. Since β is assumed to be a b-invariant, the series M has coefficients that are polynomial in b. By Corollary 5.22, if $\nu, \varphi \vdash 2n$ are, respectively, the vertex- and face-degree partitions of a map on the Klein bottle, then the b-polynomial $c_{\nu,\varphi,[2^n]}(b)$ is an element of span(B_2), and can be written in the form

$$c_{\nu,\varphi,[2^n]}(b) = \sum_{\mathfrak{m} \in \mathcal{M}_{\nu,\varphi}} b^{\beta(\mathfrak{m})} = h_{\nu,\varphi,1}(1 + b) + h_{\nu,\varphi,0}b^2.$$

Specializing to $b = 0$ shows that $h_{\nu,\varphi,1}$ is the number of rooted maps on the torus with the prescribed vertex- and face-degree partitions, but it is also the number of rooted maps in $\mathcal{M}_{\nu,\varphi}$ for which β takes the value 1. □

Remark 6.4. Similar combinatorial predictions can be made for rooted maps of higher genera, but aside from the analogous statement for rooted maps on the cross-capped torus, they do not involve bijections and are better stated in terms of equivalence classes. Generalizations of Theorem 6.3 are discussed in Section 6.3.

Remark 6.5. Every element of B_g is monic, so any common factor of the coefficients of $c_{\nu,\varphi,\epsilon}(b)$ with respect to the standard basis is also a common factor of its coefficients with respect to B_g. As a consequence, if Conjecture 5.2 and Conjecture 4.9 are both true, then they can be applied simultaneously. Thus the bijection predicted by Theorem 6.3 is expected to preserve the degree of the root face. It reasonably may be expected to also preserve the degree of the root vertex, but this is not predicted by any of the stated algebraic conjectures.

6.2 Explicit Bijections for Genus 2 Rooted Maps

To show that η is a b-invariant for rooted maps on the Klein bottle, it remains only to find the bijection predicted by Theorem 6.3. Proposition 6.2 guarantees the existence of such a bijection for rooted maps on the Klein bottle with at most six edges, but it does not give an explicit bijection. The case of monopoles offers more insight.

If φ is the face-degree partition of a rooted monopole on the torus or Klein bottle with n edges, then by Remark 4.19 and Theorem 4.22

$$c_{[2n],\varphi,[2^n]}(b) = d_{1,\varphi}(b) = h_{1,\varphi,0}b^2 + h_{1,\varphi,1}(b+1),$$

where $2h_{1,\varphi,1}$ enumerates rooted maps with 1 handle. In this case, the bijection provides a perfect matching between rooted maps with twisted handles and rooted maps with untwisted handles.

The bijection for monopoles is related to the computation of η. Attempting to extend the bijection to maps with more than 1 vertex reveals a distinction between two classes of maps, and motivates the following definition.

Definition 6.6 (*h*-rooted, *i*-rooted). *For a rooted map* $\mathfrak{m}$, *consider the process of computing* $\eta(\mathfrak{m})$ *using the recursive description from Definition 4.1. If a* handle *that is incident with the root vertex of* $\mathfrak{m}$ *is deleted during the computation of* η, *then* $\mathfrak{m}$ *is h-rooted. Otherwise, the root vertex becomes* isolated *before a handle is deleted, and the map is i-rooted.*

Remark 6.7. *If* $\mathfrak{m}$ *is an h-rooted map on the Klein bottle, then* $\eta(\mathfrak{m}) = 1$.

Lemma 6.8. *There is a vertex- and face-degree partition preserving bijection between h-rooted maps on the torus and h-rooted maps on the Klein bottle.*

Proof. One such bijection, illustrated in Figure 6.1 is described as follows.

Suppose $\mathfrak{m}$ is an *h*-rooted map of Euler genus 2. The handle found when computing η is denoted by e. A second *h*-rooted map, $\mathfrak{m}'$, is obtained from $\mathfrak{m}$ by iteratively deleting the root edge until the resulting map is rooted on e. Figure 6.1a gives a generic *h*-rooted map, $\mathfrak{m}$, with the corresponding $\mathfrak{m}'$ given in Figure 6.1b: in both figures, the vertices are arranged according to the order they are encountered in a clockwise walk around the boundary of the root face of $\mathfrak{m}'$. A vertex may occur more than once in this boundary, but except for identifying the two occurrences of each end of e, labelled u_1 and v_1 in the figures, these occurrences are to be considered distinct vertices.

Both sides of e are on faces that are incident with the root vertex. Denote the first such face encountered in a clockwise tour around the root vertex by f. Then walk around the boundary of f in a clockwise direction starting at e, denote the last vertex visited before returning to the root vertex by v', and denote the edge from v' to the root vertex by e': it is possible that $e = e'$. In the rooted map given in Figure 6.1a, the distinguished vertex is $v' = v_k$.

Since e is a handle, it connects two faces, the root face, f_1, and a second face, f_2, in the planar map $\mathfrak{m}'\backslash e$: see Figure 6.1c. Replace e by a new handle labelled e' that is twisted relative to e and runs from the root vertex in f_1 to v' in f_2 to obtain a new *h*-rooted map, $\overline{\mathfrak{m}'}$, also of Euler genus 2: see Figure 6.1d. The boundary of the root face of $\overline{\mathfrak{m}'}$ contains the same vertices as the boundary of the root face of $\mathfrak{m}'$, but in a different order: compare Figures 6.1e and 6.1b.

The image $\overline{\mathfrak{m}}$ of $\mathfrak{m}$ is constructed from $\overline{\mathfrak{m}'}$ by adding the edges deleted from $\mathfrak{m}$ to obtain $\mathfrak{m}'$, omitting e', and when $e \neq e'$, inserting an extra edge e to complete
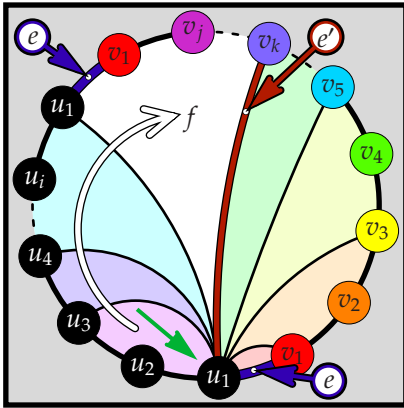
(a) An *h*-rooted map, $\mathfrak{m}$, on the torus
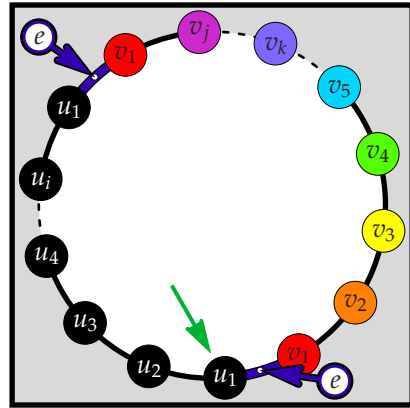
(b) Root-edge deletion produces *m'*
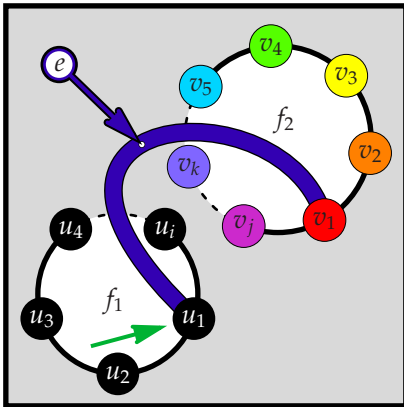
(c) The edge *e* joins two faces in $\mathfrak{m}' \backslash e$
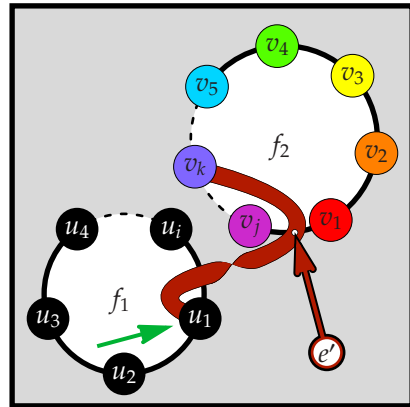
(d) Replace *e* with a twisted handle *e'*
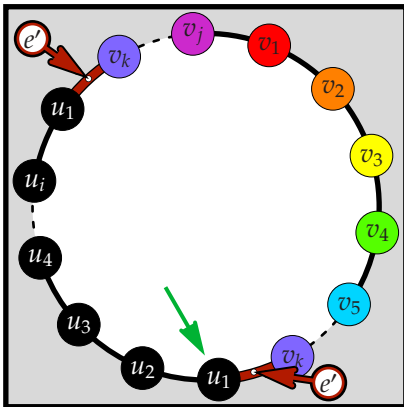
(e) This gives $\overline{m'}$
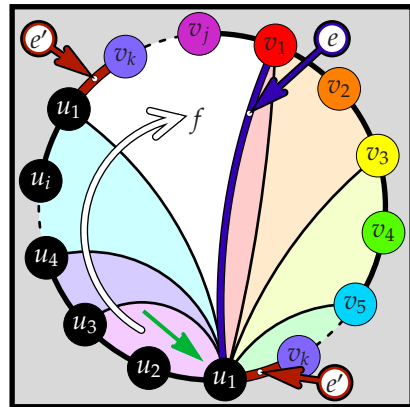
(f) The image, $\overline{\mathfrak{m}}$, on the Klein bottle

Figure 6.1: The bijection described in the proof of Lemma 6.8 pairs the rooted map on the torus, (a), with the rooted map on the Klein bottle, (f). The bijection preserves every face boundary walk, except the walk around the unshaded face *f*.

(a) A handle in a dipole on the torus

(b) A twisted handle
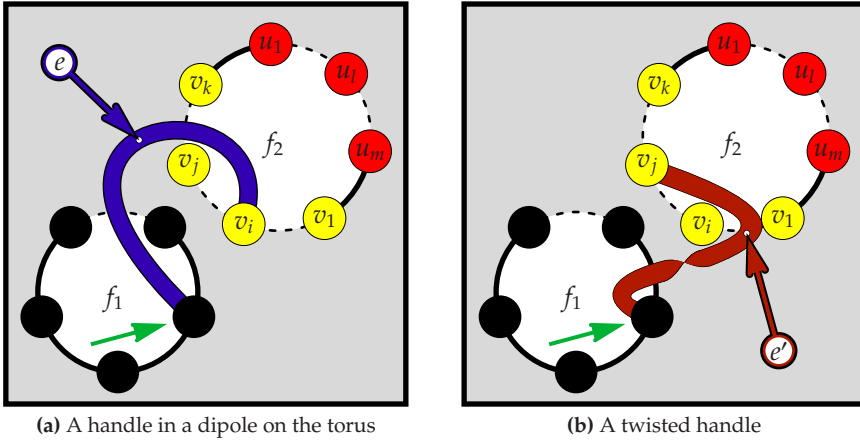
Figure 6.2: A simpler bijection for monopoles and dipoles

the boundary of f. Edges clockwise of f in $\mathfrak{m}$ are added to $\overline{\mathfrak{m}'}$ in a reversed order so that, up to dihedral symmetry, boundary walks of the faces of $\mathfrak{m}$ and $\overline{\mathfrak{m}}$ are identical for every face other than f: compare Figures 6.1f and 6.1a. Each face may contain blocks consisting of vertices not present in $\mathfrak{m}'$, and these blocks are also added to the appropriate faces.

The process is an involution, and precisely one of $\mathfrak{m}$ and $\overline{\mathfrak{m}}$ is on the torus, with the other on the Klein bottle. Since the boundaries of f in $\mathfrak{m}$ and $\overline{\mathfrak{m}}$ contain identical vertices, the required bijection is established. □

To complete the verification that η is a b-invariant for rooted maps on the Klein bottle, it remains to find a bijection between i-rooted maps on the torus and i-rooted maps on the Klein bottle for which η takes the value 1. The difficulty comes from the fact that the bijection described in the proof of Lemma 6.8 does not preserve the boundary walk of f. For rooted maps with at most two vertices, this can be rectified by modifying the proof to acknowledge the identification between vertices that occur more than once in the boundary of f_2. This produces a second bijection that preserves the vertices encountered in each face boundary walk, but acts only on rooted maps with at most two vertices. The two bijections for h-rooted maps are used in the proof of Theorem 6.11 to construct a bijection for i-rooted maps with at most three vertices.

Lemma 6.9. *There is a bijection, between h-rooted maps with at most two vertices on the torus and h-rooted maps with at most two vertices on the Klein bottle, that preserves vertex-degree partitions and face-boundary walks.*

Proof. Begin, as in the proof of Lemma 6.8, by constructing $\mathfrak{m}'$ from $\mathfrak{m}$. Denote the vertex at the non-root end of e by v, and the second vertex of the map, if it exists, by u. Since f_2 is a face of $\mathfrak{m} \backslash e$, a planar map with at most 2 vertices,

(a) A rooted map on the Klein bottle

(b) A rooted map on the torus
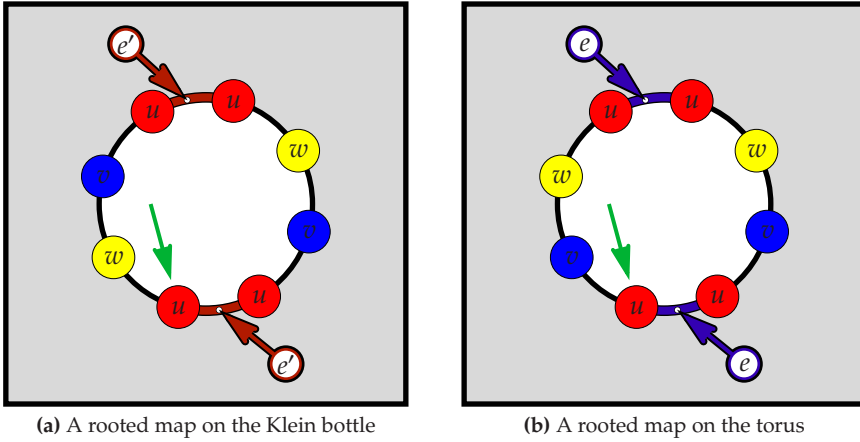
Figure 6.3: Examining the root faces of h-rooted maps with vertex-degree partition $[2^2, 4]$ and face-degree partition $[8]$ reveals that Lemma 6.9 does not extend to rooted maps with three or more vertices.

the boundary of f_2 contains $k \geq 1$ consecutive occurrences of v, and $m \geq 0$ consecutive occurrences of u: this description of the boundary is invariant under reflection. In clockwise order, denote the occurrences of v by $v_1, v_2, \ldots, v_k$, and denote the occurrences of u by $u_1, u_2, \ldots, u_m$: see Figure 6.2a.

If the f_2 end of the handle e is v_i, then replace e with a twisted handled, e', constructed in such a way that its f_2 end is v_j, where $j = k - i + 1$ if $m > 0$ and $j = i$ otherwise: see Figure 6.2b. Since a boundary walk of the root face of $\overline{\mathfrak{m}'}$ encounters vertices in the same order as a boundary walk of the root face of $\mathfrak{m}'$, proceeding as in the proof of Lemma 6.8 produces $\overline{\mathfrak{m}}$ with face-boundary walks containing the same vertices as the face-boundary walks in $\mathfrak{m}$. □

Remark 6.10. Lemma 6.9 is best possible, in the sense that it does not extend to rooted maps with three or more vertices. To see this, consider all the h-rooted maps with vertex-degree partition $\nu = [2^2, 4]$ and face-degree partition $\varphi = [8]$. One such map on the Klein bottle is given in Figure 6.3a, and a boundary walk of its root face visits the vertices in the order (u, u, v, w, u, u, v, w), but this is not a face-boundary walk of any of the six rooted orientable maps with the specified vertex- and face-degree partitions (see [JV01, pp. 90–91] for a listing). Similarly, among rooted maps on the Klein bottle, only unhandled maps have the same root-face boundary as the orientable h-rooted map given in Figure 6.3b.

Using Lemmas 6.8 and 6.9, it is now possible to describe the bijection predicted by Theorem 6.3 for i-rooted maps on the torus with at most 3 vertices. The main result of this section, Corollary 6.13, that η is a b-invariant for two new infinite classes of rooted maps on the Klein bottle, is then obtained as an immediate corollary.

(a) An *i*-rooted map

(b) The underlying *h*-rooted map
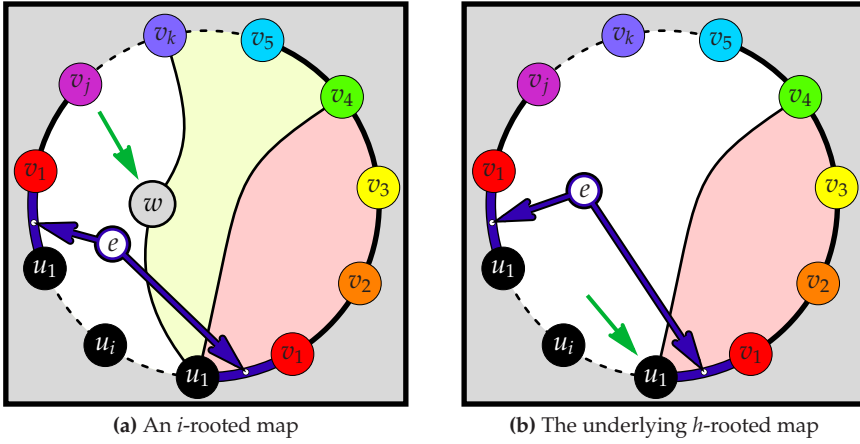
Figure 6.4: An *i*-rooted map and its associated *h*-rooted map

Theorem 6.11. *There is a vertex- and face-degree preserving bijection between rooted maps on the torus and rooted maps on the Klein bottle for which η takes the value 1.*

Proof. By Lemma 6.8, it is sufficient to describe a bijection for *i*-rooted maps. Let $\mathfrak{m}$ be an *i*-rooted map with Euler genus 2 such that $\eta(\mathfrak{m}) \leq 1$. Since $\eta(\mathfrak{m}) \neq 2$, a handle is deleted when $\eta(\mathfrak{m})$ is computed using the recursive description from Definition 4.1, and it follows that $\mathfrak{m}$ can be decomposed as a planar piece, $\mathfrak{p}$, embedded in the root face of an *h*-rooted map $\mathfrak{m}'$, with $\eta(\mathfrak{m}) = \eta(\mathfrak{m}')$. Figure 6.4 gives a schematic representation of an *i*-rooted map and its underlying *h*-rooted map.

Since $\mathfrak{m}$ has at most three vertices, $\mathfrak{m}'$ has at most two vertices, so the bijection from Lemma 6.9 applies: denote the image of $\mathfrak{m}'$ with respect to this bijection by $\overline{\mathfrak{m}'}$. Then $\mathfrak{m}'$ and $\overline{\mathfrak{m}'}$ have identical face boundaries, and $\{\eta(\mathfrak{m}'), \eta(\overline{\mathfrak{m}'})\} = \{0, 1\}$. Attaching $\mathfrak{p}$ to the root face of $\overline{\mathfrak{m}'}$ completes the desired bijection. □

Remark 6.12. A slight modification to the proof of Theorem 6.11 gives a bijection for all *i*-rooted maps on the Klein bottle with at most 6 edges, but the existence of such a bijection is already guaranteed numerically by Proposition 6.2, and the modified proof does not offer any additional combinatorial insights, since it relies on subtle symmetries that only exist for maps with a small number of edges.

Corollary 6.13. *If any b-invariant exists for rooted maps on the Klein bottle, then every invariant satisfying Definition 4.1 is a b-invariant for all rooted maps on the Klein bottle with at most three vertices.*

Proof. If β is a *b*-invariant for rooted maps on the Klein bottle, and ν and φ are the vertex- and face-degree partitions of a map on the Klein bottle with n edges

and at most three vertices, then by Corollary 5.22

$$c_{\nu,\varphi,[2^n]}(b) = \sum_{\mathfrak{m}\in\mathcal{M}_{\nu,\varphi}} b^{\beta(\mathfrak{m})} = h_{\nu,\varphi,1}(1+b) + h_{\nu,\varphi,0}b^2. \qquad (6.1)$$

But from the bijection in Theorem 6.11 and the degree bound in Theorem 4.4

$$\sum_{\mathfrak{m}\in\mathcal{M}_{\nu,\varphi}} b^{\eta(\mathfrak{m})} = a_{\nu,\varphi,0} + a_{\nu,\varphi,1}b + a_{\nu,\varphi,2}b^2 = a_{\nu,\varphi,0}(1+b) + a_{\nu,\varphi,2}b^2. \qquad (6.2)$$

Since $\beta(\mathfrak{m})$ and $\eta(\mathfrak{m})$ each equals zero precisely when $\mathfrak{m}$ is orientable, the sums in (6.1) and (6.2) agree at both $b = 0$ and $b = 1$, and the result follows. $\qquad\square$

6.3   Towards Higher Genera

The approach used to prove Corollary 6.13 involved identifying two polynomials by comparing their evaluations. With combinatorial interpretations available for two evaluations of b-polynomials, at $b = 0$ and $b = 1$, and conjectured for only one more, at $b = -1$, the approach would appear to be limited to polynomials of degree at most 2. But Corollary 5.22 offers additional structure by suggesting that b-polynomials should be expressed as elements of $\mathrm{span}(B_g)$ for appropriate choices of g. Interpreting this combinatorially gives the following generalization of Theorem 6.3.

Corollary 6.14. *If β is a b-invariant and $g = |v| - \ell(v) - \ell(\varphi) - \ell(\epsilon)$ is even, then there is a $1 : \frac{g}{2}$ map between orientable maps of Euler genus g and non-orientable maps of genus g for which β takes the value 1.*

Focusing on η and extrapolating from Theorem 4.22, if $c_{\nu,\varphi,[2^n]}(1)$ enumerates rooted maps of genus g, then the coefficient of $b^{g-2i}(1 + b)^i$ in $c_{\nu,\varphi,[2^n]}(b)$ may be expected to count equivalence classes of rooted maps with i handles, where each class consists of 2^i rooted maps with identical vertex- and face-degree partitions. Within each class the weights of maps with respect to η are distributed binomially. A combinatorial description of these equivalence classes would show that generating series for rooted maps with respect to η can be expressed in the form

$$\sum_{\mathfrak{m}\in\mathcal{M}_{\nu,\varphi}} b^{\eta(\mathfrak{m})} = \sum_{0\leq 2i\leq g} a_{\nu,\varphi,i} b^{g-2i}(1+b)^i, \qquad (6.3)$$

and would allow a generalization of Corollary 6.13.

To verify that a function is a b-invariant, subject to the existence of at least one such invariant, it is sufficient to show that the generating series for rooted maps with respect to that function takes the form seen in (6.3), and then to confirm combinatorial interpretations for enough evaluations of the corresponding b-polynomials to equate all the coefficients.

116
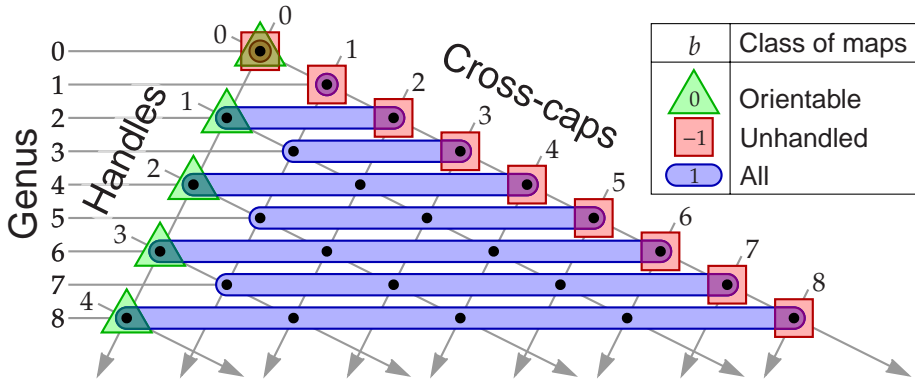
Figure 6.5: Sums of coefficients of b-polynomials obtainable using evaluations

Example 6.15. *The generating series for rooted maps on the cross-capped torus with respect to any b-invariant β should be of the form*

$$\sum_{\mathfrak{m}\in\mathcal{M}_{\nu,\varphi}} b^{\beta(\mathfrak{m})} = a_{\nu,\varphi,0}b^3 + a_{\nu,\varphi,1}b(1+b),$$

so to verify that η is a b-invariant for rooted maps on the cross-capped torus, it would be sufficient to confirm that $M(-\mathbf{x}, -\mathbf{y}, -z; -1)$ is the generating series for unhandled maps with respect to vertex- and face-degree partitions, and to then construct a vertex- and face-degree partition preserving bijection between weight 1 and weight 2 rooted maps on the cross-capped torus.

Example 6.16. *Verifying that η is a b-invariant for rooted maps of Euler genus four would involve verifying the combinatorial interpretation for $M(-\mathbf{x}, -\mathbf{y}, -z; -1)$, and then showing that the appropriate sums take the form*

$$\sum_{\mathfrak{m}\in\mathcal{M}_{\nu,\varphi}} b^{\eta(\mathfrak{m})} = a_{\nu,\varphi,0}b^4 + a_{\nu,\varphi,1}b^2(1+b) + a_{\nu,\varphi,2}(1+b)^2.$$

Figure 6.5 illustrates which sums of coefficients of b-polynomials, with respect to the basis B_g, can be obtained from evaluations of the b-polynomials. Each coefficient is represented by a black dot, and each evaluation is indicated with a shaded region. There are not enough conjectured combinatorially significant evaluations of the b-polynomials to verify that a function is a b-invariant for rooted maps on surfaces with Euler genus five or higher, but three evaluations are sufficient to identify the b-polynomials that are conjectured to enumerate rooted maps on surfaces with Euler genus at most four.

Remark 6.17. The horizontal near-symmetry of Figure 6.5 suggests that unhandled maps generalize planar maps in a sense similar to orientable maps.
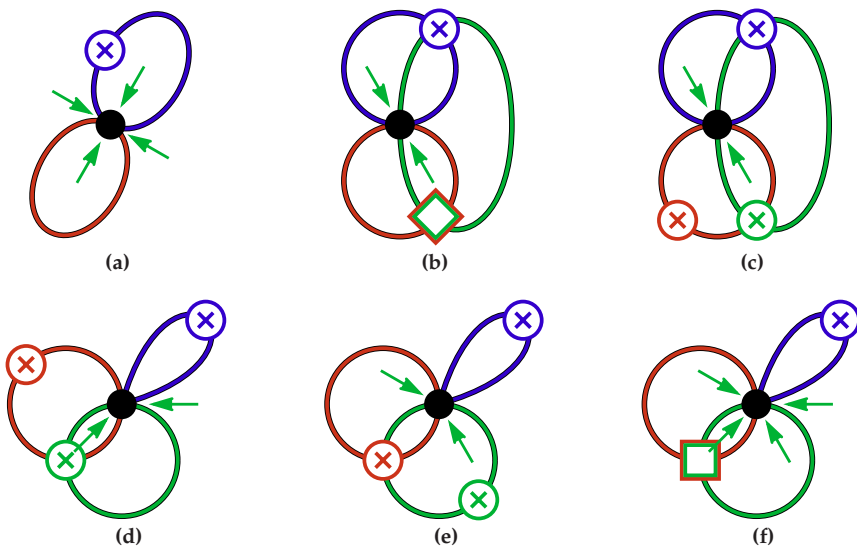
Figure 6.6: Deleting the root edges of any of the rooted maps in (b), (c), (d), (e), or (f) leaves one of the non-orientable rooted maps in (a).

6.4 Which Handles Are Twisted?

If the root edge e of a rooted map $\mathfrak{m}$ is a handle, then the involution τ described in Definition 4.1 defines a pair of handles by matching e with a handle in $\tau(\mathfrak{m})$. If $\mathfrak{m}\backslash e$ is non-orientable, then these handles are treated symmetrically by Definition 4.1, and there are marginal b-invariants both for which e is twisted and for which e is not twisted, although specifying whether e is twisted in $\mathfrak{m}$ determines whether the corresponding edge is twisted in $\tau(\mathfrak{m})$. It follows that an uncountably infinite family of marginal b-invariants satisfy Definition 4.1. This family is not sufficiently structured to permit extending the analysis from Section 6.2 to rooted maps with Euler genus greater than two.

Example 6.18. *If the root edge is deleted from any of the twelve rooted maps given in Figures 6.6b–f, then the result is one of the non-orientable rooted maps given in Figure 6.6a. It follows that functions satisfying Definition 4.1 can take any of $2^6 = 64$ combinations of values on these rooted maps. Invariants that are additive in the sense of Conjecture 3.32 must take the value 1 for the rooted maps in Figure 6.6f: this additional constraint leaves $2^2 = 4$ possible combinations of values taken by marginal b-invariants when restricted to the rooted maps given in Figures 6.6b and 6.6c.*

It is possible that the best way to analyze the map series is to avoid making a distinction between twisted and untwisted handles: this was the case, for example, in the proof of Theorem 4.22. After briefly describing this alternative, the Section proceeds by discussing two schemes for defining restricted families of invariants, each involving an explicit rule for distinguishing between twisted

and untwisted handles. The first family is related to the invariant described by Brown and Jackson in [BJ07], with twisting measured relative to spanning trees. The second family defines twisting relative to oriented faces, and provides the structure needed in Section 6.5 for extending Lemma 6.8 to h-rooted maps with Euler genus greater than two.

6.4.1 Alternatives To Twisted Handles

Corollary 5.22 predicts that the b-polynomial $c_{\nu,\varphi,[2^n]}(b)$ can be written as

$$c_{\nu,\varphi,[2^n]}(b) = \sum_{0 \le 2i \le g} h_{\nu,\varphi,i} b^{g-2i}(1+b)^i.$$

This emphasizes that b is conjectured to play two distinct combinatorial rôles: in the marginal case, as discussed in Chapter 4, factors of b correspond to cross-borders, while factors of $1+b$ correspond to handles, and this interpretation is expected to extend to all b-polynomials. It might be possible to give a direct combinatorial interpretation to the coefficients $h_{\nu,\varphi,i}$ by considering an invariant that counts cross-borders and handles independently, and ignores the distinction between twisted and untwisted handles. This refinement was predicted in the context of marginal b-polynomials by Brown in [Bro00, Sec. A.6]. The corresponding modification to the generating series would involve formally replacing $1+b$ by $2a$, as in the proof of Theorem 4.22, but this substitution cannot be made algebraically, and requires a refined family of symmetric functions to replace Jack symmetric functions in the definition of the map series.

It is difficult to predict the form that the required family of symmetric functions should take, although it does not appear to be an obvious specialization of the (q, t)-symmetric functions described by Macdonald in [Mac95, Chap. VI]. The double rôle of the Jack parameter has also been observed in an analytic context by Lassalle, who in [Las08] obtained expressions for expanding $J_\lambda(\alpha)$ in terms of power-sums when λ is a rectangular partition. Lassalle conjectured that there is a two-parameter refinement of Jack symmetric functions that reflects this directly. It is unclear whether the refinement needed for rooted map enumeration is the same refinement predicted by Lassalle.

If $M(\mathbf{x}, \mathbf{y}, z; b)$ has the conjectured combinatorial interpretation as the generating series for rooted maps with respect to η, then it may also be useful to consider two other series:

$$\sum_{n,i,\nu,\varphi} h_{\nu,\varphi,i} 2^i b^{g-i} \mathbf{x}^\nu \mathbf{y}^\varphi z^n \qquad \text{and} \qquad \sum_{n,i,\nu,\varphi} h_{\nu,\varphi,i} (1+b)^{g-i} \mathbf{x}^\nu \mathbf{y}^\varphi z^n.$$

Neither series is easily refined to recover the generating series for orientable or locally orientable rooted maps, but both correspond to invariants that are potentially easier to analyze than η. The first sum is obtained by treating all handles as twisted, and the second sum is obtained by allowing each cross-border to have both a twisted and an untwisted form.

(a) An untwisted root edge **(b)** A twisted root edge
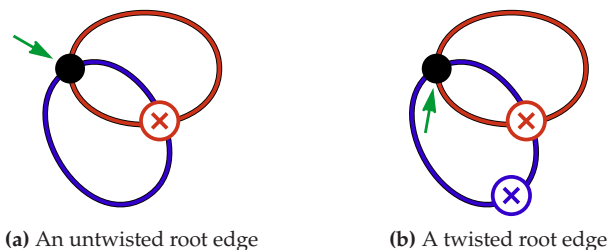
Figure 6.7: Not all twisting can be defined relative to a spanning tree.

The alternatives to specifying which handles are twisted each requires constructing new families of symmetric functions, so that a corresponding generating series can be given algebraic form. To proceed without describing these families, it is necessary to work with a restricted family of invariants.

6.4.2 Twisting Relative to a Spanning Tree

For the first restricted family, the rooting of a map is used to construct a distinguished spanning tree T, and the twisting of a handle e is determined by whether the unique cycle in $T \cup \{e\}$ is a one- or two-sided curve. Any canonical spanning tree can be used, but the particular tree consisting of the bridges encountered during the computation of η appears to be well suited for further study. When twisting is defined relative to this tree, the invariant remains constant under the operation of contracting tree edges, and as a consequence, it is additive in the sense of Conjecture 3.32. In this case, η may be studied as an invariant of rooted monopoles, since for any map $\mathfrak{m}$, the value of $\eta(\mathfrak{m})$ can be computed by contracting a spanning tree and working with the resulting monopole. Since every invariant satisfying Definition 4.1 is a b-invariant for monopoles, this is a promising decomposition.

Remark 6.19. The same choice of spanning tree was used by Brown and Jackson to define twisting for their invariant in [BJ07], though they described it as the result of a depth-first search with the search order defined by counterclockwise circulations at each vertex. This connection helped motivate the definition of η.

Example 6.20. *When twisting of handles is measured relative to a spanning tree, the root edges of the two rooted maps given in Figure 6.6b are twisted, while the root edges of the two rooted maps given in Figure 6.6c are not.*

The disadvantage of defining the twisting of handles relative to a spanning tree is that it creates two distinct forms of twisting, and breaks a potential symmetry between the descriptions of cross-borders and handles. Some untwisted edges, recognized by η as borders, are orientation reversing, as is the root edge in Figure 6.7a. Similarly, all cross-borders are twisted, but some are orientation preserving relative to a spanning tree, as is the root edge in Figure 6.7b.

120

6.4.3 Twisting Relative to Oriented Faces

For the second family of invariants, the rooting of a map is used to assign an orientation to each face of the map. Whether a handle is untwisted or twisted is determined by whether local orientation is preserved or reversed between the faces at its ends. When face orientations are chosen to be consistent across the edges of a dual-spanning tree, the second family is effectively dual to the first. Proving Lemmas 6.8 and 6.9 required comparing the relative twisting of two handles with different end points on the same face, as in Figure 6.2: defining twisting relative to oriented faces provides precisely this structure to rooted maps of genus greater than two.

Besides permitting the extension of Lemma 6.8 to rooted maps of all genera, defining twisting relative to oriented faces has the advantage of producing only one form of twisting. With this restriction, if e is the root edge of m, then e is untwisted if it preserves local orientation between its ends in $m \backslash e$, whether it is a handle, bridge, or border. Similarly, e is twisted if it reverses local orientation between its ends in $m \backslash e$, whether it is a handle or a cross-border.

At present, there does not appear to be a reason to prefer any particular method for constructing a canonical dual-spanning tree, though a tree consisting entirely of edges identified as borders during the computation of η is computationally convenient. It is necessary to use a rule to describe which borders are to be excluded from the dual-spanning tree, since in general the set of all borders is too large, a consequence of the fact that adding a handle to a rooted map has the effect of identifying two faces. Any rule that acts sufficiently locally determines an invariant that is additive in the sense of Conjecture 3.32.

Example 6.21. *When twisting of handles is measured relative to face orientations defined with respect to a dual-spanning tree, the root edges of the two rooted maps given in Figure 6.6c are twisted, while the root edges of the two rooted maps given in Figure 6.6b are not. This reverses the twisting as measured relative to a spanning tree in Example 6.20.*

Section 6.5 uses this second family to extend Corollary 6.13 by constructing equivalence classes of rooted maps with Euler genus greater than two.

6.5 The Cross-capped Torus and Beyond

This Section, uses the extra structure provided by restricting attention to the invariants described in Section 6.4.3 to verify that generating series for rooted dipoles on the cross-capped torus and doubly cross-capped torus take the form predicted by Corollary 5.22. Combined with the combinatorial interpretation of $M(\mathbf{x}, -\mathbf{y}, -z; -1)$ as the generating series for unhandled rooted maps (numerical evidence currently verifies the interpretation for rooted maps with at most six edges), this will be sufficient to show that η is a b-invariant for all rooted dipoles on surfaces with Euler genus at most four.

(a) A rooted map $\mathfrak{m}$ **(b)** Its image $\overline{\mathfrak{m}}$
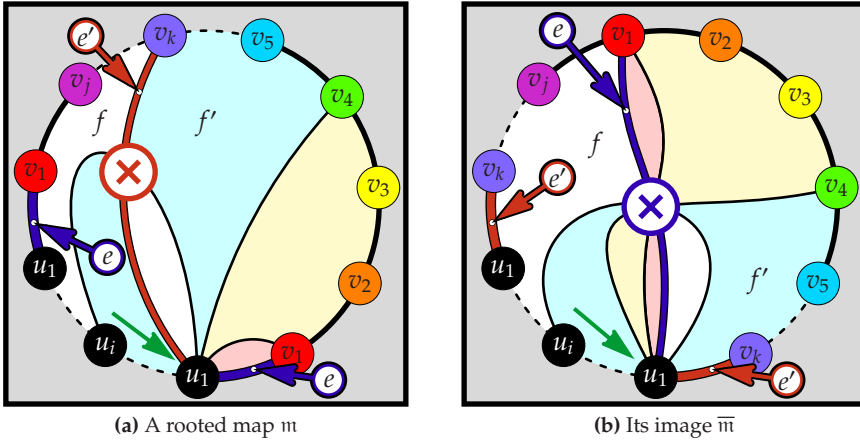
Figure 6.8: It is possible that two face boundaries, labelled f and f', differ between $\mathfrak{m}$ and its image under the bijection used to prove Theorem 6.22.

Theorem 6.22. *If ν and φ are, respectively, the vertex- and face-degree partitions of a map on the cross-capped torus with two vertices, and η satisfies Definition 4.1 with twisting of handles measured relative to a dual spanning tree, then*

$$\sum_{\mathfrak{m}\in\mathcal{M}_{\nu,\varphi}} b^{\eta(\mathfrak{m})} = a_{\nu,\varphi,0}b^3 + a_{\nu,\varphi,1}b(1+b) \in \mathrm{span}_{\mathbb{Z}_+}(B_3).$$

Furthermore, the coefficients $a_{\nu,\varphi,0}$ and $a_{\nu,\varphi,1}$ are independent of the choice of invariant.

Proof. For any two invariants satisfying Definition 4.1, the corresponding sums agree when evaluated at $b = 1$. So independence of the coefficients from the choice of invariant follows from the fact that $a_{\nu,\varphi,0}$ is the number of unhandled rooted maps with vertex-degree partition ν and face-degree partition φ.

If $\mathfrak{m}$ is a rooted map on the cross-capped torus, then Theorem 4.4 gives the bound $1 \le \eta(\mathfrak{m}) \le 3$. It is thus sufficient to establish the existence of a vertex- and face-degree preserving bijection between those rooted dipoles on the cross-capped torus for which η takes the value 1, and those for which η takes the value 2. The existence of such a bijection, which additionally preserves the degree of the root face, and hence the vertices encountered in a boundary walk of the root face, is guaranteed for monopoles by Theorems 4.16 and 4.22. As in the proof of Lemma 6.9, this is sufficient to show the existence of the required bijection for all i-rooted maps with two vertices on the cross-capped torus.

It remains only to construct an explicit bijection for h-rooted dipoles. This is accomplished as in the proof of Lemma 6.8, with the exception that, because of the possible presence of a cross-border, there may be two faces with boundaries that differ between a map and its image: consider the faces marked f and f' in Figures 6.8a and 6.8b. □

(a) An *h*-rooted map

(b) Its image under the first bijection

(c) An alternate choice of *e′*

(d) A second image
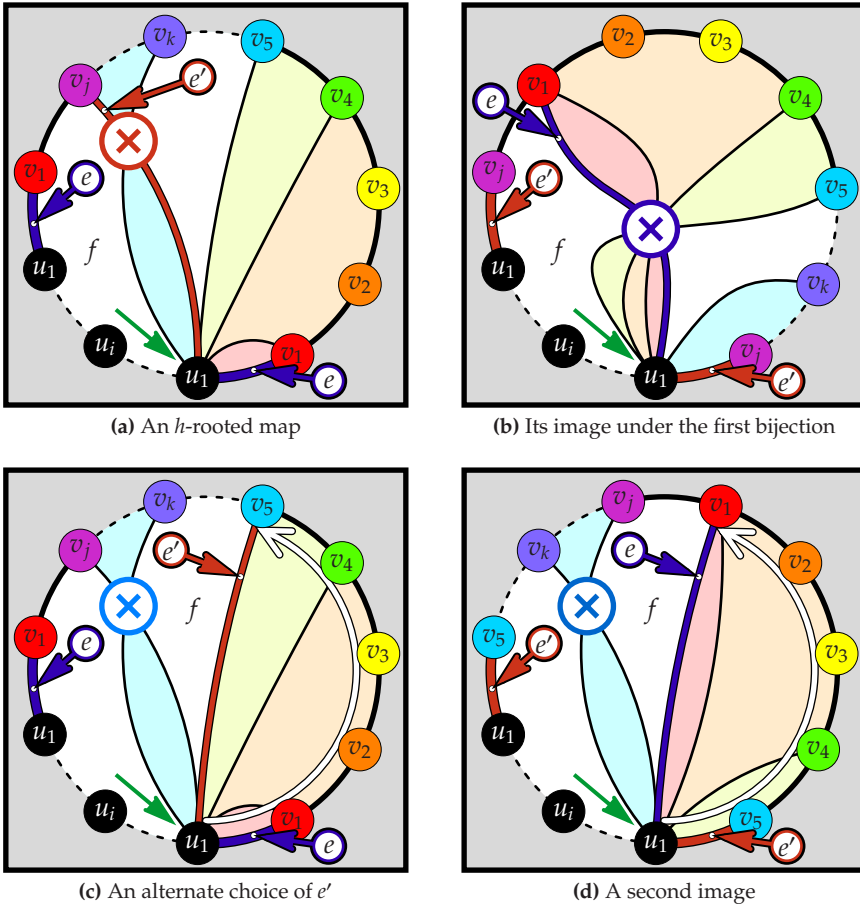
Figure 6.9: It is possible to give a second description of *e′*. The two descriptions lead to different bijections for rooted maps of genus greater than two.

Remark 6.23. An alternative description of the edge *e′* used in the proof of Lemma 6.8 leads to a second bijection for rooted maps of genus greater than two. In the terminology from that proof, *e′* can be described as the first edge bounding *f* encountered on a counterclockwise tour around the root face of $\mathfrak{m}'$. For rooted maps with genus at most two, there is no distinction between the two descriptions, but for rooted maps with Euler genus at least three, the descriptions may produce different edges, and consequently this new description gives a second bijection. There does not appear to be a reason to prefer one bijection over the other.

Example 6.24. *Contrast Figure 6.9a, where e′ is constructed as in the original description, with Figure 6.9c, where e′ is constructed using the alternative description. Their images are given in Figures 6.9b and 6.9d, respectively.*

Theorem 6.25. *If ν and φ are, respectively, the vertex- and face-degree partitions of a map with two vertices and Euler genus four, and η satisfies Definition 4.1 with twisting of handles measured relative to a dual spanning tree, then*

$$\sum_{\mathfrak{m} \in \mathcal{M}_{\nu,\varphi}} b^{\eta(\mathfrak{m})} = a_{\nu,\varphi,0}b^4 + a_{\nu,\varphi,1}b^2(1 + b) + a_{\nu,\varphi,2}(1 + b)^2 \in \mathrm{span}_{\mathbb{Z}_+}(B_4).$$

The coefficients $a_{\nu,\varphi,0}$, $a_{\nu,\varphi,1}$, and $a_{\nu,\varphi,2}$ are independent of the choice of invariant.

Proof. For any invariant satisfying Definition 4.1, the coefficient $a_{\nu,\varphi,0}$ is the number of unhandled rooted maps with the vertex-degree partition ν and face-degree partition φ. Independence of the remaining coefficients on the choice of invariant follows from the fact that the sums agree when evaluated at $b = 0$ and $b = 1$.

In the terminology from the proof of Lemma 6.8, Lemma 6.9 gives the required bijection for h-rooted maps where constructing $\mathfrak{m}$ from $\mathfrak{m}'$ involves adding two cross-borders or a handle. The remaining cases use the same constructions as in the proof of Theorem 6.22. □

Corollary 6.26. *If there is at least one b-invariant, then every invariant from the family described in Section 6.4.3 is a b-invariant for all rooted maps with Euler genus at most four, at most two vertices, and at most six edges.*

Proof. If η is such an invariant, and $\nu, \varphi \vdash 2n$ are, respectively, the vertex- and face-degree partitions of a map on the cross-capped torus with at most two vertices, then by Theorem 6.22

$$\sum_{\mathfrak{m} \in \mathcal{M}_{\nu,\varphi}} b^{\eta(\mathfrak{m})} = a_{\nu,\varphi,0}b^3 + a_{\nu,\varphi,1}b(1 + b).$$

By the existence of a b-invariant for rooted maps on the cross-capped torus, Corollary 5.22 shows that $c_{\nu,\varphi,[2^n]}(b)$ can be written in the form

$$c_{\nu,\varphi,[2^n]}(b) = h_{\nu,\varphi,0}b^3 + h_{\nu,\varphi,1}b(1 + b).$$

But combinatorial interpretations of $M(\mathbf{x}, \mathbf{y}, z; 1)$ and $M(-\mathbf{x}, -\mathbf{y}, -z; -1)$ give that when $n \leq 6$

$$a_{\nu,\varphi,0} = h_{\nu,\varphi,0} \qquad \text{and} \qquad a_{\nu,\varphi,0} + 2a_{\nu,\varphi,0} = h_{\nu,\varphi,0} + 2h_{\nu,\varphi,1},$$

so $c_{\nu,\varphi,[2^n]}(b)$ is equal to the required combinatorial sum.

Similarly, if $\nu, \varphi \vdash 2n$ are, respectively, the vertex- and face-degree partitions of a map with Euler genus four, then Theorem 6.25 applies, and combinatorial interpretations of $M(\mathbf{x}, \mathbf{y}, z; 0)$, $M(\mathbf{x}, \mathbf{y}, z; 1)$, and $M(-\mathbf{x}, -\mathbf{y}, -z; -1)$ are sufficient to equate corresponding coefficients. □

Remark 6.27. Corollary 6.26 is restricted to rooted maps with at most six edges because of computational limitations associated with directly verifying that $M(-\mathbf{x}, -\mathbf{y}, -z; -1)$ is the generating series for unhandled maps. The limitation is not inherent to the proof technique.

Remark 6.28. It may be possible to modify the proof of Theorem 6.25 to show that generating series for all dipoles on all surfaces take the form required by Corollary 5.22. For genera greater than four, the independence of the coefficients on choice of invariants will require additional analysis, and there are not enough evaluations of the map series to verify that η is a b-invariant.

Recalling Table 6.1, Corollaries 6.13 and 6.26 cover the outstanding cases required to verify the combinatorial interpretation of a b-invariant for all rooted maps with at most four edges. This gives the following corollary.

Corollary 6.29. *Every invariant from the family described in Section 6.4.3 is a b-invariant for all rooted maps with at most four edges.*

Proof. Direct computation verifies that $c_{\nu,\varphi,[2^n]}(b)$ is a polynomial with non-negative integer coefficients when $n \leq 5$, so the existence of a b-invariant for rooted maps with at most five edges is guaranteed.

It follows from Corollary 5.25 that η is a b-invariant for planar and projective planar rooted maps, from Corollary 6.13 that η is a b-invariant for rooted maps on the torus and Klein bottle with at most three vertices, from Corollary 6.26 that η is a b-invariant for rooted maps on the cross-capped torus with two vertices, and from Remark 4.19 that η is a b-invariant for all monopoles. Collectively, these classes account for all rooted maps with at most four edges. $\square$

Remark 6.30. Besides verifying the existence of a b-invariant, computer assistance in the proof of Corollary 6.29 is limited to verifying that $M(-\mathbf{x}, -\mathbf{y}, -z; -1)$ gives the generating series for unhandled rooted maps. For rooted maps with at most four edges, this verification is required only for the 260 rooted maps on the cross-capped torus with one face and two vertices, and could potentially be carried out manually by using the list of rooted maps in [JV01, pp. 131–134].

To extend Corollary 6.29 to all rooted maps with at most five edges, it would be sufficient to verify that η is a b-invariant for all rooted maps on the Klein bottle with four vertices, and for all rooted maps on the cross-capped torus with three vertices. More broadly, it might be possible to find a combinatorial proof that if ν and φ are, respectively, the vertex- and face-degree partitions of a map with Euler genus $g \leq 4$, then

$$\sum_{\mathfrak{m} \in \mathcal{M}_{\nu,\varphi}} b^{\eta(\mathfrak{m})} \in \operatorname{span}_{\mathbb{Z}_+}(B_g). \tag{6.4}$$

This would generalize Theorems 6.11, 6.22, and 6.25, and would likely require further restricting the family of invariants, or using additional symmetries of the class of rooted maps. An alternative approach, using the symmetry between $\mathbf{x}$ and $\mathbf{y}$ in $M(\mathbf{x}, \mathbf{y}, z; b)$, is discussed in Section 6.6.

6.6   An Involution to Replace Duality

To verify that a function is a b-invariant for rooted maps with six or more edges, it will be necessary to verify that it is a b-invariant for rooted maps with two vertices, one face, and genus equal to five. Without finding additional combinatorially significant evaluations of the map series, the approach outlined in Section 6.3 will not apply. Verification may, however, be possible by appealing to the symmetry between $\mathbf{x}$ and $\mathbf{y}$ in $M(\mathbf{x}, \mathbf{y}, z; b)$. Combinatorially the symmetry states that if η is a b-invariant, then

$$\sum_{\mathfrak{m} \in \mathcal{M}_{\nu,\varphi}} b^{\eta(\mathfrak{m})} = \sum_{\mathfrak{m} \in \mathcal{M}_{\varphi,\nu}} b^{\eta(\mathfrak{m})}. \tag{6.5}$$

That these sums are equal when evaluated at $b = 0$ or $b = 1$ is a consequence of the fact that duality is an involution of both orientable and locally orientable maps, but a modification to the proof of Theorem 3.35 shows that even non-additive invariants satisfying Definition 4.1 cannot be invariant with respect to duality.

Theorem 6.31. *If η satisfies Definition 4.1, then there is a map $\mathfrak{m}$, such that the multi-set of values taken by η on the rootings of $\mathfrak{m}$ is not equal to the multi-set of values taken by η on the rootings of the dual of $\mathfrak{m}$.*

Proof. As in the proof of Theorem 3.35, consider the rooted maps with one vertex, one face, and three edges, as given in Figure 3.6 on page 64. Suppose η satisfies Definition 4.1, then by Corollary 4.17, η is a marginal b-invariant, so

$$\sum_{\mathfrak{m} \in \mathcal{M}_{[6],[6]}} b^{\eta(\mathfrak{m})} = c_{[6],[6],[2^3]}(b) = 13b + 13b^2 + 15b^3.$$

Since every edge of the rooted maps given in Figures 3.6a and 3.6b is a cross-border, they collectively contribute $5b^3$ to the sum. Similarly, the rooted maps given in Figures 3.6g, 3.6h, and 3.6i collectively contribute $6b + 6b^2 + 6b^3$ to the sum, with the distribution between the maps determined by the particular invariant.

It follows that the total contribution of the rooted maps given in Figures 3.6c, 3.6d, 3.6e, and 3.6f must be $7b + 7b^2 + 4b^3$. But the map given in Figure 3.6c is dual to the map given in Figure 3.6d, and the map given in Figure 3.6e is dual to the map given in Figure 3.6f, so the total contribution of these four maps to each coefficient is even with respect to every function that is invariant under duality. □

It follows that a combinatorial proof of (6.5) will require an alternative family of invariants or an alternative explanation for the symmetry. With such a proof, Corollary 6.29 can be extended to rooted maps with at most six edges, independent of verifying (6.4), since the outstanding cases are all dual to cases covered by Corollaries 6.13 and 6.26.

While not suggesting a combinatorial proof of (6.5), the invariants satisfying Definition 4.1 offer enough structure to prove a weaker property of b-invariants. In particular, if η is a b-invariant, and $\nu \vdash 2n$, then by interchanging the rôles of ν and φ in Lemma 3.22, it follows that

$$\sum_{\varphi \vdash 2n} c_{\nu,\varphi,[2^n]}(b) = (1+b)^{n-\ell(\nu)+1} \sum_{\varphi \vdash 2n} c_{\nu,\varphi,[2^n]}(0). \tag{6.6}$$

The coefficients of the generating series for rooted maps with respect to η also satisfy this relationship. As with the invariant of Brown and Jackson, [BJ07], fixing a spanning tree of a map $\mathfrak{m}$ by depth-first search, and independently twisting each of the remaining $n - \ell(\varphi) + 1$ edges, in the sense of ribbon graphs, produces a class of rooted maps with identical vertex degrees and weights distributed consistently with (6.6), each edge contributing a factor of $1 + b$ to the expression on the right.

6.7 Conclusion

This Chapter outlined an approach for verifying that a function is a b-invariant for all rooted maps with a bounded number of edges or bounded genus. Rooted maps are classified according to genus, number of vertices, and number of edges, and then each class is analyzed individually. Additional techniques will be required to completely resolve Conjecture 3.25, since, for example, other than direct computation, there is not yet an approach that could be used to verify that a particular function is a b-invariant for all rooted maps with two vertices, two faces, and seven edges: there are $10\,392\,697$ such rooted maps, all embedded on the triply cross-capped torus. The analysis did, however, show that a restriction of Definition 4.1, described in Section 6.4.3, defines b-invariants for all rooted maps with at most four edges. In the process, this provided additional evidence for the conjectured relationship between handles and the basis B_g.

The approach identified four significant open problems, the resolution of which will confirm that η is a b-invariant for all rooted maps with at most six edges and for all rooted maps with Euler genus at most four. The problems consist of verifying each of the following statements when ν and φ are, respectively, the vertex- and face-degree partitions of a rooted map with Euler genus g.

❶ The coefficient $c_{\nu,\varphi,[2^n]}(b)$ of $M(\mathbf{x}, \mathbf{y}, z; b)$ is a polynomial in b.

❷ The generating series for unhandled rooted maps is $M(-\mathbf{x}, -\mathbf{y}, -z; -1)$.

❸ The combinatorial sum $\sum_{\mathfrak{m} \in \mathcal{M}_{\nu,\varphi}} b^{\eta(\mathfrak{m})}$ is an element of $\mathrm{span}(B_g)$.

❹ The sum $\sum_{\mathfrak{m} \in \mathcal{M}_{\nu,\varphi}} b^{\eta(\mathfrak{m})}$ is equal to $\sum_{\mathfrak{m} \in \mathcal{M}_{\varphi,\nu}} b^{\eta(\mathfrak{m})}$.

Several combinations of these problems are significant. Table 6.2 summarizes classes of rooted maps for which the approach outlined in this chapter might be used to verify that η is a b-invariant. The final column lists the open problems

Table 6.2: Verifying that η is a b-invariant

Genus	Edges	Vertices	What is needed?
≤ 1	any number	any number	❶
≤ 2	any number	≤ 3	❶
≤ 2	and number	any number	❶ and ❸
≤ 4	any number	≤ 2	❶ and ❷
≤ 4	any number	any number	❶, ❷, and ❸
any genus	≤ 4	any number	Corollary 6.29
any genus	≤ 5	any number	❸ or ❹
any genus	≤ 6	any number	❶ and ❹
any genus	any number	1	Corollary 4.17

that must be resolved to complete this verification. Two classes for which the verification is complete are included in the Table for comparison.

Chapter 7

The q-Conjecture

This Chapter gives evidence that tools developed in Chapter 4 are applicable to Conjecture 7.3, the q-Conjecture, a problem that appears otherwise unrelated to the b-Conjecture. A chain of structural observations suggests a refinement, Conjecture 7.15, of the original conjecture, and numerical evidence supports this refinement. The refinement is used to identify a special case that appears to be both more tractable than the original problem, and interesting in its own right. Since the discussion emphasizes structural similarities, the general case is more relevant than marginal particulars. Several technical details are included as footnotes, to avoid interrupting the discourse.

The q-Conjecture is based on a functional relationship, (7.1), that was discovered by Jackson and Visentin in [JV90a]. The relationship equates evaluations of generating series of two classes of rooted orientable maps, and relates the ϕ^4 and Penner models of 2-dimensional Quantum gravity, as discussed in [JPV96]. The two series, $A(u, x, y, z)$ and $Q(u, x, y, z)$, are generating series for rooted orientable maps with at least one edge and rooted orientable 4-regular maps, with respect to Euler genus,[1] number of vertices, number of faces, and number of edges. They are less combinatorially refined than the series studied in previous chapters, and are given by

$$A(u, x, y, z) := u^2 \, M\left(\frac{x}{u}\mathbf{1}, \frac{y}{u}\mathbf{1}, uz; 0\right) - xy \quad \text{and}$$

$$Q(u, x, y, z) := u^2 \, M\left(\frac{1}{u}\mathbf{x}, \frac{y}{u}\mathbf{1}, uz; 0\right)\Big|_{x_i = \delta_{i,A} x}.$$

As a mnemonic, $A(u, x, y, z)$ enumerates *all* orientable maps with at least one edge, and $Q(u, x, y, z)$ enumerates *quartic* maps. In both series, the variable u is redundant, but it is included to simplify the statement of (7.1), the motivating functional relationship.

---

[1] Maps on the n-torus are enumerated by monomials of degree $2n$ in u.

129

By factoring an exponential generating series for edge-labelled face-4-regular orientable rooted maps, the duals of the maps considered in the present discussion, Jackson and Visentin, in [JV90a], derived the relationship

$$Q(u, x, y, z) = \tfrac{1}{2} \left(A(2u, y + u, y, z^2x) + A(2u, y - u, y, z^2x) \right). \tag{7.1}$$

The second series on the right, $A(2u, y - u, y, z^2x)$, contains negative terms when expanded as a power series in $\mathbb{Q}[u, x, y][\![z]\!]$, but the sum is a generating series for appropriately decorated rooted maps. The relationship demands a combinatorial explanation, though none is currently known, since the existing proof of (7.1), as outlined in Section 7.1, is algebraic, relies on subtle properties of the character theoretic presentation of $M(x, \mathbf{y}, z; 0)$ described in Section 3.5.1, and contains inherently non-combinatorial steps.

Conjecture 7.3, the q-Conjecture, originally stated implicitly in [JV90a], extended to hypermaps in [JV99], and named the Quadrangulation-Conjecture in [JV01], predicts that there is a combinatorial explanation for (7.1). This explanation should take the form of a *natural* bijection, φ, between appropriately decorated rooted orientable maps and 4-regular rooted orientable maps. The content of the q-Conjecture rests on the meaning of the word 'natural', and it is to be interpreted as an assertion that there is a bijection that preserves additional structure, though the precise nature of this structure is not known, and at present *no* explicit bijections are known.

As a starting point, evaluating (7.1) at $u = 0$ produces the equation

$$Q(0, x, y, z) = A(0, y, y, z^2x), \tag{7.2}$$

with both sides enumerating planar maps. The *medial* construction, gives a combinatorial explanation for (7.2) in this special case by providing a natural bijection. The construction was developed in dual form by Tutte for an application to the dissection of equilateral triangles in [Tut48], and was applied to map enumeration in [Tut62] and [Tut63]. Both the medial construction, and its dual, the *radial* construction are described by Ore in [Ore67, pp. 46-47].

A natural generalization of the medial construction to higher genera is explored by Schaeffer in [Sch98, Ch. 2], and gives a bijection between rooted maps and face-bipartite 4-regular rooted maps. This bijection is used in Section 7.3 as a guide for predicting which structures might by preserved by φ. At present, the most explicit construction is one given by Brown and Jackson in [BJ02]. It generalizes the radial construction and provides a combinatorial proof of the weaker relationship

$$Q(1, x, 1, z) = \tfrac{1}{2}A(2, 2, 1, z^2x) = 2A\left(1, 1, \tfrac{1}{2}, 2z^2x\right) = 2A\left(1, \tfrac{1}{2}, 1, 2z^2x\right), \tag{7.3}$$

a special case of (7.1), with additional conditions on genus that are not apparent from the generating series.

Instead of searching for an explicit bijection, this Chapter identifies structures

that might be preserved by such a bijection, with an emphasis on involutions and products on both classes of maps. One difficulty with combinatorializing the proof of (7.1) is that the original derivation involved manipulating exponential generating series for edge-labelled rooted maps, but the combinatorial interpretation is expected only for unlabelled rooted maps. Since the proof of Theorem 4.16 avoids edge-labelled intermediaries, the construction used in Chapter 4 is taken as a starting point for the investigation. In particular, φ^{-1} induces a many-to-one function from 4-regular maps to undecorated maps, and the root-edge classification used in the proof of Lemma 4.7 is related to the cardinality of fibres of φ^{-1}. It is thus expected that the behaviour of φ is related to the root-edge classification.

Cut-edges in maps are associated with a product on rooted maps, so the required bijection φ can be used to induce products on the class of quartic rooted maps. Section 7.4 investigates the form these induced products might take, and states Conjecture 7.15, a more combinatorially refined version of the q-Conjecture. A combinatorial analysis gives an algebraic formulation for the refinement in Section 7.6, where additional equivalent statements are discussed. The Chapter concludes with a more detailed analysis of a special case involving minimally decorated rooted maps on the plane with images on the torus.

7.1 Origins of the q-Conjecture

Jackson and Visentin derived (7.1) indirectly in [JV90a] by exhibiting a multiplicative relationship between two series in two indeterminates each, but the reduction to this form eliminates features that are essential to the conjectured combinatorial interpretation. In particular, the right side of (7.1) is a generating series for a class of rooted maps with decorated vertices and handles, but the indeterminate associated with handles, u, is redundant, since by Euler's formula and degree counting,

$$Q(u^2, x, y, z) = u^2 Q\left(1, \frac{x}{u}, \frac{y}{u}, uz\right) \quad \text{and} \quad A(u, x, y, z) = u^2 A\left(1, \frac{x}{u}, \frac{y}{u}, uz\right).$$

It is sufficient to restrict consideration to evaluations of A and Q at $u = 1$, since

$$A\left(2, y + 1, y, z^2 x\right) = 4A\left(1, \tfrac{1}{2}(y + 1), \tfrac{1}{2}y, 2z^2 x\right).$$

Using the derivation of the map series from Section 3.5, specializations of A and Q at $u = 1$ can be expressed in the form

$$A(1, x, y, z) = 2z \frac{\partial}{\partial z} \ln\left(R_{\mathcal{N}}(x, y, z)\right) \quad \text{and} \tag{7.4}$$

$$Q(1, x, y, z) = 2z \frac{\partial}{\partial z} \ln\left(R_{\{4\}}(x, y, z)\right). \tag{7.5}$$

The series $R_{\mathcal{N}}(x, y, z)$ and $R_{\{4\}}(x, y, z)$ are defined implicitly, up to a constant multiple, and may be normalized to have unit constant terms. With this normalization they are generating series for maps with labelled half-edges, ordinary with respect to vertices and faces, marked by x and y, and exponential with respect to half-edges, marked by $\sqrt{z}$.

Jackson and Visentin worked with a related series, $R_{\mathcal{N}}(x, y \mid z)$, a generating series for orientable maps with directed labelled edges that satisfies $R_{\mathcal{N}}(x, y, z) = R_{\mathcal{N}}(x, y \mid \frac{z}{2})$. They showed in [JV90a, Thm. 5.1] that, when N is a positive integer,

$$R_{\{4\}}(1, 2N, z) = R_{\mathcal{N}}\left(N + \tfrac{1}{2}, N, 2z^2\right) \cdot R_{\mathcal{N}}\left(N - \tfrac{1}{2}, N, 2z^2\right), \tag{7.6}$$

which, by polynomiality, is equivalent to (7.1). Their derivation involved algebraic properties of character evaluations rather than any direct appeal to the combinatorics of rooted maps.

When $R_{\mathcal{N}}$ and $R_{\{4\}}$ are expressed as integrals, as in [JPV96], the relationship in (7.6) is a statement that an integral over $\mathbb{R}^{2N}$ factors as a product of two integrals over $\mathbb{R}^N$. This is written more compactly using the expectation operator from Definition 3.17, which for the remainder of this Chapter is specialized to $b = 0$, so that $\langle \cdot \rangle = \langle \cdot \rangle_{(N)}$ and $\langle \cdot \rangle_e = \langle \cdot \rangle_{e(N)}$ are given by

$$\langle f \rangle := \int_{\mathbb{R}^N} |V(\lambda)|^2 f(\lambda)\, e^{-\frac{1}{2} p_2(\lambda)}\, d\lambda \quad \text{and} \quad \langle f \rangle_e := \left\langle f(\lambda) e^{\sum_{k \geq 1} \frac{1}{k} x_k p_k(\lambda)\, \sqrt{z}^k} \right\rangle,$$

and the recurrence from Lemma 4.13 specializes to

$$\left\langle p_{j+2} p_\theta \right\rangle = \sum_{i \in \theta} i\, m_i(\theta) \left\langle p_{j+i} p_{\theta \setminus i} \right\rangle + \sum_{i=0}^{j} \left\langle p_i p_{j-i} p_\theta \right\rangle. \tag{7.7}$$

Using duality to interchange the rôles of $\mathbf{x}$ and $\mathbf{y}$, Corollary 4.15 states that

$$M(\mathbf{x}, N, z; 0) = \sum_{k=0}^{\infty} x_k \sqrt{z}^k \frac{\langle p_k \rangle_e}{\langle 1 \rangle_e} = x_0 N + 2z \frac{\partial}{\partial z} \ln \left\langle e^{\sum_{k \geq 1} \frac{1}{k} p_k x_k \sqrt{z}^k} \right\rangle \tag{7.8}$$

for every positive integer N. It follows that

$$R_{\mathcal{N}}(x, N, z) \langle 1 \rangle_{(N)} = \left\langle \exp\left(\sum_{k \geq 1} \frac{1}{k} p_k x \sqrt{z}^k \right) \right\rangle_{(N)} = \left\langle \prod_{i=1}^{N} \frac{1}{(1 - \sqrt{z}\, \lambda_i)^x} \right\rangle_{(N)},$$

and similarly $R_{\{4\}}(1, N, z) \langle 1 \rangle_{(N)} = \left\langle \exp\left(\tfrac{1}{4} p_4 z^2 \right) \right\rangle_{(N)}$, so the identity is given by

$$\left\langle \exp\left(\tfrac{1}{4} p_4 z^2 \right) \right\rangle_{(2N)} = c \left\langle \prod_{i=1}^{N} \frac{1}{(1 - \sqrt{2}\, z \lambda_i)^{N + \frac{1}{2}}} \right\rangle_{(N)} \left\langle \prod_{i=1}^{N} \frac{1}{(1 - \sqrt{2}\, z \lambda_i)^{N - \frac{1}{2}}} \right\rangle_{(N)}, \tag{7.9}$$

where $c = c(N) := \langle 1 \rangle_{(2N)} \langle 1 \rangle_{(N)}^{-2}$. This presentation suggests the possibility of a direct analytic proof, although none is known at present. The derivation in [JPV96] follows, in effect, the same steps as the earlier proof, after $\exp\left(\frac{1}{4} p_4(\lambda) z^2\right)$ is expanded in terms of the Schur basis for symmetric functions in λ.

Remark 7.1. Jackson, Perry, and Visentin appear to have conflated the series $R_{\mathcal{N}}(x, y, z)$ in [JPV96], defined consistently with its usage in the present setting, with $R_{\mathcal{N}}(x, y \mid z)$ from the earlier work of Jackson and Visentin in [JV90a]. Since the distinction went unnoticed when results were adapted from the earlier work, several theorems are false as they appear in [JPV96], but easily corrected to the present form by scaling the third argument of $R_{\mathcal{N}}$ by a factor of two.

The factors of (7.6) do not lend themselves to a combinatorial interpretation, but taking logarithms and partial derivatives gives an additive identity,

$$Q(u, x, y, z) = \tfrac{1}{2}\left(A(2u, y + u, y, z^2 x) + A(2u, y - u, y, z^2 x)\right). \tag{7.1}$$

If $\mathcal{A}_k$ denotes the class of rooted maps with $2k$ distinguished vertices, then

$$\tfrac{1}{2}\left(A(1, y + 1, y, x) + A(1, y - 1, y, x)\right) = \sum_{k \geq 0} \sum_{\mathfrak{m} \in \mathcal{A}_k} y^{|V(\mathfrak{m})| + |F(\mathfrak{m})| - 2k} x^{|E(\mathfrak{m})|},$$

so $\tfrac{1}{2}\left(A(2u, y + u, y, z^2 x) + A(2u, y - u, y, z^2 x)\right)$ enumerates elements of $\bigcup_{k \geq 0} \mathcal{A}_k$ with each handle decorated in one of four ways. This led Jackson and Visentin, in [JV90a], to implicitly posit Conjecture 7.3 as an explanation for (7.1).

Definition 7.2 ($\mathcal{A}_{g,n}$, $\mathcal{Q}_{g,n}$)**.** *Let $\mathcal{A}_{g,n}$ denote the class of rooted orientable maps with $n \geq 1$ edges, each handle decorated independently in one of four ways, orientable genus $g - k$, and $2k$ decorated vertices for some integer k. Similarly, let $\mathcal{Q}_{g,n}$ denote the class of rooted orientable 4-regular maps with n vertices and orientable genus g.*

Conjecture 7.3 (Jackson and Visentin [JV90a])**.** *There is a bijection*

$$\varphi \colon \bigcup_{g,n} \mathcal{A}_{g,n} \to \bigcup_{g,n} \mathcal{Q}_{g,n}, \text{ such that } \varphi(\mathcal{A}_{g,n}) = \mathcal{Q}_{g,n},$$

and φ is 'natural' in the sense that it respects additional structure.

Remark 7.4. If $\mathfrak{m}$ has f faces and v vertices, $2k$ of which are decorated, then $\varphi(\mathfrak{m})$ must have $f + v - 2k$ faces.

Remark 7.5. Without the insistence on naturality, the existence of at least one such bijection is guaranteed by (7.1). Since the sets $\mathcal{A}_{g,n}$ and $\mathcal{Q}_{g,n}$ are finite and equicardinal for every g and n, it is possible to construct an explicit bijection by assigning any total order to the elements of each set, but such a bijection does not provide any meaningful insight into the nature of maps.

Remark 7.6. By implicitly identifying handles with canonically chosen pairs of edges, Brown and Jackson represented handle decorations as distinguished
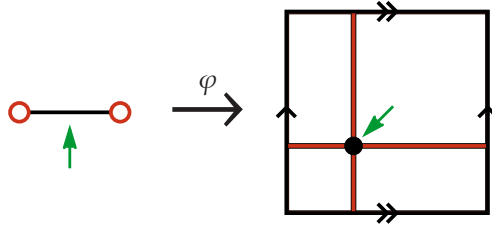
Figure 7.1: The image of the unique rooted map with two decorated vertices, indicated by hollow circles, is the rooted map with two edges on the torus.

subsets of edges in [BJ02]. Their approach has the advantage that undecorated maps are naturally identified with decorated maps in which no vertices are distinguished and the handles are decorated by the empty set of edges, but without constructing φ explicitly, it is unclear whether this is the best way to represent the decoration of handles.
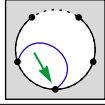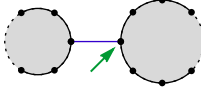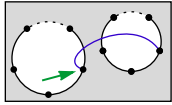
7.2 Initial Observations

Since $\left|\mathcal{A}_{1,1}\right| = \left|\mathcal{Q}_{1,1}\right| = 1$, the action of φ is known for the unique rooted map with one edge and two decorated vertices: see Figure 7.1. No other explicit values are known, but the medial construction, described in Section 7.3, provides an appropriate bijection from $\bigcup_n \mathcal{A}_{0,n}$ to $\bigcup_n \mathcal{Q}_{0,n}$. This is used as a starting point in Section 7.3 to predict which structures might be respected by φ.

The remainder of this Chapter examines Conjecture 7.3 in terms of the root-edge classification introduced in Chapter 4 for establishing Lemma 4.7, and reproduced, as it relates to orientable maps, in Table 7.1. Specializing the proof of Corollary 4.15 to $b = 0$ and $\mathbf{r} = \mathbf{y}$, and appealing to duality of orientable rooted maps, established (7.8) directly for rooted maps, without reference to edge-labelled intermediaries. Additional specialization establishes the integral expressions for $A(1, x, N, z)$ and $Q(1, x, N, z)$ while avoiding the character evaluations associated with the derivation of $R_{\mathcal{N}}(x, y, z)$ and $R_{\{4\}}(x, y, z)$. These character evaluations, though essential to the original proof of (7.6), present an obstacle to its combinatorialization. By avoiding them, it may be possible to establish the identity directly in its additive form, (7.1), and thus avoid the difficulty of finding a combinatorial interpretation for the factors in (7.6).

The root-edge classification is compatible with decorated maps: each rooted map with b borders, r bridges, and h handles corresponds to $2^r 4^h$ elements of $\mathcal{A} := \bigcup_{g,n} \mathcal{A}_{g,n}$. It is thus possible to represent elements of $\mathcal{A}$ by associating decorations to edges, with each bridge decorated in one of two ways, and each handle decorated in one of four ways: the final column of Table 7.1 lists the number of decorations that may be attached to a root-edge of each type. With this convention, root-edge deletion extends naturally to decorated maps, since the decoration of $\mathfrak{m} \backslash e$ can be inherited from the decoration of $\mathfrak{m}$.

Table 7.1: The contribution to M from maps with each root-edge type

Root type	Schematic	Contribution to M	Multiplicity
Border		$z \displaystyle\sum_{i \geq 0} \sum_{j=1}^{i+1} r_j y_{i-j+2} \frac{\partial}{\partial r_i} M$	1
Bridge		$z \displaystyle\sum_{i,j \geq 0} r_{i+j+2} \left(\frac{\partial}{\partial r_i} M \right)\left(\frac{\partial}{\partial r_j} M \right)$	2
Handle		$z \displaystyle\sum_{i,j \geq 0} j r_{i+j+2} \frac{\partial^2}{\partial r_i \partial y_j} M$	4

Remark 7.7. One way to obtain two of the required four decorative states of a handle is to allow each to be either twisted or untwisted. This interpretation helps to explain why non-orientable intermediaries appear in the bijection between $\bigcup_g \mathcal{A}_{g,n}$ and $\bigcup_g \mathcal{Q}_{g,n}$, obtained by Brown and Jackson in [BJ02].

Remark 7.8. If $\mathfrak{m}$ is rooted on a cut-edge e, or if e is the only edge of $\mathfrak{m}$, then one or both of the components of $\mathfrak{m} \backslash e$ may be the rooted map with no edges. The augmented set, $\mathcal{A}$ with the edgeless map adjoined will be denoted by $\mathcal{A}^*$. If $\mathcal{Q}^*$ is produced by adjoining an additional element to $\mathcal{Q}$, then φ can be extended so that $\varphi \colon \mathcal{A}^* \to \mathcal{Q}^*$ is a bijection. The representation of this additional element is discussed in Remark 7.12.

If $\xi \colon \mathcal{A} \to \mathcal{A}^* \cup \mathcal{A}^* \times \mathcal{A}^*$ is the operation of root-edge deletion on decorated maps and φ is extended to $\mathcal{A}^* \times \mathcal{A}^*$ by $\varphi(\mathfrak{m}_1, \mathfrak{m}_2) := \big(\varphi(\mathfrak{m}_1), \varphi(\mathfrak{m}_2)\big)$, then the q-Conjecture would be resolved by providing a natural description of the action of $\varphi \circ \xi \circ \varphi^{-1}$. This action may be expected to take two distinct forms, χ_1 and χ_2, as summarized in the following commutative diagrams,

$$
\begin{array}{ccc}
\mathcal{A}_1 & \xrightarrow{\;\xi\;} & \mathcal{A}^* \\
\downarrow{\scriptstyle\varphi} & & \downarrow{\scriptstyle\varphi} \\
\mathcal{Q} & \xrightarrow{\;\chi_1\;} & \mathcal{Q}^*
\end{array}
\qquad\qquad
\begin{array}{ccc}
\mathcal{A}_2 & \xrightarrow{\;\xi\;} & \mathcal{A}^* \times \mathcal{A}^* \\
\downarrow{\scriptstyle\varphi} & & \downarrow{\scriptstyle\varphi \times \varphi} \\
\mathcal{Q} & \xrightarrow{\;\chi_2\;} & \mathcal{Q}^* \times \mathcal{Q}^*
\end{array}
$$

with $\mathcal{A}_1 := \xi^{-1}(\mathcal{A}^*)$ and $\mathcal{A}_2 := \xi^{-1}(\mathcal{A}^* \times \mathcal{A}^*)$, so that χ_2 acts on 4-regular maps that are the images under φ of cut-edge rooted maps, and χ_1 acts on all other 4-regular maps. It is possible that Conjecture 7.3 is true but χ_1 and χ_2 lack natural descriptions. An investigation of properties expected of χ_2 leads in Section 7.4, an attempt to classify the images of maps rooted on cut-edges, to the main result of this Chapter, an identification of partitions of $\mathcal{A}$ and $\mathcal{Q}$ that appear to be respected by φ. More generally, natural descriptions of χ_1 and χ_2 should provide a description of additional correspondences between $\mathcal{A}$ and $\mathcal{Q}$.

Example 7.9. *If $\mathfrak{m}$ is a rooted orientable map with n edges and root-face degree j that can be decorated in c ways, then $\xi^{-1}(\mathfrak{m})$ consists of $2n + 1$ rooted maps. Precisely $j + 1$ of these are rooted on borders with c decorations each, while the remaining maps are rooted on handles with 4c decorations each. It follows that for $\mathfrak{q} \in Q^*$, the number $|\chi_1(\mathfrak{q})|$ determines the root-face degree of $\varphi^{-1}(\mathfrak{q})$, so a natural description of χ_1 defines a parameter of 4-regular maps corresponding to root-face degree in rooted maps.*

The medial construction, a possible specialization of the bijection required by Conjecture 7.3, is discussed in Section 7.3 in an attempt to anticipate which structures might be respected by φ.

7.3 The Medial Construction

The medial construction, described for all genera by Schaeffer in [Sch98, Ch. 2],[2] gives an explicit genus preserving bijection between rooted orientable maps and face-bipartite rooted orientable 4-regular maps. If the decoration of handles is represented in such a way that some maps in $\bigcup_{g,n} \mathcal{A}_{g,n}$ are considered undecorated, then there is a bijection between $\mathcal{A}$ and Q such that its restriction to undecorated maps is the medial construction. If it is assumed that that at least one bijection explaining Conjecture 7.3 takes this form, then any additional structure respected by φ must also be respected by the medial construction. This approach is used in Section 7.4 to attempt to predict a characterization of which 4-regular maps are the images under φ of decorated maps rooted on cut-edges.

Definition 7.10 (medial construction)**.** *If $\mathfrak{m}$ is a map, then the image of $\mathfrak{m}$ under the medial construction, denoted by $\overline{\varphi}(\mathfrak{m})$, is obtained by placing a vertex on every edge of $\mathfrak{m}$. An edge joining two vertices of $\overline{\varphi}(\mathfrak{m})$ is drawn within every face in which the corresponding edges of $\mathfrak{m}$ appear consecutively around a face boundary. This construction extends naturally to rooted maps.*

The 4-regular maps produced by the medial construction are face-bipartite: one class of faces corresponds to the faces of the original map, the other class corresponds to vertices, and the degree of every face in $\overline{\varphi}(\mathfrak{m})$ equals the degree of the corresponding face or vertex in $\mathfrak{m}$: see Figure 7.2. The rôles of vertices and faces are interchangeable, since a map and its dual have the same unrooted images under the action of $\overline{\varphi}$. The construction applies, unmodified, to maps of all genera, with its image being all face-bipartite 4-regular maps.

Example 7.11. *The first column of Figure 7.3 gives the orientable rooted maps with two edges, and the final column gives their images under the medial construction. Maps are rooted by specifying the side of an edge, and 4-regular maps are rooted by specifying a vertex-face incidence, but the convention given in Figure 2.16 is altered so that the root flag is counterclockwise of the head of the arrow in all cases.*

---

[2]Schaeffer, and other recent authors studying map enumeration, see for example [JV01], [JV90a], and [BJ02], appear to have reversed the terms 'medial' and 'radial'. The present work attempts to restore the terms to their historical meanings as used by Ore in [Ore67, pp. 46-47].
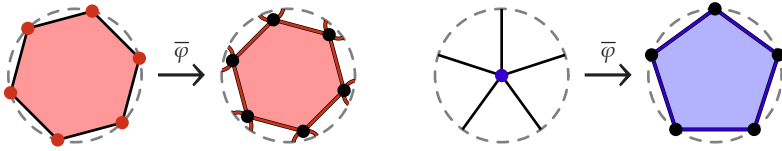
Figure 7.2: The image, under the action of $\overline{\varphi}$, the medial construction, of a degree i vertex or face in a rooted map is a degree i face in a face-bipartite 4-regular map.
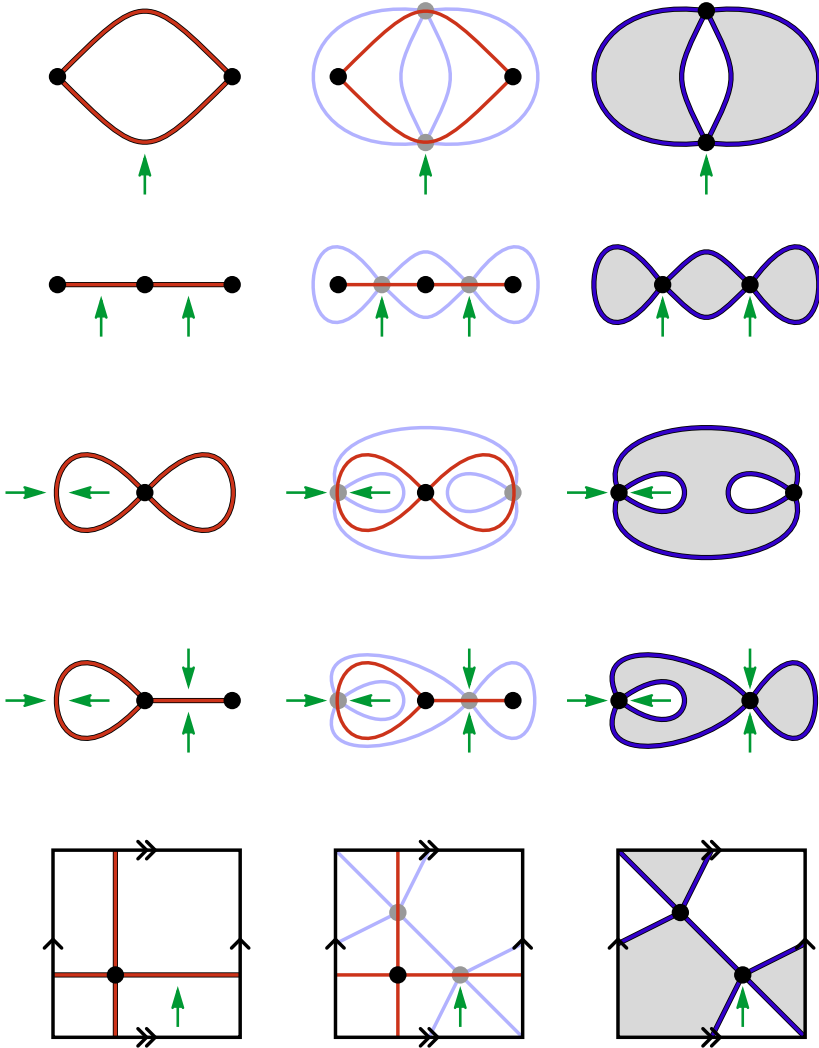
Figure 7.3: The medial construction for orientable maps sends rooted maps with two edges, given in the first column, to face-bipartite 4-regular rooted maps with two vertices, given in the third column.
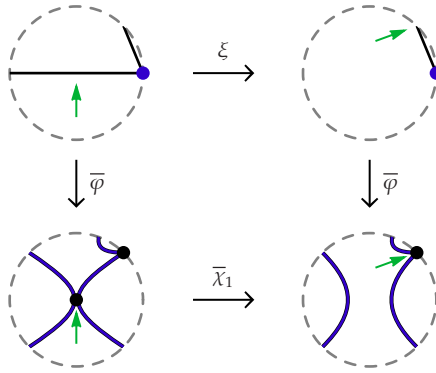
Figure 7.4: If $\overline{\varphi}$ is used to defined $\overline{\chi}_1$, an analogue of χ_1 acting on undecorated maps, then $\overline{\chi}_1$ acts locally on 4-regular maps that are the images of border rooted undecorated maps.

Root-face degree is preserved by $\overline{\varphi}$, but this does not generalize to φ, since root-face degree is not preserved by the action of φ given in Figure 7.1, where a decorated map with root-face degree two has an image with root-face degree four. The same example shows that vertex degree cannot be preserved in the general case. Similarly, even though the involution induced by duality in $\mathcal{A}$ is re-rooting in Q, this behaviour cannot be generalized to decorated maps, since the dual of the map in Figure 7.1 has only a single vertex, and thus no images on the torus. The structures preserved by φ must be more subtle.

A more abstract characterization of the medial construction, one that might generalize to φ, is that local properties of rooted maps induce local properties of 4-regular maps. Two examples are that the action of the function on Q induced by root edge deletion in $\mathcal{A}$ can be described locally, as illustrated for borders in Figure 7.4, and that topological cut-vertices[3] in face-bipartite 4-regular rooted orientable maps are the images of cut-edges and their duals in undecorated rooted orientable maps, as illustrated in Figure 7.5. An examination of possible relationships between cuts in Q and the action of φ, in Section 7.4, leads to Conjecture 7.15, a refinement of Conjecture 7.3.

Remark 7.12. With $\overline{\chi}_2$ defined analogously to χ_2, Figure 7.6 gives the action of $\overline{\chi}_2$ on $\overline{\varphi}(\mathfrak{m})$ when neither component of $\mathfrak{m}\backslash e$ is a leaf. Under the assumptions that φ acts locally, extending this to the map in which both components of $\mathfrak{m}\backslash e$ are leaves, as in Figure 7.7, suggests the action

$$\varphi: \raisebox{-2pt}{\includegraphics[height=10pt]{leaf}} \to \raisebox{-2pt}{\includegraphics[height=10pt]{circle}} \qquad \text{so that} \qquad Q^* := Q \cup \left\{ \raisebox{-2pt}{\includegraphics[height=10pt]{circle}} \right\}.$$

The additional map should be considered orientable, 4-regular, and planar. It has two faces, no vertices, and no edges.

---

[3]A *topological cut-vertex* is a vertex whose deletion disconnects the graph as a topological space. The term includes both graphical cut-vertices and all vertices incident with loops.
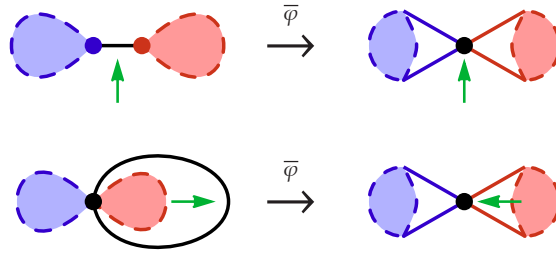
Figure 7.5: Topological cut-vertices in face-bipartite 4-regular orientable rooted maps are the images under $\overline{\varphi}$ of cut-edges and their duals.
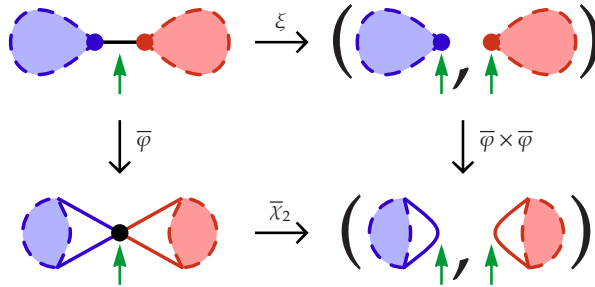
Figure 7.6: The function $\overline{\chi}_2$ is analogous to χ_2, and it acts locally.
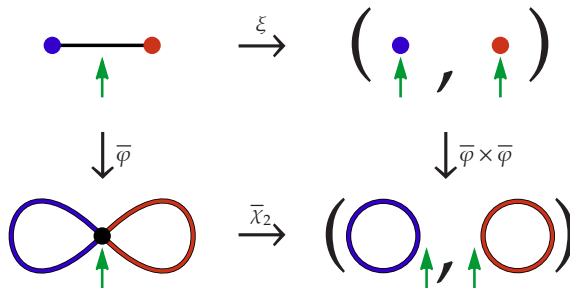
Figure 7.7: The medial construction suggests the image of the edgeless map.

7.4 Cuts, Products, and a Refined Conjecture

The medial construction induces a correspondence that relates cut-edges and their duals in rooted maps to topological cut-vertices, which occur in two forms, in face-bipartite 4-regular rooted orientable maps. Shifting attention to decorated rooted maps from rooted maps, and from face-bipartite to all 4-regular rooted orientable maps, as required by the q-Conjecture, introduces a third family of cuts on each class, but φ cannot induce a correspondence between these additional cuts since they behave differently with respect to the parameter g. With the goal of reconciling these differences, this Section describes products associated with each family of cuts, and in the process, partitions of each of $\mathcal{A}$ and Q into two qualitatively different classes of maps, with each class identifiable using properties of an appropriate product. Since numerical evidence suggests that there may be a bijection that satisfies the q-Conjecture and respects the partitions, this leads to a refined conjecture.

This Section analyzes twelve products. Three of them, ρ_1, ρ_2, and ρ_3, are defined by natural actions on $\mathcal{A}^* \times \mathcal{A}^*$, three more, π_1, π_2, and π_3, are defined by natural actions on $Q^* \times Q^*$, and the remaining six are defined implicitly by the dashed arrows in the following commutative diagrams for $1 \le i \le 3$:

$$
\begin{array}{ccc}
\mathcal{A}^* \times \mathcal{A}^* & \xrightarrow{\ \rho_i\ } & \mathcal{A} \\
{\scriptstyle \varphi \times \varphi}\big\downarrow & & \big\downarrow{\scriptstyle \varphi} \\
Q^* \times Q^* & \dashrightarrow{\scriptstyle \underline{\pi}_i} & Q.
\end{array}
\qquad
\begin{array}{ccc}
\mathcal{A}^* \times \mathcal{A}^* & \dashrightarrow{\scriptstyle \overline{\rho}_i} & \mathcal{A} \\
{\scriptstyle \varphi \times \varphi}\big\downarrow & & \big\downarrow{\scriptstyle \varphi} \\
Q^* \times Q^* & \xrightarrow{\ \pi_i\ } & Q.
\end{array}
$$

The implicitly defined products do not necessarily have natural descriptions on $\mathcal{A}^* \times \mathcal{A}^*$ and $Q^* \times Q^*$, but the products are indexed such that the actions of π_i and $\underline{\pi}_i$ on face-bipartite 4-regular rooted orientable maps agree for $i \in \{1, 2\}$, provided that the restriction of φ to undecorated maps is the medial construction. Section 7.4.3 examines the possibility that π_3 and $\underline{\pi}_3$ agree on a non-trivial subset of $Q^* \times Q^*$.

Remark 7.13. The names of the products have been selected such that the correspondence preserves subscripts, the ρ's act on $\mathcal{A}^* \times \mathcal{A}^*$, the π's act on $Q^* \times Q^*$, and a bar indicates that a product is defined implicitly. With Q sitting below $\mathcal{A}$, the position of a bar indicates the position of the implicitly defined product relative to the naturally defined product to which it corresponds.

7.4.1 Products Acting Naturally on $Q^* \times Q^*$

Deleting a topological cut-vertex separates a 4-regular map into precisely two components. Since each component is incident with the vertex along two half-edges, this induces a perfect matching on the half-edges. There are precisely three possible configurations in which a 4-regular map can be rooted at a cut-

(d) Products associated with the configurations
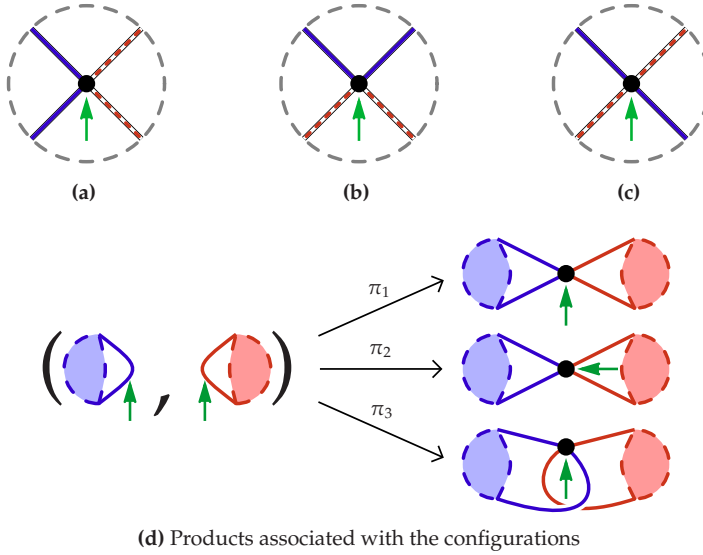
Figure 7.8: The root vertex of a 4-regular map rooted on a cut-vertex has one of three possible configurations, (a)–(c), classified by the matching on half-edges induced by the cut. Products corresponding to each configuration are given in (d), where crossing edges are treated as in ribbon graphs.

vertex, one for each perfect matching. Each configuration corresponds to a product on Q^*, and the products are denoted by π_1, π_2, and π_3 as in Figure 7.8.

Remark 7.14. As in Example 7.11, the rooting convention from Figure 2.16 is reversed for 4-regular maps relative to maps: arrows pointing at vertex-face incidences in 4-regular maps indicate flags immediately counterclockwise of their heads, while arrows pointing at edges in 4-regular maps indicate flags clockwise of their heads. The distinction may be significant since, if the refinement predicted in this Section is true, then φ does not commute with orientation reversal. The modified convention is used for the rest of the Chapter.

Both π_1 and π_2 are genus additive, but the genus of $\pi_3(\mathfrak{q}_1, \mathfrak{q}_2)$ depends on whether the root edges of $\mathfrak{q}_1$ and $\mathfrak{q}_2$ are face-separating. Table 7.2 summarizes the behaviours of π_1, π_2, and π_3, relative to whether or not the root edges of their operands are face-separating. A ✔ indicates a map with a face-separating root edge, and an ✘ indicates a map with a face-non-separating root edge.

For the purpose of Table 7.2, the map $\varphi(\overset{\bullet}{\nearrow}) = \overset{\nearrow}{\bigcirc}$, its representation suggested by Remark 7.12, has a face-separating root edge. A comparison of the genus and number of decorated vertices in $\overline{\rho}_3\,(\mathfrak{m}, \overset{\bullet}{\nearrow})$ to the same parameters in $\mathfrak{m}$ determines whether the root edge of $\varphi(\mathfrak{m})$ is face-separating. It follows that a natural description of $\overline{\rho}_3$ induces a parameter of $\mathcal{A}$ that determines which maps have images that are rooted on face-separating edges.

Table 7.2: The genus of $\pi_3(\mathfrak{q}_1, \mathfrak{q}_2)$ depends on which root edges are face-separating.

$\mathfrak{q}_1$	$\mathfrak{q}_2$	$\pi_1(\mathfrak{q}_1, \mathfrak{q}_2)$	$\pi_2(\mathfrak{q}_1, \mathfrak{q}_2)$	$\pi_3(\mathfrak{q}_1, \mathfrak{q}_2)$	Genus of $\pi_3(\mathfrak{q}_1, \mathfrak{q}_2)$
✔	✔	✔	✔	✘	$g(\mathfrak{q}_1) + g(\mathfrak{q}_2) + 1$
✔	✘	✘	✘	✔	$g(\mathfrak{q}_1) + g(\mathfrak{q}_2)$
✘	✔	✔	✔	✘	$g(\mathfrak{q}_1) + g(\mathfrak{q}_2)$
✘	✘	✘	✘	✘	$g(\mathfrak{q}_1) + g(\mathfrak{q}_2)$

7.4.2 Products Acting Naturally on $\mathcal{A}^* \times \mathcal{A}^*$

In $\mathcal{A}$, cut-edges occur in two forms, decorated and undecorated. Taken together with duals of cut-edges, which are borders, and thus never decorated, this gives three natural classes of cuts, and as with 4-regular maps, each cut is associated with a corresponding product. These products are related to, but differ from, $\overline{\rho}_1$, $\overline{\rho}_2$, and $\overline{\rho}_3$. The differences suggest a refined conjecture that limits which structures might be preserved by φ.

Recall that $\mathcal{A}_2$ is the set of decorated maps that are rooted on bridges. Such maps fall into two classes, distinguished by whether or not the root is decorated. If the decoration of bridges is indicated by decorating an even subset of vertices, as suggested by (7.1), then the two classes can be represented by $\mathcal{A}_{2e}$, those rooted maps with an *even* number of decorated vertices on each side of the cut-edge, and $\mathcal{A}_{2o}$, those rooted maps with an *odd* number of decorated vertices on each side of the cut-edge. Since $\xi \colon \mathcal{A}_{2o} \to \mathcal{A}^* \times \mathcal{A}^*$ preserves legal decorations, when ξ acts on $\mathcal{A}_{2o}$, the decoration of each resulting root vertex is changed to give each component an even number of decorated vertices. Two products, ρ_1 and ρ_3, both related to cut-edges, are then defined so that the following diagram commutes:

$$
\begin{array}{ccc}
\mathcal{A}^* \times \mathcal{A}^* & \xrightarrow{\ \rho_1\ } & \mathcal{A}_{2e} \\
{\scriptstyle \rho_3}\big\downarrow & \searrow{\scriptstyle \mathrm{id}} & \big\downarrow{\scriptstyle \xi} \\
\mathcal{A}_{2o} & \xrightarrow{\ \xi\ } & \mathcal{A}^* \times \mathcal{A}^*
\end{array}
$$

The diagram can also be used to define $\tau := \left(\rho_1 \circ \rho_3^{-1}\right) \oplus \left(\rho_3 \circ \rho_1^{-1}\right)$, an involution of $\mathcal{A}_2$ that acts as a bijection between $\mathcal{A}_{2e}$ and $\mathcal{A}_{2o}$ by changing the decoration of each vertex incident with the root edge: see Figure 7.9.
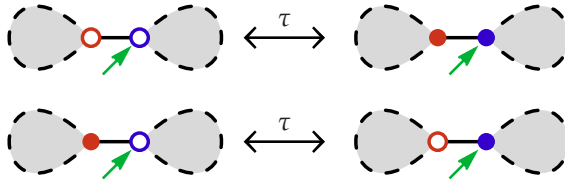
Figure 7.9: An involution of $\mathcal{A}$, denoted by τ, interchanges $\mathcal{A}_{2e}$ and $\mathcal{A}_{2o}$.
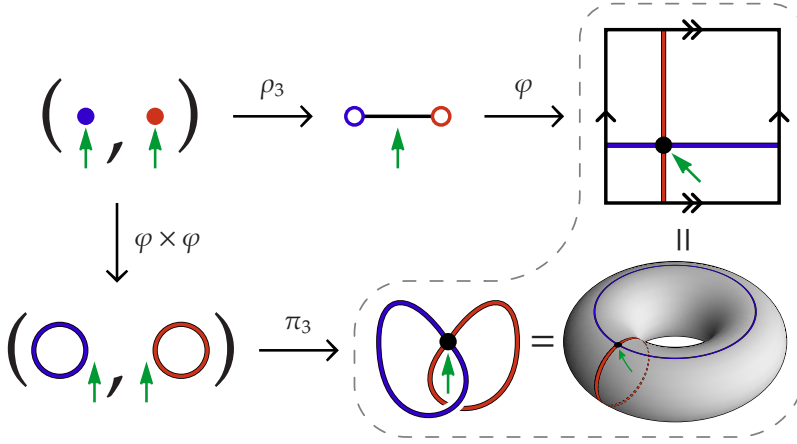
Figure 7.10: The products ρ_3 and π_3 are related.

Since the element-wise action of ρ_1, given by

is the inverse of ξ as it occurs in Figure 7.6, the products $\underline{\pi}_1$ and π_1 coincide on face-bipartite maps, provided that $\overline{\varphi}$ is the restriction of φ to undecorated maps. Both products are genus additive, and it may be expected that their coincidence extends to all decorated maps.

The second product, ρ_3, is the composition of ρ_1 with τ. Since every element of $\rho_3(\mathcal{A}^* \times \mathcal{A}^*)$ has at least two decorated vertices, it does not correspond to a product on undecorated maps. With the action of φ still unknown, a relationship between $\underline{\pi}_3$ and π_3 is only conjectured, but both products agree on $\left(\text{⊙}, \text{⊙} \right)$, as illustrated in Figure 7.10. If $\mathfrak{q}_1$ and $\mathfrak{q}_2$ are both images of rooted maps with decorated root vertices, then the genus of $\underline{\pi}_3(\mathfrak{q}_1, \mathfrak{q}_2)$ is $g(\mathfrak{q}_1) + g(\mathfrak{q}_2) - 1$, but the genus of $\pi_3(\mathfrak{q}_1, \mathfrak{q}_2)$ is at least $g(\mathfrak{q}_1) + g(\mathfrak{q}_2)$. It follows that the products $\underline{\pi}_3$ and π_3 cannot coincide for all 4-regular maps, but qualitative similarities between their behaviours suggest the existence of some relationship, and this possibility is examined in Section 7.4.3.

The third product, ρ_2, is not directly related to ξ, but corresponds instead to the duals of cut-edges. Its action is defined by

with the root vertex of $\rho_2(\mathfrak{m}_1, \mathfrak{m}_2)$ decorated as necessary to maintain parity. If $\overline{\varphi}$ is the restriction of φ to undecorated maps, then $\underline{\pi}_2$ and π_2 agree on face-bipartite 4-regular maps, but this agreement cannot extend to all maps: if the

143

Table 7.3: The products ρ_1, ρ_2, and ρ_3, are summarized. Maps are listed with the genera of their images under φ. Decorated vertices are hollow, and q_i denotes $\varphi(\mathfrak{m}_i)$.

$(\mathfrak{m}_1, \mathfrak{m}_2)$	$\rho_1(\mathfrak{m}_1, \mathfrak{m}_2)$	$\rho_2(\mathfrak{m}_1, \mathfrak{m}_2)$	$\rho_3(\mathfrak{m}_1, \mathfrak{m}_2)$
	$g(q_1) + g(q_2)$	$g(q_1) + g(q_2)$	$g(q_1) + g(q_2) + 1$
	$g(q_1) + g(q_2)$	$g(q_1) + g(q_2)$	$g(q_1) + g(q_2)$
	$g(q_1) + g(q_2)$	$g(q_1) + g(q_2)$	$g(q_1) + g(q_2)$
	$g(q_1) + g(q_2)$	$g(q_1) + g(q_2) - 1$	$g(q_1) + g(q_2) - 1$

root vertices of both $\mathfrak{m}_1$ and $\mathfrak{m}_2$ are decorated, $q_1 = \varphi(\mathfrak{m}_1)$, and $q_2 = \varphi(\mathfrak{m}_2)$, then $\underline{\pi}_2(q_1, q_2)$ has genus $g(q_1) + g(q_2) - 1$, but $\pi_2(q_1, q_2)$ has genus $g(q_1) + g(q_2)$.

Table 7.3 gives the dependence of ρ_1, ρ_2, and ρ_3 on root decoration. Both ρ_2 and ρ_3 are genus-additive, but neither preserves total number of decorated vertices, so $\underline{\pi}_2$ and $\underline{\pi}_3$, the corresponding products on Q^*, are not genus-additive. From their behaviour with respect to genus, a natural description of either $\underline{\pi}_2$ or $\underline{\pi}_3$ can be used to describe a property of 4-regular maps that distinguishes images of rooted maps with face-separating root edges from images of rooted maps with face-non-separating root edges.

7.4.3 A Comparison and a Refinement

Each of the implicitly defined products described in the preceding sections induces structure on the class of maps on which it acts. One approach to identifying the bijection φ required by Conjecture 7.3 involves trying to recognize these induced structures by comparing their expected properties to properties of structures associated with the naturally defined products. This approach leads to Conjecture 7.15, a refined conjecture that is further supported by numerical evidence.

The products $\underline{\pi}_1$, $\underline{\pi}_2$, and $\underline{\pi}_3$ induce three disjoint embeddings of $Q^* \times Q^*$ in Q.

Provided that the medial construction is the restriction of φ to undecorated maps, π_1 and π_2 agree with $\underline{\pi}_1$ and $\underline{\pi}_2$, respectively, when acting on face-bipartite 4-regular rooted orientable maps. Similarly, π_3 and $\underline{\pi}_3$ agree unconditionally when acting on $\left(\left(\text{⟲}\right), \left(\text{⟲}\right)\right)$. A dearth of natural candidates for the images of the induced embeddings, together with the prediction that π_i and $\underline{\pi}_i$ agree on restricted sets for every i, suggests that the products agree on substantially larger sets.

Comparing π_3 with $\underline{\pi}_3$ shows that the two products are distinct. For two 4-regular rooted orientable maps, $\mathfrak{q}_1 = \varphi(\mathfrak{m}_1)$ and $\mathfrak{q}_2 = \varphi(\mathfrak{m}_2)$, with the root vertex of $\mathfrak{m}_i$ denoted by v_i and the root edge of $\mathfrak{q}_i$ denoted by e_i for $i \in \{1, 2\}$, the products $\underline{\pi}_3$ and π_3 have the following behaviour with respect to genus:

$$g\left(\underline{\pi}_3(\mathfrak{q}_1, \mathfrak{q}_2)\right) = g(\mathfrak{q}_1) + g(\mathfrak{q}_2) + \begin{cases} 1 & \text{neither } v_1 \text{ nor } v_2 \text{ is decorated} \\ 0 & \text{one of } v_1 \text{ and } v_2 \text{ is decorated} \\ -1 & \text{both } v_1 \text{ and } v_2 \text{ are decorated, and} \end{cases}$$

$$g\left(\pi_3(\mathfrak{q}_1, \mathfrak{q}_2)\right) = g(\mathfrak{q}_1) + g(\mathfrak{q}_2) + \begin{cases} 1 & \text{both } e_1 \text{ and } e_2 \text{ are face-separating} \\ 0 & \text{one of } e_1 \text{ and } e_2 \text{ is face-separating} \\ 0 & \text{neither } e_1 \text{ nor } e_2 \text{ is face-separating.} \end{cases}$$

Since π_3 is genus-superadditive, the two products cannot agree on images of maps that are both rooted on decorated vertices, but comparing the operands on which the products are strictly genus-superadditive suggests a relationship between undecorated root vertices in maps and face-separating root edges in 4-regular maps.

Similarly, if $\underline{\pi}_3$ and $\overline{\rho}_3$ have natural descriptions, then $\mathcal{A}^*$ and $\mathcal{Q}^*$ carry the structure necessary for identifying which elements of $\mathcal{A}^*$ are sent to 4-regular maps rooted on face-separating edges by φ, and which elements of $\mathcal{Q}^*$ are the images of maps rooted on decorated vertices. The simplest explanation, in that it demands the least additional structure on each class, is that the structures are related by the action of φ. This is the same conclusion as the one implied by the hypothesis that π_3 and $\underline{\pi}_3$ coincide on the maximum set not excluded by their behaviours with respect to genus. Together with numerical evidence, this suggests the following refinement of Conjecture 7.3.

Conjecture 7.15 (The Refined q-Conjecture)**.** *There is a bijection φ satisfying the conditions of Conjecture 7.3 such that the root edge of $\varphi(\mathfrak{m})$ is face-separating if and only if the root vertex of $\mathfrak{m}$ is not decorated.*

Remark 7.16. In support of this refinement, even without knowing any explicit actions of φ, if $\mathfrak{m}$ is a one-faced map in which every vertex is decorated, then $\varphi(\mathfrak{m})$ also has only one face, so the root edge of $\varphi(\mathfrak{m})$ is face-non-separating.

Example 7.17. *There are 1720 rooted maps with 3 vertices on the torus, each with $4\binom{3}{2} = 12$ decorations having images on the double-torus under the action of φ. If Conjecture 7.15 is true, then $4\binom{2}{2} = 4$ of these have face-separating root edges and $4\binom{2}{1} = 8$ have face-non-separating root edges.*

Table 7.4: Number of 5-vertex maps in Q refined by genus and root-edge behaviour

g	Face-separating	Face-non-separating	Total
0	2,916	0	2,916
1	23,976	7,290	31,266
2	27,972	28,674	56,646
3	0	9,450	9,450

Table 7.5: Number of 5-edge maps refined by genus and number of vertices

g	$v=1$	$v=2$	$v=3$	$v=4$	$v=5$	$v=6$
0	42	386	1030	1030	386	42
1	420	1720	1720	420		
2	483	483				

Example 7.18. *A computer search was used to classify all* $100,278$ *of the 4-regular rooted orientable maps with* 5 *vertices according to genus and whether or not the root-edge of each is face-separating. The results appear in Table 7.4. The following calculation uses Conjecture 7.15 to express each non-zero entry of the Table in terms of coefficients of* $A(u, x, 1, z)$*, with the relevant values appearing in Table 7.5, a tabulation of the number of orientable 5-edged maps with each genus and number of vertices:*

$$2,916 = \binom{0}{0}42 + \binom{1}{0}386 + \binom{2}{0}1030 + \binom{3}{0}1030 + \binom{4}{0}386 + \binom{5}{0}42,$$

$$23,976 = \binom{2}{2}1030 + \binom{3}{2}1030 + \binom{4}{2}386 + \binom{5}{2}42$$
$$+ 4\left(\binom{0}{0}420 + \binom{1}{0}1720 + \binom{2}{0}1720 + \binom{3}{0}420\right),$$

$$27,972 = \binom{4}{4}386 + \binom{5}{4}42 + 4\left(\binom{2}{2}1720 + \binom{3}{2}420\right) + 4^2\left(\binom{0}{0}483 + \binom{1}{0}483\right),$$

$$7,290 = \binom{1}{1}386 + \binom{2}{1}1030 + \binom{3}{1}1030 + \binom{4}{1}386 + \binom{5}{1}42,$$

$$28,674 = \binom{3}{3}1030 + \binom{4}{3}386 + \binom{5}{3}42 + 4\left(\binom{1}{1}1720 + \binom{2}{1}1720 + \binom{3}{1}420\right),$$

$$9,450 = \binom{5}{5}42 + 4\binom{3}{3}420 + 4^2\binom{1}{1}483.$$

7.5 Symmetry Breaking and Chirality

This Section examines symmetries of $\mathcal{A}$ and Q, with emphasis on symmetries of $\mathcal{A}$ that preserve the root edge and symmetries of Q that preserve the root vertex. As in Section 3.6.3, where it was noted that a b-invariant must break the symmetry between three involutions acting on hypermaps in order to have a dependence on rooting, the bijection predicted by Conjecture 7.15 cannot respect all of the symmetries that are shared by $\mathcal{A}$ and Q, even those that are respected by the medial construction. In particular, the left-right symmetry exhibited by both classes must be broken by every suitable bijection.

A 4-regular rooted map has eight flags incident with each vertex, and the dihedral group with 8 elements acts on Q by re-rooting maps to new flags incident with the same vertex. The group is generated by three involutions, α_1, α_2, and α_3, and each induces a corresponding action on $\mathcal{A}$: Figure 7.11 gives the actions of α_1, α_2, and α_3, together with the actions of β_1, β_2, and β_3, the corresponding involutions induced on undecorated elements of $\mathcal{A}$ by the medial construction. All three induced actions are natural on undecorated maps and preserve root edges: β_1 and β_2 do so directly, and β_3 does so *via* the natural bijection between the flags of a map and the flags of its dual. As noted in Section 7.3, a map and its dual need not have the same number of vertices, and thus need not have images on the same surfaces. It follows that α_3 cannot correspond to duality in general. Conjecture 7.15 additionally precludes extending the actions of β_1 and β_2 given in Figure 7.11 to all decorated maps.
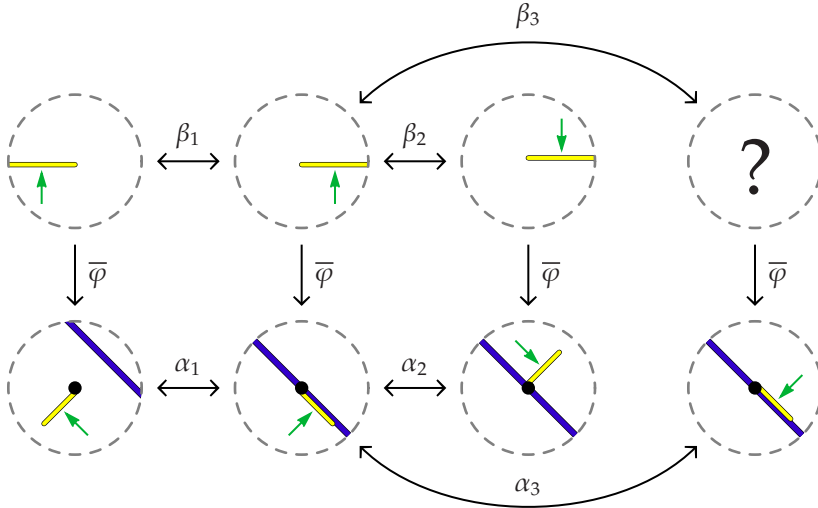
Figure 7.11: Three involutions, α_1, α_2, and α_3, act on Q by changing the root to a new flag incident with the same vertex, and generate a group of order eight. In the restriction to face-bipartite maps, they correspond, *via* the medial construction, $\overline{\varphi}$, to β_1, β_2, and β_3. The first two re-root maps to new flags on the same edge. The third, β_3, is rooted duality. It does not act locally, but it does preserve root edges.
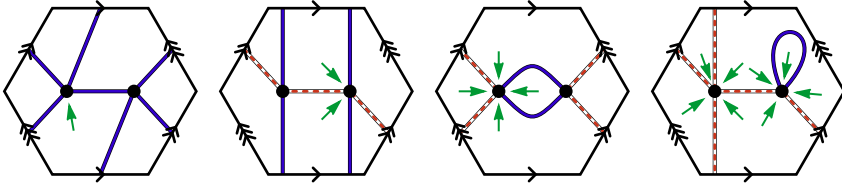
Figure 7.12: There are fifteen rooted orientable 4-regular maps with two vertices on the torus. Face-non-separating edges are indicated with broken lines, while face-separating edges are solid.
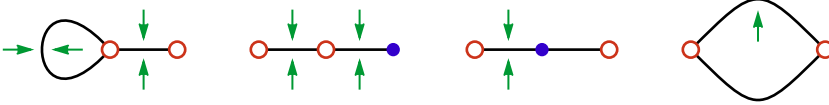
Figure 7.13: Nine of the eleven elements of $\mathcal{A}$ with two edges and images on the torus are rooted at decorated vertices, which are indicated with hollow circles.

To see that the actions of β_1 and α_1 given in Figure 7.11 do not correspond to each other in general, consider the elements of $\mathcal{A}$ with two edges and their images in Q with two vertices. Figure 7.12 gives the fifteen rooted orientable 4-regular maps with two vertices on the torus, using line-style to distinguish face-separating edges from face-non-separating edges. Eleven of these are images of the decorated planar rooted maps given in Figure 7.13, and the remaining four are images of decorated copies of the monopole with two edges on the torus, all of which have undecorated root vertices. Assuming the Refined q-Conjecture, if the correspondence between the actions of α_1 and β_1 given in Figure 7.11 extends to all maps, then φ induces a bijection between

1. elements of $\mathcal{A}_{g,n}$ with root arrows that are clockwise of decorated vertices and counterclockwise of undecorated vertices, and

2. elements of $Q_{g,n}$ with root arrows that are clockwise of face-non-separating edges and counterclockwise of face-separating edges.

Since there are three of the former in Figure 7.12 and only two of the latter in Figure 7.13, no such bijection exists.

Similarly, there are three maps in Figure 7.12 with face-separating root edges that have images under the action of α_2 with face-non-separating root edges. It follows that if Conjecture 7.15 is true, then the action on $\mathcal{A}$ induced by α_2 cannot preserve root vertices. So the correspondence between the actions of α_2 and β_2 given in Figure 7.11 does not extend to all decorated maps either.

Attempting to match involutions acting on $\mathcal{A}$ with naturally defined involutions acting on Q suggests why the q-Conjecture has remained relatively intractable: to wit, the required bijection exhibits an unexpected chirality. Even though the enumerative theories of both $\mathcal{A}$ and Q are unchanged by interchanging the senses of clockwise and counterclockwise used to determine which flag

is indicated by a particular arrow, the bijection predicted by Conjecture 7.15 cannot respect this symmetry. Since the underlying enumerative problem was introduced from a study of two models of 2-dimensional quantum gravity, this chirality might have a physical significance.

Additional insight into the q-Conjecture might be obtained by trying to match involutions acting on Q with naturally defined involutions acting on $\mathcal{A}$. In particular, the actions of β_1 and β_2 given in Figure 7.11 extend unmodified to all of $\mathcal{A}$. Similarly, the involution τ, its action on bridge-rooted maps given in Figure 7.9, acts on any decorated map by changing the state of decoration of each vertex once for every time it is incident with the root edge. By comparing fixed points, a natural description of the involution induced by τ could be used to identify the images in Q of loop-rooted maps in $\mathcal{A}$. Together, τ, β_1, and β_2, generate a group isomorphic to $\mathbb{Z}_2 \times \mathbb{Z}_2 \times \mathbb{Z}_2$ that acts on $\mathcal{A}$, but attempts to find the induced action of this group on Q have been no more successful than attempts to identify a natural action of the eight element dihedral group on $\mathcal{A}$.

To date, attempts to identify the actions that α_1, α_2, and α_3 induce on $\mathcal{A}$, or the actions that β_1, β_2, and τ induce on Q, have been unsuccessful. This suggests that perhaps the correct approach to the q-Conjecture should be to study a class of covering objects on which all of the actions described in this Chapter act naturally.

7.6   An Algebraic Formulation

Though the Refined q-Conjecture begins to answer questions of what structures might be preserved by a bijection between $\mathcal{A}$ and Q, and through Section 7.5 what structures cannot be preserved by such a bijection, it does so at the expense of certainty about existence. The existence of a bijection between $\mathcal{A}_{g,n}$ and $Q_{g,n}$ is guaranteed by the work of Jackson and Visentin in [JV90a], but the existence of a bijection that additionally sends maps rooted on decorated vertices to 4-regular maps rooted on face-non-separating edges, as required by Conjecture 7.15, is presently supported only by structural observations and numerical evidence. This Section describes the combinatorial observations necessary to give Conjecture 7.15 an algebraic reformulation that can potentially be verified using an approach similar to that used by Jackson and Visentin in [JV90a]. The desired reformulation is obtained by giving explicit expressions to the generating series of the relevant partitions of $\mathcal{A}$ and Q.

Definition 7.19 (Q_1, Q_2, $Q_1(u, x, y, z)$, and $Q_2(u, x, y, z)$). *Denote the subset of Q consisting of maps with face-separating root edges by Q_1, and denote the subset consisting of maps with face-non-separating root edges by Q_2. The generating series for these sets are $Q_1(u, x, y, z)$ and $Q_2(u, x, y, z)$, respectively.*

Finding generating series for the required partitions of $\mathcal{A}$ requires decorating the root vertex separately from the remaining vertices. Since the generating series for elements of $\mathcal{A}$ with root vertices marked by r instead of x is given by

$\frac{r}{x}A(u, x, y, z)$, dropping the condition of naturality from Conjecture 7.15 gives the following algebraic formulation.

Conjecture 7.20. *The series $Q_1(u, x, y, z)$ and $Q_2(u, x, y, z)$ are given by*

$$Q_1(u, x, y, z) = \text{bis}_u \left(\frac{y}{y + u} A\left(2u, y + u, y, xz^2\right) \right), \qquad \text{and}$$

$$Q_2(u, x, y, z) = \text{bis}_u \left(\frac{u}{y + u} A\left(2u, y + u, y, xz^2\right) \right),$$

where $\text{bis}_u\, f(u) := \frac{1}{2}\big(f(u) + f(-u)\big)$ denotes the even bisection of f with respect to u.

Neither $Q_1(u, x, y, z)$ nor $Q_2(u, x, y, z)$ specializes $M(\mathbf{x}, y, z)$, but both series can be obtained indirectly from a system of two equations involving linear combinations of Q_1 and Q_2. The first equation, $Q = Q_1 + Q_2$, is obtained by noting that Q is the disjoint union of Q_1 and Q_2. A second equation is obtained by using two different methods to compute the generating series for a class of maps with at most two vertices having degree different from four.

7.6.1 Pseudo-4-Regular Maps

Definition 7.21 (pseudo-4-regular map)**.** *A map is m-pseudo-4-regular if it has a root vertex of degree m but every other vertex has degree 4. Similarly, a map is (m, n)-pseudo-4-regular if it has a root vertex of degree m, it has a non-root vertex of degree n, and its remaining vertices all have degree 4. Classes of such maps are denoted by $\mathcal{P}_m$ and $\mathcal{P}_{m,n}$, with corresponding generating series denoted by P_m and $P_{m,n}$.*

Remark 7.22. Only $(3, 1)$-pseudo-4-regular maps are required in the present discussion, but 2-, 6-, and $(3, 3)$-pseudo-4-regular maps all arise naturally when considering minors of 4-regular maps.

The series $P_{3,1}(u, x, y, z)$ can be obtained either by considering a bijection between $\mathcal{P}_{3,1}$ and $\mathcal{Q}$, or by specializing $M(\mathbf{x}, y, z; 0)$ and appealing to Corollary 4.20 and duality. Comparing the resulting expressions gives the second equation required for determining $Q_1(u, x, y, z)$ and $Q_2(u, x, y, z)$.

If $\mathfrak{p}$ is a $(3, 1)$-pseudo-4-regular map and the edge e is incident with its degree one vertex, then a 4-regular map is obtained from $\mathfrak{p}$ by identifying its degree one vertex with its root vertex so that e becomes the new root edge. Every 4-regular map can be obtained in this way, and the operation is invertible when attention is restricted to orientable maps. It follows that the function ζ defined by the local action,
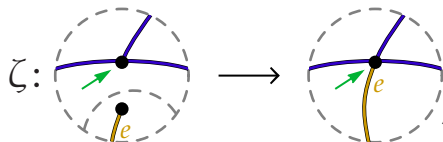
is a bijection from elements of $\mathcal{P}_{3,1}$ with k vertices to elements of $\mathcal{Q}$ with $k-1$ vertices. If the degree one vertex of $\mathfrak{p}$ is incident with its root face, then $\zeta(\mathfrak{p})$ has a face-separating root edge and one more face than $\mathfrak{p}$, so $\zeta(\mathfrak{p})$ and $\mathfrak{p}$ have the same genus. Otherwise, $\zeta(\mathfrak{p})$ has a face-non-separating root edge and one face fewer than $\mathfrak{p}$, so $\zeta(\mathfrak{p})$ has one more handle than $\mathfrak{p}$. It follows that $P_{3,1}$ is given as a linear combination of Q_1 and Q_2 by

$$P_{3,1}(u, x, y, z) = \frac{x}{y} Q_1(u, x, y, z) + \frac{xy}{u^2} Q_2(u, x, y, z). \tag{7.10}$$

Solving this simultaneously with $Q = Q_1 + Q_2$ gives the solution

$$Q_1 = y \frac{u^2 P_{3,1} - xy Q}{x(u^2 - y^2)} \qquad \text{and} \qquad Q_2 = u^2 \frac{x Q - y P_{3,1}}{x(u^2 - y^2)}, \tag{7.11}$$

so it remains only to find an expression for $P_{3,1}(u, x, y, z)$.

By duality and Corollary 4.20, if a rooted map has vertex-degree partition $[1, 3, 4^{k-1}]$, then precisely $\frac{3}{4k}$ of its rootings are on its degree three vertex. Since such a map has $2k$ edges, the operator sending f to $\int \frac{3}{2z} f \, dz$ has the effect of restricting the generating series of arbitrarily rooted maps with vertex degree partitions in the set $\left\{ [1, 3, 4^k] : k \geq 0 \right\}$ to the generating series for $(3, 1)$-pseudo-4-regular maps, and it follows that $P_{3,1}$ is given by

$$P_{3,1}(1, x, y, z) = \int \frac{3}{2z} \left([x_1 x_3] M(\mathbf{x}, y, z; 0) \right) \Big|_{x_i = \delta_{i,4} x} dz. \tag{7.12}$$

Remark 7.23. Using (7.11) and (7.12), a `Maple` program naïvely based on the specialization of (4.9) at $b = 0$ took less than two hours and less than $1\,\text{Gb}$ of memory to compute the low order terms of $P_{3,1}$ necessary to verify that Conjecture 7.15 predicts the correct distribution between Q_1 and Q_2 of the over 8×10^{10} elements of $\mathcal{Q}$ with at most 9 edges.

7.6.2 An Integral Factorization

By using the expectation operator $\langle \cdot \rangle$ to represent $P_{3,1}(1, x, y, z)$, the algebraic content of Conjecture 7.20 can be rephrased as an integral factorization. Since its form is analogous to the factorization given by Jackson, Perry, and Visentin in [JPV96], it may be resolvable using a similar approach. For this purpose, it is sufficient to work with the two-parameter series $P_{3,1}(x, N) := P_{3,1}(1, x, N, 1)$ and $Q_i(x, N) := Q_i(1, x, N, 1)$, since the remaining parameters can be recovered *via* the relationships

$$P_{3,1}(u, x, y, z) = \frac{1}{z^2} P_{3,1}\left(uxz^2, \frac{y}{u} \right), \qquad \text{and} \qquad Q_i(u, x, y, z) = \frac{1}{u^2} Q_i\left(uxz^2, \frac{y}{u} \right).$$

151

Starting from (7.8), $\sqrt{z}^{3}x_3\frac{\langle p_3\rangle_e}{\langle 1\rangle_e}$ enumerates maps with root vertex degree three, and specializing this series at $z = 1$ and $x_2 = x_5 = x_6 = \cdots = 0$ gives that, when N is a positive integer,

$$P_{3,1}(x, N) = x^2 \, [x_1 x_3] \, x_3 \frac{\left\langle p_3 \exp\left(p_1 x_1 + \frac{1}{3}p_3 x_3 + \frac{1}{4}p_4 x_4\right)\right\rangle}{\left\langle \exp\left(p_1 x_1 + \frac{1}{3}p_3 x_3 + \frac{1}{4}p_4 x_4\right)\right\rangle}\Bigg|_{x_4 = x.}$$

Since

$$p_3 \exp\left(p_1 x_1 + \tfrac{1}{3}p_3 x_3 + \tfrac{1}{4}p_4 x_4\right) = p_3(1 + p_1 x_1)\exp\left(\tfrac{1}{4}p_4 x_4\right) + O(x_1^2) + O(x_3),$$

and the odd function $p_3 \exp\left(\frac{1}{4}p_4 x_4\right)$ is annihilated by $\langle \cdot \rangle$, the only non-zero contribution to the numerator is from $x_1 \left\langle p_3 p_1 \exp\left(\frac{1}{4}p_4 x\right)\right\rangle$, so it follows that

$$P_{3,1}(x, N) = x^2 \left\langle p_3 p_1 \exp\left(\tfrac{1}{4}p_4 x\right)\right\rangle\left\langle \exp\left(\tfrac{1}{4}p_4 x\right)\right\rangle^{-1}. \tag{7.13}$$

which, when combined with (7.11), gives the following theorem.

Theorem 7.24. *If N is a positive integer not equal to 1, then*

$$Q_1(x, N) = x\,\frac{N}{1 - N^2}\left\langle (p_3 p_1 - N p_4)\exp\left(\tfrac{1}{4}p_4 x\right)\right\rangle\left\langle \exp\left(\tfrac{1}{4}p_4 x\right)\right\rangle^{-1} \quad and$$

$$Q_2(x, N) = x\,\frac{1}{1 - N^2}\left\langle (p_4 - N p_1 p_3)\exp\left(\tfrac{1}{4}p_4 x\right)\right\rangle\left\langle \exp\left(\tfrac{1}{4}p_4 x\right)\right\rangle^{-1}.$$

Remark 7.25. At $N = 1$, the linear system used to derive Q_1 and Q_2 is degenerate. Substituting (7.13) in (7.11) and multiplying by N gives

$$Q_1(x, N) + N^2 Q_2(x, N) = Nx\left\langle p_3 p_1 \exp\left(\tfrac{1}{4}p_4 x\right)\right\rangle\left\langle \exp\left(\tfrac{1}{4}p_4 x\right)\right\rangle^{-1},$$

but at $N = 1$ this gives only the trivial identity, $Q_1(x, 1) + Q_2(x, 1) = Q(1, x, 1, 1)$, since $p_3(\lambda)p_1(\lambda) = \lambda_1^3 \lambda_1 = \lambda_1^4 = p_4(\lambda)$.

Example 7.26. *The recurrence from (7.7) gives the following expectations of power-sums, with factors of $\langle 1 \rangle$ omitted for clarity:*

$$\langle p_4 \rangle = N + 2N^3,$$
$$\langle p_4^2 \rangle = 61N^2 + 40N^4 + 4N^6,$$
$$\langle p_4^3 \rangle = 1440N + 6517N^3 + 2202N^5 + 228N^7 + 8N^9,$$
$$\langle p_1 p_3 \rangle = 3N^2,$$
$$\langle p_1 p_3 p_4 \rangle = 24N + 75N^3 + 6N^5,$$
$$\langle p_1 p_3 p_4^2 \rangle = 5232N^2 + 4743N^4 + 408N^6 + 12N^8.$$

These values, in turn, are sufficient to derive all terms of $Q_1(x, N)$ and $Q_2(x, N)$ with degree at most 3 in x, by first evaluating $\left\langle \exp\left(\frac{1}{4}p_4x_4\right)\right\rangle$, $x\left\langle p_4\exp\left(\frac{1}{4}p_4x\right)\right\rangle$, and $x\left\langle p_1p_3\exp\left(\frac{1}{4}p_4x\right)\right\rangle$ as follows:

$$\left\langle \exp\left(\tfrac{1}{4}p_4x\right)\right\rangle = \langle 1\rangle + \frac{\langle p_4\rangle}{4}x + \frac{\langle p_4^2\rangle}{2\cdot 4^2}x^2 + \frac{\langle p_4^3\rangle}{6\cdot 4^3}x^3 + O(x^4)$$

$$= 1 + \frac{N+2N^3}{4}x + \frac{61N^2 + 40N^4 + 4N^6}{32}x^2 + O(x^3),$$

$$x\left\langle p_4\exp\left(\tfrac{1}{4}p_4x\right)\right\rangle = \langle p_4\rangle x + \frac{\langle p_4^2\rangle}{4}x^2 + \frac{\langle p_4^3\rangle}{2\cdot 4^2}x^3 + O(x^4)$$

$$= \left(N+2N^3\right)x + \frac{61N^2 + 40N^4 + 4N^6}{4}x^2$$

$$+ \frac{1440N + 6517N^3 + 2202N^5 + 228N^7 + 8N^9}{32}x^3 + O(x^4),$$

$$x\left\langle p_1p_3\exp\left(\tfrac{1}{4}p_4x\right)\right\rangle = \langle p_1p_3\rangle x + \frac{\langle p_1p_3p_4\rangle}{4}x^2 + \frac{\langle p_1p_3p_4^2\rangle}{2\cdot 4^2}x^3 + O(x^4)$$

$$= 3N^2x + \frac{24N + 75N^3 + 6N^5}{4}x^2$$

$$+ \frac{5232N^2 + 4743N^4 + 408N^6 + 12N^8}{32}x^3 + O(x^4).$$

Combining these according to (7.11), gives after significant cancellation,

$$Q_1(x, N) = \frac{Nx\left\langle p_1p_3\exp\left(\tfrac{1}{4}p_4x\right)\right\rangle - N^2x\left\langle p_4\exp\left(\tfrac{1}{4}p_4x\right)\right\rangle}{(1-N^2)\left\langle \exp\left(\tfrac{1}{4}p_4x\right)\right\rangle}$$

$$= 2N^3x + \left(6N^2 + 9N^4\right)x^2 + \left(117N^3 + 54N^5\right)x^3 + O(x^4), \quad \text{and}$$

$$Q_2(x, N) = \frac{x\left\langle p_4\exp\left(\tfrac{1}{4}p_4x\right)\right\rangle - x\left\langle Np_1p_3\exp\left(\tfrac{1}{4}p_4x\right)\right\rangle}{(1-N^2)\left\langle \exp\left(\tfrac{1}{4}p_4x\right)\right\rangle}$$

$$= Nx + 9N^2x^2 + \left(45N + 81N^3\right)x^3 + O(x^4).$$

The term $81N^3x^3$ in $Q_2(x, N)$, for example, corresponds to the monomial $81u^2x^3y^3z^6$ in $Q_2(u, x, y, z)$, and enumerates the three-vertex elements of $\mathbf{Q}_2$ on the torus: these 81 maps are given in Figure 7.14.

Remark 7.27. The program in Section B.6 of Appendix B uses this approach for computing Q_1, and was used to verify the predictions of Conjecture 7.20 for all rooted orientable 4-regular maps with at most 20 vertices.
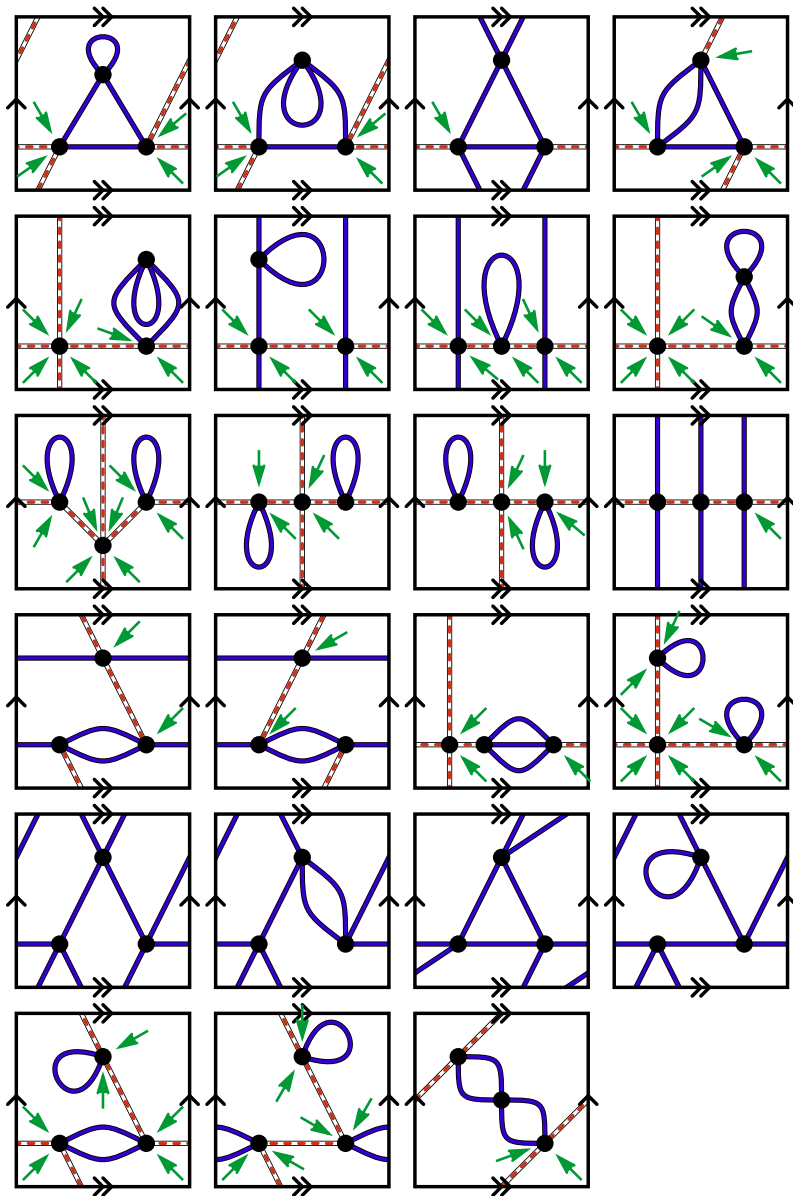
Figure 7.14: In this listing of the 4-regular maps with 3 vertices on the torus, line style distinguishes between face-separating and face-non-separating edges, and root arrows indicate the 81 elements of Q_2 on the torus that have three vertices. Rootings in Q_1 are not marked.

With some algebraic manipulation, it is now possible to use Theorem 7.24 to rephrase Conjecture 7.20 in a form similar to (7.9), and thus potentially allow a modification of the techniques from [JV90a] to resolve the question of the existence of an appropriate bijection. To this end, it is sufficient to prove Conjecture 7.20 for $u = z = 1$, in which case only the evaluations

$$A(2, y \pm 1, y, xz^2) = 4A\left(1, \tfrac{1}{2}(y \pm 1), \tfrac{1}{2}y, 2xz^2\right),$$

need to be considered. Further restricting to the case that $\tfrac{1}{2}y = N$ is a positive integer permits working exclusively with the integral representation

$$A(1, x, N, z) = \sum_{k \geq 1} x \sqrt{z}^k \frac{\left\langle p_k \exp\left(\sum_i \tfrac{1}{i} p_i x \sqrt{z}^i\right)\right\rangle}{\left\langle \exp\left(\sum_i \tfrac{1}{i} p_i x \sqrt{z}^i\right)\right\rangle},$$

of A. It is convenient to introduce $S(\mu)$ and $T(\mu)$ defined by

$$S(\mu) := \sum_{k \geq 1} \sqrt{2x}^k \left\langle p_k \prod_{i=1}^N \left(1 - \lambda_i \sqrt{2x}\right)^{-(N+\mu)}\right\rangle, \qquad \text{and}$$

$$T(\mu) := \left\langle \prod_{i=1}^N \left(1 - \lambda_i \sqrt{2x}\right)^{-(N+\mu)}\right\rangle,$$

so that $A(1, N + \mu, N, 2x) = (N + \mu) S(\mu)T(\mu)^{-1}$, and (7.9) can be rewritten as

$$c^{-1}\left\langle \exp\left(\tfrac{1}{4}p_4 x\right)\right\rangle_{(2N)} = T\left(-\tfrac{1}{2}\right)T\left(\tfrac{1}{2}\right), \tag{7.14}$$

with $c = c(N) := \langle 1\rangle_{(2N)} \langle 1\rangle_{(N)}^{-2}$ defined as before. Similarly (7.1) can be written as

$$x \frac{\left\langle p_4 \exp\left(\tfrac{1}{4}p_4 x\right)\right\rangle_{(2N)}}{\left\langle \exp\left(\tfrac{1}{4}p_4 x\right)\right\rangle_{(2N)}} = (2N + 1)\frac{S\left(\tfrac{1}{2}\right)}{T\left(\tfrac{1}{2}\right)} + (2N - 1)\frac{S\left(-\tfrac{1}{2}\right)}{T\left(-\tfrac{1}{2}\right)},$$

which when multiplied by (7.14) gives

$$c^{-1}x\left\langle p_4 \exp\left(\tfrac{1}{4}p_4 x\right)\right\rangle_{(2N)} = (2N + 1)S\left(\tfrac{1}{2}\right)T\left(-\tfrac{1}{2}\right) + (2N - 1)S\left(-\tfrac{1}{2}\right)T\left(\tfrac{1}{2}\right). \tag{7.15}$$

Using this notation, Conjecture 7.20 predicts that

$$Q_1(x, 2N) = \left(\text{bis}_u \frac{2N}{2N + u} A(2u, 2N + u, 2N, x)\right)\bigg|_{u=1}$$

$$= 2\left(\frac{2N}{2N + 1}A\left(1, N + \tfrac{1}{2}, N, 2x\right) + \frac{2N}{2N - 1}A\left(1, N - \tfrac{1}{2}, N, 2x\right)\right)$$

$$= 2N\left(S\left(\tfrac{1}{2}\right)T^{-1}\left(\tfrac{1}{2}\right) + S\left(-\tfrac{1}{2}\right)T^{-1}\left(-\tfrac{1}{2}\right)\right),$$

and also that

$$Q_2(x, 2N) = \left(\text{bis}_u \, \frac{u}{2N + u} A(2u, 2N + u, 2N, x)\right)\bigg|_{u=1}$$

$$= 2\left(\frac{1}{2N + 1} A\left(1, N + \tfrac{1}{2}, N, 2x\right) - \frac{1}{2N - 1} A\left(1, N - \tfrac{1}{2}, N, 2x\right)\right)$$

$$= S\left(\tfrac{1}{2}\right) T^{-1}\left(\tfrac{1}{2}\right) - S\left(-\tfrac{1}{2}\right) T^{-1}\left(-\tfrac{1}{2}\right).$$

Substituting the value from Theorem 7.24 into this conjectured expression then predicts, after multiplying both sides of the equation by (7.14), that

$$c^{-1}x \left\langle (p_4 - 2Np_1p_3) \exp\left(\tfrac{1}{4}p_4 x\right)\right\rangle_{(2N)} = \left(1 - 4N^2\right)\left(S\left(\tfrac{1}{2}\right) T\left(-\tfrac{1}{2}\right) - S\left(-\tfrac{1}{2}\right) T\left(\tfrac{1}{2}\right)\right),$$

or equivalently, by subtracting (7.15) and then dividing by $-2N$, that

$$c^{-1}x \left\langle p_1p_3 \exp\left(\tfrac{1}{4}p_4 x\right)\right\rangle_{(2N)} = (2N + 1)S\left(\tfrac{1}{2}\right) T\left(-\tfrac{1}{2}\right) - (2N - 1)S\left(-\tfrac{1}{2}\right) T\left(\tfrac{1}{2}\right).$$

Subtracting (7.15) again, and noting that $p_1p_3 = p_4 + m_{[1,3]}$, shows that the required bijection exists if and only if the following factorization holds:

$$c^{-1}x \left\langle m_{[1,3]} \exp\left(\tfrac{1}{4}p_4 x\right)\right\rangle_{(2N)} = (2 - 4N)S\left(-\tfrac{1}{2}\right) T\left(\tfrac{1}{2}\right).$$

This equivalence has a purely analytic statement given in the following theorem.

Theorem 7.28. *With $V(\lambda)$ denoting the Vandermonde determinant, the factorization*

$$x\left(\int_{\mathbb{R}^{2N}} V(\lambda)^2 \lambda_1 \lambda_3^2 e^{\frac{1}{4}p_4(\lambda)x - \frac{1}{2}p_2(\lambda)} \, d\lambda\right)\left(\int_{\mathbb{R}^N} V(\lambda)^2 e^{-\frac{1}{2}p_2(\lambda)} \, d\lambda\right)^2$$

$$= -\left(\int_{\mathbb{R}^N} V(\lambda)^2 \prod_{i=1}^{N}\left(1 - \lambda_i \sqrt{2x}\right)^{-N-\frac{1}{2}} e^{-\frac{1}{2}p_2(\lambda)} \, d\lambda\right)\left(\int_{\mathbb{R}^{2N}} V(\lambda)^2 e^{-\frac{1}{2}p_2(\lambda)} \, d\lambda\right)$$

$$\times \left(\int_{\mathbb{R}^N} V(\lambda)^2 \frac{\lambda_1 \sqrt{2x}}{1 - \lambda_1 \sqrt{2x}} \prod_{i=1}^{N}\left(1 - \lambda_i \sqrt{2x}\right)^{-N+\frac{1}{2}} e^{-\frac{1}{2}p_2(\lambda)} \, d\lambda\right), \quad (7.16)$$

holds for all positive integers N, if and only if Conjecture 7.20 is true, or equivalently, if and only if there is a bijection, not necessarily natural, between $\mathcal{A}_{g,n}$ and $\mathcal{Q}_{g,n}$ such that the image of a map has a face-separating root edge precisely when that map has an undecorated root vertex.

Remark 7.29. From their combinatorial interpretations, when evaluated at any positive integer N, the series appearing in (7.16) are elements of $\mathbb{R}[\![x]\!]$, and by Remark 7.27, any term that differs between the two products must have degree greater than 20 in x.

7.6.3 Characterizing the Refinement Using $\mathcal{P}_{3,1}$

Conjecture 7.20 also asserts the existence of functional relationships involving $P_{3,1}(1, x, y, 1)$, and thus offers the possibility that there is a combinatorial proof of (7.16) that avoids reference to $\mathcal{A}$. Such a proof would not require a representation for decorated handles.

With the bisections expanded explicitly, and the resulting expressions evaluated at $u = z = 1$, Conjecture 7.20 predicts two other identities that are equivalent to each other as a consequence of (7.1):

$$2\,Q_1(x, y) = \frac{y}{y+1}A(2, y+1, y, x) + \frac{y}{y-1}A(2, y-1, y, x), \qquad \text{and}$$

$$2\,Q_2(x, y) = \frac{1}{y+1}A(2, y+1, y, x) - \frac{1}{y-1}A(2, y-1, y, x).$$

Solving this system for $A(2, y+1, y, x)$ and $A(2, y-1, y, x)$ in terms of $Q_1(x, y)$ and $Q_2(x, y)$, and then applying (7.10), the conjecture holds if and only if

$$A(2, y+1, y, x) = \frac{y+1}{y}\big(Q_1(x, y) + yQ_2(x, y)\big)$$

$$= Q(1, x, y, 1) + \tfrac{1}{x}P_{3,1}(1, x, y, 1), \qquad (7.17)$$

or equivalently, if and only if

$$A(2, y-1, y, x) = Q(1, x, y, 1) - \tfrac{1}{x}P_{3,1}(1, x, y, 1). \qquad (7.18)$$

If $\overline{\mathcal{A}}$ denotes the class of rooted maps with each handle decorated in one of four ways and *any* number (even or odd) of decorated vertices, then (7.17) suggests that φ can be extended to a bisection from $\overline{\mathcal{A}}$ to $Q \cup \mathcal{P}_{3,1}$. In this extended framework images of maps with an odd number of decorated vertices are precisely the elements of $\mathcal{P}_{3,1}$, and it might be possible to describe the action of π_3 by giving an appropriate function from $\mathcal{P}_{3,1} \times \mathcal{P}_{3,1}$ to Q.

The combination of (7.17) and (7.18) also predicts a functional relationship between $P_{3,1}$ and Q. Symmetry between x and y in $A(u, x, y, z)$ gives

$$Q(1, x, y, 1) + \tfrac{1}{x}P_{3,1}(1, x, y, 1) = A(2, y+1, y, x)$$

$$= A(2, y, y+1, x)$$

$$= A(2, (y+1)-1, y+1, x)$$

$$= Q(1, x, y+1, 1) - \tfrac{1}{x}P_{3,1}(1, x, y+1, 1),$$

and after a rearrangement of terms, this is equivalent to

$$Q(1, x, y+1, 1) - Q(1, x, y, 1) = \tfrac{1}{x}P_{3,1}(1, x, y+1, 1) + \tfrac{1}{x}P_{3,1}(1, x, y, 1). \qquad (7.19)$$

This relationship suggests the existence of a bijection between two multisets of

face-decorated maps: the first multiset consists of elements of Q with n edges and k undecorated faces such that at least one face is decorated, and the second multiset consists of elements of $\mathcal{P}_{3,1}$ with n edges and k undecorated faces such that maps with no decorated faces each appear twice.

In fact, (7.19) holds if and only if Conjecture 7.20 is true. The equivalence is verified by considering the series $P'(x, y) := xA(2, y + 1, y, x) - xQ(1, x, y, 1)$. It follows from (7.1) that P' is also given by $P'(x, y) = xQ(1, x, y, 1) - xA(2, y-1, y, x)$, and so the same reasoning as above gives

$$Q(1, x, y + 1, 1) - Q(1, x, y, 1) = \tfrac{1}{x}P'(x, y + 1) + \tfrac{1}{x}P'(x, y).$$

Thus if (7.19) holds, then

$$P'(x, y + 1) + P'(x, y) = P_{3,1}(x, y + 1) + P_{3,1}(x, y),$$

which implies that $P'(x, y)$ and $P_{3,1}(x, y)$ are equal as elements of $\mathbb{Q}[y][\![x]\!]$.

The equivalence provides two additional approaches that might be used to prove Conjecture 7.20. A purely analytic approach could involve verifying (7.19) by showing that

$$\langle (p_4 + p_1 p_3) e^{p_4 x} \rangle_{(N)} \langle e^{p_4 x} \rangle_{(N+1)} = - \langle m_{[1,3]} e^{p_4 x} \rangle_{(N+1)} \langle e^{p_4 x} \rangle_{(N)}, \tag{7.20}$$

for every positive integer N. Similarly, a purely combinatorial approach could involve exhibiting an appropriate explicit bijection between face-decorated elements of Q and $\mathcal{P}_{3,1}$.

7.7 Possible Restricted Actions of φ

Although the action of φ remains known only on the rooted map given in Figure 7.1, it is possible to define actions that are consistent with Conjecture 7.15 on restricted subsets of $\mathcal{A}$. The aim is to describe consistent actions on enough restricted sets that additional actions can be deduced by the process of elimination. Care must be taken when extrapolating from such examples, since as seen in Section 7.5, symmetries that are respected on restricted classes need not be preserved by φ in general.

7.7.1 Maps With Degree One Root Vertices

One of the goals introduced in Section 7.2, the goal of describing the action of φ on maps rooted on cut-edges, would be accomplished by giving natural descriptions to the products π_1 and π_3 that were defined implicitly in Section 7.4.2. The Refined q-Conjecture was obtained in Section 7.4.3 by assuming that $\underline{\pi}_3$ and π_3 agree except where this is precluded by their behaviours with respect to genus additivity: their actions cannot coincide when acting on pairs of 4-regular maps both of which are images of maps with decorated root vertices. Extrapolating
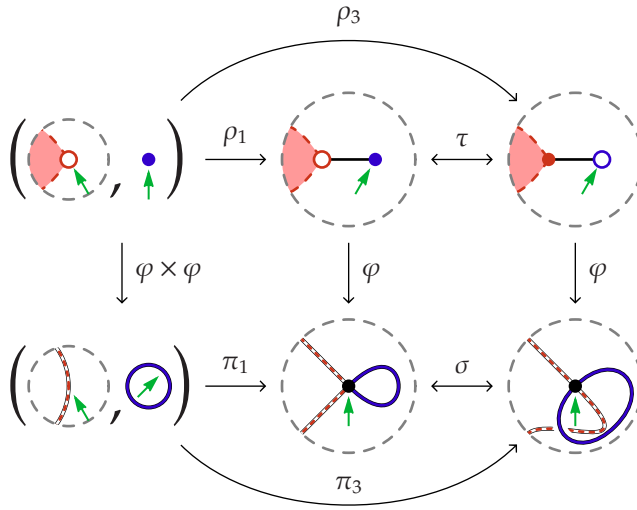
Figure 7.15: The assumption that $\underline{\pi}_3$ and π_3 coincide, except where precluded by genus, gives a possible action of φ on maps with degree one root vertices. Decorated vertices are indicated by hollow circles. The action of σ on $\mathcal{Q}$ induced by the action of τ on $\mathcal{A}$ is identical when an even number of decorated vertices are incident with the root edge.

the presumed relationship between $\underline{\pi}_3$ and π_3 gives a candidate action for φ, except when the root edge is an odd cut that separates two undecorated vertices. An edge incident with a degree one vertex induces an odd cut if and only if that vertex is decorated. So when considering only maps with degree one root vertices, no inconsistency is incurred by assuming that $\underline{\pi}_1 = \pi_1$ and $\underline{\pi}_3 = \pi_3$.

Under these assumptions, any action of φ consistent with Conjecture 7.15 on all rooted maps with at most n edges can be extended to an action consistent with Conjecture 7.15 on all maps with $n + 1$ edges that are rooted on degree one vertices: if the root vertex is undecorated, then the root edge induces an even cut, and φ can be defined in terms of π_1, otherwise, the root edge induces an odd cut, and φ can be defined in terms of π_3. More explicitly, if $\mathfrak{m}$ is rooted on a degree one vertex v, and $\xi(\mathfrak{m}) = (\mathfrak{m}', \nearrow)$, then the recursive definition,

$$
\varphi(\mathfrak{m}) := \begin{cases} \pi_1\left(\varphi(\mathfrak{m}'), \textcircled{\nearrow}\right) & \text{if } v \text{ is undecorated,} \\ \pi_3\left(\varphi(\mathfrak{m}'), \textcircled{\nearrow}\right) & \text{if } v \text{ is decorated,} \end{cases}
$$

is consistent with Conjecture 7.15. In particular, there is at least one bijection φ between $\mathcal{A}$ and $\mathcal{Q}$ for which the diagram in Figure 7.15 commutes, but it is not known if any such bijection is 'natural' on all of $\mathcal{A}$.

(a) The definition of τ and σ **(b)** The predicted action of σ extends to a larger set
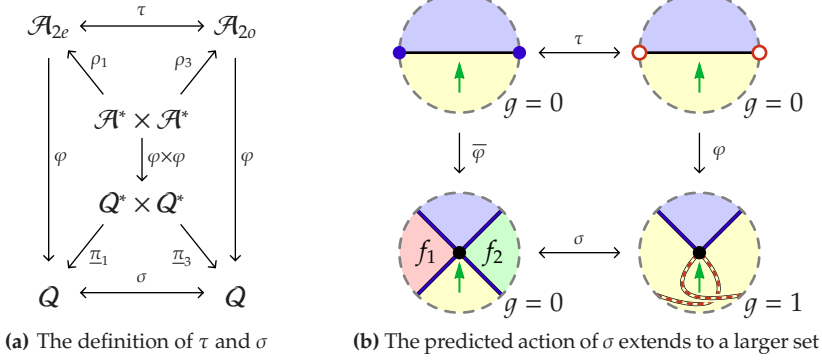
Figure 7.16: The action of $\sigma := \varphi \circ \tau \circ \varphi^{-1}$ on a restricted subset of Q is predicted in Figure 7.15 by assuming that $\underline{\pi}_1 = \pi_1$ and $\underline{\pi}_3 = \pi_3$. This action extends consistently to the images of planar maps with precisely two decorated vertices both of which are incident with the root edge.

7.7.2   Planar Maps with Two Decorated Vertices

The bijection φ sends two classes of maps to images on the torus: rooted maps on the torus with no decorated vertices, and rooted planar maps with two decorated vertices. Conjecture 7.15 predicts further that 4-regular rooted maps on the torus with face-non-separating root edges are precisely the images of planar maps with two decorated vertices, one of which is the root vertex. The action on Q induced by the action of τ on $\mathcal{A}$ suggests the behaviour of this bijection when both decorated vertices are incident with the root face.

Two involutions, τ acting on $\mathcal{A}_2$, and σ acting on a subset of Q, are defined in terms of ρ_1 and ρ_3: see Figure 7.16a. As mentioned in Section 7.5, the action of τ extends to all of $\mathcal{A}$: if the root edge of $\mathfrak{m}$ is incident with two distinct vertices, then τ acts by changing the decoration of each of these two vertices, otherwise τ acts as the identity. Similarly, the action of σ predicted in Figure 7.15 can be extended to all of Q by
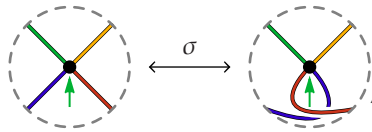
so that $\sigma \circ \overline{\varphi} \circ \tau$ gives a candidate action for φ on planar maps with two decorated vertices, both of which are incident with the root edge: see Figure 7.16b. If $\mathfrak{m}$ is such a map, then $\tau(\mathfrak{m})$ has no decorated vertices and $\overline{\varphi} \circ \tau(\mathfrak{m})$ is a planar 4-regular map with distinct faces clockwise and counterclockwise of the root. Applying σ to the result decreases the number of faces by two, increases the genus by one, and gives a map on the torus.
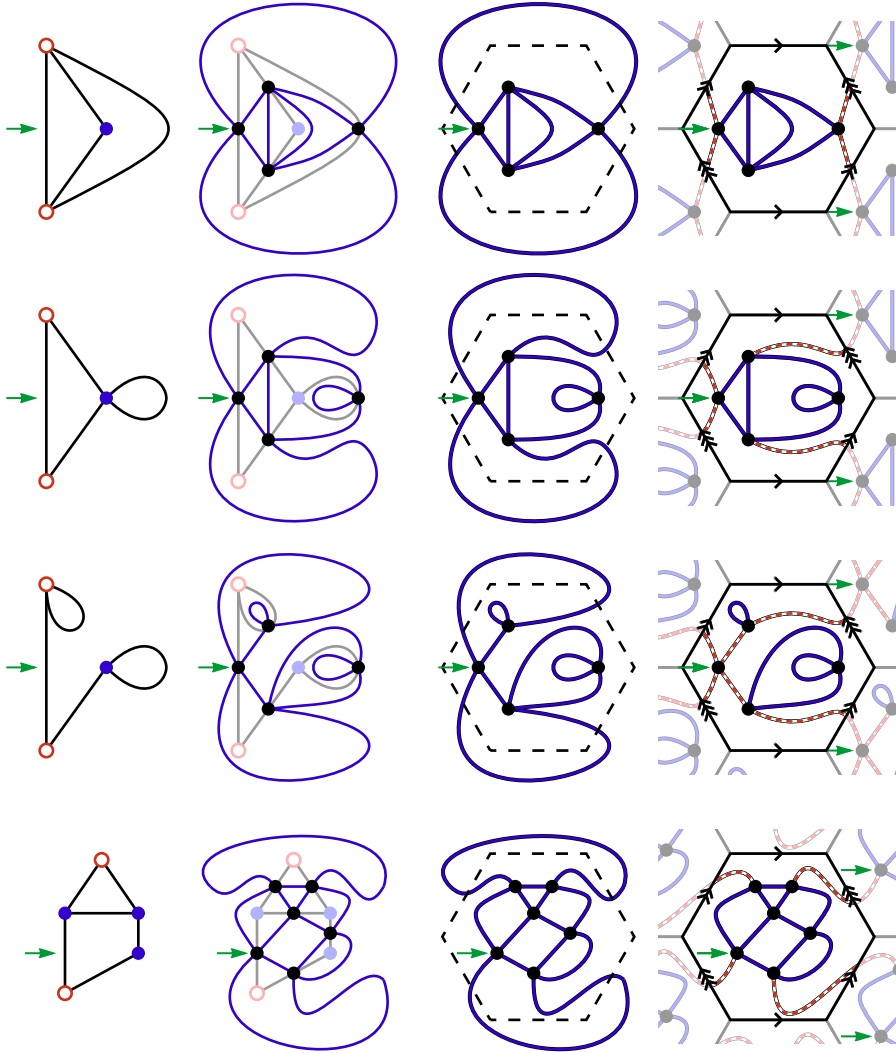
Figure 7.17: The action of $\sigma \circ \overline{\varphi} \circ \tau$ is related to the representation of the torus as a tiled hexagon. It extends from maps with both decorated vertices incident with the root edge (the first three rows) to a more general class of maps (the fourth row). The first column gives planar maps with two decorated vertices. These maps are superimposed with their images under $\overline{\varphi}$ in the second column. In the third column, hexagons are drawn intersecting edges determined by the decorated vertices. Finally, in the fourth column, the interiors of these hexagons represent tori. A partial tiling is used to emphasize face structure.

The action just described is closely related to the representation of the torus as a tiled polygon: see the first three rows of Figure 7.17. It extends, with modification, to rooted maps in which the two decorated vertices are separated by a path along the boundary of the root face that contains the root arrow and along which only undecorated vertices appear: see the fourth row of Figure 7.17.

7.7.3 Maps With Handles as Root Edges

There are only six 4-regular maps on the torus with two vertices and face-non-separating root edges. Of these, two are images of planar maps, and four are images of the rooted map on the torus with two edges. Sections 7.7.1 and 7.7.2 predict the images of the planar maps: see Figures 7.18a and 7.18b. So assuming there is a bijection between $\mathcal{A}$ and $\mathcal{Q}$ that is consistent with these actions, this gives the four images of decorated copies of the rooted map with two edges on the torus: see Figure 7.18c.

(a) An image determined by the action of φ given in Section 7.7.1

(b) An image determined by the action of φ given in Section 7.7.2

(c) The remaining four 4-regular maps on the torus with two vertices and face-non-separating edges are all images of the rooted map with two edges on the torus.
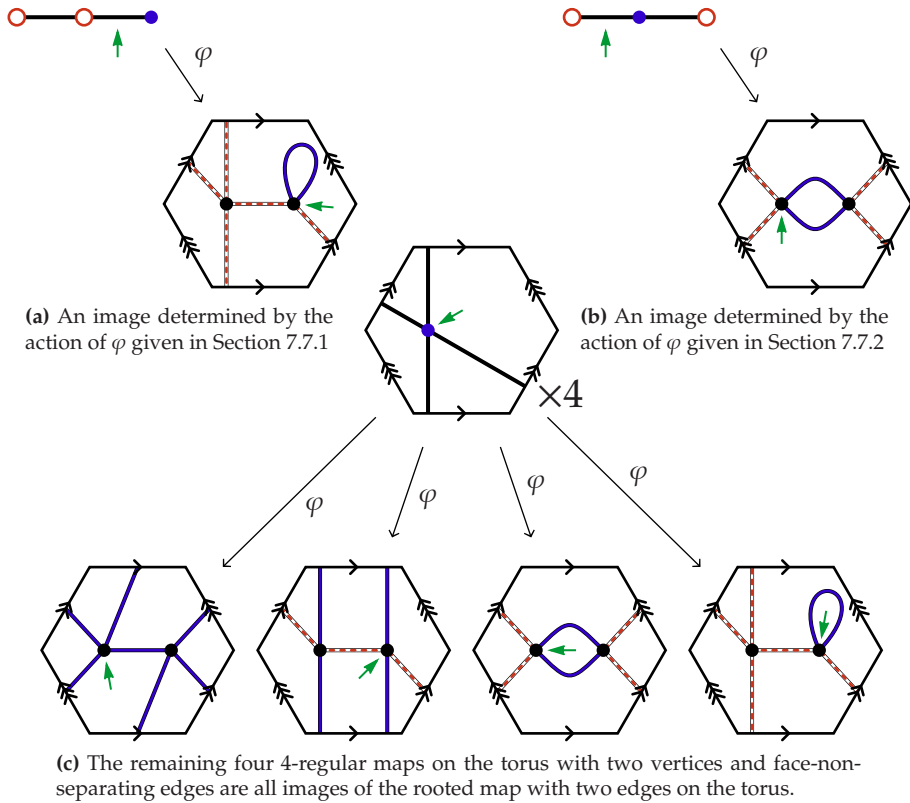
Figure 7.18: Rooted maps with undecorated root vertices and images on the torus

162
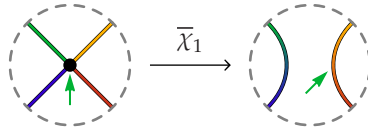
Figure 7.19: A local action on Q induced with respect to the medial construction by root-edge deletion on undecorated elements of $\mathcal{A}$ that are not rooted on cut-edges
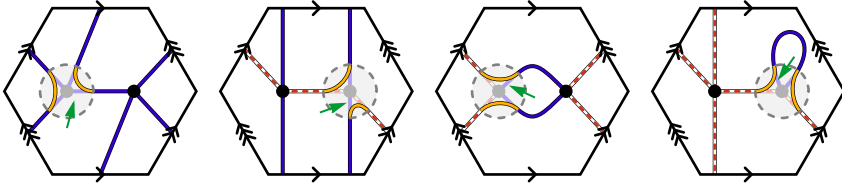
Figure 7.20: The results of applying $\overline{\chi}_1$ to the 4-regular maps in Figure 7.18c

A closer examination of these four images might reveal how the decoration of handles interacts with φ. With respect to the medial construction, Figure 7.19 gives the action $\overline{\chi}_1$ induced on Q by root edge deletion in undecorated elements of $\mathcal{A}$ that are not rooted on cut edges. Applying this action to the 4-regular maps in Figure 7.18c gives the maps in Figure 7.20, but no pattern is immediately apparent.

7.8 Summary

This Chapter examined possible structure of φ, a conjectured bijection between two classes of maps. Emphasis followed attempts to find the actions induced on one class by natural actions on the other. The medial construction, a possible restriction of φ, suggests a relationship between cut-edges in $\mathcal{A}$ and cut-vertices in Q, and an examination of structural similarities between products associated with these cuts led to the main result of the Chapter, Conjecture 7.15, a refinement of the original conjecture.

Besides predicting a chirality that may be interesting in the physical setting from which the problem originated, the Refined q-Conjecture suggests additional combinatorial relationships involving $(3, 1)$-pseudo-4-regular maps, a new class of maps introduced to permit an algebraic formulation of the conjecture. This reformulation recasts the conjecture in an analytic setting in which the approach developed by Jackson and Visentin might apply, and permits numerical testing.

Numerical evidence justifies using the refinement as a basis for conjecturing the actions of φ on two restricted classes of maps. Together, these predicted actions are sufficient to give the four images of the smallest non-planar orientable map.

Chapter 8

Future Work

8.1 On η

Chapter 4 showed that any invariant of rooted maps that satisfies Definition 4.1 is a marginal b-invariant. Algebraic properties of the series $M(x, \mathbf{y}, z; b)$ guarantee that these invariants exhibit combinatorial properties for which there are currently no combinatorial proofs. Establishing such proofs would help to resolve whether any invariant in the family is a b-invariant. Future work on these invariants should fall into two categories:

1. developing and interpreting the properties of the invariants, and
2. determining if any elements of the family are b-invariants.

The Root-Face Degree Distribution Property

Corollary 4.20, the root-face degree distribution property, states that among all rooted maps with a given number of vertices and a given face-degree partition, the degree of the root face is independent of η, for every invariant η that satisfies Definition 4.1. A combinatorial proof of this property could provide an operation analogous to re-rooting, and such an operation could simplify structural analyses, like those presented in Chapter 6.

Symmetry Between x and y

Similarly, if η is any marginal b-invariant, then the algebraic symmetry between $\mathbf{x}$ and $\mathbf{y}$ in $M(\mathbf{x}, \mathbf{y}, z; b)$ guarantees the existence of an η-preserving bijection between $\mathcal{M}_{v,f}$ and $\mathcal{M}_{f,v}$ for every pair of positive integers v and f, where $\mathcal{M}_{v,f}$ denotes the class of rooted maps with v vertices and f faces. An explicit description of such a bijection will help to answer the question of whether any such bijection additionally interchanges vertex- and face-degree partitions, as

is necessary for η to be a b-invariant. A less ambitious goal would be to establish that η is a b-invariant for one-faced maps.

The Basis B_g

Additional attention should also be directed toward determining which invariants satisfying Definition 4.1 are compatible with Theorem 5.18. That is, for which invariants η is the polynomial $\sum_{m \in \mathcal{M}_{\nu,\varphi}} b^{\eta(m)}$ an element of $\text{span}_{\mathbb{Z}}(B_g)$ for $g = 2 + n - \ell(\varphi) - \ell(\nu)$, for every $\nu, \varphi \vdash 2n$? For any such invariant, there is a vertex- and face-degree partition preserving bijection between rooted maps on the torus and rooted maps on the Klein bottle for which η takes the value one. The restricted bijections described in Chapter 6 may be a useful starting point.

A Geometric Interpretation for η

As noted in Remark 4.18, marginal b-invariants provide the combinatorial foundation that Goulden, Harer, and Jackson, in [GHJ01], conjectured could be used to explore the geometric significance of the Jack parameter in terms of an appropriately defined moduli space. As a consequence, the invariants satisfying Definition 4.1 should be examined in this geometric setting, whether or not any is a b-invariant.

8.2 On Unhandled Maps

With respect to number of vertices, face-degree partition, and number of edges, unhandled maps are enumerated by $M(-x, -\mathbf{y}, -z; -1)$. Future work should involve determining whether Jack symmetric functions are sufficiently understood in the $\alpha = 0$ limit to establish Conjecture 5.28, that $M(-\mathbf{x}, -\mathbf{y}, -z; -1)$ is the generating series for unhandled maps with respect to both vertex- and face-degree partitions. Unhandled maps might play a rôle in establishing whether or not the degree bound predicted by Corollary 5.22 is tight.

8.3 On the Invariant of Brown and Jackson

The invariant described by Brown and Jackson in [BJ07] does not appear to satisfy Definition 4.1, but it may be a marginal b-invariant. It should be possible to verify this, at least for monopoles, by considering an invariant with twisting of handles defined relative to an appropriate spanning tree, as described in Section 6.4.2. Such an invariant is not in the class to which Theorems 6.22 and 6.25 apply, but studying it could elucidate the relationship between the Jack parameter and minors.

8.4 On Map Polynomials

The question of the existence of a b-invariant, remains unresolved. Evidence suggests that invariants satisfying Definition 4.1 are appropriate candidates, and Chapter 6 introduced a framework for verifying this for rooted maps with at most six edges. In addition to verifying combinatorial properties of η, this framework requires establishing additional algebraic properties of map polynomials.

It remains to verify that the rational function $c_{\nu,\varphi,[2^n]}(b)$ is a polynomial for every $\nu, \varphi \vdash 2n$. One approach, sufficient by Corollary 5.22, would be to verify that all terms of $M(\mathbf{x}, \mathbf{y}, z; b)$ of degree less than n in z are annihilated by the differential operator $\frac{\partial^n}{\partial b^n}$. If polynomiality can be established, the conjectured combinatorial interpretation suggests that the functions should be studied with respect to the B_g basis. This leads to two additional questions for future study:

1. Are the coefficients of $c_{\nu,\varphi,[2^n]}(b)$ non-negative with respect to B_g, and

2. Can the study be given an algebraic foundation in the form of a two variable refinement of Jack symmetric functions, as discussed in Section 6.4.1?

8.5 On Jack Symmetric Functions

Theorem 4.16 establishes a concrete link between the Jack parameter and the combinatorics of rooted maps, but the link is *via* the integration formula from Theorem 3.18, and thus indirect. Analytic characterizations of Jack symmetric functions might be the key to finding a direct proof of Theorem 4.16. In particular, Jack symmetric functions in the parameter α are orthogonal with respect to the inner product $\langle \cdot, \cdot \rangle'_\alpha$ defined by

$$\langle u, v \rangle'_\alpha := \int_{T^n} |V(\mathbf{t})|^{\frac{2}{\alpha}} u(\mathbf{t}) \overline{v(\mathbf{t})} \, d\mathbf{t},$$

where $\overline{v(\mathbf{t})}$ denotes the complex conjugate of $v(\mathbf{t})$, and integration is over the n-dimensional torus

$$T^n := \left\{ \mathbf{t} = (t_1, t_2, \ldots, t_n) \in \mathbb{C}^n : |t_i| = 1 \text{ for } 1 \le i \le n \right\}.$$

It might be interesting to explore the relationship between this orthogonality and (4.2), the partial differential equation used to establish Theorem 4.16.

8.6 On the Hypermap b-Conjecture

Algebraically, the most symmetric form of the b-Conjecture is Conjecture 3.10, the Hypermap b-Conjecture. If hypermaps are identified with bipartite maps,

the dual of the standard identification, then every invariant η that satisfies Definition 4.1 induces an invariant of hypermaps. In [GJ96a], Goulden and Jackson predicted from numerical evidence that

$$[b^{n-\ell(v)}]c_{[n],v,[n]}(b) = |C_v|,$$

and asked for a convenient class of non-orientable hypermaps with this cardinality. Unhandled hypermaps appear to be such a class, and this suggests that the induced invariants are b-invariants for hypermaps.

If the two classes of vertices in a bipartite map are coloured red and blue, with the root vertex receiving the colour red and η is any invariant satisfying Definition 4.1, then the generating series for rooted hypermaps,

$$H(x, \mathbf{y}, z, \mathbf{r}; b) := \sum_{\mathfrak{h}\in\mathcal{H}} x^{\#\text{red vertices in }\mathfrak{h}}\mathbf{y}^{\varphi(\mathfrak{h})\backslash r(\mathfrak{h})}z^{\#\text{blue vertices in }\mathfrak{h}}r_{r(\mathfrak{h})}b^{\eta(\mathfrak{h})},$$

where $\varphi(\mathfrak{h})$ is the partition with parts equal to half the lengths of the face boundaries of $\mathfrak{h}$, satisfies the equation

$$
\begin{aligned}
H(x, \mathbf{y}, z, \mathbf{r}; b) = r_0 x &+ \sum_{i\geq 1}\sum_{j=1}^{i+1} r_j y_{i-j+1}\frac{\partial}{\partial r_i}H(x, \mathbf{y}, z, \mathbf{r}; b) + b\sum_{i\geq 0} i r_{i+1}\frac{\partial}{\partial r_i}H(x, \mathbf{y}, z, \mathbf{r}; b) \\
&+ \sum_{i,j\geq 0} r_{i+j+1}\left(\frac{\partial}{\partial r_i}H(x, \mathbf{y}, z, \mathbf{r}; b)\right)\left(\frac{\partial}{\partial r_j}H(z, \mathbf{y}, x, \mathbf{r}; b)\right) \qquad (8.1) \\
&+ (1+b)\sum_{i,j\geq 0} j r_{i+j+1}\frac{\partial^2}{\partial r_i \partial y_j}H(x, \mathbf{y}, z, \mathbf{r}; b)
\end{aligned}
$$

Verifying that an appropriately refined version of the algebraically defined hypermap series satisfies (8.1) would establish a root-face degree distribution property for hypermaps and provide additional evidence for Conjecture 3.27. This verification might involve using the identity

$$J_\lambda(\mathbf{x}; \alpha)|_{p_i(\mathbf{x})=N} = J_\lambda(1^N; \alpha) = \prod_{(i,j)\in\lambda}\left(N - (i-1) + \alpha(j-1)\right),$$

established by Stanley in [Sta89, Thm. 5.4] when N is a positive integer, and then appealing to the fact that Jack symmetric functions are eigenfunctions of the Laplace-Beltrami operator

$$\Box^\alpha := \frac{1}{2}\left(\sum_{k\geq 1}(\alpha-1)(k-1)p_k k\frac{\partial}{\partial p_k}\right) + \frac{1}{2}\left(\sum_{i,j\geq 1} p_i p_j(i+j)\frac{\partial}{\partial p_{i+j}} + \alpha p_{i+j} ij\frac{\partial^2}{\partial p_i \partial p_j}\right),$$

as described in [Sta89, Thm. 3.1]. A similar approach was suggested, in relation to the map series, by Brown and Jackson in [BJ07].

8.7 On the q-Conjecture

Chapter 7 suggested a way to identify the bijection predicted by the q-Conjecture: identify the actions on Q induced by root-edge deletion in $\mathcal{A}$. This appears to be more tractable when root-edges in $\mathcal{A}$ are restricted to borders and bridges, since it is not clear how best to represent the decoration of handles. The refinement predicted by Conjecture 7.15 suggests that a more restricted problem, finding an explicit bijection between planar maps with two decorated vertices, one of which is the root vertex, and 4-regular maps on the torus with face-non-separating root edges, will be more tractable than the general problem. A precise description of this restricted bijection should help isolate the rôles of borders and bridges from the rôle of handles.

The Refined q-Conjecture

Another subject for future work is to establish Conjecture 7.15, which is presently supported by structural and numerical evidence. This could be accomplished either analytically, by verifying (7.16) or (7.20), or combinatorially by verifying (7.19).

An Extension to Hypermaps

In [JV90b], Jackson and Visentin showed that (7.6), the multiplicative identity that suggested the q-Conjecture, extends to a more general setting. This led them to a generalized conjecture, with rooted maps replaced by rooted hypermaps, and 4-regular maps replaced by Eulerian maps, rooted maps in which every vertex has even degree. Since a slightly modified bijection ζ continues to apply in this setting, it should be determined whether the Refined q-Conjecture can also be generalized.

8.8 On Chirality

An unexpected relationship between the b-Conjecture and the q-Conjecture is that both conjectures appear to involve forms of chirality. By the analysis in Section 3.6.3, a b-invariant cannot be both additive and symmetric with respect to orientation reversal, and by the analysis in Section 7.5, any bijection between $\mathcal{A}$ and Q that respects the refinement predicted by Conjecture 7.15 cannot also respect the left-right symmetry exhibited by both classes of maps. These asymmetries should be examined in relation to applications of rooted maps to physics, a subject where symmetry breaking and chirality are significant themes.

Appendix A

Coefficients of b-Polynomials

This Appendix contains a tabulation, for $|v| \leq 10$, of the coefficients of each b-polynomial, $c_{v,\varphi,[2^n]}(b)$, with respect to the basis $B_g := \left\{ b^{g-2i}(1+b)^i : 0 \leq i \leq \frac{g}{2} \right\}$, where g is the Euler genus of the maps conjectured to be enumerated by $c_{v,\varphi,[2^n]}(b)$. For example, from the Table of coefficients for maps with two edges and genus two, $c_{[4],[4],[2^2]}(b) = 3b^2 + (1+b)$. A similar tabulation with respect to the standard basis was produced by Jackson and Visentin and appears in [JV01, Chap. 12].

All coefficients for $|v| \leq 16$ were computed using the `Maple` programs given in Appendix B, and each was found to be a non-negative integer, but only coefficients for $|v| \leq 10$ are reproduced exhaustively. As discussed in Section 5.6, of the computed coefficients, both non-negativity and integrality with respect to B_g are guaranteed by non-negativity and integrality with respect to the standard basis, except when $v \vdash 16$, $\ell(v) = 2$, and $\ell(\varphi) = 2$. Coefficients of the polynomials in this category are also reproduced, up to symmetry between v and φ.

Tables are organized by number of edges, and the Euler genus of the maps they are conjectured to enumerate. Within each table, entries are sorted first by decreasing number of parts of v, and then by reverse lexicographical order of v and φ. Tables that are continued into another column or onto another page are left unterminated.

A.1 b-Polynomials for Maps with 1 Edge

1 **edge, genus** 0		
v	φ	1
[2]	$[1^2]$	1
$[1^2]$	[2]	1

1 **edge, genus** 1		
v	φ	b
[2]	[2]	1

A.2   *b*-Polynomials for Maps with 2 Edges

2 edges, genus 0

ν	φ	1
$[4]$	$[1^2,2]$	2
$[1,3]$	$[1,3]$	4
$[1,3]$	$[2^2]$	0
$[2^2]$	$[1,3]$	0
$[2^2]$	$[2^2]$	1
$[1^2,2]$	$[4]$	2

2 edges, genus 1

ν	φ	b
$[4]$	$[1,3]$	4
$[4]$	$[2^2]$	1
$[1,3]$	$[4]$	4
$[2^2]$	$[4]$	1

2 edges, genus 2

ν	φ	b^2	$(1+b)$
$[4]$	$[4]$	3	1

A.3   *b*-Polynomials for Maps with 3 Edges

3 edges, genus 0

ν	φ	1
$[6]$	$[1^3,3]$	2
$[6]$	$[1^2,2^2]$	3
$[1,5]$	$[1^2,4]$	6
$[1,5]$	$[1,2,3]$	6
$[1,5]$	$[2^3]$	0
$[2,4]$	$[1^2,4]$	0
$[2,4]$	$[1,2,3]$	6
$[2,4]$	$[2^3]$	0
$[3^2]$	$[1^2,4]$	3
$[3^2]$	$[1,2,3]$	0
$[3^2]$	$[2^3]$	1
$[1^2,4]$	$[1,5]$	6
$[1^2,4]$	$[2,4]$	0
$[1^2,4]$	$[3^2]$	3
$[1,2,3]$	$[1,5]$	6
$[1,2,3]$	$[2,4]$	6
$[1,2,3]$	$[3^2]$	0
$[2^3]$	$[1,5]$	0
$[2^3]$	$[2,4]$	0
$[2^3]$	$[3^2]$	1
$[1^3,3]$	$[6]$	2
$[1^2,2^2]$	$[6]$	3

3 edges, genus 1

ν	φ	b
$[6]$	$[1^2,4]$	9
$[6]$	$[1,2,3]$	12
$[6]$	$[2^3]$	1
$[1,5]$	$[1,5]$	18
$[1,5]$	$[2,4]$	6
$[1,5]$	$[3^2]$	6
$[2,4]$	$[1,5]$	6
$[2,4]$	$[2,4]$	6
$[2,4]$	$[3^2]$	3
$[3^2]$	$[1,5]$	6
$[3^2]$	$[2,4]$	3
$[3^2]$	$[3^2]$	0
$[1^2,4]$	$[6]$	9
$[1,2,3]$	$[6]$	12
$[2^3]$	$[6]$	1

3 **edges, genus** 2			
ν	φ	b^2	$(1+b)$
[6]	[1,5]	18	6
[6]	[2,4]	9	3
[6]	[3²]	5	1
[1,5]	[6]	18	6
[2,4]	[6]	9	3
[3²]	[6]	5	1

3 **edges, genus** 3			
ν	φ	b^3	$b(1+b)$
[6]	[6]	15	13

A.4 b-**Polynomials for Maps with** 4 **Edges**

4 **edges, genus** 0		
ν	φ	1
[8]	[1⁴,4]	2
[8]	[1³,2,3]	8
[8]	[1²,2³]	4
[1,7]	[1³,5]	8
[1,7]	[1²,2,4]	16
[1,7]	[1²,3²]	8
[1,7]	[1,2²,3]	8
[1,7]	[2⁴]	0
[2,6]	[1³,5]	0
[2,6]	[1²,2,4]	8
[2,6]	[1²,3²]	4
[2,6]	[1,2²,3]	8
[2,6]	[2⁴]	0
[3,5]	[1³,5]	8
[3,5]	[1²,2,4]	8
[3,5]	[1²,3²]	0
[3,5]	[1,2²,3]	8
[3,5]	[2⁴]	0
[4²]	[1³,5]	0
[4²]	[1²,2,4]	4
[4²]	[1²,3²]	4
[4²]	[1,2²,3]	0
[4²]	[2⁴]	1

4 **edges, genus** 0 **continued**		
ν	φ	1
[1²,6]	[1²,6]	12
[1²,6]	[1,2,5]	8
[1²,6]	[1,3,4]	16
[1²,6]	[2²,4]	0
[1²,6]	[2,3²]	4
[1,2,5]	[1²,6]	8
[1,2,5]	[1,2,5]	24
[1,2,5]	[1,3,4]	8
[1,2,5]	[2²,4]	0
[1,2,5]	[2,3²]	8
[1,3,4]	[1²,6]	16
[1,3,4]	[1,2,5]	8
[1,3,4]	[1,3,4]	16
[1,3,4]	[2²,4]	8
[1,3,4]	[2,3²]	0
[2²,4]	[1²,6]	0
[2²,4]	[1,2,5]	0
[2²,4]	[1,3,4]	8
[2²,4]	[2²,4]	4
[2²,4]	[2,3²]	0
[2,3²]	[1²,6]	4
[2,3²]	[1,2,5]	8
[2,3²]	[1,3,4]	0
[2,3²]	[2²,4]	0
[2,3²]	[2,3²]	4

4 **edges, genus** 0 **concluded**		
ν	φ	1
[1³,5]	[1,7]	8
[1³,5]	[2,6]	0
[1³,5]	[3,5]	8
[1³,5]	[4²]	0
[1²,2,4]	[1,7]	16
[1²,2,4]	[2,6]	8
[1²,2,4]	[3,5]	8
[1²,2,4]	[4²]	4
[1²,3²]	[1,7]	8
[1²,3²]	[2,6]	4
[1²,3²]	[3,5]	0
[1²,3²]	[4²]	4
[1,2²,3]	[1,7]	8
[1,2²,3]	[2,6]	8
[1,2²,3]	[3,5]	8
[1,2²,3]	[4²]	0
[2⁴]	[1,7]	0
[2⁴]	[2,6]	0
[2⁴]	[3,5]	0
[2⁴]	[4²]	1
[1⁴,4]	[8]	2
[1³,2,3]	[8]	8
[1²,2³]	[8]	4

4 **edges, genus** 1		
ν	φ	b
$[8]$	$[1^3, 5]$	16
$[8]$	$[1^2, 2, 4]$	36
$[8]$	$[1^2, 3^2]$	16
$[8]$	$[1, 2^2, 3]$	24
$[8]$	$[2^4]$	1
$[1, 7]$	$[1^2, 6]$	48
$[1, 7]$	$[1, 2, 5]$	48
$[1, 7]$	$[1, 3, 4]$	56
$[1, 7]$	$[2^2, 4]$	8
$[1, 7]$	$[2, 3^2]$	16
$[2, 6]$	$[1^2, 6]$	12
$[2, 6]$	$[1, 2, 5]$	32
$[2, 6]$	$[1, 3, 4]$	24
$[2, 6]$	$[2^2, 4]$	8
$[2, 6]$	$[2, 3^2]$	12
$[3, 5]$	$[1^2, 6]$	32
$[3, 5]$	$[1, 2, 5]$	32
$[3, 5]$	$[1, 3, 4]$	16
$[3, 5]$	$[2^2, 4]$	8
$[3, 5]$	$[2, 3^2]$	8
$[4^2]$	$[1^2, 6]$	8
$[4^2]$	$[1, 2, 5]$	8
$[4^2]$	$[1, 3, 4]$	16
$[4^2]$	$[2^2, 4]$	6
$[4^2]$	$[2, 3^2]$	0

4 **edges, genus** 1 **concluded**		
ν	φ	b
$[1^2, 6]$	$[1, 7]$	48
$[1^2, 6]$	$[2, 6]$	12
$[1^2, 6]$	$[3, 5]$	32
$[1^2, 6]$	$[4^2]$	8
$[1, 2, 5]$	$[1, 7]$	48
$[1, 2, 5]$	$[2, 6]$	32
$[1, 2, 5]$	$[3, 5]$	32
$[1, 2, 5]$	$[4^2]$	8
$[1, 3, 4]$	$[1, 7]$	56
$[1, 3, 4]$	$[2, 6]$	24
$[1, 3, 4]$	$[3, 5]$	16
$[1, 3, 4]$	$[4^2]$	16
$[2^2, 4]$	$[1, 7]$	8
$[2^2, 4]$	$[2, 6]$	8
$[2^2, 4]$	$[3, 5]$	8
$[2^2, 4]$	$[4^2]$	6
$[2, 3^2]$	$[1, 7]$	16
$[2, 3^2]$	$[2, 6]$	12
$[2, 3^2]$	$[3, 5]$	8
$[2, 3^2]$	$[4^2]$	0
$[1^3, 5]$	$[8]$	16
$[1^2, 2, 4]$	$[8]$	36
$[1^2, 3^2]$	$[8]$	16
$[1, 2^2, 3]$	$[8]$	24
$[2^4]$	$[8]$	1

4 **edges, genus** 2			
ν	φ	b^2	$(1+b)$
[8]	$[1^2, 6]$	60	20
[8]	$[1, 2, 5]$	72	24
[8]	$[1, 3, 4]$	64	16
[8]	$[2^2, 4]$	18	6
[8]	$[2, 3^2]$	20	4
$[1, 7]$	$[1, 7]$	120	40
$[1, 7]$	$[2, 6]$	48	16
$[1, 7]$	$[3, 5]$	64	16
$[1, 7]$	$[4^2]$	24	8
$[2, 6]$	$[1, 7]$	48	16
$[2, 6]$	$[2, 6]$	36	12
$[2, 6]$	$[3, 5]$	32	8
$[2, 6]$	$[4^2]$	12	4
$[3, 5]$	$[1, 7]$	64	16
$[3, 5]$	$[2, 6]$	32	8
$[3, 5]$	$[3, 5]$	24	8
$[3, 5]$	$[4^2]$	8	0
$[4^2]$	$[1, 7]$	24	8
$[4^2]$	$[2, 6]$	12	4
$[4^2]$	$[3, 5]$	8	0
$[4^2]$	$[4^2]$	9	3
$[1^2, 6]$	[8]	60	20
$[1, 2, 5]$	[8]	72	24
$[1, 3, 4]$	[8]	64	16
$[2^2, 4]$	[8]	18	6
$[2, 3^2]$	[8]	20	4

4 **edges, genus** 3			
ν	φ	b^3	$b(1+b)$
[8]	$[1, 7]$	120	104
[8]	$[2, 6]$	60	52
[8]	$[3, 5]$	56	40
[8]	$[4^2]$	24	19
$[1, 7]$	[8]	120	104
$[2, 6]$	[8]	60	52
$[3, 5]$	[8]	56	40
$[4^2]$	[8]	24	19

4 **edges, genus** 4				
ν	φ	b^4	$b^2(1+b)$	$(1+b)^2$
[8]	[8]	105	160	21

A.5 b-Polynomials for Maps with 5 Edges

ν	φ	1
$[10]$	$[1^5,5]$	2
$[10]$	$[1^4,2,4]$	10
$[10]$	$[1^4,3^2]$	5
$[10]$	$[1^3,2^2,3]$	20
$[10]$	$[1^2,2^4]$	5
$[1,9]$	$[1^4,6]$	10
$[1,9]$	$[1^3,2,5]$	30
$[1,9]$	$[1^3,3,4]$	30
$[1,9]$	$[1^2,2^2,4]$	30
$[1,9]$	$[1^2,2,3^2]$	30
$[1,9]$	$[1,2^3,3]$	10
$[1,9]$	$[2^5]$	0
$[2,8]$	$[1^4,6]$	0
$[2,8]$	$[1^3,2,5]$	10
$[2,8]$	$[1^3,3,4]$	10
$[2,8]$	$[1^2,2^2,4]$	20
$[2,8]$	$[1^2,2,3^2]$	20
$[2,8]$	$[1,2^3,3]$	10
$[2,8]$	$[2^5]$	0
$[3,7]$	$[1^4,6]$	10
$[3,7]$	$[1^3,2,5]$	20
$[3,7]$	$[1^3,3,4]$	10
$[3,7]$	$[1^2,2^2,4]$	20
$[3,7]$	$[1^2,2,3^2]$	10
$[3,7]$	$[1,2^3,3]$	10
$[3,7]$	$[2^5]$	0
$[4,6]$	$[1^4,6]$	0
$[4,6]$	$[1^3,2,5]$	10
$[4,6]$	$[1^3,3,4]$	20
$[4,6]$	$[1^2,2^2,4]$	10
$[4,6]$	$[1^2,2,3^2]$	10
$[4,6]$	$[1,2^3,3]$	10
$[4,6]$	$[2^5]$	0
$[5^2]$	$[1^4,6]$	5
$[5^2]$	$[1^3,2,5]$	10
$[5^2]$	$[1^3,3,4]$	0
$[5^2]$	$[1^2,2^2,4]$	10

ν	φ	1
$[5^2]$	$[1^2,2,3^2]$	10
$[5^2]$	$[1,2^3,3]$	0
$[5^2]$	$[2^5]$	1
$[1^2,8]$	$[1^3,7]$	20
$[1^2,8]$	$[1^2,2,6]$	30
$[1^2,8]$	$[1^2,3,5]$	40
$[1^2,8]$	$[1^2,4^2]$	20
$[1^2,8]$	$[1,2^2,5]$	10
$[1^2,8]$	$[1,2,3,4]$	40
$[1^2,8]$	$[1,3^3]$	10
$[1^2,8]$	$[2^3,4]$	0
$[1^2,8]$	$[2^2,3^2]$	5
$[1,2,7]$	$[1^3,7]$	10
$[1,2,7]$	$[1^2,2,6]$	50
$[1,2,7]$	$[1^2,3,5]$	30
$[1,2,7]$	$[1^2,4^2]$	10
$[1,2,7]$	$[1,2^2,5]$	30
$[1,2,7]$	$[1,2,3,4]$	50
$[1,2,7]$	$[1,3^3]$	10
$[1,2,7]$	$[2^3,4]$	0
$[1,2,7]$	$[2^2,3^2]$	10
$[1,3,6]$	$[1^3,7]$	30
$[1,3,6]$	$[1^2,2,6]$	30
$[1,3,6]$	$[1^2,3,5]$	30
$[1,3,6]$	$[1^2,4^2]$	30
$[1,3,6]$	$[1,2^2,5]$	30
$[1,3,6]$	$[1,2,3,4]$	40
$[1,3,6]$	$[1,3^3]$	0
$[1,3,6]$	$[2^3,4]$	0
$[1,3,6]$	$[2^2,3^2]$	10
$[1,4,5]$	$[1^3,7]$	20
$[1,4,5]$	$[1^2,2,6]$	40
$[1,4,5]$	$[1^2,3,5]$	40
$[1,4,5]$	$[1^2,4^2]$	10
$[1,4,5]$	$[1,2^2,5]$	10
$[1,4,5]$	$[1,2,3,4]$	40
$[1,4,5]$	$[1,3^3]$	10
$[1,4,5]$	$[2^3,4]$	10
$[1,4,5]$	$[2^2,3^2]$	0

ν	φ	1
$[2^2,6]$	$[1^3,7]$	0
$[2^2,6]$	$[1^2,2,6]$	0
$[2^2,6]$	$[1^2,3,5]$	10
$[2^2,6]$	$[1^2,4^2]$	5
$[2^2,6]$	$[1,2^2,5]$	10
$[2^2,6]$	$[1,2,3,4]$	20
$[2^2,6]$	$[1,3^3]$	0
$[2^2,6]$	$[2^3,4]$	0
$[2^2,6]$	$[2^2,3^2]$	5
$[2,3,5]$	$[1^3,7]$	10
$[2,3,5]$	$[1^2,2,6]$	40
$[2,3,5]$	$[1^2,3,5]$	10
$[2,3,5]$	$[1^2,4^2]$	0
$[2,3,5]$	$[1,2^2,5]$	10
$[2,3,5]$	$[1,2,3,4]$	30
$[2,3,5]$	$[1,3^3]$	10
$[2,3,5]$	$[2^3,4]$	10
$[2,3,5]$	$[2^2,3^2]$	0
$[2,4^2]$	$[1^3,7]$	0
$[2,4^2]$	$[1^2,2,6]$	0
$[2,4^2]$	$[1^2,3,5]$	10
$[2,4^2]$	$[1^2,4^2]$	10
$[2,4^2]$	$[1,2^2,5]$	10
$[2,4^2]$	$[1,2,3,4]$	10
$[2,4^2]$	$[1,3^3]$	0
$[2,4^2]$	$[2^3,4]$	0
$[2,4^2]$	$[2^2,3^2]$	5
$[3^2,4]$	$[1^3,7]$	10
$[3^2,4]$	$[1^2,2,6]$	10
$[3^2,4]$	$[1^2,3,5]$	10
$[3^2,4]$	$[1^2,4^2]$	5
$[3^2,4]$	$[1,2^2,5]$	10
$[3^2,4]$	$[1,2,3,4]$	10
$[3^2,4]$	$[1,3^3]$	0
$[3^2,4]$	$[2^3,4]$	0
$[3^2,4]$	$[2^2,3^2]$	5

ν	φ	1
$[1^3,7]$	$[1^2,8]$	20
$[1^3,7]$	$[1,2,7]$	10
$[1^3,7]$	$[1,3,6]$	30
$[1^3,7]$	$[1,4,5]$	20
$[1^3,7]$	$[2^2,6]$	0
$[1^3,7]$	$[2,3,5]$	10
$[1^3,7]$	$[2,4^2]$	0
$[1^3,7]$	$[3^2,4]$	10
$[1^2,2,6]$	$[1^2,8]$	30
$[1^2,2,6]$	$[1,2,7]$	50
$[1^2,2,6]$	$[1,3,6]$	30
$[1^2,2,6]$	$[1,4,5]$	40
$[1^2,2,6]$	$[2^2,6]$	0
$[1^2,2,6]$	$[2,3,5]$	40
$[1^2,2,6]$	$[2,4^2]$	0
$[1^2,2,6]$	$[3^2,4]$	10
$[1^2,3,5]$	$[1^2,8]$	40
$[1^2,3,5]$	$[1,2,7]$	30
$[1^2,3,5]$	$[1,3,6]$	30
$[1^2,3,5]$	$[1,4,5]$	40
$[1^2,3,5]$	$[2^2,6]$	10
$[1^2,3,5]$	$[2,3,5]$	10
$[1^2,3,5]$	$[2,4^2]$	10
$[1^2,3,5]$	$[3^2,4]$	10
$[1^2,4^2]$	$[1^2,8]$	20
$[1^2,4^2]$	$[1,2,7]$	10
$[1^2,4^2]$	$[1,3,6]$	30
$[1^2,4^2]$	$[1,4,5]$	10
$[1^2,4^2]$	$[2^2,6]$	5
$[1^2,4^2]$	$[2,3,5]$	0
$[1^2,4^2]$	$[2,4^2]$	10
$[1^2,4^2]$	$[3^2,4]$	5
$[1,2^2,5]$	$[1^2,8]$	10
$[1,2^2,5]$	$[1,2,7]$	30
$[1,2^2,5]$	$[1,3,6]$	30
$[1,2^2,5]$	$[1,4,5]$	10
$[1,2^2,5]$	$[2^2,6]$	10
$[1,2^2,5]$	$[2,3,5]$	10
$[1,2^2,5]$	$[2,4^2]$	10
$[1,2^2,5]$	$[3^2,4]$	10

ν	φ	1
$[1,2,3,4]$	$[1^2,8]$	40
$[1,2,3,4]$	$[1,2,7]$	50
$[1,2,3,4]$	$[1,3,6]$	40
$[1,2,3,4]$	$[1,4,5]$	40
$[1,2,3,4]$	$[2^2,6]$	20
$[1,2,3,4]$	$[2,3,5]$	30
$[1,2,3,4]$	$[2,4^2]$	10
$[1,2,3,4]$	$[3^2,4]$	10
$[1,3^3]$	$[1^2,8]$	10
$[1,3^3]$	$[1,2,7]$	10
$[1,3^3]$	$[1,3,6]$	0
$[1,3^3]$	$[1,4,5]$	10
$[1,3^3]$	$[2^2,6]$	0
$[1,3^3]$	$[2,3,5]$	10
$[1,3^3]$	$[2,4^2]$	0
$[1,3^3]$	$[3^2,4]$	0
$[2^3,4]$	$[1^2,8]$	0
$[2^3,4]$	$[1,2,7]$	0
$[2^3,4]$	$[1,3,6]$	0
$[2^3,4]$	$[1,4,5]$	10
$[2^3,4]$	$[2^2,6]$	0
$[2^3,4]$	$[2,3,5]$	10
$[2^3,4]$	$[2,4^2]$	0
$[2^3,4]$	$[3^2,4]$	0
$[2^2,3^2]$	$[1^2,8]$	5
$[2^2,3^2]$	$[1,2,7]$	10
$[2^2,3^2]$	$[1,3,6]$	10
$[2^2,3^2]$	$[1,4,5]$	0
$[2^2,3^2]$	$[2^2,6]$	5
$[2^2,3^2]$	$[2,3,5]$	0
$[2^2,3^2]$	$[2,4^2]$	5
$[2^2,3^2]$	$[3^2,4]$	5
$[1^4,6]$	$[1,9]$	10
$[1^4,6]$	$[2,8]$	0
$[1^4,6]$	$[3,7]$	10
$[1^4,6]$	$[4,6]$	0
$[1^4,6]$	$[5^2]$	5

ν	φ	1
$[1^3,2,5]$	$[1,9]$	30
$[1^3,2,5]$	$[2,8]$	10
$[1^3,2,5]$	$[3,7]$	20
$[1^3,2,5]$	$[4,6]$	10
$[1^3,2,5]$	$[5^2]$	10
$[1^3,3,4]$	$[1,9]$	30
$[1^3,3,4]$	$[2,8]$	10
$[1^3,3,4]$	$[3,7]$	10
$[1^3,3,4]$	$[4,6]$	20
$[1^3,3,4]$	$[5^2]$	0
$[1^2,2^2,4]$	$[1,9]$	30
$[1^2,2^2,4]$	$[2,8]$	20
$[1^2,2^2,4]$	$[3,7]$	20
$[1^2,2^2,4]$	$[4,6]$	10
$[1^2,2^2,4]$	$[5^2]$	10
$[1^2,2,3^2]$	$[1,9]$	30
$[1^2,2,3^2]$	$[2,8]$	20
$[1^2,2,3^2]$	$[3,7]$	10
$[1^2,2,3^2]$	$[4,6]$	10
$[1^2,2,3^2]$	$[5^2]$	10
$[1,2^3,3]$	$[1,9]$	10
$[1,2^3,3]$	$[2,8]$	10
$[1,2^3,3]$	$[3,7]$	10
$[1,2^3,3]$	$[4,6]$	10
$[1,2^3,3]$	$[5^2]$	0
$[2^5]$	$[1,9]$	0
$[2^5]$	$[2,8]$	0
$[2^5]$	$[3,7]$	0
$[2^5]$	$[4,6]$	0
$[2^5]$	$[5^2]$	1
$[1^5,5]$	$[10]$	2
$[1^4,2,4]$	$[10]$	10
$[1^4,3^2]$	$[10]$	5
$[1^3,2^2,3]$	$[10]$	20
$[1^2,2^4]$	$[10]$	5

	5 **edges, genus** 1			5 **edges, genus** 1 **continued**	
ν	φ	b	ν	φ	b
[10]	$[1^4, 6]$	25	[4, 6]	$[2^3, 4]$	10
[10]	$[1^3, 2, 5]$	80	[4, 6]	$[2^2, 3^2]$	15
[10]	$[1^3, 3, 4]$	70	$[5^2]$	$[1^3, 7]$	30
[10]	$[1^2, 2^2, 4]$	90	$[5^2]$	$[1^2, 2, 6]$	60
[10]	$[1^2, 2, 3^2]$	80	$[5^2]$	$[1^2, 3, 5]$	30
[10]	$[1, 2^3, 3]$	40	$[5^2]$	$[1^2, 4^2]$	5
[10]	$[2^5]$	1	$[5^2]$	$[1, 2^2, 5]$	20
[1, 9]	$[1^3, 7]$	100	$[5^2]$	$[1, 2, 3, 4]$	50
[1, 9]	$[1^2, 2, 6]$	180	$[5^2]$	$[1, 3^3]$	10
[1, 9]	$[1^2, 3, 5]$	180	$[5^2]$	$[2^3, 4]$	10
[1, 9]	$[1^2, 4^2]$	90	$[5^2]$	$[2^2, 3^2]$	0
[1, 9]	$[1, 2^2, 5]$	90	$[1^2, 8]$	$[1^2, 8]$	150
[1, 9]	$[1, 2, 3, 4]$	210	$[1^2, 8]$	$[1, 2, 7]$	120
[1, 9]	$[1, 3^3]$	40	$[1^2, 8]$	$[1, 3, 6]$	180
[1, 9]	$[2^3, 4]$	10	$[1^2, 8]$	$[1, 4, 5]$	150
[1, 9]	$[2^2, 3^2]$	30	$[1^2, 8]$	$[2^2, 6]$	15
[2, 8]	$[1^3, 7]$	20	$[1^2, 8]$	$[2, 3, 5]$	80
[2, 8]	$[1^2, 2, 6]$	90	$[1^2, 8]$	$[2, 4^2]$	20
[2, 8]	$[1^2, 3, 5]$	70	$[1^2, 8]$	$[3^2, 4]$	55
[2, 8]	$[1^2, 4^2]$	30	[1, 2, 7]	$[1^2, 8]$	120
[2, 8]	$[1, 2^2, 5]$	70	[1, 2, 7]	$[1, 2, 7]$	210
[2, 8]	$[1, 2, 3, 4]$	130	[1, 2, 7]	$[1, 3, 6]$	160
[2, 8]	$[1, 3^3]$	20	[1, 2, 7]	$[1, 4, 5]$	140
[2, 8]	$[2^3, 4]$	10	[1, 2, 7]	$[2^2, 6]$	40
[2, 8]	$[2^2, 3^2]$	25	[1, 2, 7]	$[2, 3, 5]$	130
[3, 7]	$[1^3, 7]$	70	[1, 2, 7]	$[2, 4^2]$	30
[3, 7]	$[1^2, 2, 6]$	110	[1, 2, 7]	$[3^2, 4]$	50
[3, 7]	$[1^2, 3, 5]$	70	[1, 3, 6]	$[1^2, 8]$	180
[3, 7]	$[1^2, 4^2]$	40	[1, 3, 6]	$[1, 2, 7]$	160
[3, 7]	$[1, 2^2, 5]$	70	[1, 3, 6]	$[1, 3, 6]$	120
[3, 7]	$[1, 2, 3, 4]$	90	[1, 3, 6]	$[1, 4, 5]$	170
[3, 7]	$[1, 3^3]$	10	[1, 3, 6]	$[2^2, 6]$	40
[3, 7]	$[2^3, 4]$	10	[1, 3, 6]	$[2, 3, 5]$	90
[3, 7]	$[2^2, 3^2]$	20	[1, 3, 6]	$[2, 4^2]$	30
[4, 6]	$[1^3, 7]$	30	[1, 3, 6]	$[3^2, 4]$	30
[4, 6]	$[1^2, 2, 6]$	60	[1, 4, 5]	$[1^2, 8]$	150
[4, 6]	$[1^2, 3, 5]$	80	[1, 4, 5]	$[1, 2, 7]$	140
[4, 6]	$[1^2, 4^2]$	45	[1, 4, 5]	$[1, 3, 6]$	170
[4, 6]	$[1, 2^2, 5]$	50	[1, 4, 5]	$[1, 4, 5]$	110
[4, 6]	$[1, 2, 3, 4]$	80	[1, 4, 5]	$[2^2, 6]$	40
[4, 6]	$[1, 3^3]$	10	[1, 4, 5]	$[2, 3, 5]$	40

ν	φ	b
$[1, 4, 5]$	$[2, 4^2]$	50
$[1, 4, 5]$	$[3^2, 4]$	40
$[2^2, 6]$	$[1^2, 8]$	15
$[2^2, 6]$	$[1, 2, 7]$	40
$[2^2, 6]$	$[1, 3, 6]$	40
$[2^2, 6]$	$[1, 4, 5]$	40
$[2^2, 6]$	$[2^2, 6]$	15
$[2^2, 6]$	$[2, 3, 5]$	40
$[2^2, 6]$	$[2, 4^2]$	15
$[2^2, 6]$	$[3^2, 4]$	15
$[2, 3, 5]$	$[1^2, 8]$	80
$[2, 3, 5]$	$[1, 2, 7]$	130
$[2, 3, 5]$	$[1, 3, 6]$	90
$[2, 3, 5]$	$[1, 4, 5]$	40
$[2, 3, 5]$	$[2^2, 6]$	40
$[2, 3, 5]$	$[2, 3, 5]$	40
$[2, 3, 5]$	$[2, 4^2]$	30
$[2, 3, 5]$	$[3^2, 4]$	30
$[2, 4^2]$	$[1^2, 8]$	20
$[2, 4^2]$	$[1, 2, 7]$	30
$[2, 4^2]$	$[1, 3, 6]$	30
$[2, 4^2]$	$[1, 4, 5]$	50
$[2, 4^2]$	$[2^2, 6]$	15
$[2, 4^2]$	$[2, 3, 5]$	30
$[2, 4^2]$	$[2, 4^2]$	10
$[2, 4^2]$	$[3^2, 4]$	5
$[3^2, 4]$	$[1^2, 8]$	55
$[3^2, 4]$	$[1, 2, 7]$	50
$[3^2, 4]$	$[1, 3, 6]$	30
$[3^2, 4]$	$[1, 4, 5]$	40
$[3^2, 4]$	$[2^2, 6]$	15
$[3^2, 4]$	$[2, 3, 5]$	30
$[3^2, 4]$	$[2, 4^2]$	5
$[3^2, 4]$	$[3^2, 4]$	5
$[1^3, 7]$	$[1, 9]$	100
$[1^3, 7]$	$[2, 8]$	20
$[1^3, 7]$	$[3, 7]$	70
$[1^3, 7]$	$[4, 6]$	30
$[1^3, 7]$	$[5^2]$	30
$[1^2, 2, 6]$	$[1, 9]$	180
$[1^2, 2, 6]$	$[2, 8]$	90
$[1^2, 2, 6]$	$[3, 7]$	110
$[1^2, 2, 6]$	$[4, 6]$	60

ν	φ	b
$[1^2, 2, 6]$	$[5^2]$	60
$[1^2, 3, 5]$	$[1, 9]$	180
$[1^2, 3, 5]$	$[2, 8]$	70
$[1^2, 3, 5]$	$[3, 7]$	70
$[1^2, 3, 5]$	$[4, 6]$	80
$[1^2, 3, 5]$	$[5^2]$	30
$[1^2, 4^2]$	$[1, 9]$	90
$[1^2, 4^2]$	$[2, 8]$	30
$[1^2, 4^2]$	$[3, 7]$	40
$[1^2, 4^2]$	$[4, 6]$	45
$[1^2, 4^2]$	$[5^2]$	5
$[1, 2^2, 5]$	$[1, 9]$	90
$[1, 2^2, 5]$	$[2, 8]$	70
$[1, 2^2, 5]$	$[3, 7]$	70
$[1, 2^2, 5]$	$[4, 6]$	50
$[1, 2^2, 5]$	$[5^2]$	20
$[1, 2, 3, 4]$	$[1, 9]$	210
$[1, 2, 3, 4]$	$[2, 8]$	130
$[1, 2, 3, 4]$	$[3, 7]$	90
$[1, 2, 3, 4]$	$[4, 6]$	80
$[1, 2, 3, 4]$	$[5^2]$	50
$[1, 3^3]$	$[1, 9]$	40
$[1, 3^3]$	$[2, 8]$	20
$[1, 3^3]$	$[3, 7]$	10
$[1, 3^3]$	$[4, 6]$	10
$[1, 3^3]$	$[5^2]$	10
$[2^3, 4]$	$[1, 9]$	10
$[2^3, 4]$	$[2, 8]$	10
$[2^3, 4]$	$[3, 7]$	10
$[2^3, 4]$	$[4, 6]$	10
$[2^3, 4]$	$[5^2]$	10
$[2^2, 3^2]$	$[1, 9]$	30
$[2^2, 3^2]$	$[2, 8]$	25
$[2^2, 3^2]$	$[3, 7]$	20
$[2^2, 3^2]$	$[4, 6]$	15
$[2^2, 3^2]$	$[5^2]$	0
$[1^4, 6]$	$[10]$	25
$[1^3, 2, 5]$	$[10]$	80
$[1^3, 3, 4]$	$[10]$	70
$[1^2, 2^2, 4]$	$[10]$	90
$[1^2, 2, 3^2]$	$[10]$	80
$[1, 2^3, 3]$	$[10]$	40
$[2^5]$	$[10]$	1

ν	φ	b^2	$(1+b)$
$[10]$	$[1^3,7]$	150	50
$[10]$	$[1^2,2,6]$	300	100
$[10]$	$[1^2,3,5]$	250	70
$[10]$	$[1^2,4^2]$	120	30
$[10]$	$[1,2^2,5]$	180	60
$[10]$	$[1,2,3,4]$	320	80
$[10]$	$[1,3^3]$	50	10
$[10]$	$[2^3,4]$	30	10
$[10]$	$[2^2,3^2]$	50	10
$[1,9]$	$[1^2,8]$	450	150
$[1,9]$	$[1,2,7]$	450	150
$[1,9]$	$[1,3,6]$	470	130
$[1,9]$	$[1,4,5]$	420	120
$[1,9]$	$[2^2,6]$	90	30
$[1,9]$	$[2,3,5]$	240	60
$[1,9]$	$[2,4^2]$	90	30
$[1,9]$	$[3^2,4]$	130	30
$[2,8]$	$[1^2,8]$	150	50
$[2,8]$	$[1,2,7]$	270	90
$[2,8]$	$[1,3,6]$	210	60
$[2,8]$	$[1,4,5]$	180	50
$[2,8]$	$[2^2,6]$	75	25
$[2,8]$	$[2,3,5]$	160	40
$[2,8]$	$[2,4^2]$	60	20
$[2,8]$	$[3^2,4]$	65	15
$[3,7]$	$[1^2,8]$	250	70
$[3,7]$	$[1,2,7]$	260	70
$[3,7]$	$[1,3,6]$	180	50
$[3,7]$	$[1,4,5]$	180	40
$[3,7]$	$[2^2,6]$	70	20
$[3,7]$	$[2,3,5]$	120	30
$[3,7]$	$[2,4^2]$	40	10
$[3,7]$	$[3^2,4]$	40	10
$[4,6]$	$[1^2,8]$	165	55
$[4,6]$	$[1,2,7]$	180	60
$[4,6]$	$[1,3,6]$	160	30
$[4,6]$	$[1,4,5]$	180	50
$[4,6]$	$[2^2,6]$	55	15
$[4,6]$	$[2,3,5]$	90	30
$[4,6]$	$[2,4^2]$	45	5
$[4,6]$	$[3^2,4]$	35	5

ν	φ	b^2	$(1+b)$
$[5^2]$	$[1^2,8]$	105	25
$[5^2]$	$[1,2,7]$	120	30
$[5^2]$	$[1,3,6]$	100	30
$[5^2]$	$[1,4,5]$	50	10
$[5^2]$	$[2^2,6]$	30	10
$[5^2]$	$[2,3,5]$	30	0
$[5^2]$	$[2,4^2]$	30	10
$[5^2]$	$[3^2,4]$	25	5
$[1^2,8]$	$[1,9]$	450	150
$[1^2,8]$	$[2,8]$	150	50
$[1^2,8]$	$[3,7]$	250	70
$[1^2,8]$	$[4,6]$	165	55
$[1^2,8]$	$[5^2]$	105	25
$[1,2,7]$	$[1,9]$	450	150
$[1,2,7]$	$[2,8]$	270	90
$[1,2,7]$	$[3,7]$	260	70
$[1,2,7]$	$[4,6]$	180	60
$[1,2,7]$	$[5^2]$	120	30
$[1,3,6]$	$[1,9]$	470	130
$[1,3,6]$	$[2,8]$	210	60
$[1,3,6]$	$[3,7]$	180	50
$[1,3,6]$	$[4,6]$	160	30
$[1,3,6]$	$[5^2]$	100	30
$[1,4,5]$	$[1,9]$	420	120
$[1,4,5]$	$[2,8]$	180	50
$[1,4,5]$	$[3,7]$	180	40
$[1,4,5]$	$[4,6]$	180	50
$[1,4,5]$	$[5^2]$	50	10
$[2^2,6]$	$[1,9]$	90	30
$[2^2,6]$	$[2,8]$	75	25
$[2^2,6]$	$[3,7]$	70	20
$[2^2,6]$	$[4,6]$	55	15
$[2^2,6]$	$[5^2]$	30	10
$[2,3,5]$	$[1,9]$	240	60
$[2,3,5]$	$[2,8]$	160	40
$[2,3,5]$	$[3,7]$	120	30
$[2,3,5]$	$[4,6]$	90	30
$[2,3,5]$	$[5^2]$	30	0

5 **edges, genus** 2 **concluded**			
ν	φ	b^2	$(1+b)$
$[2,4^2]$	$[1,9]$	90	30
$[2,4^2]$	$[2,8]$	60	20
$[2,4^2]$	$[3,7]$	40	10
$[2,4^2]$	$[4,6]$	45	5
$[2,4^2]$	$[5^2]$	30	10
$[3^2,4]$	$[1,9]$	130	30
$[3^2,4]$	$[2,8]$	65	15
$[3^2,4]$	$[3,7]$	40	10
$[3^2,4]$	$[4,6]$	35	5
$[3^2,4]$	$[5^2]$	25	5
$[1^3,7]$	$[10]$	150	50
$[1^2,2,6]$	$[10]$	300	100
$[1^2,3,5]$	$[10]$	250	70
$[1^2,4^2]$	$[10]$	120	30
$[1,2^2,5]$	$[10]$	180	60
$[1,2,3,4]$	$[10]$	320	80
$[1,3^3]$	$[10]$	50	10
$[2^3,4]$	$[10]$	30	10
$[2^2,3^2]$	$[10]$	50	10

5 **edges, genus** 3			
ν	φ	b^3	$b(1+b)$
$[10]$	$[1^2,8]$	525	455
$[10]$	$[1,2,7]$	600	520
$[10]$	$[1,3,6]$	500	380
$[10]$	$[1,4,5]$	450	340
$[10]$	$[2^2,6]$	150	130
$[10]$	$[2,3,5]$	280	200
$[10]$	$[2,4^2]$	120	95
$[10]$	$[3^2,4]$	125	80
$[1,9]$	$[1,9]$	1050	910
$[1,9]$	$[2,8]$	450	390
$[1,9]$	$[3,7]$	500	380
$[1,9]$	$[4,6]$	390	320
$[1,9]$	$[5^2]$	210	150
$[2,8]$	$[1,9]$	450	390
$[2,8]$	$[2,8]$	300	260
$[2,8]$	$[3,7]$	250	190
$[2,8]$	$[4,6]$	195	160
$[2,8]$	$[5^2]$	105	75
$[3,7]$	$[1,9]$	500	380
$[3,7]$	$[2,8]$	250	190
$[3,7]$	$[3,7]$	190	140
$[3,7]$	$[4,6]$	150	100
$[3,7]$	$[5^2]$	90	60
$[4,6]$	$[1,9]$	390	320
$[4,6]$	$[2,8]$	195	160
$[4,6]$	$[3,7]$	150	100
$[4,6]$	$[4,6]$	155	100
$[4,6]$	$[5^2]$	75	60
$[5^2]$	$[1,9]$	210	150
$[5^2]$	$[2,8]$	105	75
$[5^2]$	$[3,7]$	90	60
$[5^2]$	$[4,6]$	75	60
$[5^2]$	$[5^2]$	20	10
$[1^2,8]$	$[10]$	525	455
$[1,2,7]$	$[10]$	600	520
$[1,3,6]$	$[10]$	500	380
$[1,4,5]$	$[10]$	450	340
$[2^2,6]$	$[10]$	150	130
$[2,3,5]$	$[10]$	280	200
$[2,4^2]$	$[10]$	120	95
$[3^2,4]$	$[10]$	125	80

\nu	\varphi	b^4	$b^2(1+b)$	$(1+b)^2$
[10]	[1, 9]	1050	1600	210
[10]	[2, 8]	525	800	105
[10]	[3, 7]	450	620	70
[10]	[4, 6]	375	535	65
[10]	$[5^2]$	189	256	33
[1, 9]	[10]	1050	1600	210
[2, 8]	[10]	525	800	105
[3, 7]	[10]	450	620	70
[4, 6]	[10]	375	535	65
$[5^2]$	[10]	189	256	33

5 **edges, genus** 4

ν	φ	b^5	$b^3(1+b)$	$b(1+b)^2$
[10]	[10]	945	2136	753

5 **edges, genus** 5

A.6 b-Polynomials for Selected Maps with 8 Edges

Table A.1: Coefficients expressing b-polynomials as elements of span(B_6) for maps with 8 edges, 2 vertices, and 2 faces. Only pairs where the largest part of ν is at least as large as the largest part of φ are listed, since the remaining coefficients are determined by symmetry.

ν	φ	b^6	$b^4(1+b)$	$b^2(1+b)^2$	$(1+b)^3$
$[1, 15]$	$[1, 15]$	2162160	6593808	4196400	308880
$[1, 15]$	$[2, 14]$	997920	3043296	1936800	142560
$[1, 15]$	$[3, 13]$	887040	2617632	1594752	110880
$[1, 15]$	$[4, 12]$	695520	2069376	1277760	90720
$[1, 15]$	$[5, 11]$	628992	1831968	1111680	78624
$[1, 15]$	$[6, 10]$	567840	1667552	1019296	71904
$[1, 15]$	$[7, 9]$	549120	1594016	972416	68640
$[1, 15]$	$[8^2]$	267120	782016	477984	33840
$[2, 14]$	$[2, 14]$	582120	1775256	1129800	83160
$[2, 14]$	$[3, 13]$	443520	1308816	797376	55440
$[2, 14]$	$[4, 12]$	347760	1034688	638880	45360
$[2, 14]$	$[5, 11]$	314496	915984	555840	39312
$[2, 14]$	$[6, 10]$	283920	833776	509648	35952
$[2, 14]$	$[7, 9]$	274560	797008	486208	34320
$[2, 14]$	$[8^2]$	133560	391008	238992	16920
$[3, 13]$	$[3, 13]$	327600	944784	560688	37968
$[3, 13]$	$[4, 12]$	258720	742240	436736	29120
$[3, 13]$	$[5, 11]$	241920	681152	395168	26208
$[3, 13]$	$[6, 10]$	217440	616512	360544	24128
$[3, 13]$	$[7, 9]$	211200	591296	343840	22880
$[3, 13]$	$[8^2]$	102480	289456	169024	11232
$[4, 12]$	$[4, 12]$	220080	627344	367444	24528
$[4, 12]$	$[5, 11]$	193536	549936	323184	21792
$[4, 12]$	$[6, 10]$	173640	495152	292736	19912
$[4, 12]$	$[7, 9]$	168960	476528	279792	18912
$[4, 12]$	$[8^2]$	81900	232764	137460	9300
$[5, 11]$	$[5, 11]$	166704	472400	279472	19472
$[5, 11]$	$[6, 10]$	151200	426336	251392	17280
$[5, 11]$	$[7, 9]$	149760	418560	245280	16800
$[5, 11]$	$[8^2]$	72240	203200	119984	8320
$[6, 10]$	$[6, 10]$	143352	401896	235224	16200
$[6, 10]$	$[7, 9]$	136320	384976	227296	15408
$[6, 10]$	$[8^2]$	65520	184928	109152	7536
$[7, 9]$	$[7, 9]$	126576	358800	214640	15056
$[7, 9]$	$[8^2]$	61200	171120	99216	6384
$[8^2]$	$[8^2]$	33810	95940	57877	4118

Appendix B

Maple Programs

Several conjectures appearing in this Thesis were tested numerically for low order terms using programs written for version 11 of `Maple`, a symbolic computation system. The programs are reproduced here, as a starting point for future investigation. The extent of the computation in each program is controlled by an appropriately named variable, and the values reproduced here are selected to ensure timely termination, rather than to reflect the limits of practical computation.

B.1   Computing $M(x, \mathbf{y}, z; b)$ using Equation 4.9

```
maxedges := 8:

scale := (n,i) -> if n>0 then i/(2*n): elif i=0 then 1: else 0: end if:
M[0]:=y[0]*x:
for edges from 1 to maxedges do
   M[edges]:=expand(add(scale(edges−1,i)*diff(M[edges−1],y[i])*
                 ((i+1)*b*y[i+2]+add(y[j]*y[i−j+2],j=1..i+1))
                 +add(y[i+j+2]*(a*j*diff(scale(edges−1,i)
                 *diff(M[edges−1],y[i]),y[j])
                 +add(scale(k,i)*diff(M[k],y[i])*scale(edges−1−k,j)
                     *diff(M[edges−1−k],y[j]),k=0..edges−1))
                 ,j=0..2*edges−i)
               ,i=0..2*edges)
):
end do:
SMP := expand(add(eval(z^edge*M[edge],{a=1+b}),edge=0..maxedges)):
```

B.2 Extracting $c_{v,\varphi,[2^n]}(b)$ from $M(\mathbf{x}, \mathbf{y}, z; b)$

```
read(BMP8): with(combinat,partition):
for nedges from 1 to 8 do
  for nu in partition(nedges*2) do
    for phi in partition(nedges*2) do
      X:=mul(x[i],i=nu);
      Y:=mul(y[i],i=phi);
      g:=nedges−nops(nu)−nops(phi)+2;
      if g>=0 then
        c[nu,phi,nedges]:=coeftayl(BMP,
            [z,seq(x[i],i=1..nedges*2),seq(y[i],i=1..nedges*2)]=
            [0,seq(0,i=1..nedges*4)],
            [nedges,seq(degree(X,x[i]),i=1..nedges*2),
              seq(degree(Y,y[i]),i=1..nedges*2)]
        );
        template:=(add(a[i]*b^(g−2*i)*(1+b)^i,i=0..g/2)):
        soln := solve({coeffs(expand(template)−c[nu,phi,nedges],b)}):
        h[nu,phi,nedges]:=eval([seq(a[i],i=0..g/2)],soln);
      end if;
    end do;
  end do;
end do;
```

B.3 Computing $M(x, \mathbf{y}, z; 0)$ and $M(x, \mathbf{y}, z; 1)$ using Matrix Integrals

```
with(linalg):

# The trace of the k'th power of an NxN matrix
M:=N−>matrix(N,N,[seq(seq(m[i,j],j=1..N),i=1..N)]):
tr:=(N,k)−>expand(trace(M(N)^k)):

# Integrate the input polynomial against all appropriate variables, one at a time
integrateit := proc(mono)
    local vari, numu, deno: global N, m, r, c, b:
    numu := mono*exp(−tr(N,2)/2/(1+b)):
    deno := exp(−tr(N,2)/2/(1+b)):
    for vari in indets(tr(N,2)) do
        numu := int(numu, vari=−infinity..infinity):
        deno := int(deno, vari=−infinity..infinity):
    end do:
    return numu/deno:
end proc:
```

```
# Initialize the entries of M
setup:=proc(N)
    global m, r, c, b: local i,j:
    m:=evaln(m): c:=evaln(c): r:=evaln(r):
    for i from 1 to N do
        for j from 1 to N do
            m[i,j]:=simplify(r[i,j]+I*c[i,j]*(b−1)):
        end do;
    end do;
    for i from 1 to N do c[i,i]:=0: end do:
    for i from 1 to N do for j from i+1 to N do
        r[j,i]:=r[i,j]: c[j,i]:=−c[i,j]:
    end do: end do:
end proc:


# Bound is the maximum number of edges to consider
bound:=3:
OMap[0]:=0: LMap[0]:=0:
for N from 1 to bound+1 do
    m:=evaln(m): b:=evaln(b):
    mo:=add(1/k/(b+1)*y[k]*zp^k*tr(N,k),k=1..bound*2):
    gene:=convert(taylor(exp(mo),zp,2*bound+1),polynom):

    b:=1: setup(N):
    simplify(eval(integrateit(expand(gene)),zp=sqrt(z))):
    LMap[N]:=expand(convert(taylor(2*(1+b)*z*diff(ln(%),z),
        z,bound+1),polynom));

    b:=0: setup(N):
    simplify(eval(integrateit(expand(gene)),zp=sqrt(z))):
    OMap[N]:=expand(convert(taylor(2*(1+b)*z*diff(ln(%),z),
        z,bound+1),polynom)):
end do:

OriMap:=sort(expand(CurveFitting[PolynomialInterpolation]
            ([seq(i,i=0..bound+1)],[seq(OMap[i],i=0..bound+1)],x)));
AllMap:=sort(expand(CurveFitting[PolynomialInterpolation]
            ([seq(i,i=0..bound+1)],[seq(LMap[i],i=0..bound+1)],x)));
```

B.4   Computing M using Jack Symmetric Functions

This program computes the map series from Jack symmetric functions. The bottleneck of the computation is constructing the Jack symmetric functions themselves. At the suggestion of Berkant Ustaoğlu, a fellow doctoral candidate in the Department of Combinatorics and Optimization at the University of Waterloo, the program avoids working with rational functions in b, and instead computes M using polynomial interpolation and an appeal to the degree bound given by Corollary 5.22. It is thus sufficient to work with evaluations of Jack symmetric functions at positive integral values of the parameter α, but the computation is only valid if the coefficients of M are polynomial in b. A slight modification to the program forces it to work over the ring of rational functions in b, but at significant cost in memory usage and run-time.

This program was used to compute the map series for all maps with at most 8 edges. The process generated 24 954 b-polynomials, each of which had non-negative coefficients as an element of span(B_g). The entire operation took approximately one week and required 2Gb of memory on a 1.7GHz processor. Speed improvements could be made by fitting the results to elements of span(B_g), thereby reducing the number of evaluations needed by a factor of two.

with(**combinat**, **partition**):
with(**combinat**, **numbpart**):

```
# Input two partitions, output true unless the first dominates the second. This is used
# to sort the monomial symmetric functions prior to applying Gram−Schmidt.
domination := proc(a,b)
  local na, nb, i:

  if add(i, i=a) < add(i, i=b) then return true: end if:
  if (nops(b) < nops(a)) then return true: end if:

  na := nops(a)+1:
  nb := nops(b)+1:
  for i from 1 to nops(a) do
    if add(op(a)[na−j], j=1..i) <
        add(op(b)[nb−j], j=1..min(i, nb−1)) then
          return true:
    end if:
  end do:
  return false:
end proc:

innerproduct := proc(v1, v2, n, alpha)
   add(coeftayl(v1,p[P]=0,1)*coeftayl(v2,p[P]=0, 1)
   *alpha^(nops(P))*macz(P), P=partition(n)):
```

end proc:

The order of the centralizer of a permutation of cycle type P
macz := **proc**(P)
  local i, output, counter, n:
  n := **add**(i, i=P):
  for i **from** 1 **to** n **do**
    counter[i]:=0:
  end do:
  for i **from** 1 **to** **nops**(P) **do**
    counter[P[i]] := counter[P[i]]**+**1:
  end do:
  return mul((i)^counter[i]*(counter[i])!, i=1..n):
end proc:

kronecker := (i,j) −> **if** i=j **then** 1 **else** 0 **end if**:

Build the Powersum symmetric functions of order n
BuildPowerSum := **proc**(n::**posint**)
  local P, p:
  for P **in** **partition**(n) **do**
    p[P] := **mul**(**add**(x[j]^i, j=1..n), i=P):
  end do:
  return p:
end proc:

Express the monomial symmetric functions of order n in the powersum basis.
MonomialFromPSum := **proc**(n::**posint**)
  local P, psum, m, avals, mydiff, coefflist, tempsum:

  # *Construct the power−sum basis for Lambda[n]*
  # *Express linear combinations of these elements in*
  # *the monomial basis, and invert the system*
  psum:=BuildPowerSum(n):

  tempsum := **add**(a[P]*psum[P], P**=partition**(n)):
  for P **in** **partition**(n) **do**
    coefflist[P] := **coeftayl**(tempsum,
      [**seq**(x[j],j=1..**nops**(P))]**=**[**seq**(0,j=1..**nops**(P))],[**seq**(P[j], j=1..**nops**(P))]):
  end do:

  for P **in** **partition**(n) **do**
    avals := **solve**({**seq**(coefflist[i] = kronecker(i,P), i=**partition**(n))}):
    m[P] := **eval**(**add**(a[P]*p[P], P**=partition**(n)), avals):
  end do:
  return m:

end proc:

Construct the Jack symmetric functions of order n with Jack parameter alpha
by applying Gram−Schmidt to the monomial symmetric function in the
powersum basis. Instead of using the built in GramSchmidt function,
the process is implemented manually to preserve the polynomial presentation
of the series and to maintain fine control over when terms are collected.
FastJack := **proc**(n::**posint**, alpha::**posint**)
  local lambda, J, P, i, oldp, m, Jnorms, j:
  global p:

  oldp := p:
  p:=**evaln**(p):
  P := **sort**(**partition**(n), domination):
  m := MonomialFromPSum(n):

  for i **from** 1 **to nops**(P) **do**
    J[P[i]] := m[P[i]]:
    for j **from** 1 **to** i−1 **do**
      J[P[i]] := **expand**(J[P[i]]
        − innerproduct(m[P[i]], J[P[j]], n, alpha) *J[P[j]] / Jnorms[j]):
    end do:
    J[P[i]] := J[P[i]]/**coeftayl**(J[P[i]], p[[**seq**(1, i=1..n)]]=0, 1):
    Jnorms[i] := innerproduct(%,%,n,alpha):
  end do:
  p := oldp:
  return J:
end proc:

BuildJack := **proc**(n::**posint**, alpha)
  # *Instead of building the functions directly as rational functions in*
  # *the Jack parameter, build evaluations of the function and then*
  # *construct the polynomials by interpolation.*
  local numerics, J, P, j:

  if type(alpha, **posint**) **then**
    return FastJack(n, alpha):
  end if:

  numerics := [**seq**(FastJack(n,i), i=1..n)]:
  for P **in partition**(n) **do**
    for j **from** 1 **to numbpart**(n) **do**
      J[P] := expand(**eval**(CurveFitting[PolynomialInterpolation]
          ([**seq**([i, numerics[i][P]], i=1..n)], v, **form=power**), v=alpha)):
    end do:
  end do:

```
      return J:
   end proc:


MapPoly := proc(maxedge, b)
   local Phi, edges, J, M, lnpart, i, curpow, P:
   Phi := 0:

   for edges from 1 to maxedge do
      # Because we want to restrict to maps, we consider only even partitions.
      J := BuildJack(2*edges, 1+b):
      print("Built ", 2*edges, 1+b);
      # The for loop is used instead of add so that coefficients
      # can be combined more frequently.
      for P in partition(2*edges) do
         Phi := expand(Phi + t^(2*edges) /
                  (innerproduct(J[P], J[P], 2*edges, 1+b)) *
                     evalindets(J[P], indexed, n->mul(x[i], i=op(n)))*
                     evalindets(J[P], indexed, n->mul(y[i], i=op(n)))*
                     coeff(J[P], p[[seq(2, i=1..edges)]])*z^edges):
      end do:
   end do:
   lnpart := Phi:
   curpow := Phi:
   for i from 2 to maxedge do
      curpow := add(coeftayl(−curpow*Phi, z=0, j)*z^j, j=1..maxedge):
      lnpart := expand(lnpart+curpow/i):
   end do:
   M := eval((1+b)*diff(lnpart, t), t=1):
   return M:
end proc:


maxedge:=3:
mydata := [seq(0, i=0..maxedge)]:
for i from 0 to maxedge do
   mydata[i+1] := expand(convert(taylor(MapPoly(maxedge,i),
                        z, maxedge+1),polynom));
end do:
frominterp := add(CurveFitting[PolynomialInterpolation](
        [seq([i, coeftayl(mydata[i+1], z=0, edge)], i=0..maxedge)],
        b, form=power)*z^edge, edge=1..maxedge):
BMP[maxedge] := simplify(expand(%)):
```

B.5 The Top Coefficient

 # The root face is represented as a sequence indicating
 # the vertices encountered in a face traversal. For
 # computational convenience, the root vertex occurs
 # both first and last.

Kronecker := (x,y)−> **if** x=y **then** 1 **else** 0 **end if**:

CrossCap := **proc**(inFace::list) option remember:
  local n:
  n := **nops**(inFace):
  return add(Reduce([inFace[1], **seq**(inFace[i−j+1],j=1..i),
             seq(inFace[j], j=i..n−1),
             [**seq**(inFace[n][j]+Kronecker(j,inFace[i])
              +Kronecker(j,inFace[1]), j=1..**nops**(inFace[n]))]
             ]), i=1..n−1):
end proc:

NewFace := **proc**(inFace::list) option remember:
  local n:
  n := **nops**(inFace):
  return add(Reduce([inFace[1], **seq**(inFace[j], j=i..n−1),
              [**seq**(inFace[n][j]+Kronecker(j,inFace[i])
               +Kronecker(j,inFace[1]), j=1..**nops**(inFace[n]))]
             ])∗y[i], i=1..n−1):
end proc:

Reduce := **proc**(inList::list) option remember:
  local i, mapping, nexti, outList, outDegrees, n, extraVertices, inDegrees:
  nexti := 1:
  n := **nops**(inList)−1:
  inDegrees := inList[n+1]:
  for i **from** 1 **to** n **do**
    if mapping[inList[i]]=**evaln**(mapping[inList[i]]) **then**
      mapping[inList[i]]:=nexti:
      outDegrees[nexti]:=inDegrees[inList[i]]:
      nexti := nexti + 1:
    end if:
    outList[i]:=mapping[inList[i]]:
  end do:
  extraVertices := 1:
  for i **from** 1 **to nops**(inDegrees) **do**
    if mapping[i]=**evaln**(mapping[i]) **then**
      extraVertices := extraVertices∗x[inDegrees[i]]:

189

```
      end if:
    end do:
    return r[seq(outList[i], i=1..n),
              [seq(outDegrees[i], i=1..nexti−1)]]*extraVertices:
end proc:


AddBridge := proc(Face1::list, Face2::list)
  local n, m, shift:
  n := nops(Face1):
  m := nops(Face2):
  shift := max(seq(Face1[i], i=1..n−1)):
  return Reduce([Face1[1], seq(Face2[j]+shift, j=1..m−1),
      seq(Face1[j], j=1..n−1),
      [seq(Face1[n][j]+Kronecker(j,Face1[1]), j=1..nops(Face1[n])),
       seq(Face2[m][j]+Kronecker(j,Face2[1]), j=1..nops(Face2[m]))]
      ]):
end proc:


BridgeMonomial := proc(inmon)
  local rop, sop, i:
  if inmon=dummyterm then
    return 0:
  end if:
  for i from 1 to nops(inmon) do
    if op(0,op(i,inmon)) = r then
      rop := op(op(i,inmon)):
    elif op(0,op(i,inmon)) = s then
      sop := op(op(i,inmon)):
    end if:
  end do:
  return AddBridge([rop],[sop])*eval(inmon,{r[rop]=1, s[sop]=1}):
end proc:


BridgePoly := proc(inpoly::polynom)
  local expoly, temp, curm:
  expoly := expand(inpoly):
  map(BridgeMonomial,expoly+dummyterm):
end proc:


AddEdge := proc(inPoly)
  # We have to use evalindets carefully, otherwise
  # the variables that appear both pre and post
  # expansion will be expanded a second time.
  evalindets(inPoly, indexed, n−>
        if(op(0,n)='r') then
            'CrossCap([op(n)])+NewFace([op(n)])'
```

190

```
        else
            n
        end if):
    return expand(%):
end proc:

maxedge := 5:
U:=0:
part[0]:=r[1,[0]];
for i from 1 to maxedge do
    part[i] := expand(
        AddEdge(part[i−1]) +
        BridgePoly(add(part[j]*eval(part[i−j−1],r=s), j=0..i−1))
    ):
    for curp in op(part[i]) do
        U := U + z^i*evalindets(curp,indexed,n−>
            if(op(0,n)=r) then
                y[nops(n)−2]*mul(x[i],i=op(n)[nops(n)])
            else
                n
            end if):
    end do:
end do:
```

```
        else
            n
        end if):
    return expand(%):
end proc:

maxedge := 5:
U:=0:
part[0]:=r[1,[0]];
for i from 1 to maxedge do
    part[i] := expand(
        AddEdge(part[i−1]) +
        BridgePoly(add(part[j]*eval(part[i−j−1],r=s), j=0..i−1))
    ):
    for curp in op(part[i]) do
        U := U + z^i*evalindets(curp,indexed,n−>
            if(op(0,n)=r) then
                y[nops(n)−2]*mul(x[i],i=op(n)[nops(n)])
            else
                n
            end if):
    end do:
end do:
```

B.6   Testing the Refined q-Conjecture

```
#Compute the order of the stabilizer of a permutation with cycle type P
macz := proc(P) option remember: local i, output, counter, n:
  n := add(i, i=P): #Find the size of the partition
  for i from 1 to n do counter[i]:=0: end do: #Compute multiplicities
  for i from 1 to nops(P) do counter[P[i]] := counter[P[i]]+1: end do:
  return mul((i)^counter[i]*(counter[i])!, i=1..n):
end proc:

delta:=table(symmetric, identity):
deletionterm := (preterm,theta) ->
   add(theta[i]*'expect'(sort([seq(theta[j]+delta[i,j]
   *(preterm),j=1..nops(theta))])), i=1..nops(theta) ):
splitterm := (preterm, theta) ->
   add('expect'(sort([i,preterm-i, op(theta)])), i=0..preterm):
expect := proc(theta) option remember: local j, thetaprime, temp:
   if theta=[] then return 1: end if:
   j:=theta[1]: thetaprime:=seq(theta[i],i=2..nops(theta)):
   if j=0 then return y*expect([thetaprime]) end if:
   temp := deletionterm(j-2,[thetaprime])+splitterm(j-2,[thetaprime]):
   return sort(expand(eval(temp))):
end proc:

maxedge:=5: maxvert:=maxedge:

#Compute A(1,x,y,z) using the expectation operator
with(combinat, partition):
add(add(expect(P)*z^i*x^nops(P)/macz(P),P=partition(2*i)),i=0..maxedge):
e1:=simplify(%): de1:=2*z*diff(e1,z):
A:=convert(simplify(taylor(de1/e1,z,maxedge+1)),polynom):

#Compute Q_1(1,x,y,1) also using the expectation operator
ep4:=add(expect([seq(4,j=1..i)])*(x/4)^i/i!,i=0..maxvert-1):
Nep4:=(1-y^2)*ep4:
xp4ep4:=add(expect([seq(4,j=1..i)])*x^i/4^(i-1)/(i-1)!,i=1..maxvert):
xp1p3ep4:=add(expect([1,3,seq(4,j=1..i)])*x^(i+1)/4^i/i!,i=0..maxvert-1):
Q1:=convert(taylor((y*xp1p3ep4-y^2*xp4ep4)/Nep4,x,maxvert+1),polynom):
Q1:=sort(expand(simplify(Q1)),x):

#Compare the two computations
eval(A,{x=y+1/2,y=y,z=2*x})/(2*y+1)+eval(A,{x=y-1/2,y=y,z=2*x})/(2*y-1):
eval(Q1,{y=2*y}):
simplify(4*y*%%-%);
```

Appendix C

PostScript Programs

The problem of visualization is a significant obstacle to the study of maps. Studying topological concepts from visual representations can provide insight that is not present when only combinatorial descriptions are available. The figures appearing in this Thesis were all written in PostScript, a stack-based programming language developed for controlling laser printers. Though not written explicitly for the purpose, most of the programs can be altered to draw different maps. This Appendix reproduces the source code of several figures, with the intention that they should be used as a framework for drawing other maps.

The figures are organized in order of increasing complexity. Each is reproduced in a separate section that contains the listing of a '.eps' file together with a thumbnail of the figure that it generates. The nature of PostScript makes it difficult to distinguish a framework for drawing figures, from the data that specifies a particular figure, so an excerpt of the source code appears beside each thumbnail to indicate the portion of the program that most directly specifies the map, though other parts of the programs can also be modified.

Section C.1 gives a framework for drawing the matching graph of a straight line embedding in the plane. Section C.2 gives a framework for drawing a planar tiling of a hexagon representing the torus. Section C.3 gives a framework for drawing a map on the surface of a torus embedded in 3-dimensional Euclidean space, and makes use of PostScript level 3 features that may cause problems on old printers. A portion of the program dealing with applying a non-linear change of co-ordinates to a PostScript path was adapted from [Lan91]. The programs are designed so that the description of maps is similar in Sections C.2 and C.3.

The framework given in Section C.4, for drawing tilings of hyperbolic space, is the most complex, but also the least polished. It contains several features that are not used in the final figure, but can be activated to draw tilings of non-orientable surfaces and surfaces of higher genera.

C.1 A Matching Graph
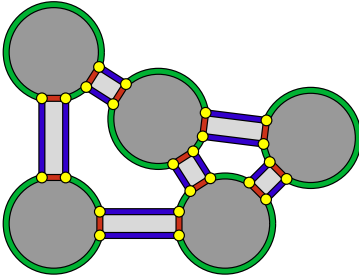
```
%!PS-Adobe-3.0 EPSF-3.0
%%BoundingBox: 0 0 154 118
%%Title: Matching_Graph.eps
%%Creator: Michael La Croix
%%CreationDate: Sat Dec 13 06:30:00 2008
%%EndComments

64 dict begin

mark
    /black 0 0 0
    /lightgrey .85 .85 .85
    /grey .6 .6 .6
    /red .8 .2 .1
    /green 0 .7 .2
    /blue .2 0 .8
    /yellow 1 1 0
counttomark 4 idiv {[ 4 1 roll /setrgbcolor cvx] cvx def} repeat pop

mark
    /v1 {23 23} /v2 {95 23} /v3 {67 67}
    /v4 {23 95} /v5 {131 59}
counttomark 2 idiv {def} repeat pop

/edges [{v4 v3}{v5 v3}{v3 v2}
        {v4 v1}{v5 v2}{v2 v1}] def
/vertices [{v1} {v2} {v3} {v4} {v5}] def

/vsize 20 def % the size of a vertex
/bandwidth 5 def % the width of a ribbon
/endoff vsize dup mul bandwidth dup mul sub sqrt def

/eedge {gsave 3 setlinewidth black stroke grestore} def
```

194

```
gsave
    bandwidth 2 mul setlinewidth 0 setlinecap
    lightgrey edges {exec moveto lineto} forall stroke
    grey vertices {exec vsize 0 360 arc fill} forall

    2 setlinewidth 0 setlinecap
    /im matrix currentmatrix def
    /flaglist [] def
    edges {
        % Set up co−ordinates so the edge runs from (0,−1) to (1,1)
        exec moveto translate currentpoint exch atan rotate
        endoff 0 translate currentpoint pop endoff sub bandwidth scale

        % Draw the sides of the edge
        0 −1 moveto 1 −1 lineto 0 1 moveto 1 1 lineto

        % Save the co−ordinates of each flag in flaglist
        [{0 −1}{0 1}{1 −1}{1 1}]{gsave
            exec moveto im setmatrix
            /flaglist [ flaglist {} forall [ currentpoint ] cvx ] def
        grestore} forall im setmatrix
    } forall blue eedge stroke

    % Add the edges to the current stroke so they can
    % be used as a mask for drawing vertex boundaries
    newpath edges {exec moveto lineto} forall
    gsave currentlinewidth bandwidth 2 mul setlinewidth
    strokepath setlinewidth
    200 0 moveto 0 0 200 0 360 arc eoclip newpath
        green vertices {exec vsize 0 360 arc eedge stroke} forall
    grestore newpath

    % Draw the edges of the edges
    red mark flaglist {exec} forall
    counttomark 4 idiv {moveto lineto} repeat eedge stroke
    cleartomark

    % Draw the flags
    black flaglist {exec 2.5 0 360 arc fill} forall
    yellow flaglist {exec 2 0 360 arc fill} forall
grestore

showpage
end
%%EOF
```

C.2 Tiling a Hexagon
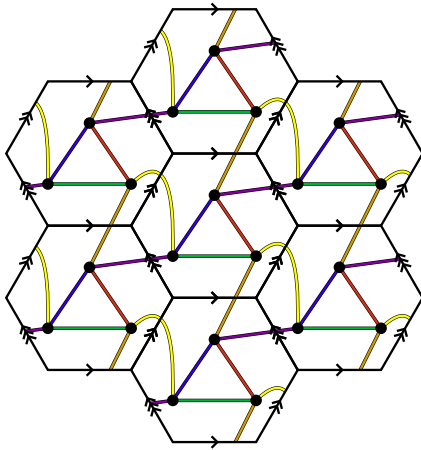

```
/themap {
    blue v1 v3 edge
    green v1 v2 edge
    red v2 v3 edge
    yellow v1 moveto v1 0 20 vadd
        v2 −d2 40 40 vadd
        v2 −d2 curveto estroke
    purple v1 v3 −d3 edge
    orange v2 v3 −d1 edge
} def
```

```
%!PS-Adobe-3.0 EPSF-3.0
%%BoundingBox: 0 0 396 410
%%Title: HexTorus.eps
%%Creator: Michael La Croix
%%CreationDate: Fri Mar 21 01:30:48 2008
%%EndComments
```

64 **dict begin**

% Some useful colors
mark
    /black 0 0 0
    /red .8 0.2 .1
    /green 0 .7 .2
    /blue .2 0 .8
    /purple .5 0 .6
    /orange .8 .6 0
    /yellow 1 1 0
counttomark 4 **idiv** {[4 1 **roll** /setrgbcolor cvx] cvx def} **repeat pop**

% Parameters of the hexagon
/side {72} **bind def**
/height {3 **sqrt** side **mul**} **bind def**
/width {side 2 **mul**} **bind def**

/skip1 {0 height} **bind def**
/skip2 {1.5 side **mul** height −1.5 **mul**} **bind def**
/origin {18 side 2 **div add** 18 height 2 **div add**} **bind def**

```postscript
/vnorm{dup mul exch dup mul add} def
/vdiv{dup 3 1 roll div 3 1 roll div exch} def
/vmul{dup 3 1 roll mul 3 1 roll mul exch} def
/vneg{−1 mul exch −1 mul exch} def
/vdup{2 copy} def
/vadd{3 2 roll add 3 1 roll add exch} def
/vsub{3 2 roll sub neg 3 1 roll sub exch} def
/vavg{vadd 2 vdiv} def

/vertex{newpath 5 0 360 arc closepath fill} def
/edge{newpath moveto lineto estroke} def

% Coloured edges are stroked with black outlines
/estroke{
    currentgray 0 ne {gsave
        currentlinewidth 1 add setlinewidth black stroke
    grestore} if stroke
} def

% A procedure to draw the arrows indicate identification of sides
/arrow{% x y angle arrowsize
    gsave
        exch 4 2 roll translate rotate newpath
        dup 2 copy neg exch moveto
        0 0 lineto neg exch neg lineto stroke
    grestore
} def

/arrowsize 5 def
/multiarrow { % x y number of arrows
    gsave
    3 1 roll exch 2 index −0.5 arrowsize mul
    mul arrowsize add add exch translate
    {
        0 0 0 arrowsize arrow
        arrowsize 0 translate
    } repeat
    grestore
} def

/hex { % x y sidelength
    newpath 3 1 roll moveto
    6 { dup 0 rlineto 60 rotate } repeat
    pop closepath
} def
```

```
% Draw a single hexagonal tile
/hextorus {
    % First draw the inside of the tile.
    0 0 side hex
    gsave clip newpath
        gsave
            % It is necessary to additionally draw the edges
            % from all the neighbours of the tile
            −1.5 side mul height −2 div translate
            2 1 8 {
                1 index exec
                3 mod 0 eq {skip2}{skip1} ifelse translate
            } for pop
        grestore

        % Draw the vertices after drawing the edges
        black vertices {cvx exec vertex} forall
    grestore stroke

    % Draw the edge identification arrows
    gsave
        1 1 3 {
            side 2 div 0 2 index multiarrow
            side 2 div height 3 −1 roll multiarrow
            side 0 translate
            60 rotate
        } for
    grestore
} def


% The co−ordinates of the vertices
/v1 {0 side 2 div} bind def
/v2 {side side 2 div} bind def
/v3 {side 2 div height side 2 div sub} bind def


% A list of all the vertices
/vertices [/v1 /v2 /v3] def


% Translations across boundaries
/d1 {height add} bind def
/−d1 {height sub} bind def
/d2 {exch 1.5 side mul add exch height 2 div sub} bind def
/−d2 {exch 1.5 side mul sub exch height 2 div add} bind def
/d3 {d1 d2} bind def
/−d3 {−d1 −d2} bind def
```

```
% A procedure for drawing edges
/themap {
    blue v1 v3 edge
    green v1 v2 edge
    red v2 v3 edge
    yellow v1 moveto v1 0 20 vadd
        v2 −d2 40 40 vadd
        v2 −d2 curveto estroke
    purple v1 v3 −d3 edge
    orange v2 v3 −d1 edge
} def

gsave
    origin translate
    2 setlinewidth

    2 1 8 {
        /themap cvx hextorus
        3 mod 0 eq {skip2}{skip1} ifelse translate
    } for
grestore
showpage

end
%%EOF
```

C.3 A Map on a Torus

The torus is modelled as the surface obtained by revolving a circle in the xz-plane with radius r_2 centered at $(r_1, 0, 0)$ about the z-axis, and then projecting into the plane $x + y + z = 0$. The surface is parametrized by $(r_3 \cos\theta, r_3 \sin\theta, r_2 \sin\varphi)$ where $r_3 = r_1 + r_2 \cos\varphi$. Hidden lines are detected for straight lines in the intrinsic co-ordinate system of the torus, but using the simplifying assumption that the only occluded portions of the torus have a negative component in the direction $(1, 1, 1)$. This assumption is not valid for the two small regions of the drawing that are more than 2 plies deep, and care should be taken to avoid drawing edges through these regions.
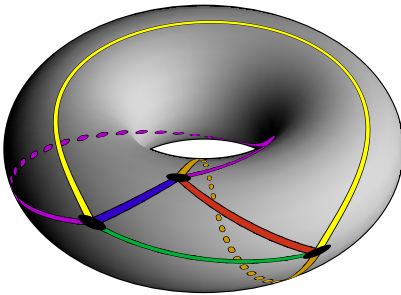

```
/lines [
    {blue v1 v3}
    {green v1 v2}
    {red v2 v3}
    {purple v1 v3 −d3}
    {orange v2 v3 −d1}
] def
/curves [
    {yellow v1 moveto v1 −40 120 vadd
    v2 −d2 20 120 vadd v2 −d2 curveto}
] def
```

```
%!PS-Adobe-3.0 EPSF-3.0
%%BoundingBox: 5 32 195 168
%%Title: TorusMap-19.eps
%%Creator: Michael La Croix
%%CreationDate: Fri Jul 25 17:30:51 2008
%%EndComments

64 dict begin

% Define some useful colours
mark
    /black 0 0 0
    /red .8 0.2 .1
    /green 0 .7 .2
    /blue .2 0 .8
    /purple .7 0 .8
    /orange .8 .6 0
    /yellow 1 1 0
counttomark 4 idiv {[ 4 1 roll /setrgbcolor cvx] cvx def} repeat pop

% Useful vector operations
/vmul {dup 4 −1 roll mul 3 1 roll mul} bind def
```

```
/vadd {exch 4 −1 roll add 3 1 roll add} bind def
/vdot {exch 3 1 roll mul 3 1 roll mul add} bind def
```

% Isometric projections of the co−ordinate axes
```
/y /x /z 90 120 360 {[ exch dup cos exch sin] cvx def} for
/isometric {
    z 3 −1 roll vmul 4 2 roll
    y 3 −1 roll vmul 3 2 roll
    x 3 −1 roll vmul vadd vadd
} def
```

% Parameters of the torus
```
/r1 {50} def % the radius to the center of the tube
/r2 {25} def % the radius of the tube
```

% Compute a point on the surface of the torus
```
/torus { % theta phi
    dup sin r2 mul 3 1 roll
    cos r2 mul r1 add exch 2 copy
    sin mul 4 1 roll cos mul 3 1 roll
} def
```

% Compute the normal to a point on the surface of the torus
```
/torusnormal {
    2 dict begin
        /phi exch def /theta exch def
        theta cos phi cos mul theta sin phi cos mul phi sin
    end
} def
```

% Determine if a point is visible by checking if its normal faces the viewpoint.
% This is cheating, because two small regions are occluded by the torus itself.
```
/isvisible{
    torusnormal add add 0 gt
} def
```

% The following code segment, from here through the definition of
% 'maxstraight' were found in the book PostScript Secrets
% by Don Lancaster, appearing there as section 32a−c.
```
/savecp {2 copy /y0 exch def /x0 exch def} def
/mt {savecp /xx0 x0 def /yy0 y0 def nlt moveto} def
/li {noshortcuts} def
/ct {savecp 3 {6 2 roll nlt} repeat curveto} def
/cp {xx0 yy0 li closepath} def
```

% nlmap applies the nonlinear transform, nlt, to the current path,

```
% leaving the transformed path on the stack for further manipulation.
% Line segments longer that maxstraight are split into curves.
/nlmap {gsave mark /newpath cvx {/mt cvx}{/li cvx}{/ct cvx}
{/cp cvx} pathforall newpath] grestore cvx} def

% We were considering drawing a line to x1 y1 from x0 y0 in the
% untransformed co−ordinate space, but they were too far apart, so
% we're splitting the line into the input number of co−ordinates.
/makecurves {floor cvi y1 y0 sub 1 index div 3 div /ydelta
exch def x1 x0 sub 1 index div 3 div /xdelta exch def {x0 y0 ydelta
add exch xdelta add exch 2 copy ydelta add exch xdelta add exch
2 copy ydelta add exch xdelta add exch ct} repeat} def

% Takes as input a point we're considering drawing a line segment to and
% computes the distance in the untransformed space to see if this is a good idea.
/noshortcuts {/y1 exch def /x1 exch def y1 y0 sub abs x1 x0 sub abs
add maxstraight div dup 1 gt {makecurves}{pop x1 y1 savecp nlt lineto}
ifelse} def

/maxstraight 5 def

/nlt {torus isometric} def

/boundary { %phi from theta
    dup cos exch sin add neg 1 atan
} def

% Directions around the torus
/−d1 {0 −360 vadd} def /d1 {0 360 vadd} def
/−d2 {−360 0 vadd} def /d2 {360 0 vadd} def
/−d3 {−360 −360 vadd} def /d3 {360 360 vadd} def

/v1 {10 20} def
/v2 {80 −10} def
/v3 {35 80} def
/vertices [{v1} {v2} {v3}] def

/lines [
    {blue v1 v3}
    {green v1 v2}
    {red v2 v3}
    {purple v1 v3 −d3}
    {orange v2 v3 −d1}
] def
/curves [
    {yellow v1 moveto v1 −40 120 vadd
```

```
        v2 −d2 20 120 vadd v2 −d2 curveto}
] def


gsave
    100 100 translate

    % Draw the inner boundary of the torus
    0 dup boundary 180 add nlt moveto
    1 1 90{dup boundary 180 add nlt lineto} for
    −270 1 −90 {dup boundary 180 add nlt lineto} for
    closepath

    % The outer boundary is an ellipse
    /currentmat matrix currentmatrix def
    −45 dup boundary torus isometric pop
    −135 dup boundary torus isometric exch pop
    scale 1 0 moveto 0 0 1 0 360 arc
    currentmat setmatrix
    gsave 1 setlinewidth stroke grestore

    % Parameters determining how finely the torus is triangulated
    /thetastep 9 def /phistep 18 def

    % Determine the color of the point with intrinsic co−ordinates (Theta, Phi)
    /lightsource [10 20 −5] def % [z y x]
    /patternpoint {% Theta Phi
        2 copy torus isometric 4 2 roll torusnormal
        lightsource{mul 3 1 roll} forall
        add add lightsource{dup mul}forall add add sqrt div
        .5 add 1.75 div dup 0 lt {pop 0}{dup 1 gt {pop 1} if} ifelse
    } def

    % Building a shading dictionary by triangulating the surface of the torus
    <<
        /PatternType 2
        /Shading
        <<
            /ShadingType 4  % Gourad
            /ColorSpace /DeviceGray  % The underlying color space
            /DataSource [−135 thetastep 45{/theta exch def
                [
                    % Draw the torus as four quadrants
                    {theta phi neg}  % back left
                    {90 theta sub phi neg} % back right
                    {theta phi}  % top left
                    {90 theta sub phi}  % top right
```

203

```
      ]{
          /phi 0 theta −45 gt {180 add neg} if def
          /cup exch def
          0 cup patternpoint
          0 cup thetastep 0 vadd patternpoint
          phistep dup 180{
              theta −45 gt {180 add neg} if
              /phi exch def
              1 cup patternpoint
              1 cup thetastep 0 vadd patternpoint
          } for
      } forall
    } for ]
  >>
>> % End prototype pattern dictionary
gsave matrix makepattern setpattern fill grestore

gsave
    3 setlinewidth

    % Draw all the lines as though they are hidden
    gsave
        1 setlinecap [2 8] 0 setdash
        lines {
            exec newpath moveto lineto
            gsave
                4 setlinewidth black
                strokepath nlmap exec fill
            grestore
            strokepath nlmap exec fill
        } forall
    grestore

    % Now draw the visible portions as solid lines
    3 dict begin
        lines {
            newpath exec
            [ 3 1 roll ] cvx /pathend exch def
            [ 3 1 roll ] cvx /pathstart exch def

            pathstart moveto
            0 5 100 {
                100 div /lambda exch def
                pathstart 1 lambda sub vmul
                pathend lambda vmul vadd
                2 copy isvisible {lineto}{moveto} ifelse
```

204

```
        } for
        gsave
            4 setlinewidth black
            strokepath nlmap exec fill
        grestore
        strokepath nlmap exec fill
    } forall
end

% Draw curves edges without detecting hidden lines
curves {
    newpath exec
    gsave
        4 setlinewidth black
        strokepath nlmap exec fill
    grestore
    strokepath nlmap exec fill
} forall
grestore

% Draw the vertices after the map is drawn
vertices {
    newpath exec 5 0 360 arc
    nlmap exec black fill
} forall
grestore

end
showpage
%%EOF
```

C.4   A Hyperbolic Tiling

This program gives a map on the double-torus as a tiling of hyperbolic space represented by the Poincaré disc model. In the current incarnation, every edge must be drawn as a geodesic. Adding an extra handle is accomplished by adding extra labels, in 4's to the array 'fundlines'. Each of these labels is used to represent one of the circular arcs bounding a fundamental tile. Translations of the fundamental tile are computed as a series of reflections together with circular inversions across these circles. To represent a non-orientable surface, it is necessary to make one of the translations introduce a reflection, and this is accomplished by setting the variable 'nonorientable' to 'true'. For non-orientable surfaces there may be any even number of labels in 'fundlines'.

Since a full tiling requires infinite detail, it is necessary to specify a maximum recursion depth. This can be specified independently for faces, edges, and vertices. Since PostScript interpreters use numerical computation, there is a practical limit to how many inversion can be computed without excessive loss of precision.
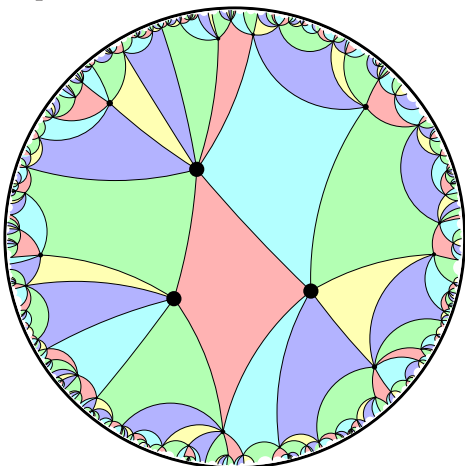

```
/facelist [
    [{va l2 ltran} {vc} {va} {vb}]
    [{vb}{vc l8 ltran}{va l1 ltran}]
    [{va l8 ltran}{vc l8 ltran}{vb}
      {vc l7 ltran}{va l2 ltran l7 ltran}]
    [{vb}{vc l7 ltran}{vb l6 ltran}{va}]
    [{va l1 ltran l4 ltran l7 ltran}
      {vc l7 ltran}{vb l6 ltran}
      {va l1 ltran l6 ltran}]
] def
```

```
/edgelist [
    {va vb l6 ltran} {va vb} {va vc} {vc l7 ltran vb l6 ltran}
    {va l1 ltran vc l8 ltran} {vb vc l7 ltran} {vb vc l8 ltran}
    {vb va l1 ltran} {vc va l2 ltran} {va l8 ltran va l2 ltran l7 ltran}
] def
```

```
%!PS-Adobe-3.0 EPSF-3.0
%%BoundingBox: 0 0 610 610
%%Title: HyperbolicGraph.eps
%%Creator: Michael La Croix
%%CreationDate: Sat Apr 12 03:08:00 2008
%%EndComments
```

64 **dict begin**
/maindict **currentdict def**

/radius {300} **def**
/origin {305 305} **def**
/backgroundcolor {white} **def**
/linecolour {black} **def**
/bordercolor {black} **def**
/skipperimeter **true def**
/skipthreshold 3 **def**
/facethreshold 5 **def**
/edgethreshold 5 **def**
/drawnthreshold 1 **def**
/nonorientable **false def**

/circle {3 **copy add moveto** 90 450 **arc**} **bind def**
/line {**newpath moveto lineto stroke**} **bind def**

/invertpointincircle { % *x y centre radius*
    5 1 **roll** 2 **copy** 7 2 **roll** vsub 2 **copy dup mul exch**
    dup mul add 4 −1 **roll dup mul exch div** vmul vadd
} **def**

/invertpoint { % *x y*
    2 **copy dup mul exch dup mul add** radius **dup mul exch div** vmul
} **def**

/cyclicorder {% *test the cyclic order of a,b,c*
    % *a < b < c OR b < c < a OR c < a < b*
    3 **copy lt** {**lt** {**gt**}{**lt**} **ifelse**} { **lt** {**lt**}{**gt**} **ifelse**} **ifelse**
} **def**

% *Draw the hyperbolic line between v1 and v2.*
/hyperbolicarc { % *v1 v2*
    4 **copy**
    2 **copy** invertpoint circlefrom3pt {
    % *v1 v2 centre radius*
    7 1 **roll** 2 **copy** 9 2 **roll**
    % *centre radius v1 v2 centre*
    2 **copy**
    6 2 **roll** % *centre radius v1 centre v2 centre*
    vsub **exch atan** % *centre radius v1 centre a2*
    5 1 **roll**
    vsub **exch atan** % *centre radius a2 a1*
    exch % *centre radius a1 a2*

207

```
    2 copy 5 index 7 index atan
    cyclicorder {arc}{arcn} ifelse
    }{% The arc is a line
    4 {pop} repeat
    moveto lineto
    } ifelse
} def

/reflectpointindirection { % point direction
    4 copy 3 −1 roll mul 3 1 roll mul add
    2 index dup mul 2 index dup mul add
    div vmul −2 vmul vadd
} def

/hyperbolicline2pt {
    2 copy dup mul exch dup mul add 0 eq
    {moveto lineto stroke}
    {2 copy invertpoint drawcircle3pt stroke}
    ifelse
} def

/drawcircle3pt {
    newpath circlefrom3pt {circle}{moveto lineto} ifelse
} def

/2ptsfromcircle {% centre radius
    % try not to make points colinear with the origin
    3 copy dup 47 cos mul exch 47 sin mul vadd
    5 2 roll dup 94.3 cos mul exch 94.3 sin mul vadd
} def

% Starting with 3 points, this procedure returns one of two things
% centre radius true − if the three points lie on a circle
% x1 y1 x2 y2 false − if the three points are colinear
/circlefrom3pt {%v1 v2 v3
    1 index 4 index eq {6 2 roll} if
    3 index 6 index eq {6 −2 roll} if
    1 index 4 index eq {pop pop false}%colinear
    {
        10 dict begin
        [/y3 /x3 /y2 /x2 /y1 /x1] {exch def} forall

        /ma y2 y1 sub x2 x1 sub div def
        /mb y3 y2 sub x3 x2 sub div def
```

```
        ma mb ne {
            % Compute the x−coordinate of the center
            ma mb y1 y3 sub mul mul
            mb x1 x2 add mul add
            ma x2 x3 add mul sub
            2 mb ma sub mul div

            % Compute the y−coordinate
            ma 0 ne {
                dup neg x1 x2 add 2 div add ma div y1 y2 add 2 div add
            }{
                dup neg x2 x3 add 2 div add mb div y2 y3 add 2 div add
            } ifelse

            % And the radius
            2 copy y1 sub dup mul exch x1 sub dup mul add sqrt
            true
        }{
            % colinear points
            x1 dup mul y1 dup mul add 0 ne {
                x1 y1 1000 vmul x1 y1 −1000 vmul
            }{
                x2 y2 1000 vmul x2 y2 −1000 vmul
            } ifelse
            false
        } ifelse
        end
        } ifelse
} def

/vneg {neg exch neg exch} bind def
/vavg {3 2 roll add 3 1 roll add 2 div exch 2 div} def
/vsub{3 2 roll sub neg 3 1 roll sub exch} def
/vadd{3 2 roll add 3 1 roll add exch} def
/vmul{dup 3 1 roll mul 3 1 roll mul exch} def

/hyperbolicline {% R theta % to center
    dup cos 2 index mul exch sin 2 index mul
    3 2 roll dup mul radius dup mul sub sqrt
    circle stroke
} def

/translateacrossfuncircle { % point circle
    revor {5 −2 roll neg exch neg exch}
      {3 copy 8 3 roll pop reflectpointindirection} ifelse
    5 2 roll invertpointincircle
```

```
} def

/buildreflectionlines {
    2 mul /reflectionlines [2 2 5 4 roll {index} for] def
} def

/notyetdrawn {% drawnlist
    1 dict begin
    /target [ 4 2 roll ] cvx def
    /retvalue true def
    {
        % There are numerical accuracy issues, we'll consider the patch drawn if
        % we've drawn a patch within 1 pt of the origin of this patch
        exec target vsub dup mul exch dup mul add sqrt
        drawnthreshold lt {/retvalue false def} if
    } forall
    retvalue
    end
} def

/drawnpatchlist [] def
/drawtranslatedpatch { % translationdepth
    4 add
    gsave
    drawnpatchlist v0 tran notyetdrawn
    skipperimeter {
        radius v0 tran dup mul exch dup mul add sqrt sub skipthreshold gt and
    } if {
        drawpatch /drawnpatchlist [ [ v0 tran ] cvx drawnpatchlist{}forall] def
    } if
    grestore
    pop
} def

% Define some useful colors
mark
    /red .8 .2 .1
    /blue .2 0 .8
    /green 0 .6 .2
    /black 0 0 0
    /white 1 1 1
    /grey .6 .6 .6
    /cyan .6 1 1
    /purple .7 0 .8
    /magenta 1 0 1
    /azure 0 .4 .8
```

```
    /orange 1 .7 0
    /yellow 1 1 0
counttomark 4 idiv {[ 4 1 roll /setrgbcolor cvx] cvx def} repeat pop

/v0 {0 0} def % The origin, used to determine if a patch has been drawn
/va {−50 90} def
/vb {100 −70} def
/vc {−80 −80} def

% tran takes a pair of co−ordinates representing a point in the
% fundamental patch and translates them to the current patch
/tran {
    reflectionlines {cvx exec translateacrossfuncircle} forall
} def

% 'va l8 ltran' translates the vertex va across the line l8
/ltran {cvx exec translateacrossfuncircle} def

% Draw a vertex at a somewhat appropriate size
/hypervertex {
    tran 2 copy
    dup mul exch dup mul add radius dup mul div neg 1 add
    15 mul newpath circle closepath fill
} def

/facelist [
    [{va l2 ltran} {vc} {va} {vb}]
    [{vb}{vc l8 ltran}{va l1 ltran}]
    [{va l8 ltran}{vc l8 ltran}{vb}
     {vc l7 ltran}{va l2 ltran l7 ltran}]
    [{vb}{vc l7 ltran}{vb l6 ltran}{va}]
    [{va l1 ltran l4 ltran l7 ltran}
     {vc l7 ltran}{vb l6 ltran}
     {va l1 ltran l6 ltran}]
] def

/edgelist [
    {va vb l6 ltran} {va vb} {va vc} {vc l7 ltran vb l6 ltran}
    {va l1 ltran vc l8 ltran} {vb vc l7 ltran} {vb vc l8 ltran}
    {vb va l1 ltran} {vc va l2 ltran} {va l8 ltran va l2 ltran l7 ltran}
] def


% Draw the faces of the map
/drawfaces {
    gsave
```

```
    3 dict begin
    /hue 0 def
    /numfaces facelist length def
    facelist {
        hue .3 1 sethsbcolor
        /central false def
        dup {exec tran dup mul exch dup mul add sqrt
            radius sub neg facethreshold gt {/central true def} if
        } forall

        central {
            [ exch {} forall dup exec moveto ]{exec lineto} forall nlt fill
        }{pop} ifelse
        /hue hue 1 numfaces 1 add div add def
    } forall
    end
    grestore
} def

% Draw the edges
/drawedges {
    1 dict begin
    gsave
    0 setlinecap 1 setlinewidth black
    edgelist {
        % Only draw edges if at least one end is far enough from the boundary circle
        /central false def
        dup exec 2 {tran dup mul exch dup mul add sqrt
        radius sub neg edgethreshold gt {/central true def} if
        } repeat

        newpath exec moveto lineto central {nlt stroke} if
    } forall
    grestore
    end
} def

% Draw vertices on the fundamental patch
/drawvertices {
    black
    [{va}{vb}{vc}]{
    /canvert exch def
    mark
        canvert 10 add tran canvert 10 sub tran canvert exch 10 add exch tran
        newpath circlefrom3pt {dup 1 ge {circle fill} if} if
    cleartomark
```

212

```
        } forall
} def


% /l1 78 cpol gives the point 78 degrees around l1
/cpol {2 copy cos mul 3 1 roll sin mul vadd} def


% Draws the lines bounding the current patch
/drawnclineslist [] def
/drawcolorlines {
    gsave mark
    newpath
    0 setlinecap 8 setlinewidth
    [
        {red l4 0}{red l8 180}{orange l3 45}{l7 225}
        {green l2 90}{green l6 270}{blue l1 135}{blue l5 315}
    ]{
        1 dict begin
        /canline exch def

        drawnclineslist canline cpol tran notyetdrawn {
        canline 45 sub cpol moveto canline 45 add cpol lineto
        gsave
            black currentlinewidth 2 add setlinewidth strokepath nlt fill
        grestore strokepath nlt fill
        maindict /drawnclineslist [ [ canline cpol tran ] cvx
            drawnclineslist{}forall] put
        } if
        end
    } forall
    cleartomark grestore
} def


/nlt {
    5 dict begin
    /hmt {tran moveto /closepoint[currentpoint]cvx def} def
    /hli {tran currentpoint 4 2 roll hyperbolicarc} def
    /hct {3{tran 6 2 roll}repeat curveto} def
    /hcp {currentpoint closepoint hyperbolicarc} def

    [ gsave /newpath cvx
    {/hmt cvx}{/hli cvx}{/hct cvx}{/hcp cvx}
    pathforall grestore ] cvx exec
    end
} def


% The fundamental lines bounding the main patch
```

213

```postscript
/fundlines [/l1 /l2 /l3 /l4 /l5 /l6 /l7 /l8] def

gsave
    origin translate

    newpath 0 0 radius circle closepath
    gsave
    0 0 radius 4 add circle closepath
    bordercolor eofill
    grestore
    gsave backgroundcolor fill grestore
    clip % Only draw in the Poincare disc

    % The number of sides bounding a fundamental patch.
    /sides fundlines length def

    % Build the hyperbolic lines bounding a
    % fundamental domain. The lines are circles
    % in the real plane represented by their
    % center and radius
    360 sides div
    radius 1 2 index 2 div sin 3 index 2 div cos div
    dup mul sub sqrt div % anglestep radius
    0 2 index 359.999 {
    1 index exch
    dup cos 2 index mul exch sin 2 index mul
    3 2 roll dup mul radius dup mul sub sqrt
    5 3 roll
    } for
    pop pop

    % To translate across a fundamental line, either
    % reflect twice or rotate and reflect
    /tranl {/revor false def} def
    /refl {/revor nonorientable def} def
    fundlines {4 1 roll
    2 index 0 eq {/refl}{/tranl} ifelse cvx
    4 packedarray cvx def
    } forall

    /maxdepth 4 def
    /recursivedraw {1 dict begin /curdepth exch def
    curdepth maxdepth le {
        curdepth buildreflectionlines
        curdepth drawtranslatedpatch
        curdepth maxdepth lt {
```

```
        fundlines {
            curdepth 1 add recursivedraw pop
        } forall
        } if
    } if
    end
} def


% The recursive depth for each type of object can be specified individually.
gsave
newpath
[
    % Drawing faces, then edges, then vertices produces a natural layout.
    {/skipperimeter false def 4 /drawfaces} %6
    {4 /drawedges} % 4
    {3 /drawvertices}

    % Uncomment the next line to draw the boundaries of tiles
    % {/skipperimeter true def /skipthreshold 3 def 4 /drawcolorlines}
]{
    exec
    /drawnpatchlist [] def
    /drawpatch exch cvx def
    /maxdepth exch def
    0 recursivedraw
} forall
grestore
grestore

end
showpage
%%EOF
```


215

Bibliography

[BG92]   N. Bergeron and A. M. Garsia, *Zonal polynomials and domino tableaux*, Discrete Math. **99** (1992), no. 1-3, 3–15. 3.5.1, 3.5.1

[BIZ80] D. Bessis, C. Itzykson, and J. B. Zuber, *Quantum field theory techniques in graphical enumeration*, Adv. in Appl. Math. **1** (1980), no. 2, 109–157. 3.3.1

[BJ02]   D. R. L. Brown and D. M. Jackson, *The quadrangulation conjecture for orientable surfaces*, J. Combin. Theory Ser. B **86** (2002), no. 1, 54–79. 7, 7.6, 7.7, 2

[BJ07]   D. R. L. Brown and D. M. Jackson, *A rooted map invariant, non-orientability and Jack symmetric functions*, J. Combin. Theory Ser. B **97** (2007), no. 3, 430–452. 1.1, 3.6.2, 4, 4.1, 4.1, 4.2, 6.4, 6.19, 6.6, 8.3, 8.6

[BR02]   B. Bollobás and O. Riordan, *A polynomial of graphs on surfaces*, Math. Ann. **323** (2002), no. 1, 81–96. 2.2.3

[Bro00] D. R. L. Brown, *Differential equations and depth first search in the enumeration of maps in surfaces*, Ph.D. thesis, University of Waterloo, 2000. 2.27, 3.4, 3.22, 3.1, 4.26, 4.7, 4.7, 4.32, 4.35, 5.19, 5.6, 6.4.1

[DES07] I. Dumitriu, A. Edelman, and G. Shuman, *MOPS: multivariate orthogonal polynomials (symbolically)*, J. Symbolic Comput. **42** (2007), no. 6, 587–620. 3.3

[GHJ01] I. P. Goulden, J. L. Harer, and D. M. Jackson, *A geometric parametrization for the virtual Euler characteristics of the moduli spaces of real and complex algebraic curves*, Trans. Amer. Math. Soc. **353** (2001), no. 11, 4405–4427 (electronic). 1, 2.27, 3, 3.19, 3.3.1, 3.4, 3.23, 3.5.2, 3.5.3, 4.18, 4.6, 4.7, 4.8, 8.1

[GJ96a] I. P. Goulden and D. M. Jackson, *Connection coefficients, matchings, maps and combinatorial conjectures for Jack symmetric functions*, Trans. Amer. Math. Soc. **348** (1996), no. 3, 873–892. 1, 2.27, 2.3, 3, 3.2, 3.10, 3.4, 3.6, 3.30, 3.6.2, 4.1, 5.3, 5.8, 8.6

[GJ96b] ———, *Maps in locally orientable surfaces, the double coset algebra, and zonal polynomials*, Canad. J. Math. **48** (1996), no. 3, 569–584. 1.1, 2.27, 3, 3.2, 3.2, 3.3, 3.5.1, 3.5.1, 3.5.1

[GJ97] ———, *Maps in locally orientable surfaces and integrals over real symmetric surfaces*, Canad. J. Math. **49** (1997), no. 5, 865–882. 3, 3.3.1, 3.3.1, 3.5.2

[GR01] C. Godsil and G. Royle, *Algebraic graph theory*, Graduate Texts in Mathematics, vol. 207, Springer-Verlag, New York, 2001. 2.2.3, 2.3

[GT01] J. L. Gross and T. W. Tucker, *Topological graph theory*, Dover Publications Inc., Mineola, NY, 2001, Reprint of the 1987 original [Wiley, New York; MR0898434 (88h:05034)] with a new preface and supplementary bibliography. 2.1, 2.1, 2.2.1, 2.2.1, 2.2.2, 2.2.3, 2.2.3, 2.3

[Her94] I. N. Herstein, *Noncommutative rings*, Carus Mathematical Monographs, vol. 15, Mathematical Association of America, Washington, DC, 1994, Reprint of the 1968 original, With an afterword by Lance W. Small. 3.5.1

[HR84] P. Hoffman and B. Richter, *Embedding graphs in surfaces*, J. Combin. Theory Ser. B **36** (1984), no. 1, 65–84. 2.2.1, 2.20, 2.3

[HSS92] P. J. Hanlon, R. P. Stanley, and J. R. Stembridge, *Some combinatorial aspects of the spectra of normally distributed random matrices*, Hypergeometric functions on domains of positivity, Jack polynomials, and applications (Tampa, FL, 1991), Contemp. Math., vol. 138, Amer. Math. Soc., Providence, RI, 1992, pp. 151–174. 3.5.1, 3.5.1, 3.5.1

[Jac71] H. Jack, *A class of symmetric polynomials with a parameter*, Proc. Roy. Soc. Edinburgh Sect. A **69** (1970/1971), 1–18. 3.1

[Jac94] D. M. Jackson, *On an integral representation for the genus series for 2-cell embeddings*, Trans. Amer. Math. Soc. **344** (1994), no. 2, 755–772. 3, 3.3.1, 3.5.2

[JPV96] D. M. Jackson, M. J. Perry, and T. I. Visentin, *Factorisations for partition functions of random Hermitian matrix models*, Comm. Math. Phys. **179** (1996), no. 1, 25–59. 7, 7.1, 7.1, 7.1, 7.6.2

[JV90a] D. M. Jackson and T. I. Visentin, *A character-theoretic approach to embeddings of rooted maps in an orientable surface of given genus*, Trans. Amer. Math. Soc. **322** (1990), no. 1, 343–363. 1, 1.1, 2.27, 3, 3.2, 3.2, 3.3, 3.5.1, 3.5.1, 7, 7, 7.1, 7.1, 7.1, 7.1, 7.3, 2, 7.6, 7.6.2

[JV90b] ———, *Character theory and rooted maps in an orientable surface of given genus: face-colored maps*, Trans. Amer. Math. Soc. **322** (1990), no. 1, 365–376. 3, 3.2, 3.2, 3.5.1, 3.5.1, 8.7

[JV99]   _____ , *A combinatorial relationship between Eulerian maps and hypermaps in orientable surfaces*, J. Combin. Theory Ser. A **87** (1999), no. 1, 120–150. 7

[JV01]   D. M. Jackson and T. I. Visentin, *An atlas of the smaller maps in orientable and nonorientable surfaces*, CRC Press Series on Discrete Mathematics and its Applications, Chapman & Hall/CRC, Boca Raton, FL, 2001. 2.2.5, 3.6.2, 5.6, 6, 6.10, 6.30, 7, 2, A

[Kad93]   K. W. J. Kadell, *An integral for the product of two Selberg-Jack symmetric polynomials*, Compositio Math. **87** (1993), no. 1, 5–43. 5.7

[KS97]   F. Knop and S. Sahi, *A recursion and a combinatorial formula for Jack polynomials*, Invent. Math. **128** (1997), no. 1, 9–22. 3.1, 5.5, 5.7

[Lan91]   D. Lancaster, *PostScript®secrets*, Synergetics Press, Thatcher AZ, 1991. C

[Las08]   M. Lassalle, *A positivity conjecture for Jack polynomials*, Math. Res. Lett. **15** (2008), no. 4, 661–681. 6.4.1

[LV95]   L. Lapointe and L. Vinet, *A Rodrigues formula for the Jack polynomials and the Macdonald-Stanley conjecture*, Internat. Math. Res. Notices **1995** (1995), no. 9, 419–424. 3.1, 5.5, 5.7

[LZ04]   S. K. Lando and A. K. Zvonkin, *Graphs on surfaces and their applications*, Encyclopaedia of Mathematical Sciences, vol. 141, Springer-Verlag, Berlin, 2004, With an appendix by Don B. Zagier, Low-Dimensional Topology, II. 2.2.6, 2.3.1, 3.5.2

[Mac87]   I. G. Macdonald, *Commuting differential operators and zonal spherical functions*, Algebraic groups Utrecht 1986, Lecture Notes in Math., vol. 1271, Springer, Berlin, 1987, pp. 189–200. 3.2

[Mac95]   _____ , *Symmetric functions and Hall polynomials*, second ed., Oxford Mathematical Monographs, The Clarendon Press Oxford University Press, New York, 1995, With contributions by A. Zelevinsky, Oxford Science Publications. 3.1, 3.1, 3.5.1, 3.5.1, 3.5.1, 5.4, 6.4.1

[Meh04]   M. L. Mehta, *Random matrices*, third ed., Pure and Applied Mathematics (Amsterdam), vol. 142, Elsevier/Academic Press, Amsterdam, 2004. 4.4, 4.4

[Oko97]   A. Okounkov, *Proof of a conjecture of Goulden and Jackson*, Canad. J. Math. **49** (1997), no. 5, 883–886. 3, 3.2, 3.3.1, 3.18

[Ore67]   O. Ore, *The four-color problem*, Pure and Applied Mathematics, Vol. 27, Academic Press, New York, 1967. 7, 2

[RW95]   L. B. Richmond and N. C. Wormald, *Almost all maps are asymmetric*, J. Combin. Theory Ser. B **63** (1995), no. 1, 1–7. 2.27, 2.2.4

[Sch98]   G. Schaeffer, *Conjugaison d'arbres et cartes combinatoires aléatoires*, Ph.D. thesis, L'Universiteé Bordeaux I, 1998. 7, 7.3

[Sta89]   R. P. Stanley, *Some combinatorial properties of Jack symmetric functions*, Adv. Math. **77** (1989), no. 1, 76–115. 3.1, 3.4, 3.5, 3.6, 3.9, 5.4, 5.11, 5.12, 5.7, 8.6

[Tho92]   C. Thomassen, *The Jordan-Schönflies theorem and the classification of surfaces*, Amer. Math. Monthly **99** (1992), no. 2, 116–130. 2.6

[Tut48]   W. T. Tutte, *The dissection of equilateral triangles into equilateral triangles*, Proc. Cambridge Philos. Soc. **44** (1948), 463–482. 7

[Tut62]   ———, *A census of slicings*, Canad. J. Math. **14** (1962), 708–722. 7

[Tut63]   ———, *A census of planar maps*, Canad. J. Math. **15** (1963), 249–271. 7

[Tut84]   ———, *Graph theory*, Encyclopedia of Mathematics and its Applications, vol. 21, Addison-Wesley Publishing Company Advanced Book Program, Reading, MA, 1984, With a foreword by C. St. J. A. Nash-Williams. 2.3, 2.3.1

[Wal75]   T. R. S. Walsh, *Hypermaps versus bipartite maps*, J. Combinatorial Theory Ser. B **18** (1975), 155–163. 2.3.2

Notation

This list of notation is organized alphabetically, using the convention that numbers precede non-alphanumeric symbols, and both classes of symbols precede letters. The Greek alphabet is considered to precede the Latin alphabet, and within each alphabet, capitals precede the corresponding minuscules.

Numbers

1	the vector $(1, 1, 1, 1, \dots)$ consisting entirely of 1's
$\mathbf{1}_N$	the vector $(1, 1, \dots, 1, 0, 0, \dots)$ of N leading 1's padded with 0's

Non-alphanumeric Symbols

$|\cdot|$	the cardinality of a set (*or*) the size of an integer partition
$\langle \cdot, \cdot \rangle_\alpha$	an inner product on the ring of symmetric functions
$\langle \cdot \rangle$	an expectation operator
$\langle \cdot \rangle_e$	an expectation operator defined in terms of $\langle \cdot \rangle$

Greek Letters

$\alpha_1, \alpha_2, \alpha_3$	involutions acting on Q by re-rooting
$\beta_1, \beta_2, \beta_3$	involutions acting on $\mathcal{A}$
Γ	a bijection from F to $E_G \cup V_G$
γ	the complex number $\frac{1}{1+b}$
$\delta_{\cdot,\cdot}$	the Kronecker delta function
$\partial \Sigma$	the boundary of a surface Σ
ϵ	the edge permutation of an orientable hypermap (*or*) the edge-degree partition of a hypermap

ζ	a bijection from $(3,1)$-pseudo-4-regular maps to 4-regular maps
η	any one of a family of invariants defined on rooted maps
θ	a partition
κ	Gaußian curvature
Λ	the ring of symmetric functions with coefficients in $\mathbb{Z}$
$\Lambda_{\mathbb{Q}(\alpha)}$	the ring of symmetric functions with coefficients in $\mathbb{Q}(\alpha)$
$\Lambda_{\mathbb{Q}(\alpha)}^{k}$	a graded piece of $\Lambda_{\mathbb{Q}(\alpha)}$
$\Lambda(\cdot,\cdot)$	$\Lambda(M_1, M_2)$ is the partition λ where 2λ consists of the lengths of cycles in $M_1 \cup M_2$ for perfect matchings M_1 and M_2
$\boldsymbol{\lambda}$	the vector $(\lambda_1, \lambda_2, \lambda_3, \ldots, \lambda_N)$
λ	a partition
λ'	the conjugate partition to λ
μ	a partition
ν	the vertex permutation of an orientable hypermap (*or*) the vertex-degree partition of a hypermap
Ξ_g	the space $\left\{ p(b) \in \mathbb{Q}(b) \colon p(b-1) = (-b)^g p\left(\frac{1}{b}-1\right) \right\}$
ξ	the operation of root-edge deletion on $\mathcal{A}$
π_1, π_2, π_3	natural products on $Q^* \times Q^*$
$\underline{\pi}_1, \underline{\pi}_2, \underline{\pi}_3$	induced products on $Q^* \times Q^*$
$\boldsymbol{\rho}$	the vector $(\rho_1, \rho_2, \rho_3, \ldots, \rho_N)$
ρ_1, ρ_2, ρ_3	natural products on $\mathcal{A}^* \times \mathcal{A}^*$
$\overline{\rho}_1, \overline{\rho}_2, \overline{\rho}_3$	induced products on $\mathcal{A}^* \times \mathcal{A}^*$
Σ	a surface
σ	the involution on Q induced by τ acting on $\mathcal{A}$
τ	an involution acting on $\mathcal{A}$ by changing the decoration of vertices
τ_e, τ_v, τ_f	fixed-point-free involutions used to define combinatorial maps
Φ	a series defined in terms of Jack symmetric functions
φ	the face permutation of an orientable hypermap $(= \epsilon\nu)$ (*or*) the face-degree partition of a hypermap (*or*) a conjectured natural bijection between $\mathcal{A}$ and Q
$\overline{\varphi}$	the medial construction
ϕ^λ	irreducible characters of $\mathcal{H}(\mathfrak{S}_{2n}, \mathfrak{B}_n)$ indexed by the partition λ
χ	the Euler characteristic of a map or surface

|	
χ_1	the action on Q induced by ξ acting on $\mathcal{A}_1$
χ_2	the action on Q induced by ξ acting on $\mathcal{A}_2$
χ^λ	an irreducible character of the symmetric group indexed by λ
$\chi_j^{(i)}$	the evaluation of $\chi^{(i)}$ at an element of C_j
$\overline{\chi}_j^{(i)}$	the complex conjugate of $\chi_j^{(i)}$
Ψ	a series related to the derivative of the logarithm of Φ
Ω	the product $\mathrm{e}^{-\frac{\gamma}{2} p_2(\mathbf{x})} |V(\mathbf{x})|^{2\gamma}$
ω_λ	the size of the centralizer of a permutation with cycle type λ

Latin Letters

$\mathcal{A}$	a class of decorated rooted orientable maps with at least one edge
$\mathcal{A}^*$	$\mathcal{A}$ together with the rooted map with no edges
$\mathcal{A}_1$	the subset of $\mathcal{A}$ not rooted on cut edges
$\mathcal{A}_2$	the subset of $\mathcal{A}$ rooted on cut edges
$\mathcal{A}_{g,n}$	a subset of $\mathcal{A}$
$A(u,x,y,z)$	the generating series for orientable maps
$a_\lambda(x)$	the arm length of a cell x in a partition λ
b	a ubiquitous parameter
B_g	a basis, $\left\{ b^{g-2i}(1+b)^i : 0 \le i \le g/2 \right\}$ for b-polynomials
$\mathfrak{B}_n$	the wreath product $\mathfrak{S}_n[\mathfrak{S}_2]$ realized as the stabilizer of the fixed-point free involution $(1,2)(3,4)\cdots(2n-1,2n)$ in $\mathfrak{S}_{2n}$
$\mathbb{C}$	the field of complex numbers
C_λ	a conjugacy class of $\mathfrak{S}_n$ indexed naturally by the partition λ
C_λ	the formal sum of elements of C_λ
$\mathbb{C}\mathfrak{S}_n$	the group algebra of $\mathfrak{S}_n$ with coefficients in $\mathbb{C}$
$c_{\lambda\mu}(\alpha)$	the coefficient of p_μ in $J_\lambda(\alpha)$
$c_{\nu,\varphi,\epsilon}(b)$	a coefficient of the hypermap series
c_{ij}	the complex component of a co-ordinate of $\mathcal{V}_N$
$\mathrm{cl}(\cdot)$	the topological closure of a set
$d_{\nu,\varphi}(b)$	the sum $\sum_{\ell(\nu)=\nu} c_{\nu,\varphi,[2^n]}(b)$
$\deg(\cdot)$	the degree of a vertex or a face
E_λ	an orthogonal idempotent of either $Z(\mathbb{C}\mathfrak{S}_n)$ or $\mathscr{H}(\mathfrak{S}_{2n}, \mathfrak{B}_n)$

E_G	the edges of G
e	the base of the natural logarithm
e	an edge, often the root edge of the map $\mathfrak{m}$ or $\mathfrak{q}$
$\mathbf{e_2}$	the vector $(0, 1, 0, 0, 0, \dots)$
e_λ	the elementary symmetric function indexed by the partition λ
$\mathcal{F}$	a closed family of discs forming a ribbon graph
f	a face of a map
G	a graph
g	genus
H_λ	the hook length product $\prod_{x \in \lambda}(1 + a(x) + l(x))$ when λ is a partition
$\mathscr{H}(\mathfrak{S}_{2n}, \mathfrak{B}_n)$	the Hecke algebra of $\mathfrak{B}_n$ as a subgroup of $\mathfrak{S}_{2n}$
$H(\mathbf{x}, \mathbf{y}, \mathbf{z}; b)$	a generating series for hypermaps
$h_{v,\varphi,i}$	a coefficient of $c_{v,\varphi,[2^n]}(b)$ with respect to the basis B_g
i	is the imaginary unit
$i\colon G \to \Sigma$	an embedding of G in Σ
i^*	the dual of the map i
$J_\lambda(\alpha)$	the Jack symmetric function indexed by λ with Jack parameter α
$\mathcal{K}_\lambda$	a double coset of $\mathfrak{B}_n$ in $\mathfrak{S}_{2n}$ naturally indexed by the partition λ
K_λ	the formal sum of the elements of $\mathcal{K}_\lambda$
$\ell(\cdot)$	the length of a partition
$l_\lambda(x)$	the leg length of a cell x in a partition λ
M	an $N \times N$ matrix in $\mathcal{W}_N$ or $\mathcal{V}_N$
$M(\cdot)$	a generating series for maps, its definition determined by context
$\mathcal{M}_{v,\varphi}$	the set of maps with vertex- and face-degree partition v and φ
M_e, M_f, M_v	perfect matchings on the matching graph of a map
$\mathcal{M}_{v,f}$	the set of maps with v vertices and f faces
$M(x, \mathbf{y}, z, \mathbf{r}; b)$	a refinement of $M(x, \mathbf{y}, z; b)$
$\mathfrak{m}$	a map
$\mathfrak{m}'$	a map, often obtained from $\mathfrak{m}$ by successive root-edge deletions
$\overline{\mathfrak{m}'}$	a map obtained from $\mathfrak{m}'$ deleting one handle and adding another
$\overline{\mathfrak{m}}$	the image of $\mathfrak{m}$ under a bijection
m_λ	the monomial symmetric function indexed by the partition λ

$m_i(\lambda)$	the multiplicity of the part i in the partition λ
m_{ij}	an indeterminate marking a half edge separating a face painted i from a face painted j (*or*) an entry in an $N \times N$ matrix M
$m_n(x, \mathbf{y}, \mathbf{r}; b)$	the coefficient of z^n in M
N	a positive integer, often the dimension of a space of integration
O	the set of equivalence classes of orientable surfaces
$O(x^n)$	a formal power series with valuation at least n
$\mathscr{P}$	the set of integer partitions
$P_{3,1}(u, x, y, z)$	a generating series for $(3, 1)$-pseudo-4-regular maps
$\mathfrak{p}$	a $(3, 1)$-pseudo-4-regular map
p_λ	the power-sum symmetric function indexed by the partition λ
$\mathbf{p}(\mathbf{x})$	the vector $(1, p_1(\mathbf{x}), p_2(\mathbf{x}), p_3(\mathbf{x}), \dots)$
$\mathbb{Q}$	the field of rational numbers
Q	the class of rooted orientable 4-regular maps
Q^*	Q together with the object ⊘
$Q_{g,n}$	a subset of Q consisting of maps with genus g and n vertices
$Q(u, x, y, z)$	a generating series for Q
Q_1	the restriction of Q to maps with face-separating root edges
Q_2	the restriction of Q to maps with face-non-separating root edges
$\mathfrak{q}$	a rooted orientable 4-regular map
$q_{v,\varphi,\epsilon}(b)$	a coefficient of Φ with respect to the power-sum basis
$\mathbb{R}$	the field of real numbers
$\mathfrak{R}(\cdot)$	the real part of a complex number
$R_{\mathscr{N}}(x, y, z)$	a series related to $A(1, x, y, z)$
$R_{\{4\}}(x, y, z)$	a series related to $Q(1, x, y, z)$
R	a semi-ring
R_+	the semi-ring of positive elements of $R \subseteq \mathbb{R}$
$\mathbf{r}$	the vector $(r_0, r_1, r_2, \dots)$, usually associated with root faces
r_{ij}	a co-ordinate of $\mathcal{W}_N$ or the real component of a co-ordinate of $\mathcal{V}_N$
$S(\mu)$	the function $\sum_{k \geq 1} \sqrt{2x}^k \left\langle p_k \prod_{i=1}^N \left(1 - \lambda_i \sqrt{2x}\right)^{-(N+\mu)} \right\rangle$
$\mathfrak{S}_n$	the symmetric group on n elements
s_λ	the Schur function indexed by the partition λ

$T(\mu)$	the function $\left\langle \prod_{i=1}^{N} \left(1 - \lambda_i \sqrt{2x}\right)^{-(N+\mu)} \right\rangle$
$t(\nu, \varphi, \epsilon)$	the number $|\nu| - \ell(\nu) - \ell(\varphi) - \ell(\epsilon)$ when ν, φ, and ϵ are partitions
$\mathcal{U}$	the class of unhandled maps
$U(\mathbf{x}, \mathbf{y}, \mathbf{z})$	the generating series for $\mathcal{U}$
$V(\lambda)$	the Vandermonde determinant $\prod_{1 \leq i < j \leq N} (\lambda_i - \lambda_j)$
V_G	the vertices of a graph G
$\mathcal{V}_N$	the space of $N \times N$ complex Hermitian matrices
v	a vertex of a graph
$v_{\lambda\mu}(\alpha)$	the coefficient of m_μ in $J_\lambda(\alpha)$ when λ and μ are partitions
$\mathcal{W}_N$	the space of $N \times N$ real symmetric matrices
$\mathbf{x}$	the vector $(x_0, x_1, x_2, \dots)$, usually associated with vertices
$\mathbf{x}^\theta$	a monomial $\prod_{i \geq 1} x_i^{m_i(\theta)}$ determined by the partition θ
$\mathbf{y}$	the vector $(y_0, y_1, y_2, \dots)$, usually associated with faces
$\mathbb{Z}$	the ring of integers
Z_λ	the zonal polynomial indexed by the partition λ
$Z(\mathbb{C}\mathfrak{S}_n)$	the centre of $\mathbb{C}\mathfrak{S}_n$
$\mathbf{z}$	the vector $(z_0, z_1, z_2, \dots)$, usually associated with edges
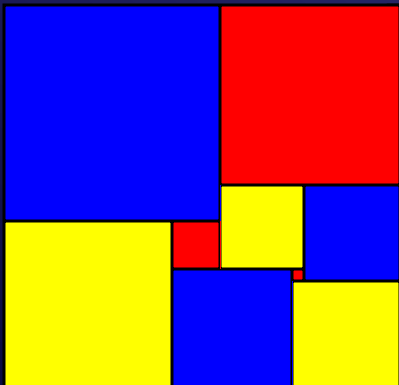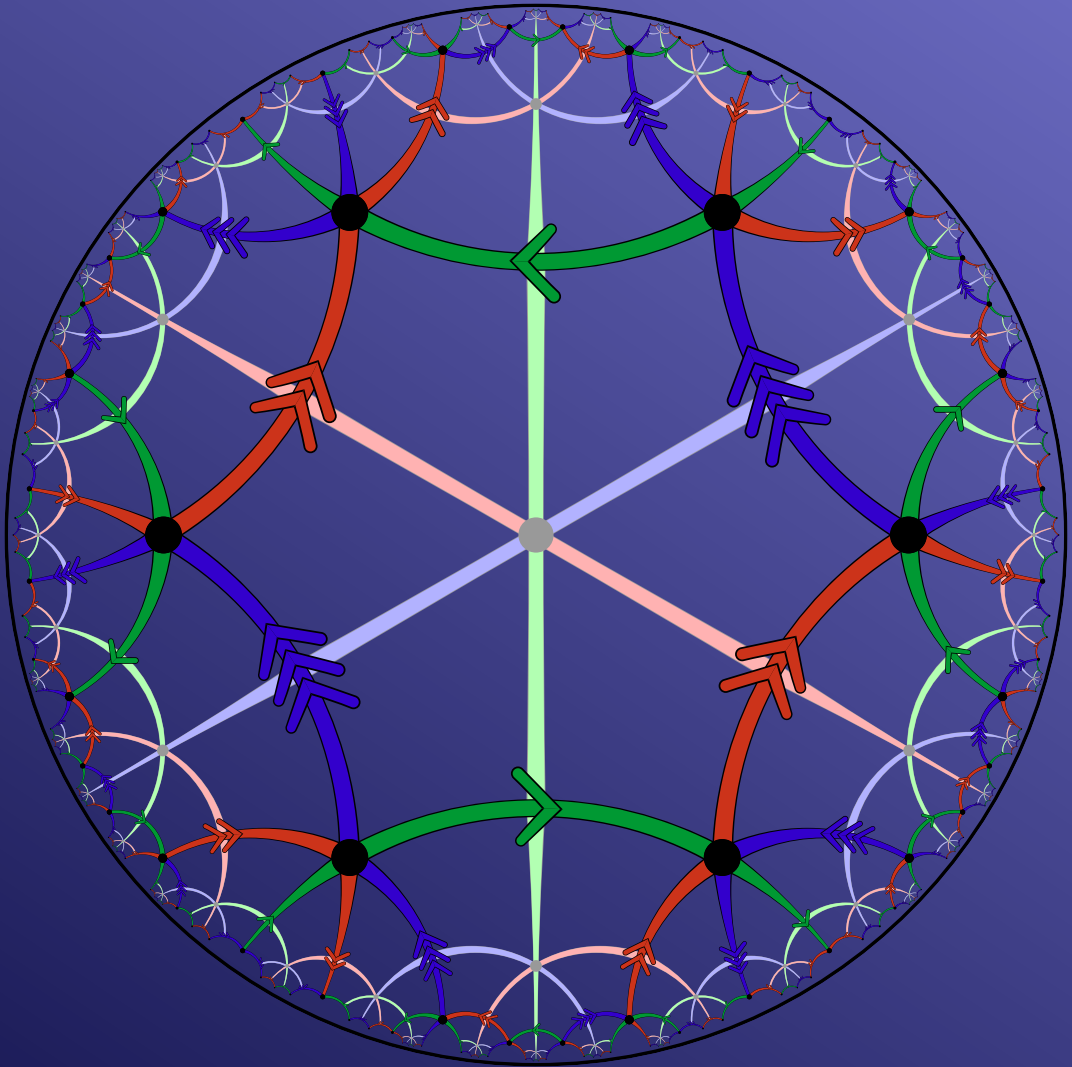
A thesis
presented to the University of Waterloo
in fulfillment of the
thesis requirement for the degree of
Doctor of Philosophy
in
Combinatorics and Optimization

An electronic copy of this text is available at
http://hdl.handle.net/10012/4561